SISSA
Scuola
Internazionale
Superiore di
Studi Avanzati

Physics Area - PhD course in
Theoretical Particle Physics

Space(time) oddity: dualities, holography and branes

Candidate:
Francesco Mignosa

Advisor:
Matteo Bertolini

Academic Year 2021-22

Abstract

In this Thesis, we study (several) aspects of three and five dimensional non-supersymmetric gauge theories. Using non-perturbative techniques, such as known strong-weak coupling dualities and holography, we present new results concerning their dynamics and phase diagrams. The thesis is divided into six Chapters.

In the first Chapter, we start reviewing some general aspects of non-supersymmetric three dimensional theories, focusing on the dynamics of gauge theory both in the absence and in presence of Chern-Simons terms. We then focus on known dualities among three dimensional theories, such as particle-vortex and bosonization duality. Thanks to these tools, we discuss what is known about the phase diagram of QCD_3, namely the three dimensional analog of four dimensional quantum chromodynamics, for various ranges of its parameters.

In Chapter two, we introduce the basics of holography, starting by reviewing the AdS/CFT correspondence. We then generalize the discussion to the case of non-conformal field theories, with particular emphasis on the description of confining theories. Finally, we review the holographic construction of four dimensional and three dimensional gauge theories, and, focusing on the latter case, we construct the gravity dual of QCD_3.

In Chapter three, we show new results regarding the phase diagram of QCD_3 in presence of flavor-breaking mass deformation. The corresponding theory, namely QCD_3 with two sets of flavors, is studied in detail, thanks to the conjectured infrared dualities characterizing gauge theories with matter in three dimensions, namely boson-fermion dualities. In particular, the low-energy phase diagram is charted, and its consistency gives additional support to the conjectured phase diagram of QCD_3. Moreover, new non-perturbative phases are observed, together with peculiar phase transitions among them, which are novel to QCD_3 with two flavors.

In Chapter four, we study the phase diagram of large N QCD_3 through its holographic dual. This novel study shows perfect agreement with the field theory analysis, giving a simple explanation of the observed peculiarity of its phase diagram, together with an holographic evidence of the validity of boson-fermion dualities.

In Chapter five, we review the main aspects of five dimensional theories. Firstly, we focus on general properties of supersymmetric gauge theories, their BPS spectrum, and their moduli spaces of vacua. Then, we study their non-perturbative dynamics using string constructions, both in type I' and in type IIB string theory. The latter type of construction, known as the pq-web or brane web construction, gives us the possibility of studying in detail many non-perturbative phenomena characterizing these theories and their superconformal ultraviolet fixed points, such as global symmetry enhancement and continuation past infinite coupling.

Finally, in Chapter six, we deal with new results involving the possible existence of five dimensional non-supersymmetric conformal field theories. Firstly, a known conjectured non-supersymmetric fixed point, obtained by soft supersymmetry breaking deformation of the E_1 superconformal field theory, is analyzed using field theory techniques. Then, a similar transition point, enjoyed by a class of superconformal field theories generalizing the E_1 fixed point, is studied via its pq-web construction. In particular, in a specific regime of the parameters, semi-classical gravitational interactions can be taken into account. In both the field theory and the string construction analysis, we give hints of the presence of a non-supersymmetric second order phase transition for some specific regime of the parameters, shading light on the possible existence of non-supersymmetric conformal field theories in five dimensions.

Forward

This thesis is divided into six chapters. In the first one, we revise some background material about three dimensional field theories and their dualities. In Chapter two we discuss some basics of holography which will be useful in the following. In Chapter three we describe new results for QCD_3 with two sets of flavors. In Chapter four new results are reported for the holographic realization of the vacuum structure of QCD_3. In Chapter five we review general aspects of five dimensional theories and their string constructions. Finally, in Chapter six we describe recent attempts to find non-supersymmetric conformal field theories in five dimensions via soft supersymmetry breaking deformations of known superconformal fixed points. The thesis is based on the following papers

1. R. Argurio, M. Bertolini, F. Mignosa and P. Niro, *Charting the phase diagram of QCD_3,* JHEP **08** (2019), 153, [arXiv:1905.01460 [hep-th]].

2. R. Argurio, A. Armoni, M. Bertolini, F. Mignosa and P. Niro, *Vacuum structure of large N QCD_3 from holography,* JHEP **07** (2020), 134, [arXiv:2006.01755 [hep-th]].

3. M. Bertolini and F. Mignosa, *Supersymmetry breaking deformations and phase transitions in five dimensions,* JHEP **10** (2021), 244, [arXiv:2109.02662 [hep-th]].

4. M. Bertolini, F. Mignosa and J. van Muiden, *On non-supersymmetric fixed points in five dimensions,* [arXiv:2207.11162 [hep-th]].

Contents

Introduction

Quantum field theory (QFT) provides the most successful framework to describe physical phenomena. Both low-energy physics, such as phase transitions in condensed matter, and high-energy physics, such as particle physics and fundamental interactions, can be described in the context of quantum field theories.
Quantum field theories are well-understood only in perturbation theory: in this framework, the couplings describing interactions among various fields are taken to be small and the various observables are calculated in a series expansion of these couplings. However, many interesting phenomena arise at strong coupling. This is the case of strong interactions or interacting conformal field theories. Phenomena such as confinement, chiral symmetry breaking, and dynamical generation of a mass gap of four dimensional gauge theories are still far from having a complete analytic understanding.
It is then of great physical interest to go beyond perturbation theory to study non-perturbative aspects of QFTs.
In recent years, many techniques have been developed in order to tackle this problem. First of all, supersymmetry gives us a huge control over quantum field theories. In some cases, the strong coupling dynamics of supersymmetric QFTs can be studied in detail, giving the possibility of understanding important physical phenomena, such as confinement from monopole condensation [1] or chiral symmetry breaking [2]. However, the real world seems to lack of supersymmetry, at least at low-energies, so although these results can help if the non-supersymmetric theory we consider is the result of a soft supersymmetry breaking of a supersymmetric theory, also other tools are needed to study non-perturbative physics.
Dualities are one such option: a theory that is strongly coupled in a certain regime can sometimes be studied using a dual weakly coupled theory that shares with it the same physics in this regime. Observables can then be easily calculated in the latter theory and the dynamics of the former can be unveiled. In the same vein, holography can give us important information about QFTs at strong coupling. The correspondence, relating a quantum gravity theory on a specific background to a quantum field theory living on the boundary of this background, is of weak-strong type. So, again, by just looking at a semi-classical theory of gravity, one can obtain non-perturbative information about the field theory dual to this gravity theory.

On top of these general tools, also studying theories in different dimensions can be helpful.
Three dimensional gauge theories, in particular, share important similarities with their four dimensional counterparts: they are strongly coupled at low-energies, confine, and show the

presence of a mass gap. In presence of fermions, they enjoy chiral symmetry breaking as in four dimensional QCD. The advantage is that we have much more control over these theories since there exist a huge variety of dualities connecting them which gives us the possibility of studying their dynamics also in absence of supersymmetry. In this way, studying the dynamics of three dimensional theories can give us a framework to better understand four dimensional theories, gaining fundamental hints of how non-perturbative physics works. This can give us also a better understanding of four dimensional dualities. For example, in the supersymmetric case, many three dimensional dualities were found to be related to known dualities in four dimensions under compactification [3]. So, thanks to three dimensional theories, we can understand better four dimensional physics.
In fact, three dimensional theories are also interesting per se. They happen to describe many phenomena relevant to condensed matter systems in three dimensions, that can be experimentally realized. For example, we can describe superfluidity and superconductivity, but also the quantum Hall effect and topological insulators. This gives a way to test theoretical predictions through experiments and a source for new phenomena that need to be theoretically explained by new models.

Similarly, five dimensional gauge theories represent an important framework to understand the physics of strongly coupled systems. They have many connections to four and three dimensional theories. This can be easily established by employing supersymmetry. Many five dimensional dualities, for example, can be obtained by lifting known four dimensional dualities [4]. Similarly, superconformal field theories in five dimensions can be related to known three and four dimensional analogs [5, 6]. Moreover, in recent years important hints were obtained that point to the possibility that any four dimensional superconformal field theory can be obtained from dimensional reduction of a six dimensional analog. We see that there is a strict relation among superconformal field theories in three, four, five, and six dimensions. So, understanding superconformal field theories in a framework where they are well-behaved can give us a tool to understand these theories in all other dimensions. This is precisely the case with five dimensional theories. These are well-behaved in presence of supersymmetry and many of them can be studied via model building in string theory. The great control gained through these constructions allowed in recent years to unveil a great variety of superconformal field theories, many of which can be obtained as UV completions of known supersymmetric gauge theories. In this way, also the non-perturbative physics of these latter theories was unveiled and studied in detail.
For this reason, the analysis of these theories is not only interesting but essential to understand how the physics of our world works.

This Thesis deals with the problem of understanding non-perturbative aspects of gauge theories in odd dimensions. Using many tools, such as supersymmetry, dualities, holography, and model building in string theory, we shed light on the dynamics of strongly coupled theories, with a particular focus on non-supersymmetric field theories.

Chapter 1

Aspects of three dimensional theories

In this Chapter, we review three dimensional non-supersymmetric Quantum Field Theories (QFT)s. We start discussing Abelian gauge theories in three dimensions and their extensions obtained by including topological terms, the Chern-Simons (CS) terms. We then introduce fermions in $(2+1)$-dimensions, their anomalies, and their relation with the CS terms. After that, we introduce the concept of infrared duality and we describe particle-vortex duality. This allows us to discuss Abelian bosonization in three dimensions and to obtain, from these basic correspondences, an intricate web of Abelian dualities between fermionic and bosonic theories. We then generalize our discussion to non-Abelian theories in presence of CS terms. We extend dualities in presence of fermionic and/or bosonic matter in the fundamental representation for non-Abelian theories. Finally, we explore the phase diagram of QCD_3, namely $SU(N)$ Yang-Mills (YM) CS theory coupled to F fundamental Dirac fermions and with CS level k, in different regimes of its parameter space.

1.1 $U(1)$ Maxwell theory

Let us start by reviewing Maxwell theory in $2+1$ dimensions.
The Maxwell Lagrangian in presence of a conserved current J^μ, normalizing the gauge field to have the coupling e in front of the Lagrangian, reads

$$\mathcal{L} = -\frac{1}{2e^2} F \wedge *F - A \wedge *J. \tag{1.1}$$

The corresponding equations of motion reads

$$d * F = e^2 * J. \tag{1.2}$$

From (1.1), we see that the gauge coupling e is relevant $[e] = 1/2$, so the theory is super-renormalizable. Moreover, the coupling e runs classically. In the UV, the theory is asymptotically free, while in the IR it is strongly coupled. In particular, a charge $J_0 = \delta^2(x)$ generates an electric field $E \sim \frac{1}{r}$, so two probes attract with a logarithmic potential $V(R) \sim e^2 \log R$ where R represents the distance between them. This is a signal of confinement of the electric charges.

This is quite different from 3+1 dimensional physics, where electromagnetism is free in the IR and develops a Landau pole in the UV.
Another difference comes from the number of degrees of freedom. The gauge potential is a three dimensional Lorentz vector. However, we have only one on-shell independent degree of freedom surviving the gauge fixing. The gauge invariant information of the Maxwell theory are encoded in the two-form field strength. In any dimension d, this has $\frac{1}{2}d(d-1)$ independent components. These are divided into an electric field $E_i = \partial_0 A_i - \partial_i A_0$ of dimension $d-1$ and a magnetic field $B_{ij} = \partial_i A_j - \partial_j A_i$ of dimension $\frac{1}{2}(d-1)(d-2)$. So we see that, for example, when $d = 5$, the electric field is four dimensional and the magnetic field is six. The first is a vector under the rotation group (as in any dimension), while the second is a tensor. In four dimensions, both the electric and the magnetic field have dimension 3 and the first is a vector, while the latter is a pseudovector. Finally, in three dimensions, the electric field has dimension two, while the magnetic field has a single independent degree of freedom

$$B \equiv B_{12} = \epsilon^{ij}\partial_i A_j \tag{1.3}$$

which is a pseudoscalar.

Let us now focus on the global symmetries preserved by the Maxwell theory, starting from discrete symmetries. The theory respects charge conservation $\mathcal{C}$, which sends

$$\mathcal{C} : A_\mu \to -A_\mu. \tag{1.4}$$

time-reversal symmetry $\mathcal{T}$ sends $(x^0, x^i) \to (-x^0, x^i)$ and

$$\mathcal{T} : (A_0, A_i) \to (A_0, -A_i) \tag{1.5}$$

so the Maxwell Lagrangian is again invariant. Standard parity $\mathcal{P} : x^i \to -x^i$ in three dimensions belongs to the Lorentz group, being a Lorentz transformation of determinant one. So, in three dimensions (as also in general odd dimensions) parity is actually a reflection along a single coordinate. In the following, we will choose this coordinate to be x^1. Parity then acts on one-forms as

$$(A_0, A_1, A_2) \to (A_0, -A_1, A_2) \tag{1.6}$$

so the Maxwell Lagrangian is left invariant.
The theory in (1.1) preserves also a continuous zero-form symmetry. Indeed, due to the Bianchi identity [7],

$$dF = 0 \tag{1.7}$$

the current

$$j_T = \frac{1}{2\pi} * F \tag{1.8}$$

is conserved. In particular, since it is conserved off-shell, the associated symmetry is topological. Its charge corresponds to the total flux of the gauge field across a two dimensional spacelike surface Σ_2

$$Q = \int_{\Sigma_2} *j_T = \frac{1}{2\pi}\int_{\Sigma_2} F. \tag{1.9}$$

This is nothing but the magnetic flux through the Σ_2 surface. States charged under this symmetry are then denoted as monopoles and their charge is an integer due to the Dirac quantization condition. In particular, gauge connections are labeled by the first homotopy group $\pi_1(U(1)) = \mathbb{Z}$ or equivalently by the first Chern number $\frac{1}{2\pi}\int_{S^2} F \in \mathbb{Z}$. To each $U(1)$ group, we associate a corresponding topological symmetry.
We can construct monopole operators as local defects associated with the monopole flux. These are defined abstractly as operators implementing a boundary condition for the gauge field in the path integral, when they are inserted in a correlation function of gauge-invariant operators $\mathcal{O}_i(x_i),\ i = 1, ..., n$. Labeling a monopole operator of charge m at a point x as $\mathcal{M}_m(x)$, the resulting path integral representation will have enforced the boundary condition for the gauge field

$$\int_{S^2_x} F = 2\pi m \tag{1.10}$$

where S^2_x represents a two-sphere centered at the point of monopole insertion x. So, the correlation function reads

$$\langle \mathcal{M}_m(x)\mathcal{O}_i(x_i)...\mathcal{O}_n(x_n)\rangle = \int_{\int_{S^2_x} F = 2\pi m} DA\ \ \mathcal{O}_i(x_i)...\mathcal{O}_n(x_n)e^{iS}. \tag{1.11}$$

We will encounter similar operators, namely instanton operators, in five dimensions.
Finally, notice that Maxwell's theory, in absence of external currents, possesses a $U(1)$ one-form symmetry [8] which is conserved by virtue of the equations of motion

$$d * F = 0. \tag{1.12}$$

The corresponding current $j_e = \frac{1}{e^2}F$ is a two-form, whose charge

$$Q = \frac{1}{e^2}\int_{\Sigma_1} *F \tag{1.13}$$

equals the electric flux passing through a spacelike cycle Σ_1. So, the symmetry generator reads

$$U_\alpha(\Sigma_1) = e^{\frac{i\alpha}{e^2}\int_{\Sigma_1} *F} \equiv W_\alpha[\Sigma_1]. \tag{1.14}$$

These are nothing but the Wilson lines associated with the cycle Σ_1. From the Lagrangian point of view, the symmetry acts as a shift of the gauge potential $A \to A + \beta$ under a closed (but not exact) one-form β. This symmetry acts on the Wilson lines $W_m[\Sigma_1]$ itself. These are gauge-invariant under a gauge transformation $A \to A + d\lambda$, due to the quantization condition $\oint d\lambda = 2\pi\mathbb{Z}$, but they transform by a phase $e^{im\alpha}$ under the generator $U_\alpha(\Sigma_1)$.

Hodge duality in three dimensions relates two-forms to one-forms. This is analogous to the four dimensional case, where electromagnetic duality relates a two-form (the electric gauge field strength) with another two-form (the field strength of the magnetic gauge field) or to the five dimensional case (where a two-form is dual to a three-form). This suggests that a gauge field can be dualized to a scalar. Let us start from (1.1) and turn off J^μ. Calculating the partition

function of the theory, we can first implement the Bianchi identity constraint $\epsilon^{\mu\nu\rho}\partial_\mu F_{\nu\rho} = 0$ using a Lagrangian multiplier ω and then change the integration measure from A_μ to $F_{\mu\nu}$

$$Z = \int \mathcal{D}A e^{-i\int d^3x \frac{1}{4e^2}F_{\mu\nu}F^{\mu\nu}} = \int \mathcal{D}F\,\mathcal{D}\omega\, e^{-i\int d^3x\left[\frac{1}{4e^2}F_{\mu\nu}F^{\mu\nu} - \frac{1}{4\pi}\omega\epsilon^{\mu\nu\rho}\partial_\mu F_{\nu\rho}\right]}. \tag{1.15}$$

We can then use the equations of motion for the field

$$F = \frac{e^2}{4\pi^2} * d\omega \tag{1.16}$$

and integrate out F, expressing the partition function in terms of a Lagrangian for the dual scalar ω

$$Z = \int \mathcal{D}\omega\, e^{i\frac{e^2}{8\pi}\int d^3x \partial_\mu\omega\partial^\mu\omega}. \tag{1.17}$$

In this frame, the topological current, thanks to eq. (1.16), can be rewritten as

$$j_T = \frac{e^2}{2\pi}\, d\omega \equiv j_s. \tag{1.18}$$

So, we see that the current j_T of the original Maxwell theory is mapped to a current j_s associated with a shift symmetry $\omega \to \omega + c$ for the scalar field ω. In fact, since F respects the Dirac quantization condition, ω is periodic $\omega \simeq \omega + 2\pi$.
In this frame, we can easily construct a monopole operator in terms of the dual scalar

$$\mathcal{M}_m(x) = e^{im\omega(x)} \tag{1.19}$$

transforming with a phase e^{imc} under the topological symmetry. We see that a disordered operator, which in the gauge theory cannot be constructed in terms of fundamental fields, now can be easily constructed in terms of the dual scalar. The charge of the previous monopole is quantized $m \in \mathbb{Z}$, since $\omega(x)$ is 2π periodic. Finally, from (1.16) we see that ω is actually odd under $\mathcal{P}$, so the monopole operator transforms as $\mathcal{M}_m \leftrightarrow \mathcal{M}_m^\dagger = \mathcal{M}_{-m}$.
The theory in (1.17) has an S^1 moduli space of vacua parametrized by the VEV of ω. At each point of this manifold, the shift symmetry is spontaneously broken and ω represents the associated Goldstone boson. Using the correspondence $j_s \leftrightarrow j_T$, this tells us that $U(1)_T$ is spontaneously broken and the Goldstone boson associated with its breaking can be interpreted as the scalar ω itself. This can be understood in the Maxwell theory by noticing that also the one-form symmetry is spontaneously broken. Then, at low energy, we have a protected Goldstone boson associated with this breaking, which is a spin 1 particle. This is nothing but the photon itself.

1.2 Abelian Chern-Simons theory

In three dimensions, on top of the usual Maxwell term in eq. (1.1), we can also construct another gauge-invariant term, the Chern-Simons (CS) Lagrangian. This is a general feature of odd dimensional gauge theories. The Lagrangian is identified with the CS term

$$\mathcal{L}_{\text{CS}} = \frac{k}{4\pi} A dA. \tag{1.20}$$

This is labeled by a dimensionless coupling k, called the CS level. The corresponding theory is denoted in literature as $U(1)_k$ pure CS theory. The Lagrangian in (1.20) changes under a gauge transformation $A \to A + d\lambda$ as [9]

$$\delta\mathcal{L}_{\rm CS} = \frac{k}{4\pi}\partial_\mu(\lambda\epsilon^{\mu\nu\rho}\partial_\nu A_\rho) \tag{1.21}$$

so it is gauge-invariant in absence of boundaries.
However, the formula is in general difficult to interpret, since A can be not globally well-defined.[1] Let us place, in particular, our theory (1.20) on a generic three dimensional manifold M_3. To define properly the CS term, we need to extend the gauge potential to a four dimensional manifold M_4 with boundary $\partial M_4 = M_3$. Now the CS is manifestly gauge-invariant and depends only on the field strength F

$$S_{\rm CS} = \frac{k}{4\pi}\int_{M_4} F\wedge F. \tag{1.22}$$

However, this extension depends on the manifold M_4 and so it is ambiguous. To eliminate this dependence, we require that, when we take two different four manifolds M_4, M_4', the action should differ only by an integer number multiplying 2π, so that the path integral is independent of the choice of the extended manifold. This implies that

$$\frac{k}{4\pi}\int_{C_4} F^2 = 2\pi m,\ \ m\in\mathbb{Z} \tag{1.23}$$

where C_4 is a closed four manifold obtained as the union of $M_4 \cup M_4'$ along their common boundary. This leads to a quantization condition for the CS level

$$k \in \mathbb{Z}. \tag{1.24}$$

Actually, the previous condition holds only for manifolds C_4 equipped with a spin structure (see [10, 11] for a nice discussion on this point). On a generic four manifold C_4 equipped with a background metric g and a spin$_c$ structure, the term (1.23) is not quantized as an integer multiplied by 2π, unless $k \in 2\mathbb{Z}$. However, when A is actually[2] a spin$_c$ connection [11] the term $\frac{1}{4\pi}\int F\wedge F$ together with a gravitational CS term

$$2{\rm CS}(g) = \frac{1}{96\pi}\int_{C_4}{\rm Tr}(R\wedge R) \tag{1.25}$$

with R the Ricci tensor, is quantized as an integer multiplied by 2π

$$\frac{1}{4\pi}\int_{C_4} F\wedge F + 2{\rm CS}(g) = 2\pi\mathbb{Z}. \tag{1.26}$$

[1] This happens, for example, in presence of monopoles. A corresponding potential can be defined only on local patches and at the intersection of two of them, the gauge potential is glued by a gauge transformation. The gauge field is a connection over the bundle.

[2] Note that, in the following, we will avoid specifying if we are dealing with a gauge field or a spin$_c$ connection.

When we deal with multiple gauge fields A^i, we can have mixed CS terms

$$\mathrm{CS}(A^i) = \int_{M_4} \frac{k_{ij}}{4\pi} A^i dA^j. \tag{1.27}$$

Their levels obey an analogous quantization condition, $k_{ij} \in \mathbb{Z}$.

The CS term is topological since it does not depend on the metric of the manifold on which the theory is defined. This represents then an example of a topological quantum field theory (TQFT) since, as we will see, its dynamics depends only on the topology of the manifold itself. Being the energy-momentum tensor the variation of the action with respect to the metric, we see that the CS energy-momentum tensor vanishes. This signals the absence of local propagating degrees of freedom, as we will see in the following.

Let us now discuss the symmetries preserved by the CS Lagrangian.
From the properties of A under discrete symmetries, we see that the CS term breaks time-reversal (and parity) symmetry. However, it preserves charge conjugation (being quadratic in the gauge field) and, due to the CPT theory, also $\mathcal{PT}$.
The electric one-form symmetry $U(1)_e$ of the original Maxwell theory here reduces to $\mathbb{Z}_k$ [8], since the Lagrangian (1.20) is no more invariant under generic shift of the gauge potential, but only on shifts $A \to A + \frac{\beta}{k}$ with $\oint \beta \in 2\pi m$.
Moreover, the CS term (1.20) couples the topological current to the gauge field

$$S_{\mathrm{CS}} = \frac{k}{4\pi} \int AdA \sim \int A \wedge *j_T. \tag{1.28}$$

So, states charged under the topological symmetry acquire an electric charge proportional to the CS term. This can be seen explicitly by looking at the path integral definition of the disordered monopole operators in (1.11). The correlation function changes under a gauge transformation as

$$\delta\langle \mathcal{M}_m(x)\mathcal{O}_1(x_1)...\mathcal{O}_k(x_k)\rangle = \frac{k}{4\pi}\left(\lambda(x)\oint_{S^2_x} F\right)\langle \mathcal{M}_m(x)\mathcal{O}_1(x_1)...\mathcal{O}_k(x_k)\rangle \tag{1.29}$$

so $\mathcal{M}_m$ has an electric charge $n_e = km$.

Let us now discuss the dynamics of the theory. In absence of sources, the equation of motion reduces to

$$F = 0 \tag{1.30}$$

so solutions are only flat connections and there are no local gauge-invariant propagating degrees of freedom. From (1.30), we see that the topological symmetry vanishes on-shell, accordingly to the fact that monopoles acquire an electric charge under the gauge group. The previous conclusion can be drawn by looking at the CS propagator in the R_ξ gauge [12]

$$S(p)_{\mu\nu} = \frac{4\pi i}{k}\frac{\epsilon_{\mu\nu\rho}p^\rho}{p^2} + i\xi\frac{p_\mu p_\nu}{p^4}. \tag{1.31}$$

This has a spurious pole at $p^2 = 0$, leading to no propagating degree of freedom.
The theory, however, in presence of a non-trivial topology for M_3, is non-trivial. Indeed, in this case, we can have non-local gauge invariant operators, the Wilson lines

$$W_m(\mathcal{C}) = e^{im \oint_{\mathcal{C}} A}. \tag{1.32}$$

Through the algebra of these operators, we can characterize the Hilbert space of the gauge theory [13, 14]. In particular, taking a two dimensional genus g surface Σ_2^g as the space of our theory, the ground state degeneracy of the Hilbert space is k^g.
Considering the one-form symmetry $\mathbb{Z}_k$, it can be shown that the Wilson loops follow perimeter law, so $\mathbb{Z}_k$ is spontaneously broken. This is the hallmark of deconfinement.

In conclusion, we saw that the pure CS theory has no local propagating degrees of freedom and no dependence on the metric. This is non-trivial in presence of a non-trivial topology. The theory is then a TQFT and its vacuum is said to be non-trivially gapped, as opposed to trivially gapped phases, where the theory in the IR is empty.

1.2.1 Anyons

To the pure CS theory in (1.20), we can add an external current J^μ coupled to the gauge field. The equations of motion are modified as

$$\frac{k}{2\pi} F = *J \tag{1.33}$$

where the current J is conserved by virtue of the Bianchi identities.
From (1.33), we deduce the analogous of Gauss law and current conservation for CS theories

$$\rho = \frac{k}{2\pi} B \tag{1.34}$$

$$J^i = \frac{k}{2\pi} \epsilon^{ij} E_j \tag{1.35}$$

where $J^\mu = (\rho, J^i)$ and B and E^i are the magnetic and the electric fields respectively.
The relation (1.34) fixes the magnetic and electric fields algebraically in terms of the external sources. Moreover, the Gauss law (1.34) attaches a magnetic flux to the electric charge. This relation remains preserved by the time evolution thanks to eq. (1.34), where the CS level plays the role of a conductivity $\sigma^{ij} = \frac{k}{2\pi}\epsilon^{ij}$, which is quantized due to the quantization of k. This property enables to describe the integer quantum Hall effect through a CS theory, where the Hall conductivity of ν filled Landau levels with $\nu = k/e^2$ coincides with the CS conductivity σ^{ij} [14]. So, we see that the Chern-Simons terms introduce a magnetic flux for an electric charge. This phenomenon is known in the literature as flux attachment.

We can now add two external electric charges m, n to the CS theory. To both particles, the CS term attaches a magnetic flux. So, when the first particle is moved adiabatically around the

latter, we expect it to pick up a phase, due to the Aharonov-Bohm (AB) effect. This phase shift depends on the magnetic flux attached to the second charge and reads:

$$e^{im \oint_C A} = e^{im \int_{D_2} F} = e^{\frac{2\pi i m n}{k}} \tag{1.36}$$

where D_2 is the area enclosed by the curve $\mathcal{C}$ and we used (1.33) in the last equality. This operation can be interpreted as a double exchange of the two particles. In particular, if these are identical, the phase that the particle picks up gives us their (naive) statistics. Since, under a single exchange, the phase shifts as

$$\Delta\theta = \frac{\pi n^2}{k}, \tag{1.37}$$

the naive spin s of the particle reads

$$s = \frac{n^2}{2k} \text{ mod } 1. \tag{1.38}$$

So, for generic levels, particles obey a new kind of statistics, with fractional spin. These particles are denoted as anyons. The possibility of having anyons in three dimensions comes from the structure of the three dimensional massive little group, which is $SO(2) \simeq U(1)$. Its universal covering is $\mathbb{R}$, so any real value for the spin is allowed for a representation.[3] Particles with zero charges mod k do not acquire any phase by winding around each other, since the AB phase is a multiple of 2π. However, they can possess non-trivial spin $\frac{k}{2}$ mod 1 when k is odd. To the worldline $\mathcal{C}$ of a static source with charge n, we can associate a Wilson line

$$W_n[\mathcal{C}] = e^{in \oint_{\mathcal{C}} A}. \tag{1.39}$$

The relation (1.38) gives us information about the Wilson lines of these theories. These are identified by their spin and their Aharonov-Bohm phases. We then see that only $|k|$ of these lines with $n = 0, ..., k-1$ are independent when k is even, while these are $2|k|$ when k is odd, since whenever $n = 0$ mod k, the AB phase vanishes. In the latter case, we can in particular have lines transparent under the AB effect, but with half-integer spins [11, 15]. These are denoted in the literature as transparent lines. This introduces the need for a spin structure and renders the CS theory non-trivial. An example comes from the $U(1)_1$ CS theory [16], which has two lines: the trivial one $n = 0$ of spin 0 and the non trivial one $n = 1$ of spin 1/2. The theory is almost trivial thanks to this transparent line. Its Hilbert space on a spatial manifold Σ_g of genus g has always a single state and the partition function $Z[g]$ of the theory can be easily determined by the action of the topologically nontrivial diffeomorphisms of Σ_g on this single state. $Z[g]$ depends then only on a gravitational CS term

$$Z[g] = e^{-2i\text{CS}(g)}. \tag{1.40}$$

Having a single gapped state for any closed manifold, this is an invertible TQFT. These theories are particularly relevant for the construction and classification of gapped phases of matter. However, their study is beyond the scope of this thesis. We refer to [17–24] for an extended discussion.

[3] Notice, though, that, a formulation of a Lagrangian for these particles is still missing.

1.2.2 Topologically massive gauge theory

Let us now consider the most general gauge invariant Lagrangian for the $U(1)$ field, including both the Maxwell and the CS terms

$$\mathcal{L} = -\frac{1}{2e^2} F \wedge *F + \frac{k}{4\pi} AdA. \tag{1.41}$$

The latter, although topological, contributes to the equations of motion as

$$d * F + \frac{m_{\mathrm{CS}}}{2} F = 0 \tag{1.42}$$

where $m_{\mathrm{CS}} = \frac{ke^2}{2\pi}$. On the right hand side, we recognize the topological current j_T, so we see that this sources electrically the gauge field. Monopoles are then charged under the electric field, as can be explicitly seen from the Gauss law

$$\partial_i E^i = \frac{ke^2}{2\pi} B. \tag{1.43}$$

So, if flux attachment associates a magnetic flux to an electric charge, the Gauss law in eq. (1.43) associates an electric flux with a magnetic charge!
The equations (1.42) can be rewritten in terms of a Hodge dual field $\tilde{F}$, defined as

$$\tilde{F} \equiv *F. \tag{1.44}$$

This is gauge-invariant and conserved in absence of magnetic charges. So, to this, it corresponds a single independent degree of freedom. The equation of motion reduces to a Klein-Gordon equation for a scalar of mass $m_{\mathrm{CS}} = \frac{ke^2}{2\pi}$:

$$\left[\Box + \left(\frac{ke^2}{2\pi}\right)^2\right] \tilde{F}_\mu = 0 \tag{1.45}$$

The statistics of the field can be inferred from the analysis of the representations of the Poincaré group. The spin turns out to be $s = \frac{k}{|k|} = \mathrm{sgn}(k)$. We see, then, that the CS term gives a mass $m_{\mathrm{CS}} = \frac{ke^2}{2\pi}$ to the gauge field without Higgsing the gauge symmetry. The Maxwell CS theory is described by the propagation of this single transverse degree of freedom $\tilde{F}$.
The same conclusion can be drawn by looking at the propagator of the gauge field (in the R_ξ gauge)

$$S_{\mu\nu}(p) = e^2 \left(\frac{p^2 \eta_{\mu\nu} - p_\mu p_\nu - i m_{\mathrm{CS}} \epsilon_{\mu\nu\rho} p^\rho}{p^2 (p^2 - m_{\mathrm{CS}}^2)} + \xi \frac{p_\mu p_\nu}{(p^2)^2} \right). \tag{1.46}$$

In particular, it can be shown that only the pole $p^2 = \left(\frac{ke^2}{2\pi}\right)^2$ is physical, so the photon is massive.
From the expression of the mass m_{CS}, we see that in the infinite coupling limit, the photon becomes extremely massive and stops propagating. This is naively expected from the Lagrangian

(1.41) since the Maxwell term is suppressed in this regime with respect to the CS one. Similarly, when we flow to low-energies, the Maxwell term, being irrelevant, is negligible with respect to the CS one, so the photon stops propagating and can be integrated out at energies smaller than the topological mass $m_{\rm CS}$. We obtain a vacuum, which is gapped but described by a leftover TQFT given by the CS theory. The low-energy physics of $U(1)_k$ CS theory is then non-trivially gapped.

1.3 Fermions in three dimensions

In this section, we introduce fermions in three dimensions, their properties under discrete symmetries and their anomalies. Many of the following concepts can be applied also to five dimensional theories, as we will see in Chapter 5.
Let us start by analyzing the spinor representation of the Lorentz group in 2+1 dimensions. The representation of the Clifford algebra

$$\{\gamma^\mu, \gamma^\nu\} = 2\eta^{\mu\nu} \tag{1.47}$$

is two dimensional. The Dirac spinor ψ is then two dimensional and complex. In the Dirac basis, the gamma matrices read

$$\gamma^0 = \sigma^3 = \begin{pmatrix} 1 & 0 \\ 0 & -1 \end{pmatrix}, \;\; \gamma^1 = i\sigma^1 = \begin{pmatrix} 0 & i \\ i & 0 \end{pmatrix}, \;\; \gamma^2 = i\sigma^2 = \begin{pmatrix} 0 & 1 \\ -1 & 0 \end{pmatrix} \tag{1.48}$$

and obey the following relations

$$\gamma^\mu\gamma^\nu = \eta^{\mu\nu} - i\epsilon^{\mu\nu\rho}\gamma_\rho$$
$$\mathrm{Tr}(\gamma^\mu\gamma^\nu\gamma^\rho) = -2i\epsilon^{\mu\nu\rho}.$$

As it happens in general odd dimensions, we have no chirality matrix, so we cannot impose a Weyl condition on ψ. However, we can impose a Majorana condition, so the smallest representation is real and given by a two-component Majorana fermion χ.
Note that, in three dimensions all the irreducible representations of the Poincaré algebra are labeled by the eigenvalues of two Casimirs, the square momentum P^2 and the Pauli-Lubanski pseudoscalar $W = P^\mu J_\mu$, where $J^\mu = \frac{1}{2}\epsilon^{\mu\nu\rho}L_{\nu\rho}$ is a pseudovector composed by the Lorentz generators $L_{\mu\nu}$. A single particle representation Φ is then classified by its mass m and spin s

$$P^2\Phi = m^2\Phi, \;\; W\Phi = -sm\Phi. \tag{1.49}$$

For a Dirac fermion, the operator J^μ can be written as

$$J^\mu = -i\epsilon^{\mu\nu\rho}p_\nu\frac{\partial}{\partial p^\rho}\mathbb{I} - \frac{1}{2}\gamma^\mu \tag{1.50}$$

so the second condition in (1.49) is nothing but the Dirac equation of a massive fermion

$$(i\gamma^\mu\partial_\mu - m)\psi = 0. \tag{1.51}$$

The spin[4] then is $\frac{1}{2}\text{sgn}(m)$. So, masses in three dimensions are real and their sign determines the spin of the fermion. This is related to the absence of chirality, so it is a common feature in odd dimensions.

We now discuss how fermions transform under discrete symmetries. Parity $\mathcal{P}$ acts as

$$\psi \to \gamma^1 \psi. \tag{1.52}$$

The action of charge conjugation $\mathcal{C}$ reads

$$\psi \to C\bar{\psi}^T \tag{1.53}$$

where C is the 2×2 charge conjugation matrix, defined by the relations $C^{-1}\gamma^\mu C = -(\gamma^\mu)^T$. In the Dirac basis, this is $C = \gamma^2$.
Finally, time-reversal $\mathcal{T}$ acts on fermions as

$$\psi \to \gamma^2 \psi. \tag{1.54}$$

From these transformations, we see that the fermionic kinetic term is invariant under all the discrete symmetries. On the other hand, a Dirac mass term is odd under time-reversal and parity transformations

$$\bar{\psi}\psi \to -\bar{\psi}\psi \tag{1.55}$$

while it is even under charge conjugation. So, adding a mass term for a Dirac fermion breaks parity and time-reversal symmetry.
Note that fermion masses and Chern-Simons terms share the same properties under discrete symmetries. So, when one of the two is present, no symmetry prevents the generation of the other. Indeed, when mass terms for fermions are present, CS terms are generated at the quantum level.[5] This will be the main topic of the next section.

1.3.1 Induced CS terms and parity anomaly

In this section, we see how massive fermions can generate a shift in the CS level and how this is related to an anomaly between parity and gauge symmetry.
Let us consider a Dirac fermion with mass m coupled to a gauge field A with charge q. In particular, we set $k = 0$. At low enough energies, we can integrate the fermion out and we remain with an Abelian gauge theory. However, the decoupling actually leaves a trace in the low-energy theory. In the integration, the one-loop diagram in figure 1.1 generates the following parity violating term

$$\Pi_{odd}(p^2, m) = 2mq^2 \int \frac{d^3l}{(2\pi)^3} \frac{1}{[(l-p)^2 + m^2][l^2 + m^2]} = \frac{1}{2\pi} \frac{m}{|p|} \arcsin\left(\frac{|p|}{\sqrt{p^2 + 4m^2}}\right). \tag{1.56}$$

[4]Similarly, we can obtain also anyonic representations with arbitrary spins s constructing an appropriated J^μ operator [9].

[5]Also the opposite happens: in presence of CS terms, masses of fermions are additively renormalized at the quantum level, see [25].

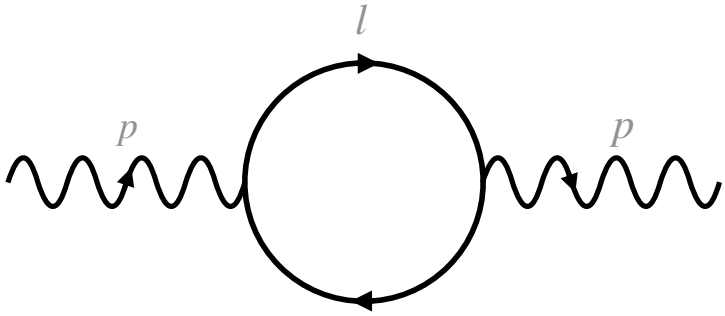

Figure 1.1: Self-energy of the gauge field A_μ.

At small momenta $|p| \to 0$ and in the infinite mass $m \to \infty$ limit, (1.56) reduces to [26, 27]

$$\Gamma^{\mu\nu}(k,m) \sim \frac{1}{4\pi}\frac{mq^2}{|m|}\epsilon^{\mu\nu\rho}p_\rho + \mathcal{O}\left(\frac{p^2}{m^2}\right) \tag{1.57}$$

leading to a Chern-Simons term for the gauge field

$$\Delta k = \frac{q^2}{2}\text{sgn}(m). \tag{1.58}$$

So, integrating out the fermion, we generated a CS term at one-loop!
This shift is one-loop exact [28], as it happens for anomalies in four dimensions. We will come back to this point later.

The shift (1.58) is not properly quantized when q is odd, being the level half-integer. To elucidate why this is the case, we need to consider what happens in presence of massless fermions. When fermions are massless, these cannot be integrated out at low-energies. However, the diagram in figure 1.1 can be calculated. Apparently, the diagram cannot give rise to a parity violating contribution, since this is preserved by the classical Lagrangian when $m = 0$. The photon self-energy is UV divergent, so we must introduce a regulator in the calculation. An example of this regulator is the Pauli-Villard (PV) one. This regulator is gauge-invariant and introduces to each field in the theory a field of mass M with the same spin but opposite statistics. Introducing this regulator for the fermions, we see that parity is explicitly broken and the regularized action $S^{PV}_{\text{reg}}[A, m = 0]$, obtained by decoupling the regulating fields sending $M \to \pm\infty$, reads

$$S^{PV}_{\text{reg}}[A, m = 0] = S[A, m = 0] - \lim_{M\to\pm\infty} S[A, M]. \tag{1.59}$$

The mass generates, though the loop in figure 1.1, a CS level proportional to $\text{sgn}(M)$. So, removing the regulator, we end up with a CS term at level

$$k = \frac{q^2}{4\pi}\text{sgn}(M). \tag{1.60}$$

So, although preserving gauge-invariance, the regulator breaks parity explicitly. In presence of a bare mass m for the fermion, we generate a total CS level in the IR

$$k_{IR} = q^2 \frac{\mathrm{sgn}(m) + \mathrm{sgn}(M)}{2} \tag{1.61}$$

which is now properly quantized!

We can ask if the previous breaking of parity is avoidable by choosing a different regulator. It can be shown that this is not the case: any gauge-invariant regulator breaks parity at the quantum level. This defines a mixed anomaly between parity and gauge symmetry: preserving one of the two, we break the other and vice versa. This is denoted as parity anomaly.
The anomaly can be obtained by looking at the partition function of the massless fermion coupled to the gauge field. We will take for definiteness $q = 1$. The partition function, as a function of the gauge field A, reads

$$Z[A] = \det \mathcal{D}_A = \det i\not{D}_A \tag{1.62}$$

with $\mathcal{D}$ is the fermion hermitian Dirac operator obtained when we integrate over the fermions in the path integral.
Hermiticity implies that all the eigenvalues λ_i of the Dirac operator are real, and so should also be its determinant. This is a manifestation of $\mathcal{T}$-invariance, since when a theory respects time-reversal symmetry, its partition function is real. The number n_- of negative eigenvalues of the operator is infinite, as well as the number of positive ones n_+, so the sign of the determinant $\det \mathcal{D}$ is not well-defined and needs to be regularized. In particular, we cannot simply choose a sign, say $+$, for a gauge field configuration $\bar{A}$ and then assign to a generic configuration A the sign obtained by looking at the number of eigenvalues that changes sign when we go from $\bar{A}$ to A. Proceeding in this way we would encounter a violation of gauge-invariance due to the phenomenon of spectral flow: the partition function calculated on a configuration A related to $\bar{A}$ by a large gauge transformation would have a different sign of $Z[\bar{A}]$, see [29]. What one can do is to regularize the difference $\frac{1}{2}(n_+ - n_-)$ by employing the representation

$$\eta = \lim_{\epsilon \to 0^+} \sum_i e^{-\epsilon|\lambda_i|} \mathrm{sign}(\lambda_i). \tag{1.63}$$

We will call the expression in (1.63) the η-invariant. The regularized partition function reads then

$$Z = |\det \mathcal{D}| e^{\mp i\pi \frac{\eta}{2}}. \tag{1.64}$$

The APS index theorem [30] allows us to write the η invariant as a CS term for the field A plus a gravitational one

$$e^{i\pi\eta} = e^{i\mathrm{CS}(A,g)} = e^{i\left(\frac{1}{4\pi}\int_W AdA + 2\mathrm{CS}(g)\right)} \tag{1.65}$$

and the result (1.64) is actually independent of the regulator. So, under a parity transformation, the partition function changes by a phase proportional to a CS term of level $k = 1$. So, as expected from the previous PV regularization, parity symmetry is broken and a CS term is generated.

Adding a mass term for the fermion to the Lagrangian breaks explicitly time-reversal invariance. At low-energies, we can integrate out the fermion, at the price of generating a new CS term

$$e^{i\text{sgn}(m)\frac{\pi}{2}\eta(A)}. \tag{1.66}$$

The IR level reduces to the expression in (1.61). On top, we have also a gravitational CS term of level

$$k_g = \frac{1}{2}(\text{sgn}(m) \pm 1). \tag{1.67}$$

Note that the value of the IR level depends on the choice of the sign in (1.64), or equivalently of the PV regulator mass. The two signs lead to two different partition functions (Z_+, Z_-), which are inequivalent, having different CS levels in the IR. In the following, we will adopt the convention of [16, 31], choosing the minus sign in (1.64). The CS level in the IR generated by a massive fermion ψ in this regularization reads

$$\mathcal{L} = \begin{cases} 0, & m > 0 \\ -\frac{1}{4\pi}AdA - 2\text{CS}(g), & m < 0. \end{cases} \tag{1.68}$$

In absence of a mass, the partition function depends then on

$$k = k_\text{b} - \frac{1}{2} \tag{1.69}$$

where k_b represents the bare level, which is the CS level the theory possesses in the IR when we add a positive mass for the fermion and we integrate it out. Since k_b is an integer, k is an half-integer and parity is broken, since we cannot choose k_b in such a way that $k = 0$ and the partition function is real. Indeed, time-reversal sends $m \to -m$ and $k_\text{b} \to -k_\text{b}$, so $k \to -k$ and parity is conserved only for $k = 0$.
With F fermions, the previous argument trivially generalizes and the level k obeys the quantization condition

$$k + \frac{F}{2} \in \mathbb{Z}. \tag{1.70}$$

This tells us that in presence of an odd number of fermions the full theory cannot respect parity[6], since k needs to be half-integer. In presence of an even number of fermions, instead, (1.70) allows having $k = 0$. Theories of this kind are distinguished, being parity and time-reversal invariant at $m = 0$. In the following, in presence of fermions, we adopt the convention of indicating the CS level of the theory as the level (1.69). So, a $U(1)$ theory with a single fermion of charge 1 and no bare CS level will be indicated as $U(1)_{-1/2} + \psi$ CS theory.

1.4 Abelian dualities

In previous sections, we saw how three dimensional gauge theories exhibit complicated IR dynamics. In presence of a CS term, the theory is non-trivially gapped. In absence of a CS term,

[6]However, parity can arise at low energies as an accidental symmetry, as we will see later.

on the other hand, pure gauge theories become strongly coupled in the infrared, due to the classical running of the coupling and are trivially gapped [32, 33].
The dynamics is even more complex in presence of matter, and the vacuum structure is sometimes difficult to determine, due to the strong coupling nature of these theories. In particular, flowing in the IR we can also reach a conformal field theory (CFT). These are theories that show conformal invariance and describe second order phase transitions. We can have then two or more theories that, along the RG-flow, end up at the same fixed point in the IR. If this happens, we say that these theories are infrared dual to each other.
Being the CFT the same, we can establish a correspondence between these two theories. In particular, the global symmetries of both theories should match in the IR, as well as the relevant deformations of their fixed point. This correspondence is commonly denoted as a duality map between the two theories.
Dualities become particularly useful whenever one of the two theories is weakly coupled at the fixed point. In this way, we can gain information about a strongly coupled theory thanks to the dual weakly coupled theory. This happens, for instance, in the well-known examples of Seiberg dualities [34] in four dimensions.
In this section, we review dualities involving Abelian gauge theories. Firstly, we discuss particle-vortex duality, one of the first dualities discovered in three dimensions. Then, we consider Abelian bosonization, relating a purely bosonic theory to a purely fermionic one, which generalizes bosonization in two dimensions. Finally, we will see how to construct new correspondences from known ones and how many of the known dualities are actually not independent, being connected by a series of operations.

1.4.1 Particle-vortex duality

Let us consider a theory of a complex scalar ϕ, preserving a $U(1)_F$ flavor symmetry $\phi \to e^{i\alpha}\phi$. Neglecting irrelevant operators (and the sextic marginal coupling), the most general Lagrangian, compatible with the global symmetry reads

$$\mathcal{L}_{\text{XY}} = |\partial_\mu \phi|^2 - m^2|\phi|^2 - \beta|\phi|^4 + ... \tag{1.71}$$

where m^2, β are the relevant couplings of dimension one. The potential is bounded from below whenever $\beta > 0$. The current corresponding to the flavor symmetry j_F reads

$$j_F = -i(\bar{\phi}\, d\phi - \phi\, d\bar{\phi}). \tag{1.72}$$

The model is also invariant under a $\mathbb{Z}_2$ symmetry acting on the scalar as $\phi \to -\phi$. Together with the global symmetry $U(1)_F \simeq SO(2)_F$, the model preserves an $O(2)$ symmetry. The theory is known in the literature as the $O(2)$ or XY model.
Strong indications suggest that this theory flows in the IR to a strongly interacting fixed point, called the Wilson-Fisher fixed point [35]. To reach this CFT, the relevant couplings m^2, β need to be tuned to some specific values. We conventionally fix the value of m^2 at the fixed point to be equal to zero. We indicate the theory of the scalar at the fixed point (or critical boson theory) by the Lagrangian

$$\mathcal{L}_{\text{WF}} = |\partial_\mu \phi|^2 - \beta|\phi^4|. \tag{1.73}$$

This fixed point possesses a relevant deformation, which can be parametrized by the mass squared m^2 itself. Turning on m^2, we flow away from the fixed point and we end up in another IR phase. When m^2 is large, these phases can be inferred by analyzing the UV theory at the semi-classical level. These are distinguished by the sign of m^2:

- $m^2 \gg 0$:
  The $U(1)$ global symmetry is preserved since the quartic potential in (1.71) has a single vacuum at $\phi = 0$. The scalar field is massive with mass m^2 and can be integrated out. At low-energies, the theory is trivially gapped. The excitations of the theory around the vacuum are given by the scalar ϕ itself, which is charged under the global symmetry with charge one.

- $m^2 \ll 0$:
  The potential has a moduli space of vacua S^1, parametrized by the VEV of the scalar field $\langle|\phi|^2\rangle = v = -\frac{m^2}{2\beta}$. This breaks spontaneously the flavor symmetry $U(1)_F$. The theory is then gapless in this phase and its IR dynamics is described by a single Goldstone boson $\sigma(x)$, associated with the phase of the scalar field $\phi(x) = \rho(x)e^{i\sigma(x)}$. The field ρ becomes massive with mass $\sim \langle\phi\rangle$ and decouples at low-energies. We have additional excitations in this phase, which are charged under the flavor group. These are topologically non-trivial configurations of the scalar field ϕ, the so-called vortex configurations $\mathcal{V}_n$. This can be studied in the low-energy effective field theory (EFT) given by the Goldstone boson Lagrangian

  $$\mathcal{L} \sim \frac{v^2}{2} d\sigma \wedge *d\sigma \tag{1.74}$$

  in the vacuum $\langle\phi\rangle = v$. In spatial polar coordinates (r, θ), these vortices read $\phi(x) = \rho(r)e^{i\sigma(\theta)}$, where in the vacuum we are studying $\rho(r) \to v$ at spatial infinity. Since $\pi_1(U(1)) = \mathbb{Z}$, there exist topological distinct configurations, labeled by a winding number n. This counts the number of times σ winds around spatial infinity S^1_∞, so

  $$\oint_{S^1_\infty} dx^i \partial_i \sigma = \int d\theta \partial_\theta \sigma = 2\pi n. \tag{1.75}$$

  A single vortex is infinitely massive, as one can verify by inserting the ansatz $\rho(r)e^{in\theta}$ inside the static energy [36]

  $$M = E \sim \int r\, dr\, d\theta\, \frac{1}{r^2}(\partial_\theta \sigma)^2 \sim v^2 n^2 \log \frac{v^2}{\Lambda} \tag{1.76}$$

  where Λ is an IR cutoff for the radius $r \leq \Lambda^{-1}$. Since $\rho(r) \to 0$ close to $r = 0$ to ensure regularity for the solution, there are no UV divergences.
  A vortex-anti vortex configuration, on the other hand, has a finite energy proportional to the logarithm of their distance R

  $$E(R) \sim v^2 n^2 \log R \tag{1.77}$$

since the total winding of the configuration is zero. These are nothing but the vortices that we observe experimentally in the superfluid phase of liquid helium. We see that the energy between the two vortices grows with R and a Coulomb force $\sim \frac{1}{R}$ attracts the two objects.

The phase diagram of the XY model is shown in figure 1.2.

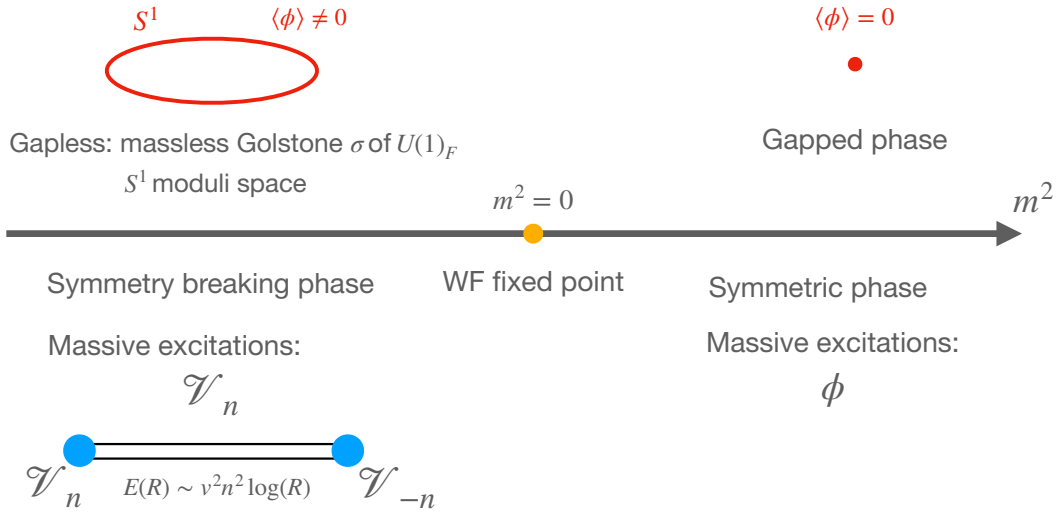

Figure 1.2: Phase diagram of the XY model.

We can now think of gauging the $U(1)_F$ symmetry of the theory. The resulting theory

$$S_{AH} = \int d^3x \left[-\frac{1}{4e^2} F_{\mu\nu} F^{\mu\nu} + |D_\mu \tilde{\phi}|^2 - \tilde{m}^2 |\tilde{\phi}|^2 - \tilde{\beta} |\tilde{\phi}|^4 \right]. \tag{1.78}$$

is denoted as the Abelian-Higgs (AH) model.
The gauging of $U(1)_F$ introduces an additional global symmetry, the topological $U(1)_T$ associated with the conserved current $j_T = *\frac{F}{2\pi}$. The theory preserves also charge conjugation, leading to an $O(2) = SO(2)_T \ltimes \mathcal{C}$ global symmetry, as in the XY model.
Let us explore the phases of this theory for large values of the mass $\tilde{m}^2$.

- $\tilde{m}^2 \gg 0$:
  The gauge symmetry is unbroken and the scalar field is massive. At low-energies, $\tilde{\phi}$ can be integrated out, leaving only the photon as a dynamical field. The latter can be dualized into a compact scalar ω. The theory is then free and gapless, with Lagrangian

$$\mathcal{L} = \frac{e^2}{8\pi} \partial_\mu \omega \partial^\mu \omega. \tag{1.79}$$

  The moduli space of vacua is an S^1 manifold. This is nothing but the theory of the Goldstone boson of the topological symmetry $U(1)_T$, which is spontaneously broken at

any point of the vacuum manifold.
In this phase, the scalar field $\tilde{\phi}$ is massive. Being charged under the gauge group, this interacts with a scalar $\tilde{\phi}^\dagger$ through an interaction energy

$$E(R) \sim e^2 \log(R) \tag{1.80}$$

where R represents the distance between the charges.
As we saw before, monopoles are present in this phase and can be written in terms of ω. On a generic vacuum $\langle\omega\rangle \neq 0$, these condense, leading to confinement in the original $U(1)$ gauge theory, due to the Polyakov mechanism [37,38]. The same mechanism was observed in [1] in the context of $\mathcal{N} = 2$ four dimensional theories.

- $\tilde{m}^2 \ll 0$:
The potential has an S^1 moduli space of vacua and the gauge symmetry is spontaneously broken by the VEV $\langle|\tilde{\phi}|^2\rangle = -\frac{\tilde{m}^2}{2\tilde{\beta}}$, leading to an Higgs phase. On the other hand, the topological symmetry $U(1)_T$ remains unbroken. The gauge field and the scalar become both massive and the theory is hence trivially gapped.
Also, in this case, we have massive vortex solutions.[7] Their energy is actually finite and they are defined as field configurations $\tilde{\phi}(r,\theta)$ that at infinite distance $r \to \infty$ behave as [9]

$$\tilde{\phi}_\infty = ve^{i\sigma(\theta)}, \;\; A_i(r,\theta) \to -\partial_i\sigma(\theta). \tag{1.81}$$

These configurations are classified by the first homotopy group $\pi_1(S^1)$, given by the number of times σ winds around spatial infinity. The associated winding number reads

$$n = \frac{1}{2\pi}\oint d\sigma. \tag{1.82}$$

A topological non-trivial configuration, by virtue of (1.81) carries a magnetic field

$$\frac{1}{2\pi}\oint d\sigma = -\frac{e}{2\pi}\oint_{S^1_\infty} A = \frac{e}{2\pi}\int_{\mathbb{R}^2} F = \frac{e}{2\pi}\Phi \tag{1.83}$$

where Φ represents the magnetic flux through $\mathbb{R}^2$. These are nothing but states produced by acting with a monopole operator $\mathcal{M}$ on the vacuum of the gauge theory.

The phase diagram of the AH model is shown in figure 1.3.

We see that we can establish a precise map among the XY and the AH models

- The phase diagrams of the two theories agree. The gapped phase of the XY model at $m^2 \gg 0$ is mapped to the gapped phase of the AH model at $\tilde{m}^2 \ll 0$. The gapless phase of the XY model with moduli space S^1 at $m^2 \ll 0$ is mapped to the gapless phase of the AH model at $\tilde{m}^2 \gg 0$ with moduli space S^1;

[7] These can be studied both in the UV Lagrangian and on the EFT Lagrangian $\mathcal{L} = \frac{v^2}{2}D\sigma$ describing superconductivity.

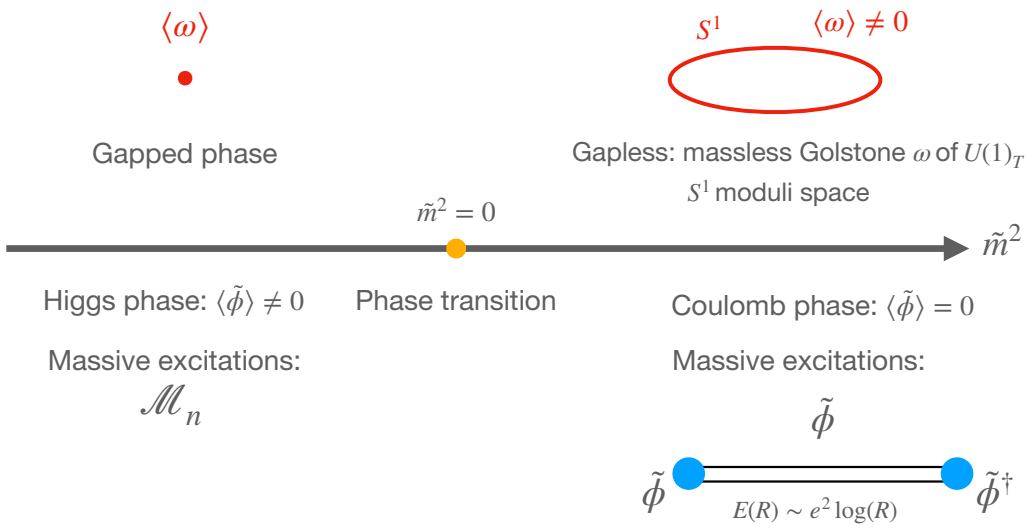

Figure 1.3: Phase diagram of the AH model.

- The flavor symmetry of the XY model matches the topological symmetry of the AH theory

$$SO(2)_F \leftrightarrow U(1)_T. \tag{1.84}$$

  Both are broken in the corresponding gapless phases and preserved in the gapped ones. Currents of these two symmetries map then as

$$j_F = -i(\bar{\phi} d\phi - \phi d\bar{\phi}) \leftrightarrow j_T = \frac{1}{2\pi} * F \tag{1.85}$$

- Excitations matches across the duality. In the gapless phase, the Goldstone boson of the $U(1)_F$ symmetry in the XY model is mapped to the dual photon, namely the Goldstone boson of the $U(1)_T$ symmetry, of the AH model. The massive excitations $\tilde{\phi}$ of the AH model match the massive vortices of the XY theory and both excitations interact with each other via a confining potential. In the gapped phases, the vortices of the AH model, charged under the topological symmetry are mapped to the scalar excitations ϕ in the XY model, charged under the $U(1)_F$ symmetry.

Note that, in the previous duality map, the matching involves gauge-invariant operators only. Indeed, in general, gauge symmetry does not need to match across the duality, while global symmetries do and represent an important tool to map operators across the correspondence.
Finally, in the AH model, we expect a phase transition to separate the two different semi-classical phases at $\tilde{m}^2 = 0$. Since at this point the global symmetry $U(1)_T$ of the theory is restored, this suggests that the transition is second order, with the order parameter corresponding to the VEV of the dual photon. We are then led to identifying this transition with the Wilson-Fisher fixed point of the XY model, and the only relevant deformation of the WF fixed point m^2 with

$-\tilde{m}^2$ parameter of the AH model. The two theories are claimed to be IR dual and to flow to the same WF fixed point. We can express this duality schematically in terms of their "IR lagrangians"

$$|D_\mu \tilde{\phi}|^2 - \tilde{\beta}|\tilde{\phi}|^4 \leftrightarrow |\partial_\mu \phi|^2 - \beta|\phi|^4 \tag{1.86}$$

where we dropped the Maxwell term at low-energies. The duality maps particles to vortices and vice versa: for this reason, this is denoted in the literature as particle vortex duality. We summarize the duality map in Table 1.1. Many other evidence suggest the duality to hold, in

	XY model	AH model
Global current	$j_F = -i(\phi d\phi - \phi d\phi)$	$j_T = \frac{1}{2\pi} * F$
Gapped phase	Massive ϕ	Massive $\mathcal{M}$
Gapless phase	SB phase with massive $\mathcal{V}$	Coulomb phase with massive $\tilde{\phi}$
Relevant deformation	$\|\phi\|^2$	$-\|\tilde{\phi}\|^2$

Table 1.1: Dictionary of the particle-vortex duality.

particular from lattice analysis [39, 40].

1.4.2 Abelian bosonization

This section is dedicated to Abelian bosonization duality in three dimensions. This generalizes the concept of bosonization in two dimensions, which represents an exact duality between a compact chiral boson and a chiral fermion. This allows rewriting bosonic theories in terms of fermionic ones and vice versa. A famous example of this duality is the relation between the Thirring model and the Sine-Gordon theory [41].
However, two dimensional physics is rather special: the massive little group is discrete and a couple of fermions differ from a couple of bosons only when we consider their behavior at coincident points of the one dimensional space. In three dimensions, it seems unlikely for a purely bosonic theory to match a fermionic one, since the little group is continuous and fermions lie in different representations of bosons. However, flux attachment shows that charges can develop a non-trivial spin in presence of magnetic monopoles. In this way, bosonic theories can hide in their spectrum some non-trivial fermionic excitations [16, 42, 43].

In three dimensions, Abelian bosonization conjectures that the Wilson-Fisher type fixed point of the AH model with CS term $k = 1$ is described by a free theory of a Dirac fermion

$$U(1)_1 + \phi \leftrightarrow \psi \tag{1.87}$$

or, in Lagrangian notation

$$\frac{1}{4\pi} AdA + |D_A \phi|^2 - |\phi|^4 \leftrightarrow i\bar{\psi}\not{D}\psi. \tag{1.88}$$

Notice that in (1.88), we omitted the kinetic term for the gauge field. Indeed, as we saw above, in presence of a CS term the gauge boson acquires a topological mass. Below this scale, we

expect the gauge field to stop propagating and the kinetic term to be negligible compared to the CS one. In this way, the kinetic term can be dropped at low enough energies. However, although naively correct, it is not completely safe to drop the kinetic term when the strong coupling scale of the theory is of the same order of the topological mass, since we cannot integrate out the gauge field before the theory develops a strong coupling dynamics.[8] However, when discussing Abelian dualities, we will adopt the assumption of [15, 16] that the kinetic term can be always dropped at low energies.

Again, the bosonic theory includes a quartic potential tuned in order to reach a WF-like fixed point. This correspondence is an example of a strong-weak coupling duality. In the bosonic description, the CFT appears strongly coupled, but in another duality frame, the theory is actually free!

Let us first consider the $U(1)_1$ model. The global symmetry of the theory is a topological $U(1)_T$. To keep track of this symmetry across the duality, we can couple the theory to a background gauge field $\hat{B}$ for the topological symmetry. Since $j_T \sim *dA$, the coupling reads

$$S[\hat{B}] = \frac{1}{2\pi}\hat{B}dA. \tag{1.89}$$

Note that this does not spoil the duality: taking two dual theories, global symmetries can be both coupled to the external gauge field associated with them. The duality then ensures that the partition function $Z_{T_1}[\hat{B}]$ of the first theory T_1 is the same as the partition function $Z_{T_2}[\hat{B}]$ of the latter theory T_2 as a function of the external gauge field $\hat{B}$.

We denote this term as the BF coupling between A and $\hat{B}$. This is gauge invariant under the gauge transformations of A and $\hat{B}$ and it is properly quantized [11]. We can move away from the fixed point by turning on a mass $m^2|\phi|^2$ for the scalar field. We can then distinguish two different phases, which can be studied in this semi-classical regime for $m^2 \gg 0$, $m^2 \ll 0$.

- $m^2 \gg 0$:
  The potential has a unique vacuum and the gauge symmetry is unbroken. The scalar ϕ is massive and can be integrated out at energies $\lesssim m$. Also, the gauge field A has a topological mass due to the CS term $m_{\text{CS}} \sim ke^2$ and it can be integrated out. At low-energies, we end up with a TQFT described by the following CS Lagrangian

  $$\mathcal{L}_{\text{CS}}[\hat{B}] = \frac{1}{4\pi}AdA + \frac{1}{2\pi}\hat{B}dA. \tag{1.90}$$

  This is a deconfined gapped phase. The theory is $U(1)_1$, so it is almost trivial. After we integrate A out, its partition function reduces to a contact term for $\hat{B}$ together with a gravitational CS term

  $$Z[\hat{B}] = e^{-\frac{i}{4\pi}\hat{B}d\hat{B}-2\text{CS}(g)}. \tag{1.91}$$

  However, the theory possesses a single transparent line of spin 1/2, which renders it non-trivial.

  The theory possesses also monopole operators. These are not gauge-invariant, being

[8] This is crucial, for instance, to determine the dynamics of large N QCD_3, see section 1.6.4.

charged under the gauge group due to the CS term. However, if a monopole of charge one $\mathcal{M} \equiv \mathcal{M}_1$ is "dressed" with a scalar field $\phi^\dagger$, the resulting operator is gauge-invariant. The scalar field is then quantized in the monopole background. In presence of a magnetic monopole of charge n, the conserved orbital angular momentum L^2 associated with an electric charge m gets modified as

$$L^2 = (\vec{r} \times (\vec{p} - 2s\vec{A}))^2 + |s|^2 \tag{1.92}$$

where $s = \frac{1}{2}nm$, and $\vec{A}$ represents the gauge potential of the monopole background. Looking at eq. (1.92), we see that representations of the angular momentum are bounded from below by the value of the s. In particular, we can focus on the representation with lowest angular momentum $L^2 = s^2$, since this represents the state of lowest energy. A particle of spin s and of charge one, in the presence of a unit monopole, acquires then an additional spin due to the Lorenz force. So, for example, a fermion in the background of the monopole acquires an integer spin and, more interestingly, a scalar develops a half-integer spin [42, 44]!
We denote the basic dressed monopole operator of the $U(1)_1 + \phi$ theory as

$$\phi^\dagger \mathcal{M}. \tag{1.93}$$

This is gauge-invariant and has spin $|s| = 1/2$. Moreover, it is charged under the global symmetry $U(1)_T$ with charge one.

- $m^2 \ll 0$:
  The potential breaks spontaneously the gauge symmetry. The photon develops a mass due to the Higgs mechanism, and so does ϕ. The theory is trivially gapped with partition function
  $$Z[\hat{B}] = 1. \tag{1.94}$$
  The lowest massive gauge invariant excitations are again the dressed monopoles $\phi^\dagger \mathcal{M}$.

Let us now analyze the fermionic theory. This has a global symmetry $U(1)_F$ which rotates the fermion as $\psi \to e^{i\alpha}\psi$. We can couple the theory to an external background $\hat{B}$

$$\mathcal{L} = i\bar{\psi} \not{D}_{\hat{B}} \psi \tag{1.95}$$

with $\not{D}_{\hat{B}}$ the covariant derivative with respect to the background field $\hat{B}$. Here, we are showing the bare CS term $k_{\rm b}$, which is set to zero. We have a natural relevant deformations defined by the mass term $\tilde{m}\bar{\psi}\psi$. We have then two phases at low-energies.

- $\tilde{m} > 0$:
  The fermion is massive and can be integrated out. This generates a shift in the CS level and at low-energy we are left with a gapped theory with no CS term
  $$Z[\hat{B}] = 1. \tag{1.96}$$
  Excitations around this vacuum are represented by ψ itself.

- $\tilde{m} < 0$:
  The fermion is massive and can be integrated out. This generates a negative shift for the CS term. The low-energy theory is then a TQFT with action

$$\mathcal{L} = -\frac{1}{4\pi}\hat{B}d\hat{B} - 2\mathrm{CS}(g). \tag{1.97}$$

  The theory is deconfined as expected. The lowest excitation is still the massive fermion.

We see that the topological symmetry of the scalar theory matches the flavor symmetry of the fermionic one. The relevant deformation m^2 of the scalar theory matches the deformation $-\tilde{m}$ of the fermion. The phases of the theory match as well, as their corresponding partition functions and their lowest massive excitation. In particular, dressed monopoles of the scalar theory are mapped to fermions of the free Dirac theory.
Both the scalar and the fermionic theories enjoy parity invariance at $m^2 = \tilde{m} = 0$, when the background field is switched off. However, both theories suffer a parity anomaly associated with their global symmetry, which manifests itself when we turn on the background gauge field $\hat{B}$ as a half-integer CS term. So the anomaly matches across the duality.
In conclusion, a $U(1)_1 + \phi$ theory is conjectured[9] to be IR dual to a theory of a free fermion, describing its IR fixed point. The CFT point, which in the bosonic case is difficult to access being strongly coupled, is conjectured to admit a weakly-coupled dual description in terms of a free fermion. The map between the two theories is summarized below:

$$j_T^\mu = \frac{e^2}{4\pi}\epsilon^{\mu\nu\rho}F_{\nu\rho} \leftrightarrow j_F^\mu = i\bar{\psi}\gamma^\mu\psi, \tag{1.98}$$

$$|\phi|^2 \leftrightarrow -\bar{\psi}\psi, \tag{1.99}$$

$$\phi^\dagger\mathcal{M} \leftrightarrow \psi. \tag{1.100}$$

1.4.3 A web of Abelian dualities

We saw above two of the main examples of three dimensional dualities. We can ask ourselves if these are the only dualities that exist among three dimensional theories and, if not, whether these are independent or they can be derived from other dualities via a series of operations. This was studied in detail in [16]. In the following, we resort mainly to this work, giving some examples of these new dualities.

We start by introducing the basic operations useful to construct new dualities. One of these is represented by gauging a global symmetry. Let us consider two different theories, which we denote by T_1 and T_2, related by an IR duality. We know that, across this duality, global symmetries need to match.[10] We can then couple both theories to background fields for their global

[9] Evidence of the validity of this duality are milder with respect to particle-vortex duality, although there are plausible arguments to infer its correctness, see [16].

[10] This, actually, needs to happen only in the IR. Indeed, the UV symmetry could not match if there is symmetry enhancement at low-energies. This is the case, for example, of self-dual QED_3 with two Dirac fermions [15, 45].

symmetry, and the partition function of the first theory T_1 with background field $\hat{B}_1$ should match the partition function of the second theory T_2 with background field $\hat{B}_2$

$$Z_{T_1}[\hat{B}_1] = Z_{T_2}[\hat{B}_2]. \tag{1.101}$$

Gauging the background fields $\hat{B}_1, \hat{B}_2$ on both sides is then equivalent to integrating the partition functions over them. These remain then equivalent also after gauging. In this way, we obtain a new duality between these gauged theories.
Adding contact terms can be important to construct new dualities. These are well-defined local terms that involve background fields. For example, the CS coupling for the global symmetry background field can be added on both sides of the duality. This operation preserves the duality and will be denoted as T.
We can also first gauge a background field and then couple it to another classical background field $\hat{C}$ through a BF-term. This operation will be denoted as S. Acting on a Lagrangian $\mathcal{L}[\hat{B}]$ coupled to a background field $\hat{B}$ with T and S, we obtain

$$T : \mathcal{L}[\hat{B}] \to \mathcal{L}'[\hat{B}] = \mathcal{L}[\hat{B}] + \frac{1}{4\pi}\hat{B}d\hat{B} \tag{1.102}$$

$$S : \mathcal{L}[\hat{B}] \to \mathcal{L}'[\hat{C}] = \mathcal{L}[B] - \frac{1}{2\pi}Bd\hat{C}. \tag{1.103}$$

Acting twice with the latter transformation, the Lagrangian changes as

$$S^2 : \mathcal{L}[\hat{B}] \to \mathcal{L}'[\hat{D}] = \mathcal{L}[B] - \frac{1}{2\pi}BdC - \frac{1}{2\pi}Cd\hat{D}. \tag{1.104}$$

The same happens acting with $(ST)^3$. Using the following path integral identity[11]

$$\int DE\, e^{\frac{i}{2\pi}EdF} = \delta(F) \tag{1.105}$$

we can eliminate C from (1.104), obtaining $\mathcal{L}[-\hat{D}]$. So, S^2 acts as charge conjugation.
Finally, we can also act with $\mathcal{T}$ and generate new dualities, if the theories related by the correspondence are not already manifestly time-reversal invariant.

Let us now use these operations to generate new dualities. In the following, we will not focus on the subtleties related to the necessity of introducing spin or spin$_c$ connection, regarding which we refer to [15, 16] for a detailed discussion.
We start from Abelian bosonization

$$\frac{1}{4\pi}AdA + \frac{1}{2\pi}Ad\hat{B} + |D_A\phi|^2 - |\phi|^4 \;\longleftrightarrow\; i\bar{\psi}\not{D}_{\hat{B}}\psi. \tag{1.106}$$

We can now apply time-reversal, which sends $\hat{B} \to -\hat{B}, A \leftrightarrow -a$ and $\phi \to \varphi$. The transformed fields a, φ are in general complicated functions of the original ones. We end up with

$$-\frac{1}{4\pi}ada - \frac{1}{2\pi}ad\hat{B} + |D_a\varphi|^2 - |\varphi|^4 \;\longleftrightarrow\; i\bar{\psi}\not{D}_{\hat{B}}\psi + \frac{1}{4\pi}\hat{B}d\hat{B} + 2\mathrm{CS}(g) \tag{1.107}$$

[11] This identity states that E acts as a Lagrangian multiplier setting F to zero [16].

We can also add background terms on both sides of the duality. In this way, we can eliminate the CS of the fermionic theory by bringing it to the bosonic side, namely

$$-\frac{1}{4\pi}ada-2\mathrm{CS}(g)-\frac{1}{2\pi}ad\hat{B}-\frac{1}{4\pi}\hat{B}d\hat{B}+|D_a\varphi|^2-|\varphi|^4 \;\longleftrightarrow\; i\bar{\psi}\not{D}_{\hat{B}}\psi. \tag{1.108}$$

The fermionic side is dual to another bosonic theory, thanks to bosonization (1.88). This establishes a new duality between purely bosonic theories

$$-\frac{1}{4\pi}ada-2\mathrm{CS}(g)-\frac{1}{2\pi}ad\hat{B}-\frac{1}{4\pi}\hat{B}d\hat{B}+|D_a\phi|^2-|\phi|^4 \;\longleftrightarrow\; \frac{1}{4\pi}AdA+|D_A\hat{\phi}|^2-|\hat{\phi}|^4+\frac{1}{2\pi}\hat{B}dA \tag{1.109}$$

which can be schematically depicted as

$$U(1)_1+\phi \;\longleftrightarrow\; U(1)_{-1}+\hat{\phi}. \tag{1.110}$$

So, the theory $U(1)_1+\phi$, which is not time-reversal invariant, flows to the same IR CFT as its time-reversal version!
The same duality can be obtained by similar manipulations from particle-vortex duality (1.86), by adding a CS term for the $U(1)$ global symmetry $\frac{1}{4\pi}\hat{B}d\hat{B}$ together with a coupling $\frac{1}{2\pi}Ad\hat{B}$ and making $\hat{B}$ dynamical. We end up with

$$\frac{1}{4\pi}(B+a+\hat{C})d(B+a+\hat{C})-\frac{1}{4\pi}(a+\hat{C})d(a+\hat{C})+|D_a\phi|^2-|\phi|^4 \;\longleftrightarrow\; \frac{1}{4\pi}AdA+|D_A\tilde{\phi}|^2-|\tilde{\phi}|^4+\frac{1}{2\pi}\hat{C}dA. \tag{1.111}$$

Indeed, the first term in (1.111) denotes a trivial $U(1)_1$ theory, which decouples in favor of a purely gravitational CS term. This matches precisely the form of the $U(1)_1 \leftrightarrow U(1)_{-1}$ duality in (1.109) by identifying $\tilde{\phi}\equiv\varphi$, $\hat{C}\equiv\hat{B}$. The relation with particle-vortex duality allows us to understand how time-reversal acts on the $U(1)_1$ theory: this transforms the scalar field ϕ into a vortex of the $U(1)_{-1}$ and a vortex of $U(1)_1$ into the scalar $\hat{\phi}$!
Moreover, this tells us also that the mass term for ϕ is odd under time-reversal, as can be shown using the particle-vortex duality dictionary $\phi^2 \leftrightarrow -\tilde{\phi}^2$.
The previous relations, moreover, show that bosonization implies particle-vortex duality. So, it is sufficient to assume the validity of the former to use the latter and construct additional dualities!

From bosonization, we can obtain additional boson-fermion dualities. We can, for example, gauge the global symmetry of the theories that enjoy the duality by making the background field $\hat{B}$ dynamical, and add the couplings $\frac{1}{2\pi}Bd\hat{C}-\frac{1}{4\pi}\hat{C}d\hat{C}$. Integrating out B in the bosonic theory, we obtain

$$i\bar{\psi}\not{D}_B\psi+\frac{1}{2\pi}Bd\hat{C}-\frac{1}{4\pi}\hat{C}d\hat{C} \leftrightarrow |D_{-\hat{C}}\phi|^2-|\phi|^4 \tag{1.112}$$

establishing a duality between a $U(1)_{-1/2}+\psi$ theory and a scalar at the WF point. We indicate the duality as

$$U(1)_{-1/2}+\psi \leftrightarrow \text{XY model}. \tag{1.113}$$

The correspondence maps monopoles to particles: a monopole $\mathcal{M}^\dagger$ dressed with a fermion ψ in the fermionic theory is charged under $U(1)_T$ with charge -1 and maps to ϕ in the $O(2)$ model, which is charged with charge -1 under $U(1)_F$.

As a final example, we comment on the possibility of obtaining dualities involving fermionic theories only. Starting from (1.112), we can add a CS term $\frac{k}{4\pi}\hat{C}d\hat{C}$ for the $U(1)$ global symmetry. We can then act with S, introducing a new background field $\hat{D}$ for the topological symmetry $j_T \sim *dC$, obtaining

$$\frac{k}{4\pi}CdC + \frac{1}{2\pi}Cd\hat{D} + |D_{-C}\phi|^2 - |\phi|^4 \leftrightarrow i\bar{\psi}\not{D}_B\psi + \frac{k-1}{4\pi}CdC + \frac{1}{2\pi}BdC + \frac{1}{2\pi}Cd\hat{D}. \quad (1.114)$$

We can then choose $k = -1$ and use (1.107), ending with a purely fermionic duality

$$i\bar{\psi}\not{D}_B\psi + \frac{1}{2\pi}BdC - \frac{2}{2\pi}CdC + \frac{1}{2\pi}Cd\hat{D} \leftrightarrow i\bar{\psi}\not{D}_{\hat{D}}\psi + \frac{1}{4\pi}\hat{D}d\hat{D} + 2\mathrm{CS}(g). \quad (1.115)$$

This can be interpreted as a fermionic version of particle-vortex duality [16, 43, 46–48] since on one side we have a Dirac fermion charged under a gauge group, while on the other side the fermion is free. Actually, in order to make this statement precise, we should integrate out C. This leads to a wrong quantization condition since the integration enforces $C = \frac{1}{2}(B + \hat{D})$, which is not correctly quantized as a $U(1)$ field. So, in the following, we will refer to this duality as

$$"U(1)_0 + \psi \leftrightarrow \psi" \quad (1.116)$$

to recall this subtlety. The web enjoyed by these dualities is shown in figure 1.4.

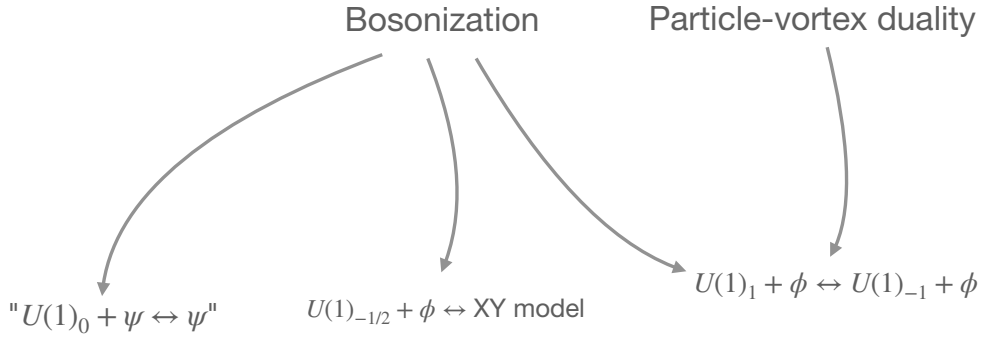

Figure 1.4: Web of Abelian dualities.

From these dualities, using the previous operations, we can obtain other correspondences for quiver or more complicated fermionic and bosonic theories. We refer the reader to [7, 16] for a detailed discussion about these dualities.

1.5 Non-Abelian theories

In this section, we discuss non-Abelian gauge theories in three dimensions. We first start reviewing pure $SU(N)$ and $U(N)$ YM theories, their symmetries, and their low-energy dynamics. Then, we analyze pure CS theories in the non-Abelian case, their spectrum of Wilson lines, and dualities. Finally, we study the dynamics of YM CS theories, focusing on their vacuum structure.

1.5.1 Non-Abelian Yang-Mills theory

Let us consider the Lagrangian of pure Yang-Mills theory

$$\mathcal{L} = -\frac{1}{2g^2}\mathrm{Tr}F \wedge *F. \tag{1.117}$$

In the following, we restrict the analysis to SU and U gauge groups.
The $U(N)$ theory possesses a topological symmetry $U(1)_T$ associated with the current

$$j_T = \frac{1}{2\pi} * \mathrm{Tr}F. \tag{1.118}$$

This is preserved by virtue of the Bianchi identities and it is associated with the Abelian factor of the $U(N)$ gauge group. Indeed, the unitary group can be written (globally) as a product of an $SU(N)$ group together with an Abelian $U(1)$ as $U(N) = \frac{SU(N)\times U(1)}{\mathbb{Z}_N}$. The gauge field associated with the Abelian factor is nothing but the trace of A, while the traceless field is associated with the $SU(N)$ part. On the other hand, this topological symmetry is absent in the $SU(N)$ case.
In presence of the topological symmetry, we can construct monopole operators. As we reviewed in section 1.2, these are disordered operators creating a magnetic flux. This flux, in particular, can be chosen to lie in the Cartan subalgebra of the $U(N)$ gauge group [49]. Any magnetic monopole $\mathcal{M}(x)$ is then identified by its magnetic fluxes q_i associated with each Cartan, the so-called GNO charges.[12] A monopole operator of charges $\{q_1, ..., q_N\}$ will be then denoted as

$$\mathcal{M}_{\{q_1,...,q_N\}}(x). \tag{1.119}$$

Note that the charge Q of the monopole under $U(1)_T$ equals the sum of all GNO charges $\sum_i q_i = Q$.

The $SU(N)$ group possesses a center $\mathbb{Z}_N$, associated with a one-form symmetry, acting on the field A by a shift of a $\mathbb{Z}_N$ flat connection. This $\mathbb{Z}_N$ symmetry acts on the Wilson lines of the theory, which now are labeled by their representation R under the gauge group

$$W_R[\mathcal{C}] = Pe^{i\oint A_R^a T_R^a} \tag{1.120}$$

where T_R^a are the generators of the algebra in the representation R and P is the path ordered prescription. When the lines close into loops, they represent a non-local gauge-invariant operator of the field theory.

[12] These charges belong to the magnetic dual lattice of the Lie algebra, due to the Dirac quantization condition.

The $U(N)$ group, on the other hand, possesses a $U(1)$ continuous one-form symmetry, descending from the one-form symmetry associated with the Abelian factor of $U(N)$ [8].
Since the $SU(N)$ YM coupling g is relevant, the theory is strongly coupled in the IR. This is expected to confine at low-energies, as it happens in the Abelian case. The expectation value of the fundamental Wilson loop, in particular, is then expected to satisfy area law, and the one-form symmetry $\mathbb{Z}_N$ to be preserved in the IR. Moreover, $SU(N)$ YM in three dimensions is believed to develop a mass gap of order $\sim g^2$, corresponding to the mass of the lightest glueball. The theory is then trivially gapped.

1.5.2 Chern-Simons theories

We now generalize the notion of CS theory to the non-Abelian case. To ensure gauge invariance under local gauge transformations, the original Abelian CS Lagrangian should be equipped with an additional term, which is cubic in the gauge field. The non-Abelian CS term reads then

$$\mathcal{L}_{\text{CS}} = \frac{k}{4\pi}\text{Tr}\left(AdA - \frac{2}{3}iA^3\right). \tag{1.121}$$

A pure $SU(N)$ CS theory equipped with this term is denoted as $SU(N)_k$. For unitarity groups $U(N)$, the nomenclature is more involved. Indeed, the $SU(N)$ and $U(1)$ factors of the $U(N)$ gauge group can have different CS levels

$$\mathcal{L} = \frac{k}{4\pi}\text{Tr}\left(AdA - \frac{2}{3}iA^3\right) + \frac{n}{4\pi}\text{Tr}A d\text{Tr}A \tag{1.122}$$

being the two terms separately gauge-invariant.
Writing $A = \tilde{A} + \frac{1}{N}\text{Tr}A$, we see the $SU(N)$ factor has CS level k, while the $U(1)$ factor has level $N(nN+k)$. Rewriting $k' \equiv nN + k$, the resulting theory is denoted as

$$U(N)_{k,k'} = \frac{SU(N)_k \times U(1)_{k'N}}{\mathbb{Z}_N}. \tag{1.123}$$

Choosing $n = 0$, $k' = k$, we obtain the CS action of the $U(N)_{k,k} \equiv U(N)_k$ CS theory.

As in the Abelian case, CS levels are quantized. The quantization, in particular, ensures gauge-invariance of the theory under large gauge transformations. Let us take the $SU(N)$ theory and act with a large gauge transformation $A_\mu \to g^{-1}A_\mu g + ig^{-1}\partial_\mu g$. This is labeled by the third homotopy group of $SU(N)$, being the gauge transformations maps from $\mathbb{R}^{1,2}$ to $SU(N)$. Since $\pi_3(SU(N)) = \mathbb{Z}$, the classes to which a transformation g belongs are labeled by the winding number

$$W(g) = \frac{1}{24\pi^2}\int \text{Tr}(g^{-1}dgg^{-1}dgg^{-1}dg) = n \in \mathbb{Z}. \tag{1.124}$$

The variation of the CS action (1.121) under large gauge transformations (up to boundary terms) reads

$$\delta\mathcal{L}_{\text{CS}} = -\frac{k}{12\pi}\text{Tr}(g^{-1}dgg^{-1}dgg^{-1}dg) = 2\pi kn. \tag{1.125}$$

To ensure gauge invariance, this shift of the action should be then proportional to an integer multiplied by 2π. This leads to the quantization condition

$$k \in \mathbb{Z}. \tag{1.126}$$

The same reasoning can be done for $U(N)$, leading to the conditions $k \in \mathbb{Z}$ and $k'N \in \mathbb{Z}$ (namely $\frac{k'-k}{N} \in \mathbb{Z}$).

Let us now discuss the dynamics of these theories.
As in the Abelian case, the equations of motion are solved by flat connections

$$F = 0 \text{ with solutions: } A_\mu = ig^{-1}\partial_\mu g. \tag{1.127}$$

We again have no local propagating degrees of freedom (as we can see also from the CS propagator), as expected from the topological nature of the CS term (1.121). The Wilson loops represent the gauge-invariant non-local observables of these theories

$$W_R[\mathcal{C}] = \mathrm{Tr}_R P e^{i \oint A}. \tag{1.128}$$

The Hilbert space of these theories was first analyzed in [13], together with the correlation functions of Wilson lines. It was shown that these correlation functions compute topological invariants of the manifolds on which the theory lives, known as knot invariants. We will not discuss any further these aspects, which are beyond the goal of this thesis.
Much information about these theories is known thanks to the exact duality between CS theories and WZW models [50].
First of all, not all the lines contribute to the Hilbert space of the theory due to the interrelations between them. Putting the theory on a spatial torus, for example, only lines in integrable[13] representations of the $SU(N)$ group contribute. The number of these representations equals the dimension of the Hilbert space of the theory and reads

$$\dim\mathcal{H} = \frac{(k+N-1)!}{k!(N-1)!}. \tag{1.129}$$

For $SU(2)$, we have a more general result [51] coming from the CS-WZW correspondence, which gives us the dimension of the Hilbert space on a generic genus g surface through the Verlinde formula

$$\dim\mathcal{H} = \left(\frac{k+2}{2}\right)^{g-1} \sum_{j=0}^{k} \left[\sin\frac{(j+1)\pi}{k+2}\right]^{2-2g}. \tag{1.130}$$

Second, we can show that many CS theories are dual to each other by looking at their corresponding WZW models [50]. For example, $SU(N)_1$ on the torus has a Hilbert space of dimension N, which is the same dimension as the Hilbert space of a $U(1)_N$ theory, see section 1.2. This holds also for $g > 1$ [51], showing that the dimension of the Hilbert space of both theories agrees

[13] These are representations whose Young tableaux have the width of their first row smaller or equal to the CS level k.

on generic manifolds and reads N^g. This is an example of a level/rank duality [15, 50]. These dualities relate $SU(N)$ and $U(N)$ pure CS theories via the correspondence

$$SU(N)_{\pm k} \longleftrightarrow U(k)_{\mp N,\mp N} \tag{1.131}$$

$$U(N)_{k,k+N} \longleftrightarrow U(k)_{-N,-N-k}. \tag{1.132}$$

The theories have the same lines and isomorphic Hilbert spaces and corresponding equal partition functions. This represents an exact duality between different TQFTs.
Note that, looking at the first row in (1.131), we conclude that $U(N)_1$ is almost trivial since $SU(1)$ is empty. This generalizes the almost triviality of $U(1)_1$ to generic $N > 1$.
Finally, let us mention that the previous methods used to establish new Abelian dualities can be also employed here to construct new level/rank dualities. In this way it is possible to obtain, for example, the $U(N)_{k,k-N} \longleftrightarrow U(k)_{-N,-N+k}$ duality [15].

1.5.3 Yang-Mills CS gauge theory

Adding a CS term of level k to the YM action, we obtain the YM CS action at level k

$$\mathcal{L}_{\text{YM CS}} = -\frac{1}{2g^2}\text{Tr}F \wedge *F + \frac{k}{4\pi}\text{Tr}\left(AdA - \frac{2}{3}iA^3\right). \tag{1.133}$$

In presence of a CS term, monopoles become charged under the topological symmetry due to flux attachment. Take for definiteness a $U(N)_k$ CS theory. In this theory, a monopole with charges $\{q_1, ..., q_n, 0, 0, .., 0\}$ breaks the gauge symmetry down to $U(1)^n \times U(N-n)$ and the monopole is charged under the n $U(1)s$ with electric charge kq_i [49]. This conclusion can be drawn by looking at the transformation of the monopole operator under the Cartan of $U(N)$, adapting the Abelian analysis in (1.29).
The one-form symmetry in the $SU(N)$ case remains $\mathbb{Z}_N$ [8]. In the $U(N)_k$ theory, instead, the $U(1)$ one-form symmetry of the Abelian factor gets reduced to $\mathbb{Z}_{kN}$ due to the CS level and to $\mathbb{Z}_k$ due to the $\mathbb{Z}_N$ quotient between the $SU(N)$ and the $U(1)$ group $U(N) = \frac{SU(N)\times U(1)}{\mathbb{Z}_N}$.

From the analysis of the propagator, we see again that the A field acquires a gauge-invariant mass $m = \frac{|k|g^2}{2\pi}$ without breaking the gauge symmetry. As a consequence, the theory possesses two mass scales: the topological mass $\sim |k|g^2$ and the strong coupling scale $\sim Ng^2$. We can then have two distinct regimes: $|k|g^2 \gg Ng^2$ and $|k|g^2 \ll Ng^2$. In the first case, gluons can be semi-classically integrated out at energies smaller than $|k|g^2$, since the dynamics of the YM theory is weakly coupled at this scale. The kinetic term can be then safely dropped and we are left with a deconfined CS theory. This is also what we expect by looking at the Lagrangian (1.133): the first term becomes subleading in the strong coupling regime and can be dropped out. However, in the $|k|g^2 \ll Ng^2$ regime (such as in the large N, small k limit), we cannot anymore integrate out the gauge field semi-classically, since at the scale of the topological mass the theory is already strongly coupled. Nevertheless, the theory is believed to deconfine and reduce to the same $SU(N)_k$ TQFT at low-energies. This expectation changes in presence of matter fields, as we will see when discussing QCD_3 in various limits of its parameters.

1.6 QCD_3: generalities

1.6.1 Chern-Simons matter dualities

Above, we saw how three dimensional theories share some interesting behavior. In the Abelian case, we saw an intricate web of dualities, involving matter theories, which can be obtained consistently from bosonization or particle-vortex duality. Moreover, in the non-Abelian case, we saw that pure CS theories are related by exact correspondences, namely by level/rank dualities. A natural generalization comes from considering dualities among non-Abelian CS matter theories. These are known as Aharony dualities [49], and can be also seen as a non-supersymmetric generalization of the three dimensional $\mathcal{N} = 2$ dualities of [3, 52–54]. The original Aharony dualities read

$$U(N)_{-k} \text{ with } F\ \psi \longleftrightarrow SU(k+F/2)_N \text{ with } F\ \phi \tag{1.134}$$

$$SU(N)_{-k} \text{ with } F\ \psi \longleftrightarrow U(k+F/2)_N \text{ with } F\ \phi \tag{1.135}$$

$$U(N)_{-k,-k-N} \text{ with } F\ \psi \longleftrightarrow U(k+F/2)_{N,N+k+F/2} \text{ with } F\ \phi. \tag{1.136}$$

In the relations above, scalars and fermions are always in the fundamental representation of the gauge group.
As for the Abelian dualities, these relations hold in the infrared: a theory of F bosons shares the same IR physics as a theory of F fermions with a different gauge group and CS level. Moreover, as in the Abelian case we will assume that the kinetic term of the gauge field can be safely dropped in the IR.
A gauge theory coupled to fundamental fermions suffers, in general, from parity anomaly. This tells us that, in order to preserve gauge-invariance, we need to break parity at the quantum level. In presence of F fermions in a complex[14] representation R, a quantum CS term is generated and reads [15]

$$\Delta k = -F h_R \text{sgn}(m) \tag{1.137}$$

where h_R is the Dynkin index of the representation $\text{Tr}(T_R^a T_R^b) = 2h_R\delta^{ab}$. Again, the partition function depends on the renormalized level $k = k_b - F h_R$, which is in general half-integer. When F fermions are massive with mass m, the CS level in the IR reads

$$k_{IR} = k + F h_R\, \text{sgn}(m) \tag{1.138}$$

where again k is the renormalized level $k = k_b - h_R$.
In this way, integrating out the fermions, k_{IR} is always an integer, and gauge-invariance is preserved. Let us take for instance F fermions in the fundamental representation f. We see that whenever $m = 0$, parity is broken if F is odd since the renormalized level k obeys the quantization condition

$$k + \frac{F}{2} \in \mathbb{Z}, \tag{1.139}$$

[14] If the representation R is instead real, $\Delta k = -\frac{F}{2} h_R \text{sgn}(m)$.

[15] This can be seen, for example, by calculating the contribution in the PV regularization with the minus sign prescription. In the following, consistently with the Abelian case, we will stick with the minus prescription for the CS term.

being $h_f = \frac{1}{2}$.
If, on the other hand, F is even, we see that the theory with $k = 0$ possesses time-reversal invariance. This parallels the Abelian case.
In writing eq.s (1.134)-(1.136), due to parity anomaly, we stick with our convention and associate with the fermionic theories the renormalized level, instead of the bare one (again adopting the $-$ convention for the shift of the level).
Many of the previous Abelian and non-Abelian dualities can be obtained as limits of the Aharony ones. For example, the case $F = 0$ reduces to level/rank dualities and their time-reversed versions. If $N = F = 2k = 1$, we obtain Abelian bosonization $U(1)_1 + \phi \leftrightarrow \psi$, as well as $U(1)_{-1/2} + \psi \leftrightarrow$ XY model . Note that actually, Aharony dualities are a subset of a more general group of dualities, known as master or Benini's dualities [55], from which they can be derived. In the following, we will not cover master dualities in detail, limiting ourselves to the dualities useful for our purpose.
In particular, we will focus on the non-Abelian bosonization duality

$$SU(N)_k \text{ with } F\ \psi \longleftrightarrow U(k + F/2)_{-N} \text{ with } F\ \phi, \tag{1.140}$$

representing the time-reversal version of (1.135). In the following, we assume k to be non-negative since theories with negative CS levels can be studied by applying a time-reversal transformation. The theory on the left-hand side of the duality, namely $SU(N)_k$+F fundamental fermions and CS level k, is denoted in the literature as QCD_3. Its dynamics was studied in various range of parameters since this theory shows many interesting phenomena common to four dimensional QCD. In the following, we will focus on the study of its phase diagram and the duality in (1.140) will be a useful tool to achieve our goal. For reasons that will become clear later, we first start analyzing its vacuum structure for the case $k \geq F/2$, and after we will discuss the $k < F/2$ case.

1.6.2 QCD_3: $k \geq F/2$ case

Let us first focus on the phase diagram of QCD_3.
The deformation of the (conjectured) fixed point of the fermionic theory is represented by turning on a mass $m\bar{\psi}\psi$ common to all the fermions, which preserves the $U(F)$ global symmetry. Depending on the sing of m, in the semi-classical regime $|m| \gg g^2$, fermions can be integrated out and the mass generates a shift of the CS level. At low-energies, we end up with the following phases

$$\mathcal{L} = \begin{cases} SU(N)_{k+F/2}, & m > 0 \\ SU(N)_{k-F/2}, & m < 0 \end{cases} \tag{1.141}$$

which are nothing but two deconfined TQFTs. Supposing that no other phase is present in the small mass regime, the phase diagram of the theory is shown in figure 1.5.
It is easy to show that the phase diagram of the bosonic dual in (1.140), in the range $k \geq F/2$, matches the one of QCD_3. Let us first see how symmetries are mapped across the duality. On the bosonic side, the gauge group is unitary, so the F scalars enjoy a $SU(F)$ flavor symmetry. Moreover, the theory preserves a topological symmetry $U(1)_T$. On the fermionic side, the gauge

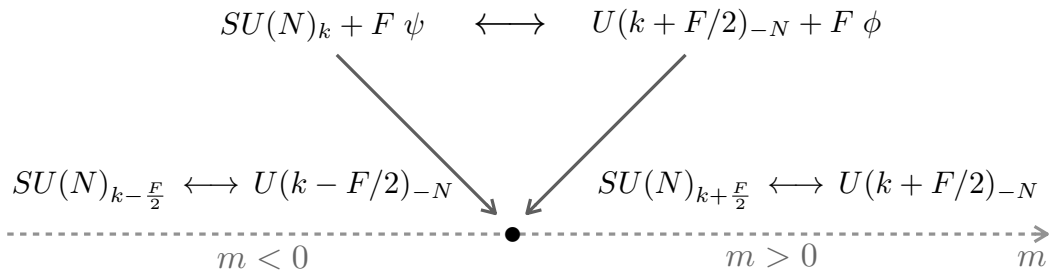

Figure 1.5: Phase diagram of $SU(N)_k + F\ \psi$ in the case $k \geq F/2$. The phase transition between the two gapped phases is indicated by the black dot.

group is special unitary, so fermions enjoy a $SU(F) \times U(1)_B$ flavor symmetry, where $U(1)_B$ represents the baryon number.[16] The global symmetries then match, identifying the baryon number with the topological symmetry $U(1)_B \leftrightarrow U(1)_F$. This correspondence generalizes the duality map of symmetries of Abelian bosonization. Moreover, also anomalies can be matched across the duality [56].
We can now draw the phase diagram of the bosonic dual of QCD_3. We expect the deformation $m\bar{\psi}\psi$ of the fermionic theory to map into a common mass $M^2\phi^2$ for the ϕs. Integrating out the bosonic fields with positive mass leaves a $U(k+F/2)_{-N}$ CS theory. When the mass square is negative, on the other hand, scalars condense and partially Higgs the gauge group. In particular, by a suitable choice of the potential[17] we have maximal Higgsing for the group, which gets broken to $U(k-F/2)$. Note that the bound $k \geq F/2$ is crucial: only for this range of k, part of the gauge symmetry is preserved by the VEV. In the process, the flavor symmetry is unbroken, thanks to color-flavor locking[18]. All the scalars are then massive, together with the gauge fields associated with the broken generators of the gauge group. The remaining gluons acquire a topological mass due to the CS term and we end up, at low-energies, with a CS theory

$$U(k-F/2)_{-N}. \tag{1.142}$$

Looking at the topological phases, we see that the phase diagram of the fermionic theory matches the bosonic one by the identification

$$\bar{\psi}\psi \leftrightarrow \phi^\dagger\phi. \tag{1.143}$$

This generalizes the bosonization map to the non-Abelian case.

Another evidence of the validity of the duality comes from the matching of gauge-invariant operators across the correspondence.

[16] Here we are simplifying the analysis, since the global symmetry that acts faithfully on gauge-invariants is actually $U(F)/\mathbb{Z}_N$ together with a charge conjugation symmetry. This can be seen to match across the duality, see [56].

[17] We will comment about the precise structure of this potential in section 3.1

[18] Namely, the action of the global symmetry together with a constant gauge transformation leaves the vacuum invariant, preserving a diagonal $SU(F)$ symmetry.

The gauge-invariant operators associated with the $U(1)$ global symmetry are dressed monopoles in the bosonic case and baryons in the fermionic case. The correspondence can be made precise by looking at the dimension of the lowest charge operators. Let us start considering the $F = 1$ case. An explicit calculation of monopole dimension was made in [57, 58]. We expect the lowest dimensional operator to be the monopole with charges $\{q_i\} = (1, 0, ..., 0)$ and topological charge one. Due to the CS term, this is charged under the first generator of the Cartan torus with charge $-N$. To make it gauge-invariant, this must be dressed with N scalars ϕ to compensate for the charge. The total classical dimension is then $\Delta = N\Delta_{scalar} + \Delta_{monopole}$. The weight Δ_{scalar} represents the dimension of the scalar in a monopole background and it is equal to one for a monopole with a unit of flux. The total dimension then reads $\Delta = N$ [49]. Moreover, ϕ has spin $\frac{1}{2}$ in the monopole background [59] due to flux attachment, so in total we have 2^N states with spin s up to $N/2$.
Baryons of the fermionic theory, on the other hand, can be written as the antisymmetrization in the color indices of N ψs

$$B = \epsilon_{a_1 a_2 ... a_n} \psi^{a_1} ... \psi^{a_n}. \tag{1.144}$$

The operator B has then baryon charge one and classical dimension N, matching the dimension of the monopole operator.[19] The total number of states is 2^N since they carry different spins up to $N/2$. This matches precisely the number of states and spins of the monopole operator, justifying the duality map. The same analysis can be done in the $F > 1$ case, showing that also the global $SU(F)$ quantum numbers of the two operators match across the duality.

The duality is also self-consistent, meaning that assuming it to hold for fixed (N, k, F), this can be proven to hold also for lower values of F and higher values of k. This can be seen performing a mass deformation. In particular, we can add a mass term to each side of the duality for the F-th flavor (keeping an $SU(N_f - 1)$ global symmetry). On the bosonic side, the sign of the mass deforms the theory to $U(k + 1/2 + (F - 1)/2)_{-N} + (F - 1)\ \phi$ for $M^2 > 0$ or $U(k + (F - 1)/2)_{-N} + (F - 1)\ \phi$ for $M^2 < 0$. On the fermionic side, when we integrate out the flavor we end up with $SU(N)_{k\pm 1/2} + (F - 1)\ \psi$, depending on the sign of the mass. We see then that, if we assume the duality for (N, k, F), this holds also for $(N, k \pm 1/2, F - 1)$.

Let us comment on the bound $k \geq F/2$ that we assumed in the previous analysis. We saw that, when we deform the scalar theory with a negative mass, we have maximal Higgsing and preservation of the global symmetry due to color-flavor locking. This is no more the case if $k < F/2$: in this regime, the gauge group is completely Higgsed and the global symmetry gets broken to $S[U(F/2 - k) \times U(F/2 + k)]$. The theory is gapless, described at low-energies by Goldstone bosons with Grassmannian target space

$$\mathrm{Gr}(F/2 + k, F) = \frac{SU(F)}{S[U(k + F/2) \times U(F/2 - k)]}. \tag{1.145}$$

There is no analog semi-classical phase for the fermionic theory, which does not manifest neither symmetry breaking nor gapless excitations. A modification of the previous correspondence

[19] This suggests that their classical dimension does not acquire quantum corrections [49].

is then needed, in order for a bosonic theory to describe the phase diagram of QCD_3 for $k < F/2$.

Finally, let us comment on the order of the phase transition in figure 1.5. It is not at the moment established if this phase transition is actually first or second order. However, we saw a large number of checks that show the validity of these dualities. Indeed, also in presence of first order phase transitions (or weakly-first order), in general, dualities can be predictive. For example, the matching of the phase diagram can be used to determine the vacuum structure of a strongly coupled theory, whenever this has a weakly coupled dual. Moreover, when the transition is weakly-first order, there is an approximate scale invariance related to the phenomenon of walking (this can be associated with tuning or complex CFTs, see [60,61]), so the physics of the theory resembles very much the one of a conformal field theory. In this case, the correspondence reminds a lot of a standard IR duality. So, in the following, we will use the bosonic duals to describe the phase diagram of QCD_3 regardless of the order of the phase transitions.

1.6.3 QCD_3: $k < F/2$ case

In the previous section, we saw how the duality in (1.140) apparently fails if $k < F/2$, since the semi-classical non-linear sigma-model (NLSM) phase (1.145) that the bosonic theory enjoys, has no trace in the semi-classical phase diagram of QCD_3, as happens in figure 1.5. However, although semi-classically the fermionic theory does not enjoy a gapless phase, we cannot exclude that, at the quantum level, the global symmetry of the theory can be spontaneously broken. For example, the Vafa-Witten theorem [62–64] does not rule out this possibility, suggesting a symmetry breaking pattern for QCD_3 at $k = 0$ of the form $U(F) \leftrightarrow U(F/2) \times U(F/2)$. This is compatible with the symmetry breaking pattern of the $U(k+F/2)_{-N}$ bosonic theory for $k = 0$. Similarly, the analysis of domain walls in four-dimensional QCD with F flavors [65] gives evidence that $SU(N)_{F/2-1}$ theory with F fermions enjoys a phase where its global symmetry $U(F)$ is spontaneously broken to $U(1) \times U(F-1)$, as happens for the bosonic dual (1.145). These suggest that the mismatch of the semi-classical phases among the theories that enjoy Aharony's duality may not be a symptom of the lack of validity of the bosonic description, but a hint of a possible quantum phase, invisible in the fermionic theory but accessible from the bosonic side. This is the guiding principle of the analysis in [31], which extended Aharony's dualities to the $k < F/2$ case.
The proposal of [31] is that the fermionic theory, on top of the semi-classical asymptotic phases $SU(N)_{k-F/2}$ and $SU(N)_{k+F/2}$ at large m, actually admits an inherently quantum phase for masses $|m| \sim g^2$, where the quark bilinear condenses as

$$\psi\psi^\dagger = \mathrm{diag}(x, ..., x, y, ..., y)$$

with x appearing $F/2+k$ times and y $F/2-k$ times with $x \neq y$, breaking $U(F) \to U(F/2+k) \times U(F/2-k)$. The theory is then gapless, described at low-energies by Goldstone bosons with target space

$$\mathrm{Gr}(F/2+k, F) = \frac{U(F)}{U(F/2+k) \times U(F/2-k)} \ , \tag{1.146}$$

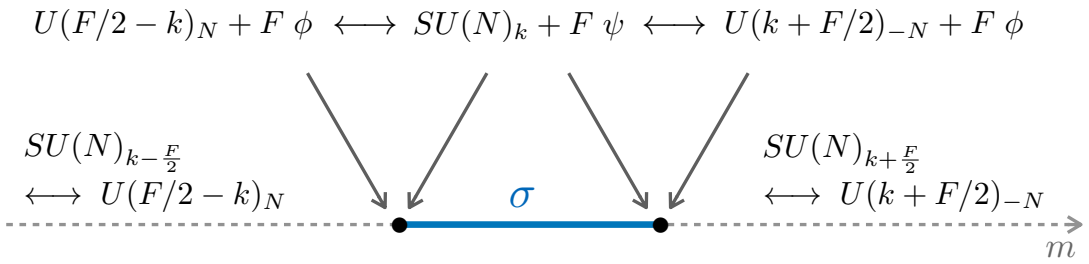

Figure 1.6: Phase diagram of $SU(N)_k + F\ \psi$ in the case $k < F/2$. For $|m| \lesssim g^2$ the theory enters a quantum phase, with complex Grassmannian (1.146). The two phase transitions, at negative and positive mass, are described by two different bosonic duals.

accompanied with a Wess-Zumino term Γ with coefficient N, see *e.g.* [66–68]. This resembles the chiral symmetry breaking of four dimensional QCD and it is clearly a strong coupling effect.

So, in this case, the phase diagram of the fermionic theory enjoys two phase transitions, where the gapless phase separates the two semi-classical topological phases. The vicinity of these two transitions can be then described by two distinct dual bosonic theories, $U(F/2-k)_N$ and $U(F/2+k)_{-N}$, each coupled to F complex scalars. When the squared masses of the scalars in the two theories, $\widehat{M}^2$ and M^2 respectively, are large and positive, they flow respectively to the large negative and large positive mass phases of the fermionic theory. Instead, when the squared masses of the scalars are negative, both theories flow to the same NLSM with target space (1.146). We see that this identified the duality map

$$\widehat{M}^2 \leftrightarrow -m, \quad M^2 \leftrightarrow m \tag{1.147}$$

looking close to the first (resp. second) phase transition. The phase diagram in the $k < F/2$ case is summarized in figure 1.6. The proposal shows the power of these dualities: a purely quantum phase of the fermionic theory can be accessed, in the semi-classical limit, by studying the corresponding bosonic duals!

There are several consistency checks for the validity of this proposal.
First of all, similarly to the $k \geq F/2$ case, it is possible to show that dualities are consistent under mass deformations.
Secondly, when $k = 0$ and the theory is time-reversal invariant, the Vafa-Witten theorem [62–64] suggests[20] that the global symmetry of the fermionic theory can be spontaneously broken down to $U(F/2) \times U(F/2)$, leading at low-energies to a theory of Goldstone bosons with target space

$$\mathrm{Gr}(F/2, F) = \frac{U(F)}{U\left(\frac{F}{2}\right) \times U\left(\frac{F}{2}\right)}. \tag{1.148}$$

Holography [69] shows a similar indication as well. We will come back to this point later in Chapter 3.

[20] We will discuss later the subtleties related to the VW theorem in section 1.6.4.

This matches the more general proposal for the non-linear sigma-model phase of eq. (1.145) and the corresponding phase diagram of $U(k+F/2)_{-N}$.
Moreover, the Goldstone bosons describing the resulting phase match the mixed anomaly between time-reversal symmetry and the $U(F)$ flavor symmetry [31].
The matching between monopoles and baryons that we saw in the $k \geq F/2$ case still holds in this regime. Let us first see the correspondence from the point of view of the fermionic theory. As in four dimensions, when we have chiral symmetry breaking in QCD, the Skyrme model represents the effective field theory that describes the dynamics of mesons. In particular, baryons are realized in the model as solitons, known as skyrmions. These are charged under a topological symmetry of the model and are classified by their winding number. This realizes the baryonic charge in the EFT. The model is equipped with a Wess-Zumino (WZ) term $k'\Gamma$, where k' denotes its level. This gives us the statistics of the skyrmions. If k' is odd, the Skyrmion have half-integer spin, while if k' is even, they have integer spin [66, 67, 70, 71]. In the same vein, in the NLSM phase of QCD_3 we can describe baryons as Skymions of the Grassmannian model, equipped with a WZ term. Since, baryons of the $SU(N)_k$ theory are bosons if N is even and fermions if N is odd, the level k' compatible with the correct statistic is $k' = N$.
Analogously, constructing the NLSM coming from the bosonic theory, the CS terms of the bosonic theories reduce to the WZ term of the Skyrme model. The monopole charge reduces then to the winding number of the skyrmions. So, again, monopoles can be identified with baryons, being both described in the NLSM as skyrmions!

Let us finally comment on the range of validity of the previous proposal. All the previous analysis remains valid until F is sufficiently small. The large F limit of QCD_3, namely $F \gg k, N$ with $F \to \infty$ was analyze in [72, 73]. In this regime, QCD_3 simplifies, since only a subset of Feynman diagrams is dominant and contributes to the correlation functions of the theory. These can be efficiently resummed and, the theory can be solved explicitly in perturbation theory. The analysis showed that for $F > F^*$ with F^* a function[21] of k, N [72], the phase diagram reduces to the $k \geq F/2$ case, where the transition at $m = 0$ is second-order and described by an interacting conformal field theory.[22] No bosonic dual is known for this fixed point. So, the previous analysis holds whenever $F < F^*$.
If we assume the phase diagram in figure 1.6 to be correct for $k = 0$ and $F < F^*$, it remains correct for any value of k. Indeed, starting from $(N, k = 0, F)$ with $F < F^*(N, k = 0)$, we can decouple f flavors and reach the theories $(N, k' \equiv \pm f/2, F' \equiv F - f)$. The bound $F' < F^*(N, k = 0) - 2k'$ remains compatible with $F < F^*$, so if the global symmetry is spontaneously broken at $k = 0$, it is broken also at $k \neq 0$ and the symmetry breaking pattern matches the proposed Grassmannian phase.

The limit k, N large with 't Hooft coupling $\lambda_{\text{CS}} \equiv \frac{N}{k}$ fixed was analyzed in detail in [75–81]. In this regime, the theory simplifies and can be studied consistently in a large k expansion. The phase diagram of QCD_3 reduces to the $k \geq F/2$ one, namely the two semi-classical phases are

[21] Estimations for its value can be found in [74].
[22] In particular, in this regime, 't Hooft anomalies are no more matched by the NLSM, but by the CFT itself.

separated by a single phase transition. Moreover, the transition was found to be second-order and the fixed point to be interacting. However, note that this analysis was derived by first decoupling the YM term from the Lagrangian, namely by studying the pure CS theory in presence of matter. As mentioned above, this is justified only when $k \gg N$, namely $\lambda_{\rm CS} \ll 1$, since gluons acquire a topological mass $\sim kg^2$ much bigger than the strong coupling scale $\sim Ng^2$ and can be integrated out before reaching strong coupling. However, if $k \ll N$, we cannot safely integrate out the gluons and drop the Yang-Mills term. The low-energy dynamics is indeed richer in this limit, as we will see in detail in the next section.

1.6.4 QCD_3 at large N

In this section, we describe the large N limit of QCD_3. This regime is obtained by sending N to infinity, keeping both k and F subleading to N, as opposed to the 't Hooft limit in three dimensions, where both k and N are sent to infinity, keeping the coupling $\lambda_{\rm CS} \equiv \frac{N}{k}$ fixed. In the following, we indeed keep fixed the scale $\Lambda = Ng^2$, which will be denoted as the 't Hooft coupling of the theory. This is nothing but the strong coupling scale of the theory. So, this limit resembles the standard 't Hooft limit of four dimensional QCD [82]. Indeed, the limit can be also studied using holography, as we will do in Chapter 3. Let us start from the Lagrangian of QCD_3

$$\mathcal{L}_{\rm YM\ CS} = -\frac{N}{2\Lambda}\mathrm{Tr}(F \wedge *F) + \frac{k}{4\pi}\mathrm{Tr}\left(AdA - \frac{2}{3}iA^3\right) + i\bar{\psi}_i \not{D}_A \psi^i - m_i^{\ j}\bar{\psi}_j\psi^i \tag{1.149}$$

with a generic mass term $\mathbf{m} = m_i^{\ j}$. This can be diagonalized using an $SU(F)$ symmetry to $\mathbf{m} = \mathrm{diag}(m_1, ..., m_F)$. The theory is time-reversal invariant if and only if $m = k = 0$. The vacuum structure can be explored by studying the VEV of the mesonic operator

$$M_j^{\ i} = \frac{1}{N}\bar{\psi}_i\psi^j, \quad (M_i^{\ j})^\dagger = M_j^{\ i}. \tag{1.150}$$

This represents an order parameter for the flavor and the time-reversal symmetries (when $k = 0$). Note that, being the matrix M in the adjoint of $U(F)$, its VEV can give us only some specific symmetry breaking patterns. However, this is sufficient to analyze the breaking of the $SU(F)$ symmetry. In particular, $\langle \mathbf{M} \rangle$ can be diagonalize via an $SU(F)$ transformation as

$$\langle \mathbf{M} \rangle = \Lambda^2 \mathrm{diag}(x_1, ..., x_F), \ \ x_i \in \mathbb{R}, \ \ i = 1, ..., F \tag{1.151}$$

where $x_i, \ \ i = 1, ..., F$ are the dimensionless eigenvalues of $\mathbf{M}$, scaling as $\mathcal{O}(1)$ in the large N limit. These are ordered using the Weyl group of $SU(F)$ as

$$x_1 \leq ... \leq x_F. \tag{1.152}$$

The symmetry breaking pattern, and the phase diagram, were obtained by constructing an effective potential for the meson VEV $V(\langle \mathbf{M} \rangle)$ at leading and subleading order in N in [25]. In the following, we do not describe the large N calculation in detail, limiting our analysis to the resulting phase diagrams.

- Leading order: the potential reads

$$V(x_i) = N\Lambda^3 \sum_{i=1}^{F} F(x_i) + N\Lambda^2 \sum_{i=1}^{F} m_i x_i \tag{1.153}$$

where $F(x)$ has two degenerate minima at $x = \pm 1$. At $m_i = 0$, we have $F+1$ degenerate vacua parametrized by the number p of positive eigenvalues $x_i = +1,\ i = 1, ..., p$. On the p-th vacuum, the global symmetry is broken spontaneously to $U(p) \times U(F-p)$ by the VEV of the mesonic operator, and the low-energy dynamics is described by a theory of Goldstone bosons with target space

$$\mathrm{Gr}(p, F) = \frac{U(F)}{U(p) \times U(F-p)}. \tag{1.154}$$

The pion decay constant f_π of this non-linear sigma-model can be shown to be large in the large N limit $f_\pi^2 \sim N\Lambda$ [83], so the model is weakly coupled.
When $m_i \neq 0$ for some i, the degeneracy is spoiled. Choosing

$$m_1 \geq m_2 \geq ... \geq m_p \geq 0 \geq m_{p+1} \geq ... \geq m_F,\ \ p \in \{0, ..., F\} \tag{1.155}$$

the vacuum

$$x_1 = ... = x_p = -1, \quad x_{p+1} = ... = x_F = 1 \tag{1.156}$$

is energetically favorable. The energy barrier that separates two vacua with two distinct symmetry breaking patterns is then of order N. Whenever one of the negative masses m_j changes sign, we encounter a first order phase transition which separates the p-th vacuum from the $(p+1)$-th one.
All the previous vacua are accompanied by a TQFT.[23] This can be inferred from the semi-classical analysis where $m_i \gg \Lambda$ and it is conjectured to remain true also at $m_i \ll \Lambda$. The p-th vacuum reads

$$\mathrm{Gr}(p, F) \times SU(N)_{k+p-F/2}. \tag{1.157}$$

From now on, we set the mass term $\mathbf{m} = m\mathbb{I}$, in order to obtain the phase diagram of QCD_3 at leading order in the large N limit. This is shown in figure 1.7. This is consistent also with Vafa-Witten theorem. In particular, the theorem predicts a symmetry breaking pattern $U(F) \to U(F/2) \times U(F/2)$ for massless QCD_3 at $k = 0$. However, this pattern was obtained by equipping QCD_3 with a time-reversal invariant mass, namely[24] $m_i = m,\ \ i = 1, ..., F/2$ and $m_i = -m,\ ,\ i = F/2+1, ..., F$ and sending it to zero. Doing the same by tuning in this way (1.156), we indeed obtain the same symmetry breaking pattern. However, the theorem does not exclude additional vacua with different symmetry breaking patterns, which can appear as degenerate states together with the VW vacuum, as happens for the phase diagram in figure 1.7.

[23] The CS term can be neglected in the calculation in the strict large N limit since diagrams including this term are suppressed by a power of k/N (or equivalently the topological mass $m_{\mathrm{CS}} \sim \frac{k\Lambda}{N}$ vanishes in the strict large N limit). However, this is still responsible for the deconfinement of the theory at low-energies.

[24] Actually, the theory is invariant under the simultaneous action of the Weyl group W of $SU(F)$ and $\mathcal{T}$, namely only $W\mathcal{T}$ is preserved.

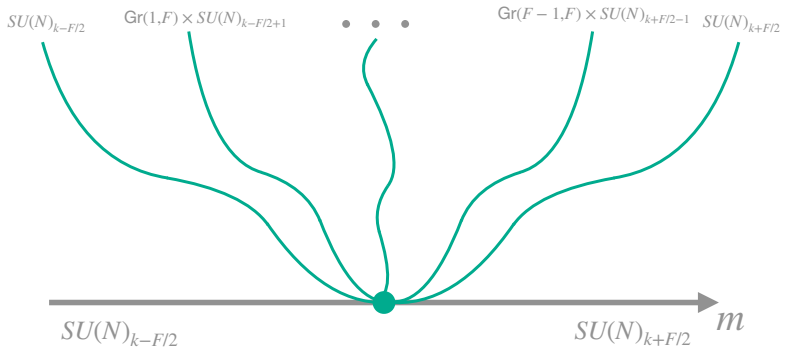

Figure 1.7: Phase diagram of large N QCD_3 at leading order. The green dot indicates a first order phase transition where $F+1$ vacua are degenerate.

- $1/N$ corrections: the potential is modified by a $\mathcal{O}(1)$ term, representing an interaction between the x_i eigenvalues

$$V_{\text{int.}} = \Lambda^3 \Delta \sum_{i,j} x_i x_j \tag{1.158}$$

where crucially[25] $\Delta > 0$. The degeneracy at $m = 0$ that we observed in the large N limit is now resolved by an energy contribution of order $\sim \mathcal{O}(1)$, as we can see by looking at the value of the potential (1.158) on the p-th vacuum

$$V_{\text{int.}} = \Lambda^3 \Delta (F - 2p)^2. \tag{1.159}$$

In particular, the VW vacuum $p = F/2$ is selected.
Taking care of the mass term, we see that the potential becomes

$$V_{\text{int.}} = \Lambda^3 \Delta (F - 2p) \left(F - 2p + \frac{Nm}{\Lambda \Delta} \right) \tag{1.160}$$

and for the value of the common mass

$$m(p) = \frac{4\Lambda\Delta}{N}(p - F/2 + 1/2) \tag{1.161}$$

we have a phase transition between the p-th and the $(p+1)$-th vacua. This is again first order, since the two vacua become degenerate but distinct at the transition point, while one of the two dominates whenever m is smaller or larger than $m(p)$.
Finally, k now contributes to the potential. Its contribution consists of a shift of the mass m by a factor $\frac{k\Lambda}{N}$. This is nothing but the additive renormalization of the mass caused by a CS term, which parallels the additive renormalization of the CS level caused by the fermionic mass that we saw in section 1.3. The phase diagram is depicted in figure 1.8.

[25] This was assumed in [25], in order to respect the VW theorem.

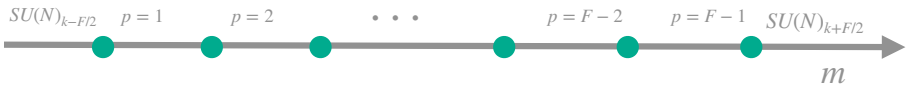

Figure 1.8: Phase diagram with $1/N$ corrections.

As it happens for generic k, F, and N, the whole phase diagram can be described by at most two bosonic theories. For $k \geq F/2$, this is described by a single bosonic theory, namely $U(k+F/2)_{-N}$ with F ϕ. For $k < F/2$, we need two bosonic duals, namely $U(F/2-k)_N$ and $U(F/2+k)_{-N}$. In this case, the former theory describes the first $F/2-k$ phases of the diagram, from $p=0$ to $p=F/2-k$, while the phases $p=F/2-k,...,F$ are described by the latter bosonic theory. Both for $k \geq F/2$ and $k < F/2$, the bosonic theory needs to be equipped with a sextic potential to correctly describe the phase diagram [25].
Since the CS levels of the bosonic duals are $\pm N$ and their ranks are $F/2 \pm k$, we are in the 't Hooft limit of these theories, so these are actually in a weakly coupled regime. It is then sufficient to study the bosonic theories in the semi-classical limit to understand the large N limit of QCD_3.

In conclusion, we saw that QCD_3 at leading order in the large N limit possesses a single first order phase transition between the two semi-classical topological phases $SU(N)_{k-F/2}$ and $SU(N)_{k+F/2}$, at which $F+1$ vacua become all degenerate.
Taking into account $1/N$ corrections, the theory develops a series of F phase transitions, and each of the $F+1$ phases is described by a Goldstone model with target space $\mathrm{Gr}(p,F)$ accompanied by a $SU(N)_{k+p-F/2}$ TQFT. The phase diagram of the theory is reproduced by two bosonic theories, equipped with a sextic potential.
Note that, since for $k \gg N$ it is known, as we reviewed above, that QCD_3 actually enjoys a second order phase transition separating the two semi-classical phases, varying k/N from $k/N \ll 1$ to $k/N \gg 1$, we expect to encounter a multicritical point for $k \sim N$ at which the F different first order phase transition coalesce into the single second order one [84].
We remark that since all the transitions the phase diagram enjoys are first order, this is an example of a "weak" duality, namely QCD_3 and the bosonic theories do not enjoy the same fixed point in the IR. Nevertheless, the phase diagrams match, as well as their excitations. In this way, we can use the weakly coupled description to infer properties of the strongly coupled fermionic theory, so the duality remains predictive.

Chapter 2

Holographic aspects of three dimensional theories

Holography represents a correspondence between a strongly coupled gauge theory and a weakly coupled quantum gravity theory. For this reason, it is a very powerful tool to understand non-perturbative physics of QFTs. In the following, we will employ this correspondence to shed light on the low-energy phase diagram of QCD_3. To do so, in this Chapter, we first review the basics of the gauge/gravity duality, with a particular focus on holographic duals of QCD theories. In section 2.1, we review the large N limit for vector and matrix models and its connection to string theory. In Section 2.2, we briefly review the Maldacena limit [85], the AdS/CFT dictionary, and the methods to extend the correspondence to non-conformal and/or non-supersymmetric theories. Finally, in Section 2.3 we review the construction of holographic models for QCD in four [86–89] and three dimensions [69, 90], in order to study the vacuum structure of QCD_3 in Chapter 4.

2.1 Large N limit

Non-Abelian gauge theories in four and three dimensions are notoriously difficult to analyze in the IR, being strongly coupled. However, field theories can simplify when we take the limit of a large number of fields. In this regime, only a particular set of Feynman diagrams contributes to the physics of the theory. In some cases, all diagrams can be resummed and the theory is solvable, as it happens for vector theories such as the $O(N)$ model [91–93]. In other cases, as for matrix theories, physics simplifies but the theory is still not solvable completely.
Vector models are an example of this simplification. These are theories in which the fundamental fields are vectors ϕ^a with N components $a = 1, ..., N$. In the large N limit, only a finite amount of Feynman diagrams, namely bubble diagrams, are relevant and they can be geometrically resummed. This happens, for example, for QED_3 coupled to N electrons in the large N limit [94]. This simplification regards also correlation functions. For any correlation function of m-operators, the disconnected and the connected parts scale differently with N. In particular, the connected part is suppressed, and all correlation functions can be calculated by

Wick contractions, like for weakly coupled field theories. This property is denoted as large N factorization.
In this section, we focus on the large N limit of matrix theories. These theories have fields that are $N \times N$ matrices. This is the case of pure $U(N)$ gauge theories, for example. These types of theories simplify in the large N limit. This simplification was studied in the context of pure YM theory by 't Hooft [82], which focuses on $SU(N)$ Yang-Mills theory in four dimensions. Denoting the gauge coupling as $g_{\rm YM}$, in order to take a meaningful limit, we want the β function of $g_{\rm YM}$

$$\frac{\partial g_{\rm YM}}{\partial \log \mu} = -\frac{11}{48\pi^2} N g_{\rm YM}^3 + \mathcal{O}(g_{\rm YM}^5) \tag{2.1}$$

to remain non-trivial in the large N limit. This can be ensured by keeping fixed the RG invariant scale $\Lambda_{QCD} = \Lambda_{UV} e^{-\frac{3}{22}\frac{(4\pi)^2}{N g_{\rm YM}^2}}$ at large N. This is achieved by keeping constant

$$\lambda \equiv N g_{\rm YM}^2 \tag{2.2}$$

as $N \to \infty$. In doing so, the β function remains non-trivial and organizes as a series in λ

$$\frac{\partial \lambda}{\partial \log \mu} = -\frac{11}{24\pi^2} N \lambda^2 + \mathcal{O}(\lambda^5). \tag{2.3}$$

The limit is denoted in literature as 't Hooft limit or the large N limit of $SU(N)$ YM theory in four dimensions.
In this regime, only a subset of Feynman diagrams contributes to the dynamics. To see how this happens, let us start by considering a $U(N)$ YM theory

$$S = -\frac{1}{2g_{\rm YM}^2} \int d^4x \mathrm{Tr} F^2. \tag{2.4}$$

and then extrapolate the finding to $SU(N)$. The gauge bosons $(A_\mu)^a_{\ b} = A^A_\mu (T^A)^a_{\ b}$ are in the adjoint of the $U(N)$ gauge group, so they can be represented as $N \times N$ matrices. The Lagrangian (2.4) has an explicit dependence on N and on the 't Hooft coupling as

$$S = -\frac{N}{2\lambda} \int d^4x \mathrm{Tr} F^2. \tag{2.5}$$

From (2.5), it seems that by sending N to infinity, we are actually reaching a semi-classical limit, where the factor $1/N$ plays the role of $\hbar$. This is what happens, for example, when we are dealing with vector theories. However, this time the number of fields grows as N^2 instead of N, so we need to be careful regarding this simplification. In fact, taking the propagator of the gluons, in Feynman gauge

$$\langle (A^\mu)^a_{\ b} (A^\nu)^c_{\ d} \rangle = \delta^a_d \delta^c_b \frac{g_{\rm YM}^2 \eta^{\mu\nu}}{p^2 + i\epsilon}, \quad \sum_A (T^A)^a_{\ b} (T^A)^c_{\ d} = \delta^a_d \delta^c_b \tag{2.6}$$

We see that this scales like $1/N$. We can represent this schematically using a double line notation, as in figure 2.1(a).

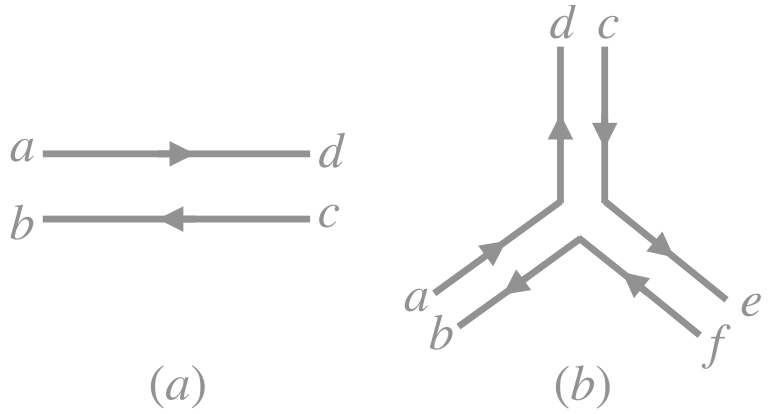

Figure 2.1: Double line notation for the propagator (a) and the triple vertex (b).

To each δ-function in the propagator (2.6), we associate a line connecting the corresponding two indices. These lines connect the various indices contracted in a vertex, see figure 2.1(c), Feynman diagrams are then constructed in this notation connecting lines in vertices and propagators. Any time a single line closes into a loop, we are summing $\sum_a \delta^a_a$ and so we get a factor of N. A gluon vertex as the one in figure 2.1(b) contributes as $g_{\rm YM}^{-2} = \frac{N}{\lambda}$. So, a generic Feynman diagram with V vertices, I internal propagators, and L loops scales with N as

$$\propto (g^2)^{I-V} N^L = N^{L-I+V} \lambda^{I-V} = N^{2-2g} \lambda^{I-V} \tag{2.7}$$

where g is the genus associated with the diagram. Indeed, each diagram can be mapped to a closed, compact, and oriented surface where edges correspond to propagators and faces to closed lines, see figure 2.2. This tells us that diagrams of smaller genus are dominant in the large N limit. So, when we consider, for example, the partition function Z of the theory, we see that only planar vacuum diagrams (namely surfaces of zero genus) are relevant at leading order in N. So, to determine Z, it is sufficient to resum only these diagrams. Although this represents a huge simplification, still efficiently resumming planar diagrams is a hard task in quantum field theory.
Looking at the next orders, we see that the partition function of the theory organizes in a genus expansion in $\frac{1}{N}$, see Fig 2.2.
This resembles what happens in closed oriented string theory [82] where interactions are organized into a genus expansion in the string coupling g_s. As we will see, the similarities between string theory and gauge theories do not stop here.
Also for gauge theories, in the large N limit correlation functions factorize. Consider a set of single trace operators $\mathcal{O}_a$, with normalization

$$\hat{\mathcal{O}}_a = \frac{1}{N} \mathcal{O}_a \tag{2.8}$$

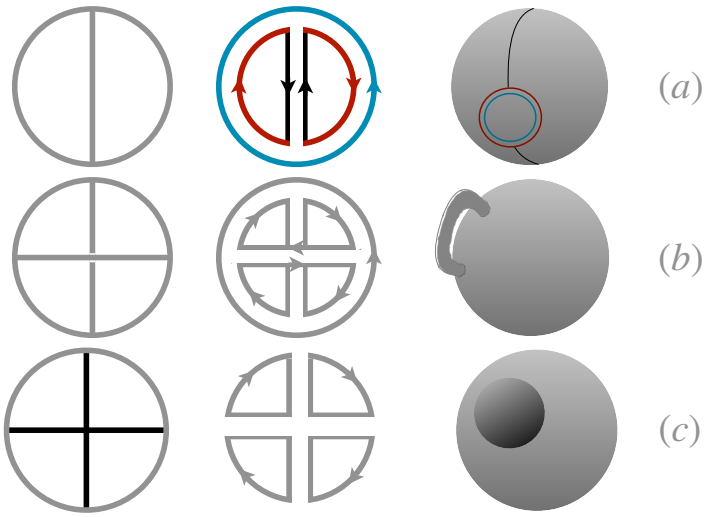

Figure 2.2: Genus expansion of Feynman diagrams. Planar diagram (a), non-planar diagram (b) and diagram with a fundamental loop (c).

so to keep two-point functions finite in the large N limit.[1] Correlation functions can be computed by adding a source J_a to its corresponding operator $\mathcal{O}_a$

$$\mathcal{L} \to \mathcal{L} + \sum_{a=1}^{n} J_a \hat{\mathcal{O}}_a. \tag{2.9}$$

where J_a/N is kept fixed to have a non-zero source in the large N limit. The connected correlation functions scale then as

$$\langle \hat{\mathcal{O}}_1 .... \hat{\mathcal{O}}_r \rangle_c \propto N^{2-r}. \tag{2.10}$$

We see that, for any r, the connected contribution is sub-leading with respect to the disconnected one

$$\langle \hat{\mathcal{O}}_1 \rangle ... \langle \hat{\mathcal{O}}_r \rangle \propto N^{2r} \tag{2.11}$$

realizing large N factorization.
Correlation functions of single trace operators are then similar to correlation functions of vertex operators in closed-oriented string theory.
In the multi-trace case, correlators are suppressed[2] by some powers of N. Correspondingly, their contribution is subleading in the strict large N limit.

The same reasoning holds, at leading order in the large N limit, also for $SU(N)$ YM, since

[1] Normalizing in this way allows states created by acting with the operator on the vacuum to have finite norm in the large N limit.

[2] These have different normalizations with respect to the single trace, to ensure the correct scaling of their two-point function in the large N limit.

their gluon loops scale in this regime $\sum_A (T^A)^a_b (T^A)^c_d = \delta^a_d \delta^c_b + \mathcal{O}\left(\frac{1}{N}\right)$, as happens for the $U(N)$ case. In presence of fundamental matter, the previous analysis can be adapted. In particular, each fundamental contributes as a vector in the large N counting. Let us take F of them and require F to be subleading to N. In double line notation, the propagator of this field is a single line, since each fundamental has a single gauge index. A fundamental loop contribues then $\propto F/N$. The counting in eq.(2.7) gets modified as

$$\propto (g^2)^{I-V} N^{L-L_F} = N^{2-2g-b} \lambda^{I-V} \tag{2.12}$$

where L_F is the number of fundamental loops. They play the role of boundaries b of the associated surface and they are suppressed with respect to pure gluon diagrams. In this limit, the flavors are said to be quenched.
We see then that field theories in the large N limit share many similarities with the genus expansion of closed-oriented string theory (in presence of only adjoint matter) or open and closed string theory (in presence of fundamentals). The expansion parameter in the string theory g_s corresponds to the expansion parameter $1/N$ of the field theory. Correlation functions of single trace operators correspond to correlation functions of vertex operators.
The previous reasoning adapts to $SO(N)$ and $Sp(N)$ theories also. In these cases, since the fundamental representation is real, there is no direction in the lines defining the propagators. The surfaces corresponding to the Feynman diagrams are then non-orientable. So, the large N expansion organizes as a genus expansion in an unoriented string theory.
These similarities between the large N expansion of gauge theories and the perturbative expansion in string theory are made precise via the gauge/gravity correspondence program, which will be reviewed in the next section.

2.2 Gauge/gravity correspondence

In this section, we review the main aspects of the gauge/gravity correspondence. This will help us in the study of the low-energy dynamics of three dimensional theories. We first start by reviewing the AdS/CFT correspondence and the associated dictionary. We then focus on the description of confinement in holography and, in the end, we discuss generalizations of the duality involving non-conformal field theories.

2.2.1 AdS/CFT

Holography relates a quantum gravity theory in a $d+1$ dimensional spacetime to a QFT on its d-dimensional boundary. In particular, in the AdS/CFT correspondence, this space is a $d+1$ dimensional Anti-de Sitter space (AdS_{d+1}), and the gravity theory is dual to the CFT living on its boundary. The quantum gravity theory can be thought of as a hologram of the CFT at the boundary. This idea was suggested in the past both by the large N limit of gauge theories that we saw, but also from black hole thermodynamics [95]. However, the main evidence of the duality came out in the seminal work of Maldacena [85]. In this section, we first introduce

some notions on type II string theories and their supergravity limits. We then review the Maldacena argument in detail and we uncover the dictionary between supergravity in AdS and the conformal field theory on its boundary. Finally, we focus on how confinement can be realized holographically.

Type IIA and IIB supergravities represent the low-energy limits of type IIA and IIB string theories, respectively. These are supersymmetric theories preserving 32 supercharges. Type IIA is non-chiral $\mathcal{N} = (1, 1)$ in ten dimensions, so the two Majorana-Weyl spinors ϵ_L, ϵ_R associated with its conserved supercharges $\epsilon_L Q^L + \epsilon_R Q^R$ satisfy opposite chirality conditions

$$\epsilon_{L,R} = \pm\bar{\gamma}\epsilon_{L,R} \tag{2.13}$$

where $\bar{\gamma} = \gamma^0 ... \gamma^9$ is the ten dimensional chiral matrix. Type IIB is instead chiral $\mathcal{N} = (2, 0)$, so both Majorana spinors satisfy the chirality condition $\epsilon_{L,R} = \bar{\gamma}\epsilon_{L,R}$. The two theories have different bosonic field content

- Type IIB has two scalars, the dilaton ϕ, and the axion C_0, a metric g_{MN}, a NSNS field B_2 and a set of RR p-forms C_p. In particular (due to the choice of GSO projection in the corresponding string theory), only p-forms of even dimensions are allowed. The VEV of e^ϕ represents the type IIB string coupling g_s. The axion C_0 is periodic $C_0 \sim C_0 + 1$ and appears in the supergravity Lagrangian, together with the dilaton, only in a complex combination, the axio-dilaton τ, defined as

  $$\tau = C_0 + ie^{-\phi}. \tag{2.14}$$

  The forms C_p are related by Hodge duality to $C_{9-\mathrm{p}}$. So, only the forms C_0, C_2, C_4 are independent. In particular, the C_4 field strength is self-dual

  $$F_5 = *F_5. \tag{2.15}$$

- Type IIA contains a dilaton ϕ, a metric g_{MN}, a NS-NS two-form B_2 and the RR p-forms C_p with p odd. Again, there are three independent forms C_1, C_3, C_9. The VEV of e^ϕ represents the type IIA string coupling.

Supergravity represents the low-energy limit of string theory. Indeed, at low enough energy, massive string states can be integrated out and, if energies are smaller compared to the string mass $\sim \frac{1}{\sqrt{\alpha'}}$, the dynamics of massless string states is described by the corresponding local supergravity theory. This approximation remains valid until the curvature R_s of the background around which we expand supergravity is small enough compared with the string scale. So, supergravity remains valid only in the regime

$$R_s \ll \frac{1}{\alpha'}, \quad E \ll \frac{1}{\sqrt{\alpha'}}, \quad g_s \ll 1. \tag{2.16}$$

In particular, g_s is kept small to have a perturbative description of the corresponding string theory. In the following, we will mainly work in this regime.

Closed string perspective

Both in type IIA and IIB there exist 1/2 BPS solitons. These are the p-branes [96]. They have codimension 10-p and are charged under the $C_{\mathrm{p}+1}$ fields of the theory through the minimal coupling

$$S_{\text{coupling}} \propto \int_{\mathcal{M}_{p+1}} C_{p+1} \tag{2.17}$$

where $\mathcal{M}_{\mathrm{p}+1}$ represents their worldvolume. In flat space, this is nothing but $\mathbb{R}^{1,\mathrm{p}}$, spanned by $\mathrm{p}+1$ coordinates x^μ, $\mu = 0, ..., \mathrm{p}$. This generalizes the concept of worldline for a particle charged under a gauge field through a minimal coupling. So, only branes with an even (resp. odd) p exist in type IIA (resp. IIB). Being solitons of supergravity, they source a non-trivial metric [97]

$$ds^2 = H_{\mathrm{p}}^{-1/2}\eta_{\mu\nu}dx^\mu dx^\nu + H_{\mathrm{p}}^{1/2}dx^i dx^i, \tag{2.18}$$

where

$$H_{\mathrm{p}} = 1 + \left(\frac{L_{\mathrm{p}}}{r}\right)^{7-\mathrm{p}} \tag{2.19}$$

is an harmonic function of the transverse coordinate of the branes $r = x^i x^i$ and $i = p+1, ..., 10$. In the formula, the scale L_{p} reads

$$L_p^{7-p} = (4\pi)^{\frac{5-\mathrm{p}}{2}}\Gamma\left(\frac{7-\mathrm{p}}{2}\right) g_s N(\alpha')^{\frac{7-\mathrm{p}}{2}}. \tag{2.20}$$

This metric preserves an $SO(1,\mathrm{p}) \times SO(9-\mathrm{p})$ isometries.
Branes, moreover, are charged under $C_{\mathrm{p}+1}$ fields and correspondingly source a flux for them. They couple to the dilaton as well, introducing, in general, a non-trivial background for it. The complete solution of the supergravity equations of motion includes then also the non-trivial profiles [97]

$$C_{\mathrm{p}+1} = -(H_{\mathrm{p}}^{-1} - 1)g_s^{-1}dx^0 \wedge ... \wedge dx^{\mathrm{p}}, \;\; e^{2\phi} = g_s^2 H_p^{\frac{3-\mathrm{p}}{2}} \tag{2.21}$$

for the $(\mathrm{p}+1)$-form and the dilaton. The charge of this brane Q_{Dp} equals the flux of the Hodge dual of the $p+2$ field strength $F_{\mathrm{p}+2}$ across an $S^{8-\mathrm{p}}$ sphere surrounding the brane

$$Q_{\mathrm{Dp}} = \frac{1}{2\kappa_0^2}\int_{S^{8-\mathrm{p}}} *F_{(\mathrm{p}+2)} = \mu_{\mathrm{p}} \tag{2.22}$$

where $2\kappa_0^2 = (2\pi)^7\alpha'^4$ and $\mu_{\mathrm{p}} = (2\pi)^{-p}(\alpha')^{-\frac{p+1}{2}}$ [98].
The solution can be shown to preserve 16 of the original 32 supercharges of the supergravity theory. Being the solution BPS, we can also align N Dp branes along the same directions preserving the same amount of supersymmetries. In the transverse space, they lie in general at different points $\vec{r}_i$, $i = 1, ..., N$. The background generated by this system remains the same, up to a change of H_{p}

$$H_{\mathrm{p}} = 1 + \sum_{i=1}^{N} \frac{L_{\mathrm{p}}^{7-\mathrm{p}}}{|\vec{r} - \vec{r}_i|^{7-\mathrm{p}}} \tag{2.23}$$

which is now a multi-centered harmonic function. When all the branes coincide at a point $\vec{r}_i = 0$ of the transverse space, the harmonic function reduces to (2.19) whose length $L_{\rm p}$ is rescaled to $L_{\rm p} N^{\frac{1}{7-{\rm p}}}$.
As was shown in [99], these solutions are nothing but the low-energy limit of Dp branes, namely hyperplanes describing the dynamics of open strings obey Dirichlet boundary condition. In the next section, we focus on this aspect.

Open string perspective

Open strings whose worldsheet fields $X^i,\ i = {\rm p}+1, ..., 10$ obey Dirichlet boundary conditions and have their endpoints lying on a hyperplane extended along the remaining directions. These hyperplanes are denoted as Dp branes. On the other hand, the worldsheet fields $X^\mu,\ \mu = 0, ..., {\rm p}$, parametrizing the other directions, satisfy Neumann boundary conditions. The directions $x^{{\rm p}+1}, ..., x^{10}$ transverse to the branes are denoted as Dirichlet, while the directions $x^0, ...x^{\rm p}$ along the branes as Neumann.
We can impose these boundary conditions on open strings living in a type II background. These preserve sixteen supercharges and can be identified at low-energies [99] as the solitonic p-branes of type II closed string theory described previously!
The dynamics of the excitations associated with these hyperplanes is described, at low energies, by a supersymmetric quantum field theory of a ${\rm p}+1$ dimensional $U(1)$ vector multiplet living on the brane worldvolume and interacting with the closed string fields via the DBI action[3]

$$S_{DBI} = -T_{\rm p} \int_{\mathcal{M}_{{\rm p}+1}} d^{{\rm p}+1}x\ e^{-\phi} \sqrt{-\det\left(P[g] + \mathcal{F}\right)} + \mu_{\rm p} \int_{\mathcal{M}_{{\rm p}+1}} e^{\mathcal{F}} \wedge \sum_q C_q \equiv S_{\rm open} + S_{\rm int}. \quad (2.24)$$

In eq. (2.24), $T_{\rm p}$ and $\mu_{\rm p}$ are respectively the tension and the charge of the Dp brane, $P[g]$ is the pullback of the string frame metric g on the Dp brane worldvolume, $\mathcal{F} = B_2 + 2\pi\alpha' F$ with B_2 the closed string NS-NS field and F is the gauge field living on the Dp brane. The first term in (2.24) represents the coupling between the NS-NS fields and the gauge field. The last term, instead, is a generalized CS term, where $\sum_q C_q$ is a poly-form obtained by the sum of all the RR fields of the theory. Zero modes describing the shape of the brane in the transverse space correspond to the scalars $X^i(x^\mu)$ belonging to the vector multiplet of the SYM theory living on its worldvolume.[4] The pullbacks are then obtained through this parametrization of the brane worldvolume

$$P[g]_{\mu\nu} = g_{MN} \partial_\mu X^M \partial_\nu X^N \quad (2.25)$$

where $X^M = (x^\mu, X^i(x^\mu))$.
The DBI factorizes into an action involving only the fields on the brane, denoted as $S_{\rm open}$, and an action involving interactions between open and closed string fields, denoted as $S_{\rm int}$.
The tension T_p and the charge μ_p of the branes are related by the equation

$$\mu_{\rm p} = T_{\rm p} = (2\pi)^{-{\rm p}} (\alpha')^{-\frac{{\rm p}+1}{2}} \quad (2.26)$$

[3] Here, we show only the bosonic part of the DBI.
[4] Here, we are choosing static gauge [97].

since the branes are 1/2 BPS.
In a flat background $g_{MN} = \eta_{MN}$ and $B_2 = 0$, so we can expand the kinetic part of the DBI for energies[5] $E \ll 1/\sqrt{\alpha'}$. Keeping the expansion up to two derivatives[6], we obtain the action of SYM in $\mathrm{p}+1$ dimensions. Its corresponding gauge coupling reads

$$g^2_{\mathrm{SYM}} = 2g_s(2\pi)^{\mathrm{p}-2}{\alpha'}^{\frac{\mathrm{p}-3}{2}} \tag{2.27}$$

where $e^{\phi_0} = g_s$.
The previous analysis can be generalized when we consider a stack of N branes. When these coincide in transverse space, the gauge group living on their worlvolume enhances to $U(N)$. This is Higgsed partially when some of the branes are separated in the transverse directions. In particular, the endpoints of the open string carry a representation of the gauge group through a corresponding CP factor. So, the gauge enhancement comes when the excitations of a string connecting one brane with another become massless, namely when the branes coincide at the same transverse point. This introduces additional massless vector multiplets in the worldvolume theory, leading to the gauge enhancement $U(1)^N \to U(N)$.

Let us now specify the discussion on D3 branes. Their low-energy effective dynamics is $U(N)$ $\mathcal{N} = 4$ SYM in four dimensions. The scalars parametrizing the six directions transverse to the brane corresponds to the six scalars of $\mathcal{N} = 4$ SYM. Its R-symmetry is $SU(4)_R \simeq SO(6)_R$ and maps to the $SO(6)$ isometry of the transverse space, as we can see from the R-symmetry representation of the X^i scalars. The gauge coupling is $g^2_{\mathrm{SYM}} = 4\pi g_s$. Moreover, a θ angle can be introduced in the theory as a VEV for the axion $\langle C_0 \rangle = \frac{\theta}{2\pi}$. As in type IIB supergravity, only a complex combination of the two couplings, the complexified gauge coupling $\tau = \theta/2\pi + i/g^2_{\mathrm{SYM}}$, appears in the SYM Lagrangian. The $U(1)$ part of $U(N)$ describes the center of mass position of the branes and it is decoupled from the rest of the theory. We are then left with $\mathcal{N} = 4$ $SU(N)$ SYM in four dimensions. The β function of the corresponding coupling vanishes at all orders in perturbation theory and non-perturbatively [100]. The theory is then classically exact and conformal for any value of complexified gauge coupling τ. This is a superconformal field theory (SCFT) with superalgebra $\mathfrak{psu}(2,2|4)$. Its bosonic subalgebra is given by the conformal algebra in four dimensions $\mathfrak{so}(2,4)$ and the R-symmetry one $\mathfrak{so}(6)_R$.

Maldacena limit

Let us consider a set of D3 branes in type IIB string theory. Their low-energy dynamics is described by massless closed string states together with massless open string excitations localized on their worlvolume. The two types of excitations interact via the interaction part S_{int} of the DBI. Massive string states indeed are expected to be negligible for energies smaller than $\frac{1}{\sqrt{\alpha'}}$ or equivalently in the $\alpha' \to 0$ limit. Interactions between the open string and the closed string modes, mediated by S_{int}, scale as

$$S_{\mathrm{int}} \propto g_s(\alpha')^2. \tag{2.28}$$

[5]Indeed, at energies of order α' the DBI starts to be highly non-local [97].
[6]The first higher derivative correction goes like ${\alpha'}^2 F^4$.

So, in the $\alpha' \to 0$ limit, closed string fields actually decouple from the D-brane theory. Moreover, looking at Newton's constant of type IIB

$$G_N = \frac{(2\pi)^7 \alpha'^4 g_s^2}{16\pi} \tag{2.29}$$

we see that in the $\alpha' \to 0$, G_N goes to zero. So, in the same limit, gravity becomes free. We are then left with two decoupled sectors: the gauge theory on the brane and the free supergravity theory in the bulk.

D3 branes are also type IIB solitons. They source a non-trivial metric and a flux for C_4. When we deal with a large number N of them in flat spacetime, their gravitational backreaction modifies the original flat space background. We are then left with type IIB string theory on the background generated by the D3 branes. Their geometry (2.18) has an horizon[7] at $r = 0$. Due to this horizon, the energy E_R of an excitation located at a point $r = R$ and the energy E_∞ of the same excitation measured at infinity are related by a redshift factor

$$E_R \sim \frac{1}{\sqrt{-g_{00}}} E_\infty \sim H_3^{1/4} E_\infty. \tag{2.30}$$

So, the energy E_0 of an excitation close to the horizon redshifts to zero at infinity. Any excitation close to the throat is then seen as a low-energy one at infinity. At the same time, gravity is free at small energies, since the dimensionless coupling describing the interaction $\hat{G}_N = G_N E^8$ goes to zero for $E \to 0$.
We remain with two types of low-energy excitations from the perspective of an observer at infinity: the ones with arbitrary energies close to the horizon (in the "throat" of the brane) and the ones associated with the free bulk gravity. The latter type is decoupled from the former since no excitation can escape the "throat" due to the gravitational potential and any excitation at infinity have a vanishing cross-section on the stack at low-energies $\sigma \sim E^3 L_3^8$ [101].
So, again, we are left with two decoupled excitations: the near-horizon ones and free gravity. The latter matches the free supergravity sector we found before performing the backreaction. We are then led to identifying the former with the $\mathcal{N} = 4$ SYM theory on the D3 branes. Measuring excitations at infinity, we then require $r \to 0$, $\alpha' \to 0$ with r/α' fixed, in order to have E_∞ in (2.30) finite for a near horizon excitation.
Relabeling $R \equiv L_3$ and changing variables $z = \frac{R^2}{r}$, the geometry reduces in this limit to

$$ds^2 = R^2 \left(\frac{dx^\mu dx_\mu + dz^2}{z^2} + d\Omega_5^2 \right) \tag{2.31}$$

which is nothing but the Poincaré patch of AdS_5 together with an S^5 metric. Both have the same radius R. The AdS geometry possesses a boundary at $z = 0$, which is $\mathbb{R}^{1,3}$ in the Poincaré patch. On this boundary lives $\mathcal{N} = 4$ $SU(N)$ SYM theory. We then establish the correspondence

$$\mathcal{N} = 4 \text{ SYM at large } N \text{ and } \lambda \text{ on } \partial \mathrm{AdS}_5 \leftrightarrow \text{type IIB SUGRA on } \mathrm{AdS}_5 \times S^5 \tag{2.32}$$

[7]Notice that this is true only for D3 branes, since for generic Dp branes the compact space $S^{8-\mathrm{p}}$ shrinks to zero at $r = 0$. If $\mathrm{p} = 3$, instead, S^5 as a radius $R^2 = \alpha'(4\pi g_s N)^{1/2}$ [97].

where

$$R^4 = 4\pi\lambda\alpha'^2, \;\; g^2_{\rm SYM} = 4\pi g_s \tag{2.33}$$

with λ the $SU(N)$ 't Hooft coupling $\lambda \equiv N g^2_{\rm SYM}$.
The previous analysis relies heavily on supergravity. This is valid whenever the curvature of the background is small with respect to the string length, and g_s is small. Using the map in eq. (2.33), these requirements

$$\frac{R^4}{\alpha'^2} \sim \lambda \gg 1, \;\; g_s \sim g^2_{\rm SYM} \ll 1 \tag{2.34}$$

map to the following conditions in field theory[8]

$$N \gg 1, \;\; \lambda = g^2_{\rm SYM} N \gg 1. \tag{2.35}$$

So we see that in the large N limit, we can describe a strong coupling QFT via a classical theory of gravity.
Corrections in α' and g_s map then to $\frac{1}{\lambda}$ and $\frac{1}{N}$ corrections respectively. When these corrections are strong, we are far away from the Maldacena limit. However, there is strong evidence that the correspondence remains valid also taking into account these corrections. So the duality in its stronger version actually relates a string theory on $\mathrm{AdS}_5 \times S^5$ to $\mathcal{N} = 4$ SYM at its boundary

$$4d\,\mathcal{N} = 4 \;\; SU(N)\,\text{SYM on } \partial\mathrm{AdS}_5 \leftrightarrow \text{type IIB string theory on } \mathrm{AdS}_5 \times S^5. \tag{2.36}$$

The dictionary

The previous correspondence is even more powerful since it establishes a dictionary between operators of the CFT on the boundary and states in the gravity theory. Since the correspondence maps a strong coupling QFT to a weak supergravity theory, having a precise dictionary gives us a great advantage: observables of the strong coupling CFT, as correlation functions, can be obtained in supergravity by a semiclassical computation!

Let us start reviewing the dictionary by considering the superconformal algebra of SYM. Above, we saw that the R-symmetry of SYM theory on the D3 branes was realized as the isometry of the $\mathbb{R}^6$ space transverse to the branes. After the backreaction, the superconformal algebra of the CFT $\mathfrak{psu}(2,2|4)$ with bosonic subalgebra $\mathfrak{so}(2,4) \oplus \mathfrak{so}(6)$ is reproduced by the isometries of $\mathrm{AdS}_5 \times S^5$ and the supersymmetries preserved by the background. In the Poincaré patch only the isometries $\mathfrak{so}(3,1) \oplus \mathfrak{so}(1,1)$, namely the Lorentz group and dilations, are manifest. In particular, dilations act as

$$x^M \equiv (x^\mu, z) \to \lambda(x^\mu, z) \tag{2.37}$$

on the AdS_5 coordinates.
The $\mathfrak{so}(6)$ symmetry maps instead into the isometry of S^5. So, the bosonic subalgebra of the superconformal algebra of the CFT at the boundary maps to the isometry of $\mathrm{AdS}_5 \times S^5$, while the supersymmetries preserved by the CFT are mapped to supersymmetries preserved by the

[8] This ensures that non-perturbative states are heavy. The other limit $g_s \gg 1$ and $N \ll 1$ is invalid since D-string becomes actually light, breaking the gravity approximation [101].

background itself.

The correspondence relates operators in the CFT to states in supergravity. In particular, operators of the CFT represent boundary conditions for the supergravity fields. This identification can be inferred by looking at (2.33). We see that the gauge coupling $g^2_{\rm SYM}$ changes when the string coupling g_s does. The latter represents the asymptotic value of the dilaton at infinity, namely at the boundary of AdS. So, changing the gauge coupling changes the boundary condition for the dilaton. From the field theory point of view, this is equivalent to changing a source for the Maxwell operator $-\frac{1}{4}{\rm Tr}F^{\mu\nu}F_{\mu\nu}$. Considering for example a scalar operator $\mathcal{O}_\phi(x)$ in the CFT, adding a source $\phi_0(x)$ to it corresponds in the supergravity theory to impose a specific boundary condition $\phi_0(x)$ for a scalar field $\phi(x,z)$ in the bulk. At the level of the partition function, the correspondence can be recast as

$$Z_{\rm string}\left[\phi(x,z)\big|_{z=\epsilon}=\phi_0(x)\right]=\langle e^{\int d^4x\,\phi_0(x)\mathcal{O}_\phi(x)}\rangle_{CFT}. \tag{2.38}$$

In generic dimension d, this can be made precise by studying the equations of motion for a scalar field $\phi(x,z)$ in ${\rm AdS}_{d+1}$ spacetime

$$(\Box_{AdS}-m^2)\phi=0. \tag{2.39}$$

Close to the boundary $z=0$, solutions of the equations of motion scale as

$$\phi(x,z)\sim A(x)z^{\Delta_+}+B(x)z^{\Delta_-} \tag{2.40}$$

where $\Delta_\pm=\frac{d}{2}\pm\sqrt{\frac{d^2}{4}+m^2R^2}$.
Not all modes are normalizable: for $m^2>0$, z^{Δ_-} diverges at the boundary, while z^{Δ_+} decays. Let us take $m^2>0$ and impose boundary conditions on the non-normalizable mode at $z=\epsilon\ll 1$

$$\phi(x,z)\Big|_{z=\epsilon}=\epsilon^{\Delta_-}\phi_0(x). \tag{2.41}$$

The fields ϕ_0 live on the boundary. It transforms under dilation as $\phi_0\to\lambda^{-\Delta_-}\phi_0$, being $\phi(x,z)$ a scalar field. This boundary condition is interpreted in the CFT as a source of the corresponding dual scalar operator $\mathcal{O}_\phi$ of weight

$$\Delta_+=d-\Delta_-. \tag{2.42}$$

Note that the weight is above the unitarity bound for a scalar in a CFT $\Delta_+\geq\frac{d-2}{2}$.
This establishes also a map between the correlation functions of the two theories. We can calculate connected correlation functions of n local operators $\mathcal{O}_{\phi_i}$ in the CFT by deriving the string partition function in their corresponding sources ϕ_0^i. This can be done by renormalizing the on-shell action and rewriting the supergravity fields (and then the action) as functions of the boundary condition ϕ_0^i. This prescription is known as holographic renormalization [102]. In this way, we can, for example, calculate the two-point function of a local operator $\mathcal{O}_{\phi_i}$ and show that this has the same structure as the correlation function of operators of dimension Δ_+ in the CFT. By calculating the one-point function, we can also see that $A(x)$ in (2.40) is proportional

to the VEV of the operator $\mathcal{O}_\phi$ itself.

All the operators that we constructed above are irrelevant or marginal, having $\Delta_+ \geq d$. This comes from our choice $m^2 > 0$ for the mass of the scalar in AdS. However, in AdS, scalar fields can have a small negative mass, if this respects the Breitenlonher-Freedman (BF) bound

$$\frac{d^2}{4} \geq -m^2 R^2. \tag{2.43}$$

This is related to the need of imposing decay boundary conditions at the boundary of AdS.[9] Whenever this bound is respected, the operator corresponding to Δ_+ has always a weight satisfying the unitarity bound, while when m is smaller, the weight becomes complex. So, we see that we can get marginal operators when $m^2 = 0$ and relevant operators if

$$-\frac{d^2}{4} \leq m^2 R^2 < 0. \tag{2.44}$$

Moreover, for $m^2 < 0$, Δ_- is positive and it can also be above the unitarity bound if the mass lies in the interval

$$-\frac{d^2}{4} \leq m^2 R^2 \leq -\frac{d^2}{4} + 1. \tag{2.45}$$

So, in this regime, also Δ_- is a good weight for an operator $\mathcal{O}$. We can then impose the boundary condition on the other mode and describe an operator with weight Δ_-. This possibility is known as double quantization.

The previous analysis holds also for fields with arbitrary spins on AdS_{d+1}. For example, the metric g_{MN} can be mapped in the stress-energy tensor $T_{\mu\nu}$ of the CFT. Gauge symmetries in the bulk A_M are mapped to conserved currents on the boundary J_μ. More generally, we can show that any protected (namely BPS) single trace operator at the boundary is mapped to a one-particle state in the bulk, while multi-trace operators are mapped to multi-particle states [101]. Finally, also anomalies match across the duality (see for example [103] for the computation of the Weyl anomaly).

Confinement in holography

In this section, we comment on how we can test confinement using holography.
In general, studying confinement can be a hard task, since gauge theories confine when they are strongly coupled. In field theory, confinement was explored in the context of SQCD [104], as well as in two dimensions [105]. However, thanks to the gauge/gravity correspondence, we should be able to understand confinement via semi-classical computations in the corresponding supergravity theory, which are expected to be more manageable.
We would like then to understand confinement through holography. The hallmark of strict

[9] Basically, AdS acts as a box for the scalar field [98]

confinement in field theory comes from the behavior of Wilson loops. As reviewed in Chapter 1, this is a non-local gauge-invariant operator defined on a closed curve $\mathcal{C}$ as

$$W_R[\mathcal{C}] = \mathrm{Tr}_R P e^{i \oint_{\mathcal{C}} A} \tag{2.46}$$

where $A = A^a T_R^a$ is the gauge potential and R denotes the representation of the generators T_R^a. Taking the loop large, its VEV gives us information about the behavior of the IR dynamics of the theory. This loop, indeed, can be thought of as the worldline of two static sources in the representation R (a quark and an antiquark) generated from the vacuum at a certain time $t = -T/2$, separated by a distance L and finally annihilated at $t = T/2$, see figure 2.3.

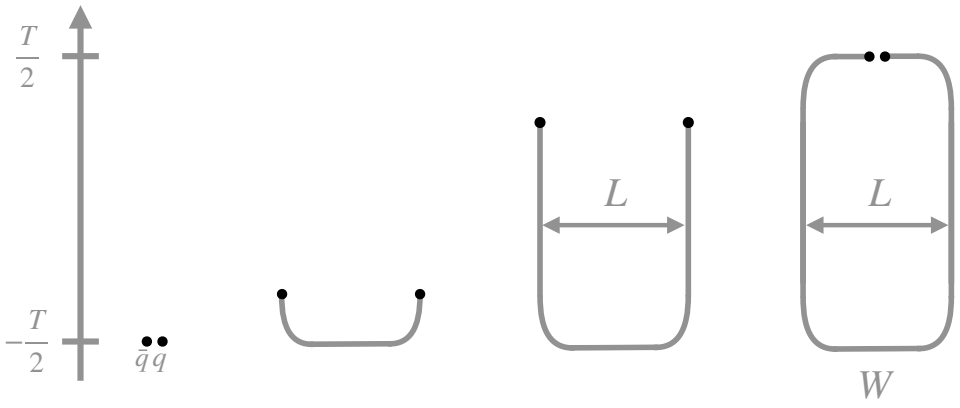

Figure 2.3: Wilson loop as wordlines of a quark-antiquark pair.

In Euclidean signature, the VEV of the loop reads then $\langle W \rangle \sim e^{-TV(L)}$ with $V(L)$ representing the interaction potential between the two probe particles. In a confining theory, the potential goes like $V(L) = T_R L$. The electric field between the two probes has a fixed cross-sectional area and forms a flux tube between the two quarks. Its tension is T_R and depends on the representation of the probes. This, in four dimensional pure YM theory, is proportional to the dynamically generated scale Λ_{YM}

$$T_R \sim \Lambda_{\mathrm{YM}}^2. \tag{2.47}$$

We see then that if this VEV goes as the exponential of the area of the loop (area law), test particles interact with a linear potential $V(L) \sim L$ and the theory confines. If, on the other hand, the exponent is proportional to the perimeter of the loop, the theory deconfines. In the first case, the VEV for large loops goes to zero. In the second case, instead, we can always add local counterterms to the loop and set its VEV to one. In presence of a one-form symmetry acting on this loop, we see then that in the first case the symmetry is preserved, while in the latter case it is spontaneously broken.

We want now to analyze confinement in holography.
Let us consider the case of a fundamental Wilson loop. Holographically, a fundamental static source can be introduced in the D3 theory by adding a D3 brane separated from the stack. The gauge symmetry of the system is $SU(N) \times U(1)$ for the stack and the single brane respectively

and strings stretching between the two types of branes are in the fundamental representation of $SU(N)$. The mass of the corresponding strings is proportional to the distance of the single D3 brane from the stack. So, to have a static source for the Wilson loop, we have to send the D3 far away from the stack. Holographically, the string then ends on the boundary of AdS [101]. So, the boundary conditions associated with this string maps to a Wilson loop operator in the QFT. The expectation value of the Wilson loop corresponds then to the on-shell action of the string of minimal surface insisting on the loop at the boundary of AdS. The VEV reads (in Euclidean signature)

$$\langle W_C \rangle = e^{-S^{\text{on-shell}}(\Sigma)}\Big|_{\partial\Sigma=C} \tag{2.48}$$

with $S^{\text{on-shell}}(\Sigma) = \frac{1}{2\pi\alpha'}\int_\Sigma \sqrt{-\det P[g]}$ the on-shell action of the string.

In AdS, the surface is favorite to bend towards the horizon, since the metric diverges at the boundary. However, boundary conditions tend to compensate for this behavior, so the more the loop is small the more the surface is close to the boundary, see figure 2.4.

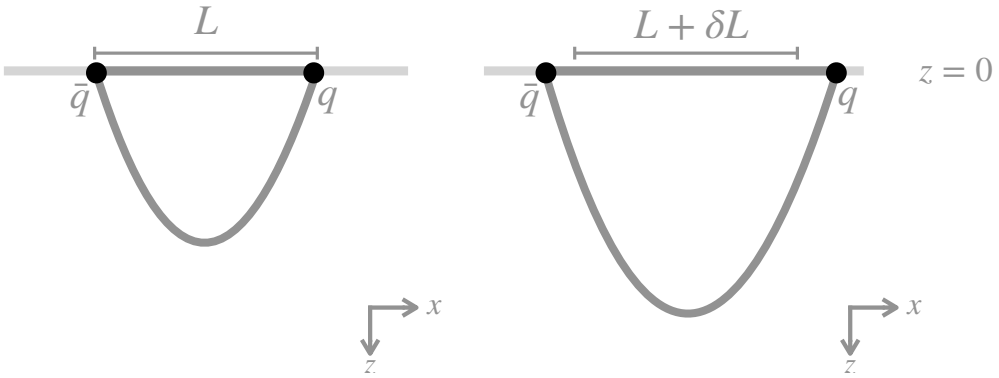

Figure 2.4: Minimal surface in AdS dual to Wilson loop of length L (a) and $L + \delta L$ (b).

The on-shell action of the resulting configuration goes like [103]

$$S^{\text{on-shell}} \sim \sqrt{\lambda}\frac{T}{L} \tag{2.49}$$

as expected from conformal invariance. The theory is then deconfined. To obtain confinement, we need to modify the AdS metric, such to have a minimal surface signaling a linear potential between the probes. Since this requires the presence of the tension T_R, which is a dimensionful quantity, we see that we need to break conformality in the gauge theory. This will be the main topic of the next section.

2.2.2 Non-AdS/non-CFT

AdS/CFT correspondence provides a powerful setup to study strongly coupled conformal field theories. However, many theories of physical interest are characterized by very complicated

dynamics along some RG-flow. This is the case for asymptotically free theories, which confine in the IR. These theories are then not conformal. Moreover, they can also develop a mass gap, as happens for YM theory in four and three dimensions. This tells that the spectrum is bounded from below by the lightest color singlet bound state (glueball) of mass

$$m_G \sim \Lambda_{\rm YM} \tag{2.50}$$

and the theory is empty in the IR. We would then like to generalize AdS/CFT correspondence to non-conformal theories.
Moreover, we should also generalize the duality to theories with less supersymmetry (like $\mathcal{N}=1$ or $\mathcal{N}=0$), which are of most interest to us. In the following, we briefly list some of the main methods to generalize the correspondence, focusing in particular on models for confining theories.

There are several ways to break conformality. The most natural one consists in starting from a CFT in the UV and turning on a relevant deformation by sourcing or giving a VEV to a relevant operator $\mathcal{O}_{\phi_i}$. In the supergravity theory, this is equivalent to imposing a specific boundary condition for the corresponding field, including it in the solution of the equations of motion. This, then, contributes to the background solution with a non-trivial profile and source also the metric due to its energy-momentum tensor. The resulting RG-flow in the field theory can end on another CFT in the infrared. In the supergravity framework, this tells us that the new metric interpolates between an AdS background at the boundary and a different AdS background at $z=\infty$.[10] The AdS metric is then modified by a warp factor $A(z)$ as

$$ds^2 = e^{2A(z)}(dz^2 + dx^\mu dx_\mu). \tag{2.51}$$

This factor interpolated between an AdS in the UV and the IR. As a consequence, $A(z)$ satisfies the condition $e^{2A(z)} \to \frac{1}{z^2}$ as $z \to 0$ and a similar condition at $z \to \infty$. The holographic direction z can be then interpreted as an energy scale parametrizing the RG-flow. An example of these flows is the FGPW flow [107], which is related to a relevant deformation of $\mathcal{N}=4$ SYM preserving $\mathcal{N}=1$ supersymmetry.

Another way to break conformality comes from considering branes wrapping cycles of a CY with non-trivial topology [108] or by adding fractional branes to the system [109]. We will not review these approaches and we refer the reader to [110] for a very nice review. Let us only note that with these methods, we can have good control on the solutions also with a small amount of supersymmetry (normally $\mathcal{N}=2$ or $\mathcal{N}=1$). In this way, it was possible to construct an holographic model of $\mathcal{N}=1$ SYM [108] and for the duality cascade of Klebanov-Strassler [109].

Another method to break conformality comes from introducing an IR bound on the holographic coordinate. This introduces a mass gap in the corresponding field theory. Indeed, a theory with a mass gap M_{KK} has no propagating degrees of freedom at energies smaller than M_{KK}.

[10] In particular, the two AdS differ by their radius. Being the radius related to the central charge c of the CFT, the two AdS spaces have radius $R_{UV} \geq R_{IR}$, in accordance with the c-theorem that states $c_{UV} \geq c_{IR}$ [106].

The theory is then either empty or a TQFT. Holographically, the coordinate z parametrizes the energy scale in the CFT. So, introducing a bound for the energy scale introduces a bound for the coordinate z. This can be done in several ways: adding singularities at a finite value of the holographic coordinate $z = z_0$ for the fields parametrizing a domain wall solution [98, 111, 112], introducing a sharp cutoff (a Hard Wall [98, 113]) or a smooth ending of space-time at finite $z = z_0$ (as for [69, 87, 89]). In all these cases, z_0 assumes the role of the mass gap for the theory. Moreover, we can also realize confinement through these methods. Indeed, now the string insisting on a Wilson loop cannot extend down to $z = \infty$, due to the cutoff at $z = z_0$. Moreover, when the warp factor in (2.51) has a minimum at $z = z_0$, the more the loop becomes large, the more the string is favored to extend at $z = z_0$, where the warp factor is minimized, see figure 2.5. Calculating the on-shell action of the string, the potential between two probe sources [98]

$$V(L) \propto L \tag{2.52}$$

is linear and the theory confines!

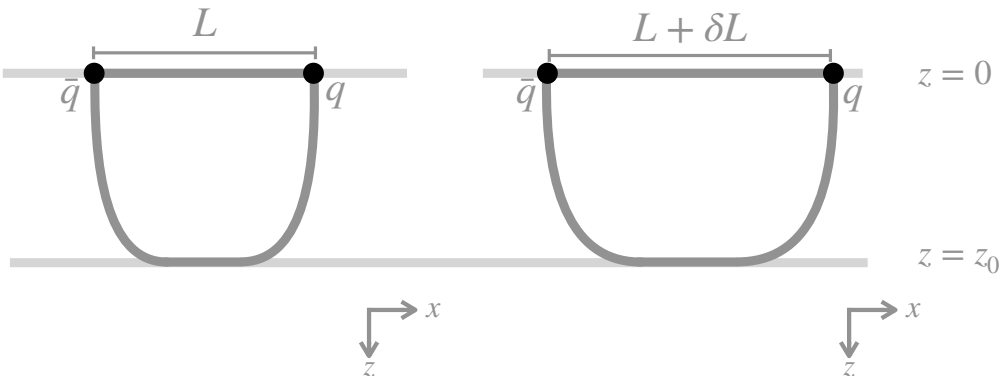

Figure 2.5: Minimal surface in presence of an IR regulator for AdS.

2.3 Holographic QCD

In this section, we review two holographic constructions of QCD in four and three dimensions respectively: the Sakai-Sugimoto (SS) model and its three dimensional counterpart. Both models realize confinement and chiral symmetry breaking holographically. In the Sakai-Sugimoto model, both the spectrum of the masses and the pion Lagrangian can be obtained by a classical analysis in supergravity. Its three dimensional analog, on the other hand, gives a holographic realization of deconfinement of YM CS theories [114] and of non-Abelian boson fermion dualities [114, 115].
In the following, we start first by reviewing the Witten model, which realizes conformal and supersymmetry breaking and gives us the holographic realization of pure YM theory. We then introduce flavors in the holographic realization of YM_4 in the quenched approximation à la Sakai-Sugimoto, obtaining the holographic description of QCD_4. Finally, in the last section, we construct analogously the holographic dual of QCD_3 with CS term k and F flavors.

2.3.1 Witten circle

A way to obtain a holographic dual of four dimensional YM theory is to compactify $\mathcal{N}=4$ SYM on a thermal circle S^1 of length β. This is equivalent to increase the temperature T of the system to $T=\beta^{-1}$. The thermal circle breaks conformal symmetry. The original theory in the UV, namely $\mathcal{N}=4$ SYM, at energies below $M_{KK}\equiv\frac{2\pi}{\beta}$ is effectively three dimensional since all the KK modes coming from the compactification can be integrated out. Fermions need to obey antiperiodic boundary conditions on the thermal cycle [86] while bosons have periodic boundary conditions. Then, the adjoint fermions acquire a non-zero mass at tree level proportional to $\sim M_{KK}$ due to the antiperiodic boundary conditions, while adjoint scalars acquire a similar mass at one loops [86]. We are then left, at sufficiently low energies, with pure YM in $\mathbb{R}^3$ (YM_3).
From the brane perspective, compactify $\mathcal{N}=4$ SYM maps to compactify the branes on a thermal circle. The resulting background is the non-extremal limit of (2.18). Its metric and fluxes can be obtained by first performing a Wick rotation on the extremal metric (2.18), compactifying on the Euclidean thermal circle and then Wick rotating the solution back. The operation gives rise to a black brane [86] with metric

$$ds^2_{BH}=R^2\left[\frac{dz^2}{z^2f(z)}+\frac{1}{z^2}\left(f(z)dt^2+dx^idx^i\right)+d\Omega_5^2\right] \tag{2.53}$$

$$e^{\phi}=g_s,\qquad \frac{1}{(2\pi l_s)^4}\int_{S^5}F_5=N,\qquad f(z)=1-\frac{z^4}{z_0^4} \tag{2.54}$$

where $i=1,2,3$ and $R^4=4\pi\lambda\alpha'^2$. Ignoring the compact direction, this resembles a Schwarzschild black hole in AdS extended along $\mathbb{R}^3$. The operation, on the other hand, does not modify the dilaton and the F_5 flux backgrounds, which remain the same. In the Lorentz signature, z_0 is the horizon of the black hole. In Euclidean signature, on the other hand, close to z_0 the metric reduces to [86]

$$ds^2\simeq R^2\left\{d\rho^2+\frac{4\rho^2}{z_0^2}d\tau^2+\frac{1}{z_0^2}dx^idx^i+d\Omega_5^2\right\} \tag{2.55}$$

where $z=z_0(1-\rho^2)$ and τ is the Euclidean time.
We see that there is no horizon at $\rho=0$, since spacetime ends smoothly at this point. The first two factors in (2.55) resemble a metric over $\mathbb{R}^2$. In particular, to avoid conical singularities, the radius of the thermal circle must be related to the endpoint z_0 as [86]

$$\beta=\pi z_0. \tag{2.56}$$

In the limit $z\to 0$, we are far away from the BH and the metric reduces to $\mathrm{AdS}_5\times S^5$.
The topology of the spacetime is $(S^1_\beta\times\mathbb{R}^+)\times\mathbb{R}^3\times S^5$ where the radius of S^1_β shrinks to zero smoothly at $z=z_0$. The shape of $(S^1_\beta\times\mathbb{R}^+)$ is then a cigar $\mathcal{C}_{z,\tau}$, depicted in figure 2.6. On the other hand, the radius of S^5 remains finite at the tip of the cigar.

In Minkowski, this background describes then $\mathcal{N}=4$ SYM compactified on a thermal circle, which reduces to YM_3 in $\mathbb{R}^3$ at sufficiently low energies. The same reasoning can be done also in finite volume S^3 [86], where the dynamics is richer and we have a first-order phase transition

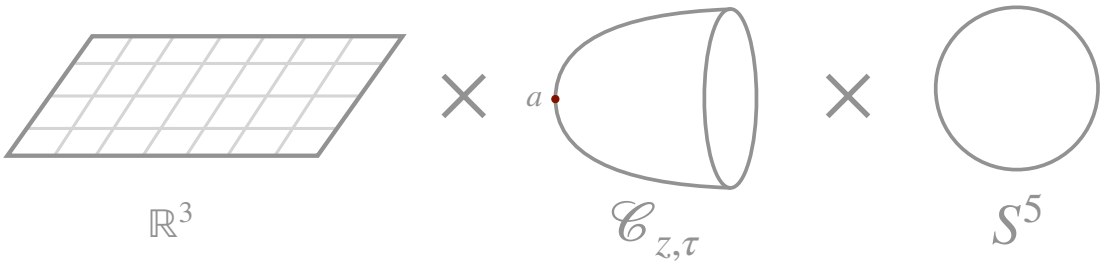

Figure 2.6: Geometry of Euclidean solution.

driven by the temperature [86], the so-called Hawking-Page phase transition [86, 116].

We saw how, in Euclidean coordinates, compactification gives rise to a space with an IR cutoff, namely the $\mathcal{C}_{z,\tau}$ of the Witten circle metric. As we reviewed in the previous section, smooth endings of spacetimes are the hallmark of confining theories. As a consequence, we would like to reproduce the same behavior in Minkowski spacetime and obtain a holographic dual of YM in four dimensions. This can be done via wrapping the stack of N D4 branes around a compact direction. In this case, notice that conformal invariance is broken even before compactification: the near-horizon limit of the background generated by a Dp brane with $\mathrm{p} \neq 3$ is only conformally equivalent to $\mathrm{AdS}_{\mathrm{p}+2} \times S^{8-\mathrm{p}}$ in the string frame. In particular, the dilaton reads

$$e^{\phi} = g_s \left(\frac{r}{L_{\mathrm{p}}}\right)^{\frac{(7-\mathrm{p})(\mathrm{p}-3)}{4}} \tag{2.57}$$

and the metric is conformal to $\mathrm{AdS}_{\mathrm{p}+2} \times S^{8-\mathrm{p}}$ via a Weyl transformation $ds^2 \to ds^2_{dual} = (Ne^{\phi})^{\frac{2}{\mathrm{p}-7}} ds^2$ followed by a change of variables $U^2 = \left(\frac{5-\mathrm{p}}{2}\right)^2 \alpha' L_{\mathrm{p}}^{\mathrm{p}-7} r^{5-\mathrm{p}}$. The dilaton after this transformation reads

$$e^{\phi} = B_{\mathrm{p}} U^{\frac{(\mathrm{p}-3)(7-\mathrm{p})}{2(5-\mathrm{p})}}, \quad B_{\mathrm{p}} = g_s \alpha'^{\frac{(\mathrm{p}-3)}{2}} C^{\frac{(7-\mathrm{p})(\mathrm{p}-3)}{2(5-\mathrm{p})}} \left(\frac{2}{5-\mathrm{p}}\right)^{\frac{(7-\mathrm{p})(\mathrm{p}-3)}{2(5-\mathrm{p})}} \tag{2.58}$$

where $C = \left(\frac{5-\mathrm{p}}{2}\right) \frac{\alpha'^{1/2}}{L_{\mathrm{p}}}$. The running in (2.58) is the signal of the classical running of the gauge coupling of the $\mathrm{p}+1$ dimensional gauge theory for $\mathrm{p} \geq 4$, which is classically irrelevant. For $\mathrm{p} = 4$, in this frame we can see that a decoupling limit compatible with the supergravity approximation $e^{\phi} \ll 1$ (namely $N \to \infty$ and λ fixed) still exists. In the $\mathrm{p} = 5$ the limit is singular since U becomes a constant. Finally, for $\mathrm{p} = 6$ we cannot decouple gravity anymore from the theory on the Dp branes [98].
Four dimensional YM theory is then obtained by compactifying on a spatial circle our brane

stack. Doing so, we obtain the background [86, 87]

$$ds^2 = \left(\frac{r}{L}\right)^{\frac{3}{2}} (\eta_{\mu\nu} dx^\mu dx^\nu + f(r) d\tau^2) + \left(\frac{L}{r}\right)^{\frac{3}{2}} \frac{dr^2}{f(r)} + L^{3/2} r^{1/2} d\Omega_4^2, \tag{2.59}$$
$$e^\phi = g_s \left(\frac{r}{L}\right)^{3/4}, \quad \frac{1}{(2\pi l_s)^3} \int_{S^4} F_4 = N, \quad f(r) = 1 - \frac{r_0^3}{r^3}$$

where we renamed $L^3 \equiv L_4^3 = \pi \lambda \alpha'^{3/2}$. In eq. (2.59), $\mu = 0, ..., 3$ and τ is periodic

$$\tau \sim \tau + \frac{4\pi}{3} \frac{L^{3/2}}{r_0^{1/2}} \equiv \tau + \delta\tau \tag{2.60}$$

and parametrizes the spatial circle.
In Lorentzian signature, the geometry ends smoothly at r_0 and the topology of spacetime reduces to $(S^1_\beta \times \mathbb{R}^+)$ times $\mathbb{R}^{1,3}$ times a sphere S^4. In this way, we realize a mass gap $M_{KK} = \frac{3}{2} \frac{r_0^{1/2}}{L^{3/2}}$ and confinement. In particular, the string tension of a flux tube between two probe quarks reads [87]

$$T = \frac{2}{27\pi} \lambda M_{KK}^2. \tag{2.61}$$

On the field theory side, by compactifying on the circle, we can impose antiperiodic boundary conditions for the fermions. In this way, both fermions and scalars in the adjoint representation acquire a mass proportional to M_{KK} and can be integrated out at low enough energies. In the compactification, the gauge coupling g_5 on the D4 branes, which is dimensionful with $[g_5] = M^{-1/2}$, is multiplied by the compactification length $\sim \frac{1}{M_{KK}}$. The resulting four dimensional coupling $1/g^2_{\rm YM}$ is dimensionless and reads

$$\frac{1}{g^2_{\rm YM}} = \frac{1}{2\pi g_s} \frac{1}{M_{KK} l_s}. \tag{2.62}$$

In this way, we are left with pure Yang-Mills theory in four dimensions!
Let us now comment on the regime of validity of the supergravity background. The maximal curvature occurs at the tip of the cigar $r = r_0$ and is of order $(r_0 R^3)^{-1/2}$, while the dilaton runs as in (2.59). The supergravity approximation then holds if

$$e^\phi \ll 1, \;\; (r_0 L^3)^{-1/2} \gg l_s^{-2} \to g^4_{\rm YM} \ll \frac{1}{g^2_{\rm YM} N} \ll 1, \;\; \lambda \gg 1 \tag{2.63}$$

and $r_0 \ll r_{crit}$ with $r_{crit} \sim \frac{N^{1/3} M_{KK} l_s^2}{g^2_{\rm YM}}$. When $r \gtrsim r_{crit}$, the string coupling cannot be small and the approximation breaks down. This is the signal of non-renormalizability of the five dimensional theory on the D4 branes. Indeed, at energies larger than the compactification scale, the theory is five dimensional $\mathcal{N} = 2$ SYM. This is known to have a UV completion only in six dimensions [86, 87, 117] in terms of a $(2, 0)$ theory.

In conclusion, this model, taking account of the previous limits, realizes some of the main

qualitative features of YM in four dimensions. However, it is worth noticing that the model does not realize YM theory at all scales. Indeed, in the UV, when energies are much bigger than the compactification scale, the theory becomes five dimensional and it is not asymptotically free. Moreover, it is not even possible to decouple all the spurious five dimensional modes at low energies. This is so since the mass gap of pure YM is proportional to the strong coupling scale of the theory, $\Lambda_{\rm YM} \sim M_{KK}$ and the string tension of flux tubes to λM_{KK}^2. Then, in the range of validity of supergravity $\lambda \gg 1$, the spurious KK modes cannot be decoupled from the YM sector and can spoil the low energy dynamics. This is known as the decoupling problem and affects all holographic duals of confining theories [87, 108, 110].
Fortunately, our model and YM in four dimensions share the same qualitative feature (and holographic QCD will do as well). In particular, the two theories are believed to belong to the same universality class [89].

2.3.2 The Sakai-Sugimoto model

To describe QCD in four dimensions, we need to introduce quarks. In the discussion of Section 2.1, we associated with the genus expansion of gauge theories with fundamental matter, the perturbative expansion of an open string theory. In the following, we will work in the limit of quenched flavors, where F is subleading with respect to N.
In holography, a simple way to introduce flavors comes from adding F Dp branes of lower codimension to the system [118]. Taking the background in (2.59), flavors can be introduced, for example, adding D6 branes [87] or D8 branes [89]. The gauge theory on the worldvolume of these branes decouples from the D4 one in the Maldacena limit since the ratio between the Dp and the D4 gauge coupling

$$\frac{\lambda_{Dp}}{\lambda_{D4}} = \frac{F}{N}(2\pi)^{p-4}\alpha'^{(p-4)/2} \tag{2.64}$$

goes to zero for $p > 4$. On the other hand, strings stretching between the D4 stack and the higher dimensional branes contribute to the D4 dynamics. Looking at their CP factors, we see that these are in the fundamental representation of both the D4 and the D8 groups. Their lowest mass excitations are then the flavors of the four dimensional theory.
In general, the lowest excitation of the string, in absence of supersymmetry, can be either bosonic or fermionic. This depends on the number of mixed Neumann-Dirichlet directions $\#_{ND}$ between the D4 and the Dp branes. In particular

- If $\#_{ND} = 4, 8$ supersymmetry is preserved between the branes. The low energy excitations of the strings stretching between the two branes are then in a supersymmetric multiplet with both bosonic and fermionic excitations;
- If $\#_{ND} = 6$, supersymmetry is broken and the lightest excitation of the strings is fermionic;
- If $\#_{ND} = 2$, supersymmetry is broken and the lightest excitation is bosonic.

In this way, we can introduce fermions or bosons depending on how we place the Dp branes with respect to the lower dimensional branes. A mass for these fundamental fields can be introduced

by separating the "flavor" Dp branes from the stack in a Dirichlet direction common to all the branes. The fundamental strings acquire a finite length Δx and their lowest excitations a mass $m \sim \frac{\Delta x}{2\pi\alpha'}$.

We can now ask what happens when we backreact the D4 branes. The stack is replaced by its geometry and we end up with the type IIA background in eq. (2.59). On the other hand, the probe branes do not backreact and remain as branes living in the background geometry. Since their number is small compared to the stack, these can be treated as probes in the D4 background.
The corresponding strings living on their worldvolume will then be gauge singlets, charged under the flavor group. So, gauge-invariant bilinears of fundamental fields[11] in the field theory are related to fluctuations of the probe branes in the D4 background. This statement holds in general for systems of Dp branes probing the background of many Dq branes (with p > q) and generalizes the gauge/gravity correspondence in presence of fundamental fields [118].

Let us now specialize our analysis on the Sakai-Sugimoto model. This is realized by a stack of N D4 branes along 01234 compactified along the x^4 circle and F D8-$\overline{\text{D8}}$ pairs branes along 012356789, see Table 2.1. The two different stacks of branes have 6 mixed directions, so the 4-8

	0	1	2	3	4	5	6	7	8	9
N D4	–	–	–	–	–	·	·	·	·	·
F D8-$\overline{\text{D8}}$	–	–	–	–	·	–	–	–	–	–

Table 2.1: Brane system

strings add fermions to the field theory. In particular, fermions realized by 4-8 strings and 4-$\bar{8}$ strings are Weyl spinors with opposite chirality. This ensures anomaly cancellation in the four dimensional theory. The gauge theory on the D8 (resp. $\overline{\text{D8}}$) stack can be then interpreted as the left (resp. right) flavor symmetry of QCD $U(F)_L$ (resp. $U(F)_R$).
Compactifying along the fourth direction, at energies lower than the Kaluza-Klein scale M_{KK}, we remain with pure YM_4 theory.[12] The quarks, on the other hand, do not acquire a mass, due to the $U(1)_A \subset U(F)_L \times U(F)_R$ axial symmetry (which is non-anomalous in the large N limit, see [87, 120, 121]). The low energy theory is then QCD with F flavors and N colors. Due to the absence of a common Dirichlet direction among the D4 and the flavor branes, we cannot introduce a mass directly by separating the flavor and the color stack. This can be done in a more refined way [89], but in the rest of the discussion, we will keep the quarks massless. The brane-anti brane pairs are expected to annihilate due to the presence of a tachyon in the spectrum of the strings connecting D8 and $\overline{\text{D8}}$. However, the tachyon becomes massive whenever we separate the D8 from the $\overline{\text{D8}}$ by a distance Δx^4 bigger then $\Delta x^4 > \sqrt{2}\pi l_s$ on the S^1. In the following, we will impose these boundary conditions for our probes.

[11] On the contrary, baryons, for example, are introduced as branes wrapping the S^4 at the tip, as in [99, 119].

[12] Actually, the trace part of the fourth component of the gauge boson is protected by a shift symmetry [89], but since it interacts only via irrelevant coupling, at low energies, we can neglect it. The same holds for the trace parts of the adjoint scalars.

After backreaction, we are left with the D4 background in eq. (2.59). Its non-trivial metric modifies the shape of the probe D8-$\overline{\text{D8}}$ pairs. These will follow geodesics in the D4 background. Their form can be obtained by minimizing their DBI action [118]. In particular, we can parametrize the shape of the D8 in static gauge as a profile $r(\tau)$. The corresponding DBI reads

$$S_{D8} \propto \int d^4x d\tau\, r^4 \sqrt{f(r) + \left(\frac{L}{r}\right)^3 \frac{r'^2}{f(r)}}. \tag{2.65}$$

The action is independent of shifts of τ, so the following quantity

$$\mathcal{I} \equiv \frac{r^4 f(r)}{\sqrt{f(r) + \left(\frac{L}{r}\right)^3 \frac{r'^2}{f(r)}}} \tag{2.66}$$

is conserved. The corresponding equations of motion can be solved imposing boundary conditions $r(0) = \tilde{r}$, $r'(0) = 0$ and the solution reads

$$\tau(r) = \tilde{r}^4 f(\tilde{r})^{1/2} \int_{\tilde{r}}^{r} \frac{dr}{\left(\frac{r}{L}\right)^{3/2} f(r) \sqrt{r^8 f(r) - \tilde{r}^8 f(\tilde{r})}}. \tag{2.67}$$

We see that the branes coming into the interior of the cigar bends and the derivative of τ diverges at $r = \tilde{r}$. The brane does not extend over this point. So, due to charge conservation, this has to merge with an $\overline{\text{D8}}$, forming a unique U-shape probe, see figure 2.7. Note that, when $\tilde{r} = r_0$, τ is a constant $\tau(r) = \delta\tau/4$ and the brane is antipodal to the anti-brane, and they merge only at the tip, as we can see in figure 2.7. This configuration was shown to be stable under

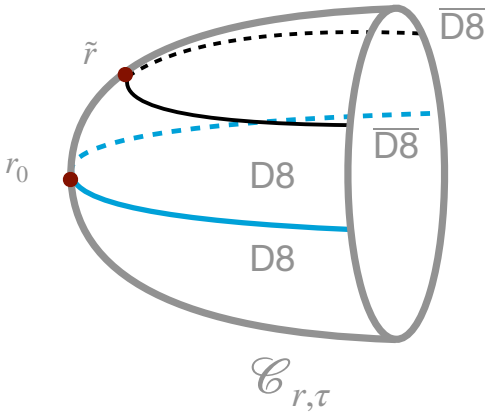

Figure 2.7: U-shape configurations of brane-anti brane pairs. In blu, we show the antipodal configuration, where the two branes meet at the tip of the cigar.

fluctuations [89]. In the following, we will focus on this type of solution.
We see then that, far away from the center of the stack, flavor branes do not feel the geometry of the D4 and behave as in flat space. Here, the D8 and the $\overline{\text{D8}}$ are separated and antipodal on

the circle. The symmetry of the theory is then $U(F)_L \times U(F)_R$. This simply tells us that in the UV we have a preserved chiral symmetry in field theory.
However, when we go into the interior of the cigar, the D8 branes feel the geometry of the stack and eventually merge at the tip of the cigar. The global symmetry then spontaneously breaks to a diagonal subgroup $U(F)_L \times U(F)_R \to U(F)_D$. So, at low-energies, we see holographically the chiral symmetry breaking of QCD_4!
The analysis of the non-Abelian DBI of the D8 branes [89] reveals the presence of the corresponding massless pions, which are the Goldstone bosons of chiral symmetry breaking. The Lagrangian of these fluctuations reduces to the effective Lagrangian which describes interactions among pions, namely the Skyrme model. Moreover, we can see that massive fluctuations around this background describe the mesons of QCD_4. Their holographic mass shows a good agreement with the experimental data for meson masses of QCD.
Baryons, on the other hand, are described holographically by D4 branes wrapping the S^4 compact space [89, 119]. From the point of view of the Skyrme effective field theory on the D8 branes, these are instantons. Indeed, the D4 has four mixed ND directions with respect to the D8 branes. Moreover, all its Neumann directions lie inside the D8 worldvolume, so the D4 dissolved in the D8 represents an instanton of the D8 gauge theory [97]. This matches with the description of baryons in the Skyrme model: these are nothing but solitonic configurations, namely skyrmions, of the theory. The mass of these baryons

$$m_b = \frac{1}{27\pi} M_{KK} N \lambda. \tag{2.68}$$

scales as $\sim N$, as expected from large N QCD calculations.

The model reproduces also the chiral anomaly of QCD and the mass for the η' when $1/N$ corrections are taken into account. The same model was also analyzed at finite temperature [122], revealing a rich dynamics, such as a deconfinement-confinement phase transition and chiral symmetry restoration at high temperatures.

2.3.3 Holographic description of QCD_3

In this section, we present the holographic set-up describing QCD_3 at large N. We first discuss how CS terms can be introduced holographically and then we add quarks in the quenched approximation. In Chapter 4, we will use the resulting background to study QCD_3 with CS level k and F flavors in the large N limit.

Yang-Mills theory with a Chern-Simons term

As we saw above, three dimensional $SU(N)$ Yang-Mills can be engineered by N D3-branes wrapping a circle in one compactified direction, $x^3 \simeq x^3 + 2\pi M_{KK}^{-1}$, with supersymmetry-breaking anti-periodic boundary conditions for the fermions. The metric and fluxes are basically the same as the black three-brane solution (2.53) where now the x^3 direction takes the role of time. The

metric, written in the holographic coordinate r, reads

$$\begin{aligned} ds^2 &= \frac{r^2}{L^2}\left(\eta_{\mu\nu}dx^\mu dx^\nu + f(r)(dx^3)^2\right) + \frac{L^2}{r^2 f(r)}dr^2 + L^2 d\Omega_5^2\,, \\ e^\phi &= g_s\,, \qquad \frac{1}{(2\pi l_s)^4}\int_{S^5} F_5 = N\,, \end{aligned} \tag{2.69}$$

where $\mu,\nu = 0,1,2$ and

$$L^4 = 4\pi g_s N l_s^4\,, \quad f(r) = 1 - \left(\frac{r_0}{r}\right)^4\,, \quad r_0 = \frac{M_{KK}L^2}{2}\,, \tag{2.70}$$

with l_s the string length and g_s the string coupling. Similarly to the four dimensional case reviewed above, the geometry is given by a flat $\mathbb{R}^{1,2}$, a constant S^5 and a cigar-shaped (r, x^3) subspace, where the holographic coordinate r goes from $r_{UV} = \infty$ to the tip of the cigar $r = r_0$, where it smoothly ends, thus giving rise to a mass gap and to confinement. In particular, two probe quarks at distance d interact with a linear potential $V = \sigma d$, with [101]

$$\sigma = \frac{\sqrt{g_s N}M_{KK}^2}{4\sqrt{\pi}} = \frac{\sqrt{\Lambda M_{KK}^3}}{4\sqrt{2\pi}}\,, \tag{2.71}$$

where Λ is the scale of large N QCD_3

$$\Lambda \equiv g_{3d}^2 N = \frac{g_{4d}^2}{2\pi M_{KK}^{-1}}N = \frac{4\pi g_s}{2\pi M_{KK}^{-1}}N = 2g_s N M_{KK}\,. \tag{2.72}$$

The limit $L \gg l_s$, where the supergravity approximation is reliable, is equivalent to $g_s N \gg 1$, i.e. $\Lambda \gg M_{KK}$, so there are spurious KK fields in this regime. In principle we should take the opposite limit $\Lambda \ll M_{KK}$, but this does not allow to use the supergravity approximation. This is again a manifestation of the decoupling problem.

The D3 background reviewed above is dual to the strongly coupled regime of Yang-Mills theory. We now discuss the inclusion of a Chern-Simons term [90]. The D3-brane theory admits a coupling with the RR axion C_0

$$S_{C_0} = \frac{1}{4\pi}\int_{D3} C_0 \mathrm{Tr}(F\wedge F) = -\frac{1}{4\pi}\int_{S^1} dC_0 \int_{\mathbb{R}^{1,2}} \omega_3(A)\,, \tag{2.73}$$

where $\omega_3(A)$ is the Chern-Simons form in three dimensions and we have assumed that the gauge field on the D3-branes does not depend on x^3 and it does not have any components along S^1. If we choose (take k_b non-negative)

$$dC_0(x^3) = -\frac{k_b}{2\pi M_{KK}^{-1}}dx^3\,, \tag{2.74}$$

then we get the following term in the D3-brane action

$$S_{C_0} = \frac{k_b}{4\pi}\int_{\mathbb{R}^{1,2}} \omega_3(A)\,, \tag{2.75}$$

which is exactly a Chern-Simons term at level k_b. Clearly, we are neglecting the backreaction of the axion field on the D3 background, which is valid at leading order in k_b/N. Thus, the Minkowski part of the worldvolume of the D3-branes hosts an $SU(N)_{k_b}$ Yang-Mills theory at large N, with fixed k_b. At very low energies, this theory is believed to flow to a pure $SU(N)_{k_b}$ Chern-Simons theory.

At strong coupling, the stack of D3-branes is replaced by the cigar geometry, while the presence of a non-vanishing RR flux needs to be supported by a magnetic source for C_0. This is provided by k_b probe D7-branes, which indeed couple magnetically to C_0. Being the number of branes an integer, this gives a holographic proof of the quantization of the Chern-Simons level. The CS branes wrap the S^5, share with the color D3-branes the three dimensions of Minkowski spacetime, and are pointlike on the (r, x^3) cigar.

	0	1	2	3	r	Ω_5
N D3	–	–	–	–	·	·
k_b D7	–	–	–	·	·	–

Table 2.2: Brane system describing $SU(N)_{k_b}$.

Such D7-branes are located at its tip $r = r_0$, where the x^3 circle shrinks to a point, in order to minimize their energy density, see figure 2.8. In this situation, the worldsheet of a string that is attached to a Wilson loop at the boundary can end on the D7-branes at the tip of the cigar. This configuration is energetically favorite, as it has been explicitly computed in [123], and signals a perimeter law for the Wilson loop. This shows, holographically, that in presence of a Chern-Simons term the theory does not confine.

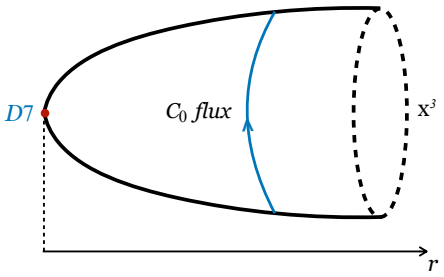

Figure 2.8: Chern-Simons D7-branes are located at the tip of the cigar and act as a source for the RR axion flux around S^1.

Following the standard holographic dictionary, the free energy density (in the three dimensional sense) can be extracted from the on-shell value of the DBI action and reads, for a single CS brane

$$E_{\rm CS} = -\frac{S_{D7}}{V_3} = T_{D7} V_5 L^2 r_0^3 \simeq N(g_s N) M_{KK}^3 \ , \tag{2.76}$$

where $T_{D7} = (2\pi)^{-7} l_s^{-8} g_s^{-1}$ is the tension of the D7-brane, V_3 is the volume of three dimensional Minkowski spacetime and V_5 is the volume of the unit five-sphere. In the strict large N limit

	0	1	2	3	4	5	6	7	8	9
N D3	–	–	–	–	·	·	·	·	·	·
F D7	–	–	–	·	–	–	–	–	–	·

Table 2.3: Brane system describing QCD_3.

probe D-branes do not interact. Therefore, in this limit, the energy density of k_b CS branes will just be $k_b E_{\text{CS}}$, which is linear in N.

At energies below the S^5 inverse radius, the D7-brane theory reduces to a three dimensional $U(k_b)$ gauge theory. Moreover, the presence of a background RR five-form flux induces a Chern-Simons term at level $-N$ from the corresponding Wess-Zumino term in the D7-brane action

$$S_{C_4} = \frac{1}{2(2\pi)^5 l_s^4}\int_{D7} C_4 \wedge \text{Tr}(F\wedge F) = -\frac{1}{2(2\pi)^5 l_s^4}\int_{S^5} F_5 \int_{\mathbb{R}^{1,2}} \omega_3 = -\frac{N}{4\pi}\int_{\mathbb{R}^{1,2}} \omega_3\,. \tag{2.77}$$

At very low energies, all excitations on the D7-branes decouple and we are left with a pure $U(k_b)_{-N}$ Chern-Simons theory. Thus, gauge/gravity duality in this set-up precisely reduces to the well-known level/rank duality $SU(N)_{k_b} \leftrightarrow U(k_b)_{-N}$ [90].

Note that if we take a negative k_b the axion monodromy changes sign, meaning that we should put $|k_b|$ D7-branes with reversed orientation. This implies that there is a sign change in (2.77), giving rise to the level/rank duality $SU(N)_{-|k_b|} \leftrightarrow U(|k_b|)_N$ at low energies, in agreement with QFT expectations.

Adding flavors in the holographic set-up

As we reviewed above, we can introduce fundamental matter by adding flavor branes in the background geometry. In our case, we add F copies of fundamental flavors by putting F probe D7-branes, transverse to the compactified x^3 direction and spanning the Minkowski spacetime $\mathbb{R}^{1,2}$ and five of the six directions which are transverse to the D3-branes worldvolume. The leftover direction x^9 is transverse to both D3 and D7-branes. This configuration has 6 mixed Neumann-Dirichlet boundary conditions, thus breaking supersymmetry completely even in the case of a SUSY D3 background (i.e. when the compactification mass scale is zero $M_{KK} = 0$). In this way, we construct[13] the holographic dual of QCD_3. A bare mass for the flavors which breaks parity in QCD_3 can be introduced by imposing a separation between color and flavor branes along x^9 at the UV boundary, as opposed to the Sakai-Sugimoto case. Indeed, the D7 worldvolume scalar corresponding to the x^9 direction couples to the fermionic mass operator. Consequently, the x^9 direction changes sign under the 3d parity transformation [69, 114]. According to the holographic dictionary, the profile of the flavor brane along x^9 is dual to the meson operator $\bar{\psi}\psi$ on the field theory side.

Having introduced the set-up, we will dedicate Chapter 4 to the analysis of the flavor branes embeddings and their field theory interpretation. This will allow us to chart the phase diagram of large N QCD_3 holographically at both leading and next subleading order in N.

[13]Note that the construction includes the kinetic term for the gauge field. This will be crucial in order to reproduce the vacuum structure of large N QCD_3.

Chapter 3

QCD_3 with two sets of flavors

In this Chapter, based on the original work in [124], we extend the analysis of [31] to the case in which the phase diagram has a two dimensional structure. The simplest way to do this is to study an $SU(N)_k$ gauge theory coupled to p fundamental fermions of mass m_1 and $F-p$ of mass m_2. Concretely, we are allowing mass deformations to explicitly break the global symmetry $U(F)$ to $U(p)\times U(F-p)$.[1] We will explore the phase diagram varying the two mass parameters and check that the dual bosonic theories, conjectured in [31], admit the same phases as the fermionic theory, after deforming them with symmetry-breaking mass terms. Without loss of generality, we will consider $0 \leq p \leq F/2$.

On one hand, our analysis provides a non-trivial check that the conjectured boson-fermion dualities can be extended to more complicated cases and still maintain their validity. On the other hand, two dimensional phase diagrams show a richer structure and novel phenomena with respect to one-family QCD_3 (including phase transitions between new gapless phases) and allow to perform some interesting vacuum analysis on the bosonic side of the duality, as well.

In section 3.1, we comment on the potential inducing maximal Higgsing (see section 1.6.2) for negative mass deformations for a $U(n)$ gauge theory coupled to f fundamental scalars with global symmetry $SU(f)$. Taking $n = F/2 \pm k$ and $f = F$, the potential gives back the correct vacuum structure for the scalar theories, useful to describe the phase diagram of QCD_3. In section 3.2, we present our main results [124], *i.e.* our proposal for the phase diagram when two different masses are varied independently. Section 3.3 contains several checks of our proposal and gives also more details on the meaning of the different phases the theory enjoys and of the phase transitions between them. We first focus on asymptotic phases, where one of the two masses is sent to $\pm\infty$. These asymptotic regions are effectively one dimensional and the phase diagrams should reduce to those of QCD_3 with one species of matter fields. We then discuss in some detail the $k = 0$ case, which is useful to perform some non-trivial consistency checks regarding time-reversal invariance and the VW theorem [62–64]. We then analyze the vacua of the dual bosonic theories, conjectured from boson-fermion dualities, and show that they match the fermionic description in the neighborhoods of each critical point. Finally, we

[1] The global symmetry is actually given by the quotient $U(F)/\mathbb{Z}_N$, together with a discrete charge conjugation symmetry [56]. However, this does not affect our analysis and we will naively refer to the global symmetry as $U(F)$.

analyze some relevant deformations of the mass-degenerate sigma-model phase, which confirm, in a yet different way, our findings in a parametrically small neighborhood of the region with maximal global symmetry. Section 3.4 contains a discussion and an outlook.

3.1 Maximal Higgsing via quartic potential

Let us start remarking what is the general structure of the scalar potential of the $U(n)$ bosonic duals necessary to induce maximal Higgsing and to reproduce the correct phases in order to describe the phase diagram of QCD_3 in section 1.6.3.
Let us consider a three dimensional gauge theory with gauge group $U(n)$ and Chern-Simons level l, coupled to f scalar fields in the fundamental representation ϕ_i^α, where $\alpha = 1, ..., n$ is the gauge index and $i = 1, ..., f$ the flavor index.

The gauge-invariant operator which can be built out of the scalar fields is the meson field $X = \phi\phi^\dagger$. In components

$$X_i^{\ j} = \phi_i^\alpha \phi_\alpha^{*j} \ , \tag{3.1}$$

which is an $f \times f$ Hermitian matrix whose rank r satisfies

$$r \leq \min(n, f) \ . \tag{3.2}$$

This matrix can be diagonalized and put in the form

$$X = \mathrm{diag}(x_1, x_2, ..., x_r, 0, ..., 0) \, , \tag{3.3}$$

where x_i are the r positive eigenvalues of X.

The potential which preserves the $U(f)$ global symmetry reads, up to quartic terms in the scalar fields

$$V = \mu(\mathrm{Tr}X) + \lambda(\mathrm{Tr}X)^2 + \widetilde{\lambda}(\mathrm{Tr}X^2) \, , \tag{3.4}$$

where we take $\widetilde{\lambda} > 0$, which requires $\widetilde{\lambda} + \min(n, f)\lambda > 0$ in order to make the potential bounded from below. If $\mu \geq 0$ then the minimum of the potential is achieved for $X = 0$. This corresponds to the case where the gauge group is not Higgsed, so that at low energies the (massive) scalars can be integrated out and the effective theory is pure $U(n)$ at level l. If $\mu < 0$, instead, minimizing the potential one gets the following equation for the eigenvalues x_i

$$\mu + 2\lambda \mathrm{Tr}X + 2\widetilde{\lambda}\, x_i = 0 \ , \tag{3.5}$$

which implies that

$$x_i = \frac{-\mu}{2\lambda r + 2\widetilde{\lambda}} \quad \forall i = 1, ..., r \ , \tag{3.6}$$

meaning that all non-vanishing eigenvalues are degenerate. Moreover, on these minima the potential is

$$V = -\frac{\mu^2 r}{4\lambda r + 4\widetilde{\lambda}} \ , \tag{3.7}$$

which is minimized when r is maximum, *i.e.* when $r = \min(n, f)$. Note that the condition for the eigenvalues x_i being positive is the same which assures the stability of the potential.

If $f < n$ this means that the Higgsing is maximal, the gauge group is broken in f independent directions, and the global symmetry $U(f)$ is unbroken. After integrating out the massive fluctuations of the scalars around their minimum configuration, we get as the resulting IR theory pure $U(n-f)$ at level l.

If $f > n$ the gauge group is completely Higgsed and the global symmetry is spontaneously broken to $U(n) \times U(f-n)$, leading to an IR dynamics described by a non-linear sigma model with target space

$$\mathrm{Gr}(n, f) = \frac{U(f)}{U(n) \times U(f-n)} \ , \tag{3.8}$$

and a Wess-Zumino term with coefficient $|l|$.

Note that the above result, *i.e.* maximal Higgsing for $f < n$ and degeneracy of non-vanishing eigenvalues for $f > n$, depends crucially on assuming a quartic scalar potential with a single trace contribution (similar observations were done, in a different context, in [125, 126] and also appear in [25]). One should also assume $\widetilde{\lambda}$ to be positive to get the aforementioned pattern. Indeed, for negative $\widetilde{\lambda}$ the minimum of the potential (whose stability now requires $\lambda + \widetilde{\lambda} > 0$) is achieved at $r = 1$, meaning that only one scalar field condenses, giving rise to a different vacuum structure in the negative squared mass phase.

If one allows higher-order terms in the potential, one would expect that there still exists a region in such a larger space of couplings for which the above extremization pattern holds. When applied to QCD_3 with one species of fermions, this explains, upon use of boson-fermion duality, the level/rank dualities in the $m < 0$ regime, as well as the structure of the Grassmannian (1.146), see figures 1.5 and 1.6.

As we will see in section 3.3.3, allowing a scalar potential with all possible gauge-invariant operators only up to quartic terms has the same effects as those discussed here also in the more intricate two dimensional phase space.

3.2 The two dimensional phase diagram

The phase diagram of $SU(N)_k$ gauge theory coupled to p fundamental fermions ψ_1 and $F-p$ fundamental fermions ψ_2, as a function of m_1 and m_2, turns out to have a different structure, depending on the value of the Chern-Simons level k at fixed F and p: $k \geq F/2$, $F/2 - p \leq k < F/2$ and $0 \leq k < F/2 - p$.

A property of all phase diagrams is that on the diagonal line $m_1 = m_2$, where the global symmetry is enhanced to the full $U(F)$, one correctly recovers the corresponding one dimensional diagram reviewed Chapter 1. We now illustrate the three different phase diagrams in turn.

$k \geq F/2$

In this case the phase diagram, which is shown in figure 3.1, presents only phases which are visible semiclassically. Consistently, as we are going to show in section 3.3.3, the full phase

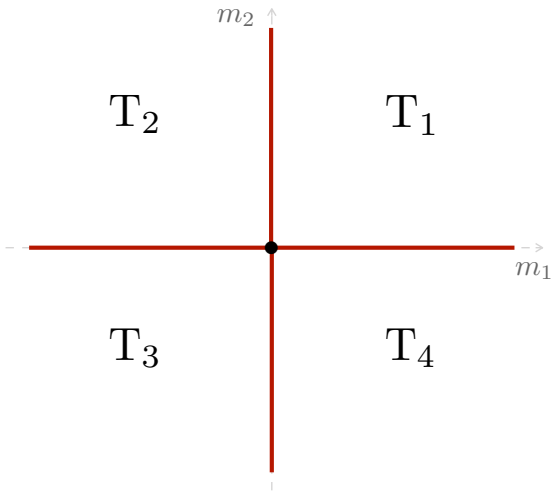

Figure 3.1: Phase diagram of $SU(N)_k + p\ \psi_1 + (F-p)\ \psi_2$ in the case $k \geq F/2$.

space can be equivalently described in terms of a *unique* dual bosonic theory, with gauge group $U(k+F/2)_{-N}$ and two sets of p and $F-p$ complex scalars in the fundamental representation.

Conventions are as follows. The black dot at the origin represents the usual phase transition of the $SU(N)_k + F\ \psi$ theory. Perturbing it by two independent mass deformations, proportional to m_1 and m_2, one covers a two dimensional space, enjoying four different topological phases T_i defined as

$$\mathrm{T}_1 : SU(N)_{k+\frac{F}{2}} \quad \longleftrightarrow \quad U(k+F/2)_{-N} \tag{3.9}$$

$$\mathrm{T}_2 : SU(N)_{k+\frac{F}{2}-p} \quad \longleftrightarrow \quad U(k+F/2-p)_{-N} \tag{3.10}$$

$$\mathrm{T}_3 : SU(N)_{k-\frac{F}{2}} \quad \longleftrightarrow \quad U(k-F/2)_{-N} \tag{3.11}$$

$$\mathrm{T}_4 : SU(N)_{k-\frac{F}{2}+p} \quad \longleftrightarrow \quad U(k-F/2+p)_{-N} \tag{3.12}$$

where $\longleftrightarrow$ stands for level/rank duality. Note that in the limiting case $k = F/2$, the topological theory T_3 becomes trivially gapped. Note also that, consistently, T_1 and T_3 are the same topological phases one expects for the theory with common mass $m = m_1 = m_2$ in the range $k \geq F/2$ (cf figure 1.5) for positive and negative m, respectively, and which one should recover on the bisector of the first and third quadrants of figure 3.1.

Red lines represent phase transitions in the (m_1, m_2) plane which are absent in the one dimensional phase diagrams. For instance, each point on the red line separating phases T_1 and T_2 defines a critical theory $SU(N)_{k+\frac{F}{2}-\frac{p}{2}} + p\ \psi_1$. In bosonic language, this can be equivalently described by $U(k+F/2)_{-N} + p\ \phi_1$. The same logic applies to all other red lines. Consistency with boson-fermion duality, which we elaborate upon in section 3.3.3, suggests that the four red lines do indeed meet at a single point (black dot in the figure).

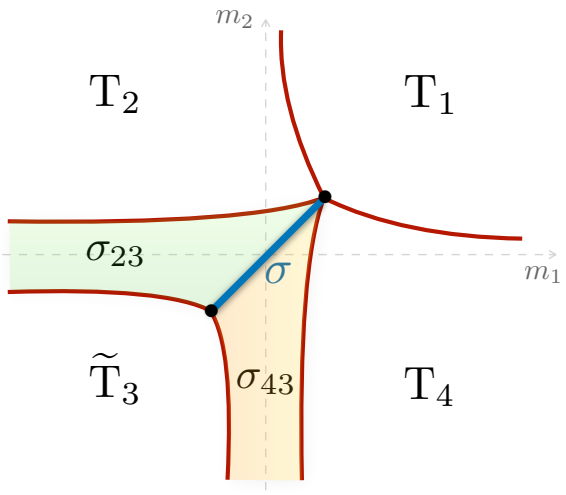

Figure 3.2: Phase diagram of $SU(N)_k + p\ \psi_1 + (F-p)\ \psi_2$ in the case $F/2 - p \leq k < F/2$.

$F/2 - p \leq k < F/2$

In this case, besides genuine topological phases, the phase diagram presents three inherently quantum phases. This implies, as we show explicitly in section 3.3.3, that two different dual bosonic descriptions are needed to cover the full fermionic phase diagram, *i.e.* $U(F/2-k)_N + p\ \phi_1 + (F-p)\ \phi_2$ and $U(F/2+k)_{-N} + p\ \phi_1 + (F-p)\ \phi_2$.

The phase diagram is reported in figure 3.2. The black dots represent the two phase transitions of the degenerate mass case, $m_1 = m_2$, cf figure 1.6. The topological theories are now

$$\mathrm{T}_1 : SU(N)_{k+\frac{F}{2}} \quad \longleftrightarrow \quad U(k+F/2)_{-N} \tag{3.13}$$

$$\mathrm{T}_2 : SU(N)_{k+\frac{F}{2}-p} \quad \longleftrightarrow \quad U(k+F/2-p)_{-N} \tag{3.14}$$

$$\widetilde{\mathrm{T}}_3 : SU(N)_{k-\frac{F}{2}} \quad \longleftrightarrow \quad U(F/2-k)_{N} \tag{3.15}$$

$$\mathrm{T}_4 : SU(N)_{k-\frac{F}{2}+p} \quad \longleftrightarrow \quad U(k-F/2+p)_{-N} \tag{3.16}$$

where, again, T_1 and $\widetilde{\mathrm{T}}_3$ are the correct topological phases one should find on the bisector, cf figure 1.6. The blue line represents a quantum phase, with target space (1.146) and a Wess-Zumino term with coefficient N. Finally, the shaded regions in the plane refer to sigma-model phases, where the IR dynamics is not gapped, but it is described by non-linear sigma models with different target spaces and a Wess-Zumino term with coefficient N. In particular, the target space of σ_{23} is the complex Grassmannian

$$\mathrm{Gr}(F/2-k, F-p) = \frac{U(F-p)}{U(F/2-k)\times U(k+F/2-p)}\ , \tag{3.17}$$

and that of σ_{43} is

$$\mathrm{Gr}(F/2-k, p) = \frac{U(p)}{U(F/2-k)\times U(k-F/2+p)}\ . \tag{3.18}$$

In the limiting case $k = F/2$ all sigma-model phases σ_{23}, σ_{43} and σ trivialize, as well as the topological phase $\widetilde{\mathrm{T}}_3$. Thus, the two phase diagrams in figures 3.1 and 3.2 become topologically equivalent, as expected. In the other limiting case, $k = F/2 - p$, to which we connect next, it is the sigma-model phase σ_{43} and the topological phase T_4 which trivialize, instead.

As in figure 3.1, red lines represent phase transitions in the (m_1, m_2) plane. Here, however, there also exist lines separating topological and massless phases. For instance, each point on the red line separating T_2 and σ_{23}, and the corresponding one separating the latter with $\widetilde{\mathrm{T}}_3$, are the two phase transitions one expects for $SU(N)_{k-\frac{p}{2}} + (F-p)\ \psi_2$. These two phase transitions are described by two different bosonic duals, $U(k + F/2 - p)_{-N} + (F-p)\ \phi_2$ and $U(F/2-k)_N + (F-p)\ \phi_2$, respectively (similar arguments hold when looking at σ_{43} as the gapless phase separating the topological phases T_4 and $\widetilde{\mathrm{T}}_3$, the relevant fermionic theory on the red lines being now $SU(N)_{k-\frac{F}{2}+\frac{p}{2}} + p\ \psi_1$).

Note that not all lines cutting through the two dimensional phase diagram can be effectively reduced to a one dimensional phase diagram of a single family theory. This applies, in particular, to the region of small masses, where different gapless quantum phases meet and σ becomes a phase transition itself, which separates the gapless phases σ_{23} and σ_{43}. This is a novel phenomenon, which does not have any counterpart in one-family QCD_3. Indeed, in our case the pattern of symmetry breaking is richer, giving a variety of quantum phases which meet in the region where both masses are, in modulus, $\lesssim g^2$.

$0 \leq k < F/2 - p$

Also in this range of parameters the phase diagram presents three different quantum phases. The two dual bosonic descriptions needed to cover the full phase space are again $U(F/2-k)_N + p\ \phi_1 + (F-p)\ \phi_2$ and $U(F/2+k)_{-N} + p\ \phi_1 + (F-p)\ \phi_2$. The phase diagram, where the same conventions as before are adopted, is shown in figure 3.3.

The topological phases are now

$$\mathrm{T}_1 : SU(N)_{k+\frac{F}{2}} \quad \longleftrightarrow \quad U(k+F/2)_{-N} \tag{3.19}$$

$$\mathrm{T}_2 : SU(N)_{k+\frac{F}{2}-p} \quad \longleftrightarrow \quad U(k+F/2-p)_{-N} \tag{3.20}$$

$$\widetilde{\mathrm{T}}_3 : SU(N)_{k-\frac{F}{2}} \quad \longleftrightarrow \quad U(F/2-k)_N \tag{3.21}$$

$$\widetilde{\mathrm{T}}_4 : SU(N)_{k-\frac{F}{2}+p} \quad \longleftrightarrow \quad U(F/2-p-k)_N \tag{3.22}$$

The sigma-model phases σ and σ_{23} are as before while σ_{14} has target space the complex Grassmannian

$$\mathrm{Gr}(F/2+k, F-p) = \frac{U(F-p)}{U(F/2+k) \times U(F/2-p-k)}\ , \tag{3.23}$$

and a Wess-Zumino term with coefficient N.

In the limiting case $k = F/2 - p$, the phase σ_{14} and the topological phase $\widetilde{\mathrm{T}}_4$ trivialize. For $k = F/2 - p$, the two phase diagrams in figure 3.2 and 3.3 become thus topologically equivalent, as expected. Again, the quantum phase σ separates two different phases described by the two Grassmannians (3.17) and (3.23). Note, in particular, that for sufficiently low values of $|m_2|$,

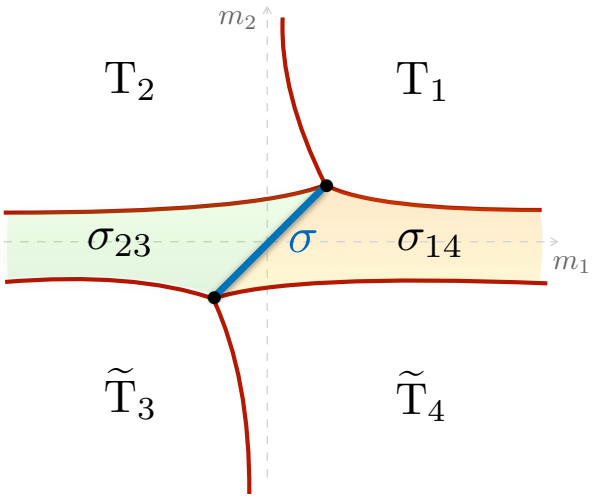

Figure 3.3: Phase diagram of $SU(N)_k + p\ \psi_1 + (F-p)\ \psi_2$ in the case $0 \leq k < F/2 - p$.

the theory enjoys only sigma-model phases for all values of m_1 (the asymmetry between m_1 and m_2 is due to our choice $p \leq F/2$).

Let us close this discussion considering a few specific values for p.

When $p = 0$ the phase diagram of figure 3.2 disappears since its allowed range for k becomes an empty set. Figures 3.1 and 3.3, instead, collapse to a single vertical line, the m_2 axis, and their topology becomes the same as the one dimensional diagrams of figures 1.5 and 1.6, respectively, as one should clearly expect. In particular, the sigma models σ, σ_{14} and σ_{23} become identical for $p = 0$, while $\mathrm{T}_1 = \mathrm{T}_2$, $\mathrm{T}_3 = \mathrm{T}_4$ and $\widetilde{\mathrm{T}}_3 = \widetilde{\mathrm{T}}_4$.

When $p = F/2$, the phase diagrams in figure 3.1 and 3.2 should be symmetric with respect to the $m_1 = m_2$ line, while it is the phase diagram in figure 3.3 which now disappears. Consistently, the sigma models with target spaces σ_{23} and σ_{43} coincide for $p = F/2$, as well as the topological phases T_2 and T_4.

3.3 Consistency checks and beyond

We now present various checks for the validity of our proposed two dimensional phase diagrams.

3.3.1 Asymptotic phases: matching ordinary QCD_3

The proposed two dimensional phase diagrams should satisfy various consistency checks, in order to be compatible with the one dimensional case. The simplest one is that the phase diagram of one-family QCD_3 should be recovered on the $m_1 = m_2$ line, where the global symmetry is enhanced to $U(F)$. This is something we have already noticed to hold. A more intricate set of checks comes by studying extreme mass regimes.

Starting from the original $SU(N)_k + p\ \psi_1 + (F-p)\ \psi_2$ theory, let us consider the four different

theories one obtains by integrating out, with either signs for the mass, one of the two fermion families, ψ_1 and ψ_2. These are $SU(N)$ gauge theories with a shifted Chern-Simons level and coupled to p or $F-p$ fundamental fermions with mass m_1 or m_2, respectively. The IR phases of these theories are easily constructed by the same methods we used in the one dimensional case. Such phases should coincide with the ones of our two dimensional diagrams, figures 3.1, 3.2 and 3.3, in the asymptotic, large mass regions. The four asymptotic theories and their one dimensional phase diagrams are the following:

1. $m_1 \to +\infty$: one ends up with $SU(N)_{k+\frac{p}{2}}+(F-p)\ \psi_2$, which has only the two semiclassical phases if $k \geq F/2-p$. Its phase diagram has the following structure:

   - $k \geq F/2-p$: the two phases are T_1 (for positive m_2) and T_4 (for negative m_2). The dual bosonic theory is $U(k+F/2)_{-N}+(F-p)\ \phi_2$.
   - $0 \leq k < F/2-p$: the topological phases are T_1 (for positive m_2) and $\widetilde{\mathrm{T}}_4$ (for negative m_2), while the intermediate sigma-model phase is σ_{14}. The dual bosonic theories are $U(k+F/2)_{-N}+(F-p)\ \phi_2$ (for positive m_2) and $U(F/2-k-p)_N+(F-p)\ \phi_2$ (for negative m_2).

2. $m_1 \to -\infty$: one gets $SU(N)_{k-\frac{p}{2}}+(F-p)\ \psi_2$, which has only the two semiclassical phases if $k \geq F/2$. Its phase diagram has the following structure:

   - $k \geq F/2$: the two phases are T_2 (for positive m_2) and T_3 (for negative m_2). The dual bosonic theory is $U(k+F/2-p)_{-N}+(F-p)\ \phi_2$.
   - $0 \leq k < F/2$: the topological phases are T_2 (for large positive m_2) and $\widetilde{\mathrm{T}}_3$ (for large negative m_2), while the intermediate sigma-model phase is σ_{23}. The dual bosonic theories are $U(k+F/2-p)_{-N}+(F-p)\ \phi_2$ (for positive m_2) and $U(F/2-k)_N+(F-p)\ \phi_2$ (for negative m_2).

3. $m_2 \to +\infty$: one ends up with $SU(N)_{k+\frac{F}{2}-\frac{p}{2}}+p\ \psi_1$, which has only two semiclassical phases for any non-negative k. The two phases are T_1 (for positive m_1) and T_2 (for negative m_1). The dual bosonic theory is $U(k+F/2)_{-N}+p\ \phi_1$.

4. $m_2 \to -\infty$: one gets $SU(N)_{k-\frac{F}{2}+\frac{p}{2}}+p\ \psi_1$, which has only two semiclassical phases if $k \geq F/2$ or $0 \leq k \leq F/2-p$. Its phase diagram has the following structure:

   - $k \geq F/2$: the two phases are T_4 (for positive m_1) and T_3 (for negative m_1). The dual bosonic theory is $U(k-F/2+p)_{-N}+p\ \phi_1$.
   - $F/2-p \leq k < F/2$: the topological phases are T_4 (for positive m_1) and $\widetilde{\mathrm{T}}_3$ (for negative m_1), and the intermediate sigma-model phase is σ_{43}. The dual bosonic theories are $U(k-F/2+p)_{-N}+p\ \phi_1$ (for positive m_1) and $U(F/2-k)_N+p\ \phi_1$ (for negative m_1).
   - $0 \leq k < F/2-p$: the two phases are $\widetilde{\mathrm{T}}_4$ (for positive m_1) and $\widetilde{\mathrm{T}}_3$ (for negative m_1). The dual bosonic theory is $U(F/2-k)_N+p\ \phi_1$.

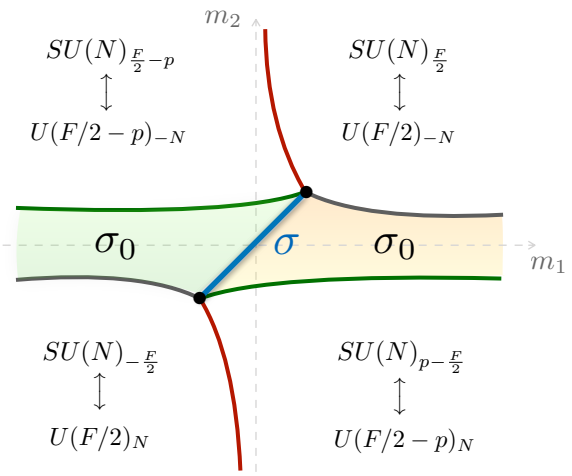

Figure 3.4: Phase diagram of $SU(N)_0 + p\ \psi_1 + (F-p)\ \psi_2$. The transition lines with the same color are described by the same theories, up to a time-reversal transformation.

It is easy to check that our proposed phase diagrams, figures 3.1, 3.2 and 3.3, exactly reproduce this intricate structure in the large $|m_1|$ and/or $|m_2|$ regions.

3.3.2 $k = 0$: time-reversal and Vafa-Witten theorem

One interesting non-trivial check comes by taking $k = 0$, in which the theory we study becomes $SU(N)_0 + p\ \psi_1 + (F-p)\ \psi_2$. Since $k = 0$, time-reversal acts on this theory just flipping the sign of the mass terms of the two sets of fermions. As a consequence, the two dimensional phase diagram should be symmetric with respect to the origin, modulo the flipping of the effective Chern-Simons levels of the specular phases. This symmetry can be nicely observed in the phase diagram in figure 3.3, which we report in figure 3.4 for the particular case $k = 0$.

It is a further consistency check that the sigma models with target spaces (3.17) and (3.23) coincide for $k = 0$. We labeled this sigma model with σ_0, whose target space is

$$\mathrm{Gr}(F/2, F-p) = \frac{U(F-p)}{U(F/2) \times U(F/2-p)}\ , \tag{3.24}$$

and which includes a Wess-Zumino term with coefficient N. The sigma-model phases σ_0 and σ enjoy time-reversal invariance for $k = 0$, as expected.

In addition to $k = 0$, let us also take $p = F/2$, *i.e.* we consider the same number of fermions in the two sets. In this case the phase diagram should be also symmetric with respect to the $m_1 = m_2$ line, besides being symmetric with respect to the origin. The phase diagram for $k = 0$ and $p = F/2$ is depicted in figure 3.5. We easily see that σ_0 trivializes, as well as the topological theories $SU(N)_{p-\frac{F}{2}}$ and $SU(N)_{\frac{F}{2}-p}$, leaving a trivially gapped phase in the second and fourth quadrants. Moreover, the theories on the two red curves are the same, up to the sign of the Chern-Simons level.

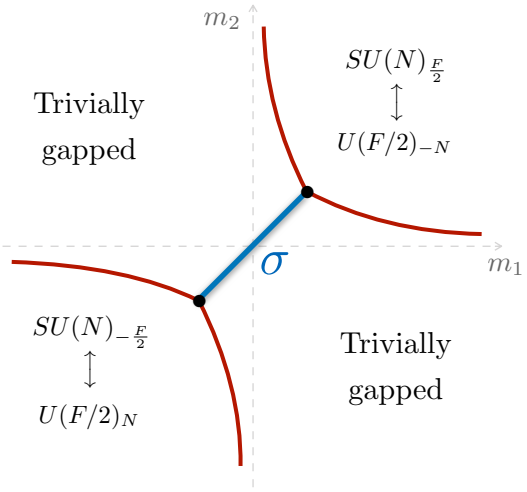

Figure 3.5: Phase diagram of $SU(N)_0 + F/2\ \psi_1 + F/2\ \psi_2$. In the bosonic dual picture, the red transition lines in the first and third quadrant are described by $U(F/2)_{\mp N} + F/2\ \phi$, respectively. On the two black spots, where the global symmetry is enhanced, the number of scalars is F.

Another interesting check when $k = 0$ and $p = F/2$ is related to the expected enhancement of time-reversal symmetry on the full $m_2 = -m_1$ line. On this one dimensional slice of the diagram of figure 3.5, the fundamental fermions are actually gapped in a parity preserving way, so we expect the VW theorem to hold. The theorem suggests then that the full $U(F)$ global symmetry should be broken down to $U(F/2) \times U(F/2)$ at strong coupling (if not classically preserved) and prevents this theory from developing a further symmetry breaking of flavor and time-reversal symmetry along the line $m_2 = -m_1$. As a consequence, on such line fermions can be safely integrated out, leading to a trivially gapped vacuum outside the origin. At the origin, the breaking $U(F) \to U(F/2) \times U(F/2)$ gives rise to the target space (1.146) with $k = 0$. The diagram in figure 3.5 exactly reproduces all these features.

3.3.3 Dual bosonic theories: matching the phase transitions

In section 3.3.1 we have checked our two dimensional phase diagrams in the large mass regime, where they become effectively one dimensional, against one-family QCD_3. Here we want to focus on the region near the critical points, *i.e.* the black dots in figures 3.1, 3.2 and 3.3. This is done using boson-fermion duality, properly adapted to the two-family case. This will also work as a nice consistency check of the duality itself.

From the conjectured boson-fermion duality of the one-family case, one can argue that the bosonic theories one should consider near the critical points are

$$U(n)_l + p\ \phi_1 + (F - p)\ \phi_2\ , \tag{3.25}$$

where $(n, l) = (F/2 \pm k, \mp N)$ and ϕ_1, ϕ_2 are scalar fields in the fundamental representation of the gauge group. Here, we have explicitly split the F scalars in two different sets, since we

want to deform the massless theories describing the critical points with the independent massive deformations, M_1^2 and M_2^2 respectively.

We can reproduce the desired vacuum structure assuming that, when at least one of the two sets condenses, the gauge group is maximally Higgsed and the unbroken global symmetry is maximized. In fact, exactly as for the one-family model discussed above, it is possible to show that these assumptions hold true if we consider the scalar potential of the critical theory up to quartic order in the scalar fields, and then deform it with symmetry-breaking mass operators. In terms of the gauge-invariant operators $X = \phi_1\phi_1^\dagger$, $Y = \phi_2\phi_2^\dagger$ and $Z = \phi_1\phi_2^\dagger$, we can write the (deformed) potential as

$$V = M_1^2 \mathrm{Tr}X + M_2^2 \mathrm{Tr}Y + \lambda(\mathrm{Tr}^2 X + \mathrm{Tr}^2 Y + 2\mathrm{Tr}X\mathrm{Tr}Y) + \widetilde{\lambda}(\mathrm{Tr}X^2 + \mathrm{Tr}Y^2 + 2\mathrm{Tr}ZZ^\dagger) \ , \quad (3.26)$$

where X and Y are positive semidefinite Hermitian matrices of dimension p and $F-p$, respectively, whereas Z is a $p \times F-p$ rectangular matrix. Note that the quartic couplings in the potential are chosen to respect the full $U(F)$ symmetry. This is because we are limiting ourselves to perturbations due to massive deformations only. In principle, there could be other $U(p)\times U(F-p)$ preserving relevant deformations besides massive ones. If boson-fermion duality is correct, these deformations should have a counterpart on the fermionic side, but we do not consider them here.

For the same reasons as the one-family case discussed above, we take $\widetilde{\lambda} > 0$, which requires $\widetilde{\lambda} + \min(n, F)\lambda > 0$ in order for the potential to be bounded from below.

In the first quadrant of the (M_1^2, M_2^2) plane, where both M_1^2 and M_2^2 are positive, X, Y and Z vanish on shell. This implies that there is no scalar condensation, all matter fields are massive and can be integrated out, leading to a $U(n)_l$ topological theory in the IR.

In all other cases, the vacuum equations imply that $Z = 0$, while X and Y are diagonal with respectively r_1 and r_2 degenerate non-negative eigenvalues given by

$$\begin{aligned} x &= \frac{-(\widetilde{\lambda} + \lambda r_2)M_1^2 + \lambda r_2 M_2^2}{2\widetilde{\lambda}^2 + 2\lambda\widetilde{\lambda}(r_1 + r_2)} \ , \\ y &= \frac{-(\widetilde{\lambda} + \lambda r_1)M_2^2 + \lambda r_1 M_1^2}{2\widetilde{\lambda}^2 + 2\lambda\widetilde{\lambda}(r_1 + r_2)} \ . \end{aligned} \quad (3.27)$$

The positivity condition on x and y implies that a simultaneous condensation of both ϕ_1 and ϕ_2 is only allowed in a subregion $\mathcal{R}$ of the third quadrant of the (M_1^2,M_2^2) plane, which includes the line $M_1^2 = M_2^2$. Outside this region and above (below) the bisector, only x (y) can be non-zero, meaning that only ϕ_1 (ϕ_2) can condense. The ranks r_1 and r_2 are non-negative integers which satisfy the constraints

$$0 \leq r_1 \leq \min(n, p) \quad , \quad 0 \leq r_2 \leq \min(n, F-p) \quad , \quad r_1 + r_2 \leq \min(n, F) \ , \quad (3.28)$$

and have to be determined by minimizing the vacuum potential, seen as a function of (r_1, r_2). Once we determine these values, the spontaneous symmetry breaking of the flavor symmetry follows the pattern

$$U(p) \times U(F-p) \longrightarrow U(r_1) \times U(p-r_1) \times U(r_2) \times U(F-p-r_2) \ . \quad (3.29)$$

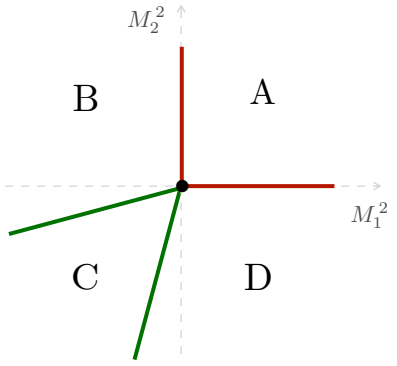

Region	r_1	r_2	Phase
A	0	0	$U(n)_l$
B	p	0	$U(n-p)_l$
C	p	$F-p$	$U(n-F)_l$
D	0	$F-p$	$U(n-F+p)_l$

Figure 3.6: Phase diagram of the bosonic theory in the case $p \leq F-p \leq F \leq n$. The region $\mathcal{R}$ of double condensation coincides with C.

This leads, in the region where x and y do not vanish simultaneously, to a sigma model with coset

$$\mathrm{Gr}(r_1, p) \times \mathrm{Gr}(r_2, F-p) = \frac{U(p)}{U(r_1) \times U(p-r_1)} \times \frac{U(F-p)}{U(r_2) \times U(F-p-r_2)} \ , \tag{3.30}$$

and an appropriate Wess-Zumino term. As we will show, the maximal symmetry pattern selects, in all cases, values of r_1 and r_2 such that this target space reduces to a single complex Grassmannian, which exactly matches the phases σ_{23}, σ_{43}, σ_{14} of figures 3.1, 3.2 and 3.3. Interestingly, these values correspond to minimizing the dimension of the target space (3.30) with respect to r_1 and r_2, once we take into account the constraints they obey.

In addition, the scalar condensation leads to a partial or total Higgsing of the gauge group following the pattern

$$U(n) \longrightarrow U(n-r_1-r_2) \ . \tag{3.31}$$

In the same spirit section 3.1, one can show that the on-shell potential as a function of (r_1, r_2) is never minimized inside the region defined in (3.28), so that the minimum of the potential is achieved at the boundaries of this region. The maximal degeneracy of the eigenvalues implies that, under our assumptions, there is never a case in which a sigma model coexists with a TQFT in a given phase. In addition, all the other excitations get a mass either by Higgs mechanism or from the scalar potential, and hence can be safely integrated out.

In order to find the values of (r_1, r_2) and the pattern of Higgsing and global symmetry breaking, one should consider four qualitatively different cases, depending on the value of n, see figures 3.6, 3.7, 3.8 and 3.9. Tables collect all data necessary to pinpoint the phase the scalar theory enjoys on the (M_1^2, M_2^2) plane, which can be either a TQFT or a sigma model.

Starting from the first quadrant, region A, where all scalars have positive mass, red and green lines represent the critical theories where one of the two sets becomes massless and condenses, whereas the blue line is the quantum phase of one-family QCD_3. On the red lines the first set of scalars condenses, partially or totally Higgsing the gauge group. In the former case, the components of the second set of scalars charged under the unbroken gauge group may

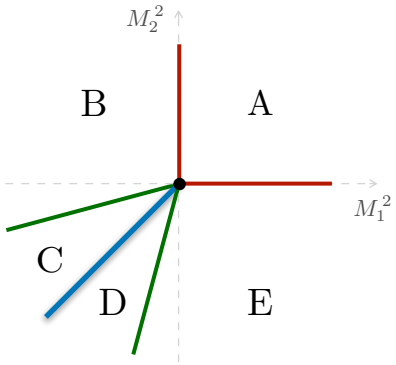

Region	r_1	r_2	Phase
A	0	0	$U(n)_l$
B	p	0	$U(n-p)_l$
C	p	$n-p$	$\mathrm{Gr}(n-p, F-p)$
D	$n-F+p$	$F-p$	$\mathrm{Gr}(n-F+p, p)$
E	0	$F-p$	$U(n-F+p)_l$

Figure 3.7: Phase diagram of the bosonic theory in the case $p \leq F-p \leq n < F$. The region $\mathcal{R}$ of double condensation coincides with $C+D$, including the blue line.

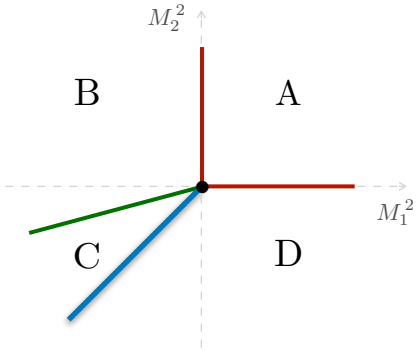

Region	r_1	r_2	Phase
A	0	0	$U(n)_l$
B	p	0	$U(n-p)_l$
C	p	$n-p$	$\mathrm{Gr}(n-p, F-p)$
D	0	n	$\mathrm{Gr}(n, F-p)$

Figure 3.8: Phase diagram of the bosonic theory in the case $p \leq n < F-p \leq F$. The region $\mathcal{R}$ of double condensation coincides with C, including the blue line.

still become massless and condense, this locus corresponding to the green lines in the figure. Neutral components receive instead an additional positive contribution to their squared mass from quartic terms of the potential. One can easily see that this contribution makes their squared mass always positive, so that they never condense and can be integrated out in the whole phase space. When the gauge group is completely Higgsed by the first condensation, instead, all scalars that have not condensed first cannot give rise to any other critical line.

Let us now specify the values of n to make contact with our conjecture and explore the topological structure of the diagrams around the critical points.

If $n = F/2 + k$, the allowed diagrams are given in figures 3.6, 3.7 and 3.8. It is now easy to check that the range of validity of each diagram and its various phases exactly reproduce the topological structure of the fermionic diagrams in figures 3.1, 3.2 and 3.3, respectively, in the neighborhood of the black dot in the first quadrant.

If $n = F/2 - k$, the allowed diagrams are given in figures 3.8 and 3.9. It is again easy to check that the range of validity of each diagram and its various phases exactly reproduce

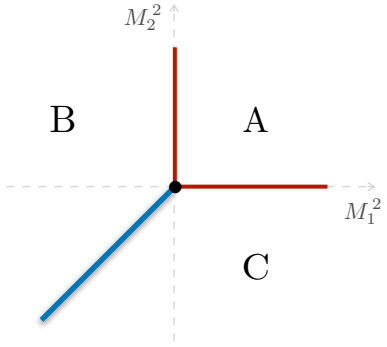

Region	r_1	r_2	Phase
A	0	0	$U(n)_l$
B	n	0	$\mathrm{Gr}(n,p)$
C	0	n	$\mathrm{Gr}(n,F-p)$

Figure 3.9: Phase diagram of the bosonic theory in the case $n < p \leq F-p \leq F$. In this case, the region $\mathcal{R}$ of double condensation shrinks to the blue line only.

the topological structure of the fermionic diagrams in figures 3.3 and 3.2, respectively, in the neighborhood of the black dot in the third quadrant. Note that in this case, as in the one-family case, cf figure 1.6, the orientation of the bosonic diagrams should be reversed.

To summarize, we have shown that the two dimensional phase diagrams of the bosonic theories are perfectly consistent with the fermionic ones, in the regions of the phase diagrams where the duality is supposed to hold. In particular, we have reproduced the peculiar structure with critical points where more than three critical lines meet.

3.3.4 Perturbing σ via massive deformations

Previously we have shown that the vacuum structure of the fermionic theory is exactly reproduced by the corresponding bosonic dual theories near each transition point. We now want to see what happens when we perturb the non-linear sigma model σ (the blue line in figures 3.2 and 3.3) with a small mass term which explicitly breaks the $U(F)$ symmetry to $U(p)\times U(F-p)$.

A similar symmetry-breaking deformation was considered in the one dimensional case, to check consistency under flowing down from F to $F-1$ (*i.e.* a flow in the space of theories), see section 1.6. Our philosophy, here, is to choose a symmetry-breaking perturbation that does not change the theory but allows us to investigate the planar region in a neighborhood of the quantum phase σ.

To do that, we deform the mass of the p scalars ϕ_1 with a small perturbation δM^2. If $\delta M^2 > 0$ (< 0) we are investigating the region $M_2^2 < M_1^2$ ($M_2^2 > M_1^2$) where the set ϕ_2 (ϕ_1) condenses first. In fermionic language $M_2^2 < M_1^2$ corresponds to $m_2 < m_1$ (*i.e.* below the $m_1 = m_2$ line) for the bosonic theory $U(F/2+k)$ and $m_2 > m_1$ (*i.e.* above the $m_1 = m_2$ line) for the bosonic theory $U(F/2-k)$. Viceversa, for the case $M_2^2 > M_1^2$.

Let us call n the rank of the bosonic theory gauge group, which can be either $F/2+k$ or $F/2-k$. In these conventions, the target space of the sigma-model phase σ reads

$$\mathrm{Gr}(n,F) = \frac{U(F)}{U(n)\times U(F-n)} \ . \tag{3.32}$$

Massive deformations act modifying the target space, but they do not change the coefficient N of the Wess-Zumino term. Let us now analyze the different possibilities, performing our analysis in the underlying gauged linear model.

- If $\delta M^2 > 0$ and $F - p > n$, the $(F-p)$ ϕ_2 condense first and completely Higgs the gauge group $U(n)$, whereas the p ϕ_1 do not play any role. Indeed, since there is no more gauge group, all the surviving ϕ_1 are neutral and can be safely integrated out. The resulting sigma model has target space $\mathrm{Gr}(n, F-p)$.

- If $\delta M^2 > 0$ and $F - p < n$ then the $(F-p)$ ϕ_2 cannot Higgs completely the gauge group, but as they condense they Higgs it down to $U(n - F + p)$ and then can be integrated out. The charged components of the p ϕ_1 then condense, whereas the neutral ones have a positive squared mass around this configuration. This leads to a sigma model with target space $\mathrm{Gr}(F-n, p)$.

- If $\delta M^2 < 0$ and $p < n$, then the p ϕ_1 condense first and Higgs the gauge group to $U(n-p)$. By the same mechanism as before, the $(F-p)$ ϕ_2 condense, eventually, leading to a sigma model with target space $\mathrm{Gr}(F-n, F-p)$.

- If $\delta M^2 < 0$ and $p > n$ then the p ϕ_1 condense first and completely Higgs the gauge group, whereas the $(F-p)$ ϕ_2 do not play any role. This leads to a sigma model with target space $\mathrm{Gr}(n, p)$.

It is a tedious but simple exercise to check that specifying the above analysis to the case of interest, *i.e.* $n = F/2 \pm k$, the resulting sigma models coincide with those living in the shaded regions around the quantum phase σ of phase diagrams in figures 3.2 and 3.3.

It is worth noticing that the above check is not entirely independent from the discussion of the previous section, since we are actually using the underlying gauged linear sigma model. It would be nice to have a proof directly in non-linear sigma-model terms. While the above results would not change, at least qualitatively, such an analysis might shed light on the nature of the phase transition around σ.

Note that by adopting the same philosophy of section 1.6, instead, one can consistently flow from the theory coupled to F flavors to the one coupled to $F-1$ flavors. This can be done by giving a large mass to, say, one of the p fermions ψ_1. After this deformation we get the same duality with parameters

$$(N, k, F, p) \longrightarrow (N, k \pm 1/2, F-1, p-1)\,, \tag{3.33}$$

for a positive (negative) mass deformation.

Using the same approach one can also play with k. As already observed in section 3.3.2, our proposal for $k = 0$ and $p = F/2$ is consistent with the Vafa-Witten theorem which holds on the entire $m_2 = -m_1$ line, figure 3.5. We can use massive deformations to increase the value of k, and show that if our proposal is correct for $k = 0$, it remains true even for $k > 0$. In particular, all values of k up to $F/2-p$ can be reached by integrating out by mass deformations the p fields in the first set, whereas bigger values of k, up to $F/2$, are reached by acting on the second set. This shows that one can consistently flow to (N, k, F, p) for any $k \leq F/2$.

3.4 Comments and outlook

In this Chapter we have constructed the phase diagram of two-family QCD_3, extending the analysis carried out in [31] for the degenerate mass case. While our results agree with [31] in the limits where the two dimensional phase diagram becomes effectively one dimensional, there exist ranges in the parameter space which present novel phenomena. These are inherent to the $m_1 \neq m_2$ case, *e.g.* the shaded regions in figures 3.2, 3.3 and 3.4, which describe new gapless phases, and phase transitions between them along σ.

We now want to discuss a few directions along which this analysis could be extended.

As far as the bosonic analysis is concerned, we have limited ourselves to quartic couplings. This is done in analogy to ordinary Wilson-Fisher fixed points for $O(N)$ vector models, and it has been, in fact, the general approach when considering boson-fermion dualities. However, the scalar theory one is dealing with is a gauged $U(N)$ linear sigma model and, as of today, a full understanding of the nature of its fixed points (if any) has not yet been achieved. Strictly speaking, one cannot exclude that along the RG-flow higher order operators acquire large (negative) anomalous dimensions and the effective low-energy theory should take several such operators into account. What one usually does is to start considering those operators whose dimensions near the Gaussian fixed point are the lowest, *i.e.* quadratic and quartic couplings. In three space-time dimensions sextic scalar operators are classically marginal, so including them in the analysis would be the first natural extension one should look for. This was partially discussed for large N QCD_3 with a single set of flavors in [25], where sextic couplings were introduced in order to correctly reproduce the phase diagram.
In a similar vein, one could consider quartic couplings not respecting the full $U(F)$ global symmetry but just $U(p) \times U(F-p)$. This could correspond to yet other relevant deformations of the massless theory, different from mass terms.

If boson-fermion duality is correct, all these (putative) novel relevant deformations should have a counterpart on the fermionic side of the duality (the first natural guess being Gross-Neveu-Yukawa couplings, in analogy with [125]). In this respect, the two-family QCD_3 case could work as the simplest laboratory to extend (and check) boson-fermion dualities beyond present understanding.

The analysis does not address the issue of the actual order of the phase transitions in QCD_3. While it is known that in certain limits such phase transitions are second order, we saw above that in the large N limit we have only first order phase transition in the phase diagram of QCD_3. Having a clear picture of this aspect would give crucial insights on how we should think about boson-fermion dualities in general.

In our two dimensional phase diagrams, there are some phase transitions that might be more amenable to treatment, namely the transitions between different sigma models. It would be nice to have a more detailed description of these transitions directly in non-linear sigma-model terms.

Finally, one could explore other situations where two dimensional phase diagrams are expected. For instance, situations where matter fermions are in other representations of the gauge group. Recently, a particular case, namely QCD_3 with two adjoint fermions, was explored in [127].

Chapter 4

Holographic QCD_3

In this Chapter, based on the original work in [115], we study holographically the vacuum structure of QCD_3, in the large N limit. Our aim is to provide a simple string theory understanding of the various vacua that one finds as parameters are varied, and of the phase transitions between them.

The vacuum structure depends on the following parameters, both discrete and continuous: the rank N, the number of flavors F, the Chern-Simons (CS) level k, and flavor masses m. In principle, flavors can have different masses, but we will always take them to be equal, unless otherwise stated, and call m this common mass. The CS level can be defined in two equivalent ways: we can define a bare CS level k_b by integrating out all fermions after giving them a large positive mass. Alternatively, we can define $k = k_b - F/2$ which has the property of flipping its sign under a time-reversal transformation. We will actually see a natural string theory interpretation of both. Finally, we allow ourselves the slight abuse of language of calling N the 'rank' of $SU(N)$.

In section 1.6, we reviewed the state of the art regarding the phase diagram of QCD_3. Here, we briefly summarize its phase diagram in various limits of the parameters. The recent regain of interest started with [75–81] where the large N, large k limit was studied in the presence of a small number of flavors, and a conformal field theory (CFT) was conjectured to arise at vanishing flavor masses. Evidence were also presented for a dual description of such fixed point in terms of a theory with bosonic matter. This led, eventually, to the conjecture [49] that such boson-fermion duality (a.k.a. bosonization) also holds at finite N, for $k \geq F/2$, as we reviewed in section 1.6.2. In this regime, there is still a single phase transition at a critical value of m, but there is no direct handle to determine its order (but for the two cases where F or k are large enough, where it is known that the transition is second order [72,73]). In section 1.6.3 also the case $k < F/2$ was contemplated, and the phase diagram was conjectured to consist of three phases as m is varied, with a purely quantum phase at small m where the flavor symmetry $U(F)$ is spontaneously broken and the low-energy physics is captured by the corresponding Grassmannian σ-model. Again, little can be said about the order of the two phase transitions. Finally, in the large N limit at finite k and F was studied in [25] and reviewed in section 1.6.4. A somewhat surprising result was found: irrespective of whether $k < F/2$ or $k \geq F/2$, a total of $F + 1$ different phases were found, with generically a coexistence of topological and σ-model

sectors. Moreover, they are separated by phase transitions that can be determined to be first order, following reasonings similar to the ones of [128–130]. Quite interestingly, one should then expect a multicritical point for a (large) value of the CS level k in which the phase transitions merge into a single second-order phase transition [84].

Below, we will propose a string theory picture for QCD_3, or more precisely for a gauge theory that we believe reproduces the low-energy behavior of QCD_3.[1] It refines a proposal made in [69, 114], where (probe) flavors were added on the non-supersymmetric holographic description of Yang-Mills in three dimensions (YM_3), see section 2.3.3. In the body of the Chapter, we will describe the technical details of our proposal, and some results concerning the phase diagram. Here, we want to outline by simple pictorial arguments how string theory helps us to find the different vacua of QCD_3, giving also evidence for the phase transitions being first order in the limit we are considering, which is the large N limit at finite k and F reviewed in section 1.6.4.

A sketch of the brane construction for the QCD_3 vacua

Our strategy for building a string theory configuration reproducing the physics of QCD_3 in the large N limit with a finite CS level and a finite number of flavors is to start from the string theory realization of YM_3 of section 2.3.3 and then add both a CS term and flavors in a probe approximation. We already analyze separately both the addition of the CS and the flavors in section 2.3.3. After backreaction of the D3s, we see that there are two important differences with respect to the Sakai-Sugimoto model. First, the D7-branes have an extra orthogonal direction in which to go (in other words, they wrap an $S^4 \subset S^5$), in addition to the angular coordinate on the cigar, so that they do not need to go back as anti-D7 branes. This is related to the fact that there is no gauge anomaly in 3d, hence anti-D7 branes are not required in the first place. Second, again because the D7-branes have the possibility to move along x^9, see Table 2.3, they are allowed to feel the repulsive force from the D3-branes, which is due to the fact that they have six mutually orthogonal directions. After backreaction, this is translated into the flavor D7-branes being slightly repelled from the tip of the cigar.

This is depicted in figure 4.1, which should be taken as an artistic rendering of the brane configuration, and similarly the following ones. Numerically exact graphs of the brane embeddings will be presented later.

The embedding of the flavor D7-branes will depend on the boundary condition at infinity along the $x^4 \cdots x^8$ directions. Since before backreaction and interactions are taken into account, the minimal distance between the D7-branes and D3-branes is given by the value of x^9 at which we place the D7s, we see that we will have massless fermions only if we set the D7s at $x^9 = 0$. Otherwise, the (bare) mass of the fermions will be proportional to the asymptotic value of x^9 of the D7-brane embedding.[2] Note that this gives fermions a mass whose sign is flipped when the parity transformation is implemented by reversing the sign of x^9. In figure 4.1 we have taken a

[1] A string theory realization of QCD_3 at finite N, giving rise to bosonization and symmetry breaking phases in terms of a magnetic Seiberg dual theory, was proposed in [83, 131].

[2] This is another difference with respect to the Sakai-Sugimoto model, where it is notoriously subtle to introduce a mass for the fermions, as we already mentioned above.

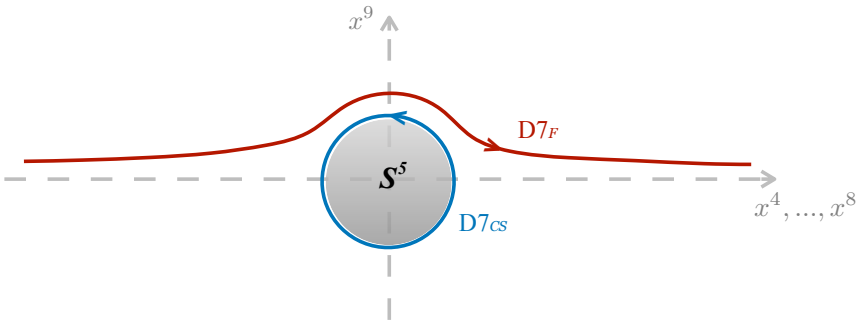

Figure 4.1: An artistic view of our brane set-up: the disk represents the S^5 at the tip of the cigar; the CS D7-branes wrap it, while the flavor D7-branes avoid it crossing the x^9 axis.

positive value for x^9 at infinity, and we henceforth associate it to a positive fermion mass.

Let us now consider a configuration with one negative mass flavor and no CS branes, figure 4.2. The embedding with minimal energy goes below the 'disk.'

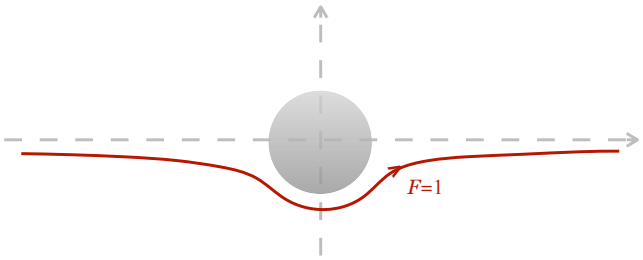

Figure 4.2: One flavor with negative mass and no CS branes.

If we now slowly bring the mass to positive values, i.e. bring the asymptotic value of the embedding to positive values of x^9, the embedding will be deformed to a non-minimal one, still passing below the disk, as shown in figure 4.3 (left). However, there is another embedding with the same asymptotic value for x^9 and, importantly, the same D7 charge around the tip of the cigar: it is a minimal embedding going above the disk, accompanied by a CS brane wrapping the disk counterclockwise (same figure, right).

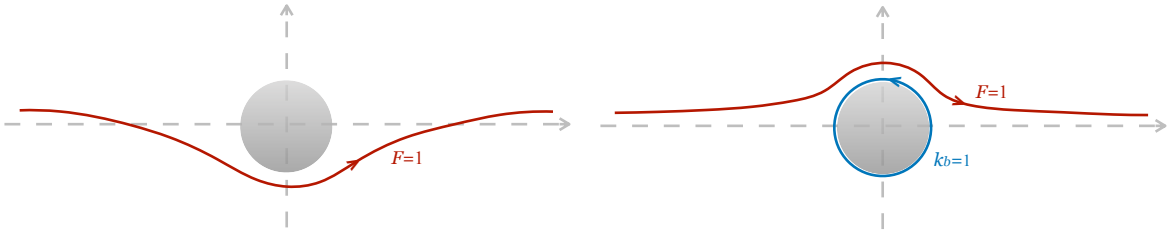

Figure 4.3: The two embeddings for positive mass: the non-minimal without CS branes, and the minimal with one CS brane.

As we will discuss in detail, there is a critical bare mass above which the energetics will favor the figure on the right. Hence we are witnessing a transition between a theory whose vacuum is trivial, i.e. $SU(N)_0$, for negative masses, to a theory with a topologically non-trivial vacuum, i.e. $SU(N)_1$, for positive masses. This is nothing else but the two phases of the theory denoted as $SU(N)_{1/2}$ with one Dirac fermion in the fundamental.

Let us now take a generic situation, with F flavor D7-branes. In order to implement a well-defined CS level, we specify a bare CS level k_b, which is an integer, by wrapping k_b D7-branes on the S^5 disk, counterclockwise if $k_b > 0$ (and clockwise if $k_b < 0$), when the flavors have a positive mass, i.e. when flavor D7s are above the disk (figure 4.4).

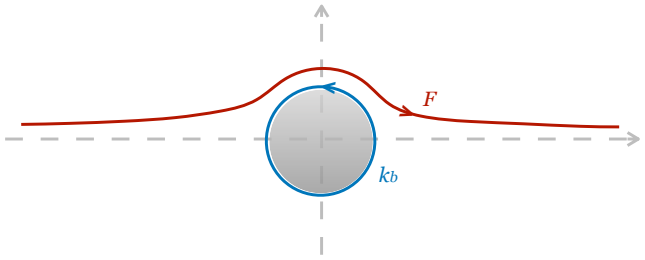

Figure 4.4: F flavors with positive mass and a bare CS level given by k_b (chosen to be positive in the figure).

The gauge theory on the CS D7-branes is $U(k_b) = U(k + F/2)$, where we used the relation between k_b and k in a theory with F flavors, $k = k_b - F/2$. Its level is the same as in the YM_3 case, i.e. $-N$. Hence for large positive mass, the vacuum is a topological theory, which by level/rank duality can be denoted by $SU(N)_{k+F/2}$. Note that the flavor D7-branes also carry a $U(F)$ gauge group, but since they extend infinitely in a direction orthogonal to $\mathbb{R}^{1,2}$, their coupling vanishes and it then corresponds to the global flavor symmetry of QCD_3.

Now bring all F flavor branes below the disk, by tuning their mass to be large and negative. The minimal energy embedding will now pass below the disk, but in the rearranging process, or in other words, to conserve the D7 charge around the angular variable of the cigar, the number of CS D7-branes has to decrease by F units.

If $k_b \geq F$ (i.e. $k \geq F/2$), we are left with $k_b - F$ CS branes, leading to a topological phase with $U(k_b - F)_{-N} = U(k - F/2)_{-N}$, level/rank dual to $SU(N)_{k-F/2}$.

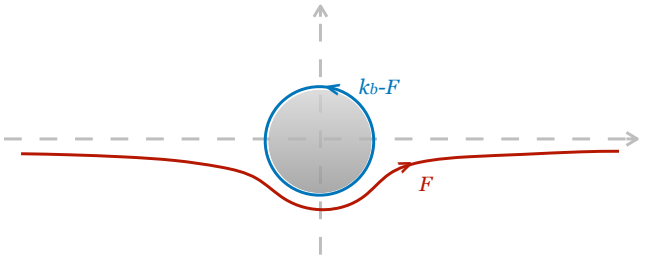

Figure 4.5: F flavors with negative mass, and $k \geq F/2$.

If $k_b < F$ (i.e. $k < F/2$), we are left with $F - k_b$ clockwise CS branes, leading to a topological phase with $U(F-k_b)_N = U(F/2-k)_N$, in agreement with the field theory result. The level of the gauge theory flips sign since the D7-branes wrap the S^5 in the opposite way. The level/rank dual is $SU(N)_{k-F/2}$. The two situations are depicted in figures 4.5 and 4.6, respectively.

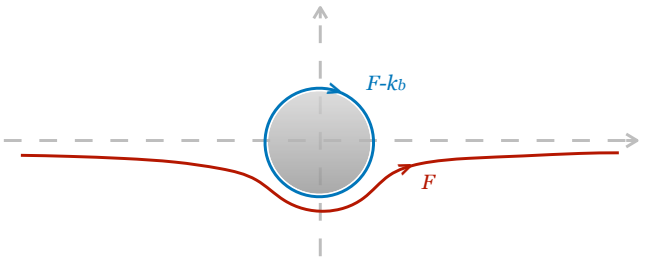

Figure 4.6: F flavors with negative mass, and $k < F/2$.

We can now ask what happens for small masses, i.e. for embeddings that asymptote to a small value of x^9. Take for instance the embedding that asymptotes to $x^9 = 0$, equivalent to a vanishing bare mass for the fermions. Obviously, the embeddings going above or below the disk have the same energy, since they are actually related by flipping the sign of x^9, i.e. by a parity transformation. Since wrapping CS D7-branes on the S^5 costs some energy, we are then to conclude that the most favorable embedding is the one with the fewest CS branes. When $k_b < F$, this means that the true vacuum should not contain any CS brane at all, i.e. there should not be any topological theory in the IR, as depicted in figure 4.7.

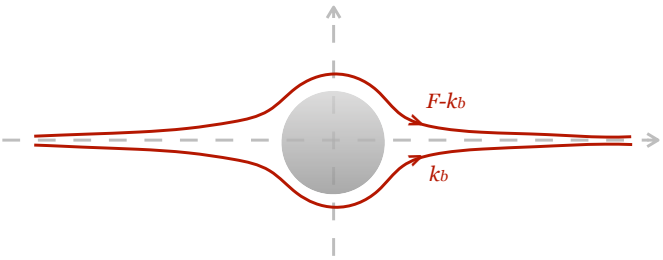

Figure 4.7: F flavors with zero mass, splitting in such a way that no CS branes are left.

However, the IR theory is not empty, since the flavors have to split into $F - k_b$ above and k_b below. Hence the flavor symmetry is spontaneously broken as

$$U(F) \to U(F-k_b) \times U(k_b) = U(F/2-k) \times U(F/2+k) \ , \tag{4.1}$$

and a σ-model parametrizing the Grassmannian $\mathrm{Gr}(F/2-k, F)$ arises from the corresponding Goldstone bosons.

It is now manifest that there has to be a critical asymptotic value of x^9 such that the two configurations in figure 4.3 are isoenergetic. As we will see, this will happen for some positive value of the mass, m^*.

Importantly, note that at such a critical mass there will be, generically, a degeneracy of more than two phases. Indeed, taking e.g. $k_b \geq F$, all configurations represented in figure 4.8 as p is varied from 0 to F, have the same energy.

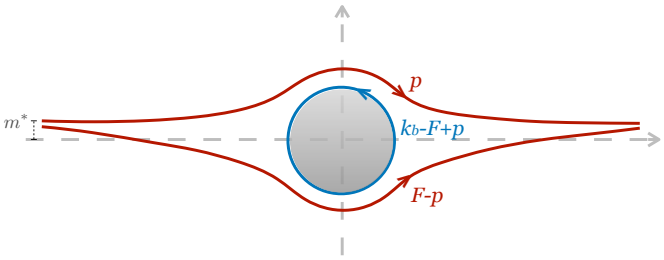

Figure 4.8: F flavors at critical mass m^*, splitting in $F+1$ different ways, depending on the value of p.

For every value of p such that $0 \leq p \leq F$, we have at low energies a σ-model on $\mathrm{Gr}(p,F)$ together with a topological CS theory $U(k_b - F + p)_{-N} = U(k - F/2 + p)_{-N}$, for $k_b - F + p > 0$. If $k_b - F + p < 0$, the topological theory is $U(F - p - k_b)_N = U(F/2 - p - k)_N$. In both cases the level/rank dual theory is $SU(N)_{k-F/2+p}$. The Grassmannians accompanied by the topological theories are exactly the degenerate phases for large N QCD_3 we saw in section 1.6, and we see them arising in this string theory construction in a very straightforward way.

Last but not least, we see pictorially that going from one phase to another requires some flavor branes to snap from above to below the disk. This clearly implies that the degenerate vacua are separated in field space, and therefore that the transitions are all first order.

The rest of the Chapter is organized as follows. In section 4.1 we provide details about the holographic model and we discuss the geometric properties of Chern-Simons and flavor probe branes. We use the holographic dictionary to extract information about the free energy and the fermion condensate on the field theory side. In section 4.2 we discuss the structure of brane configurations describing the different vacua of our holographic model and derive its phase diagram at leading order in the large N expansion. We explicitly prove that there are multiple vacua and that the phase transitions in our model are first-order. In section 4.3 we compute the $1/N$ corrections to the leading order phase diagram, and show how these modify its structure. Finally, in section 4.4, we focus on boson-fermion dualities and we show that our geometric set-up gives a simple understanding on how a dual bosonic description of QCD_3 arises at low-energies. We conclude in section 4.5 with few more comments regarding the validity of the large N expansion, brane backreaction and the existence of an IR fixed point.

4.1 Holographic description of QCD_3

In this section, employed with the holographic setup of section 2.3.3, we study the embedding of the D7 flavor branes in the massless and massive cases, obtaining the equations of motion describing their profile and calculating their corresponding energies. Finally, via the holographic

dictionary, we extract information about the free energy and the fermion condensate on the field theory side.

Massless case

It is convenient to describe the embedding in isotropic coordinates in the $x^4 \cdots x^9$ directions, transverse to the D3-brane worldvolume. To achieve this, we first define a new radial coordinate ρ from the holographic coordinate r in eq. (2.69) such that

$$r(\rho) = \left(\rho^2 + \frac{r_0^4}{4\rho^2}\right)^{1/2} . \tag{4.2}$$

The ambiguity in inverting this relation is solved by choosing the branch $\rho^2 \geq r_0^2/2$, so that spacetime in the transverse directions does not extend towards the origin, but a five-sphere with radius $r_0/\sqrt{2}$ is excluded. In these coordinates the metric can be rewritten as (now $r = r(\rho)$)

$$ds^2 = \frac{r^2}{L^2}\left(\eta_{\mu\nu}dx^\mu dx^\nu + f(r)(dx^3)^2\right) + \frac{L^2}{\rho^2}\left(d\rho^2 + \rho^2 d\Omega_5^2\right) . \tag{4.3}$$

We now separate the six transverse coordinates in the $x^4 \cdots x^8$ directions, which are part of the flavor branes worldvolume and for which we choose spherical coordinates λ and Ω_4 (with $\lambda \geq 0$), and the transverse 9 direction $u \in (-\infty, +\infty)$. The final form of the metric is

$$ds^2 = \frac{r^2}{L^2}\left(\eta_{\mu\nu}dx^\mu dx^\nu + f(r)(dx^3)^2\right) + \frac{L^2}{\rho^2}\left(d\lambda^2 + \lambda^2 d\Omega_4^2 + du^2\right) , \tag{4.4}$$

where $r = r(\rho)$ as in (4.2) and $\rho^2 = \lambda^2 + u^2 \geq r_0^2/2$. With this choice the D7-brane worldvolume is spanned by the eight coordinates $s = (x^\mu, \lambda, \Omega_4)$ and its embedding is described by $(x^3, u) = (x^3(s), u(s))$, as we can verify by looking at Table 2.3. We set x^3 to a constant, meaning that the D7-brane is localized on the circle, and by translational and rotational symmetry $u = u(\lambda)$. We have reduced the problem of finding the D7-brane embedding to the problem of finding the profile of a real function of a single real and positive variable. Recall that a parity transformation acts as $u(\lambda) \to -u(\lambda)$ and that, in the massless case, we have to impose the following boundary conditions ($\dot{u} \equiv du/d\lambda$ from now on)

$$\dot{u}(0) = 0 , \qquad u(\lambda_\infty) = 0 , \tag{4.5}$$

where λ_∞ is the location of the boundary, related to the UV cutoff on the field theory side. Now we are ready to compute the differential equation that $u(\lambda)$ should satisfy. First of all, the induced metric on the D7 takes the form

$$ds^2|_{D7} = \frac{r^2}{L^2}\eta_{\mu\nu}dx^\mu dx^\nu + \frac{L^2}{\rho^2}\left((1+\dot{u}^2)d\lambda^2 + \lambda^2 d\Omega_4^2\right) , \tag{4.6}$$

so that the action for a single D7 is

$$S_{D7} = -\frac{1}{(2\pi)^7 l_s^8}\int d^8s\; e^{-\phi}\sqrt{-g|_{D7}} = -T_{D7}V_3V_4L^2\int d\lambda \left(\rho^2 + \frac{r_0^4}{4\rho^2}\right)^{3/2}\frac{\lambda^4}{\rho^5}\sqrt{1+\dot{u}^2} , \tag{4.7}$$

where $T_{D7} = (2\pi)^{-7} l_s^{-8} g_s^{-1}$ is the D7-brane tension, V_3 is the volume of Minkowski spacetime and V_4 is the one of the unit four-sphere. The Euler-Lagrange equation of motion describing the D7-brane embedding is

$$\frac{d}{d\lambda}\left[(r_0^4+4\rho^4)^{3/2}\frac{\lambda^4}{8\rho^8}\frac{\dot{u}}{\sqrt{1+\dot{u}^2}}\right] = -(r_0^4+\rho^4)(r_0^4+4\rho^4)^{1/2}\frac{\lambda^4 u}{\rho^{10}}\sqrt{1+\dot{u}^2}\,, \tag{4.8}$$

to be solved with boundary conditions (4.5). Few observations are in order.

- If $r_0 = 0$, then the equation of motion reads

$$\frac{d}{d\lambda}\left[\frac{\lambda^4\dot{u}}{\rho^2\sqrt{1+\dot{u}^2}}\right] = -\frac{2\lambda^4 u}{\rho^4}\sqrt{1+\dot{u}^2}\,. \tag{4.9}$$

  Being the right-hand side non-vanishing, it is easy to see that a constant profile for $u(\lambda)$ is a solution only if $u(\lambda) \equiv 0$.[3] The solution $u(\lambda) = 0$ implies no symmetry breaking at all (being invariant under $u \to -u$), so we expect it to be unstable, as it was verified, for instance, in [133].

- An exact solution of (4.8) is given by the profile which wraps half of the five-sphere and then sits at $u = 0$ to $\lambda = \infty$, i.e.

$$u(\lambda) = \begin{cases} \pm\sqrt{r_0^2/2 - \lambda^2} & \text{if } 0 \le \lambda \le r_0/\sqrt{2}\,, \\ 0 & \text{if } \lambda \ge r_0/\sqrt{2}\,. \end{cases} \tag{4.10}$$

  There are two solutions, corresponding to the two signs in (4.10), one being a D7-brane wrapping the upper half-five-sphere and the other a D7-brane wrapping the lower one, as shown in figure 4.9. We will refer to these profiles as the maximal embeddings, since we will show that these solutions correspond to the ones having maximal energy, among all possible solutions to (4.8).

- In this choice of coordinates, the embedding $r = r_0$ representing the CS D7-branes discussed in section 2.3.3 takes the form

$$u^2(\lambda) = r_0^2/2 - \lambda^2\,, \tag{4.11}$$

  so that the full sphere is wrapped by the CS branes, which do not reach the UV boundary (and hence they do not introduce new degrees of freedom on the dual field theory side), see figure 4.10. We can choose an orientation for the CS branes, which are semicircles in the (λ, u) plane. In the conventions where the flavor D7-branes are taken to be oriented from left to right, a positive (negative) k_b is given by $|k_b|$ counterclockwise (clockwise) CS D7-branes. As we will explain in the next section, this is consistent with integrating out massive fermions in QCD_3.

[3] As opposite to what happens for the D4/D6 system of [87] and for the D3/D5 system of [132], where any constant profile is a solution for $r_0 = 0$. This reflects the fact that even in the supersymmetric case $M_{KK} = 0$ the D3/D7 system we consider is non-BPS.

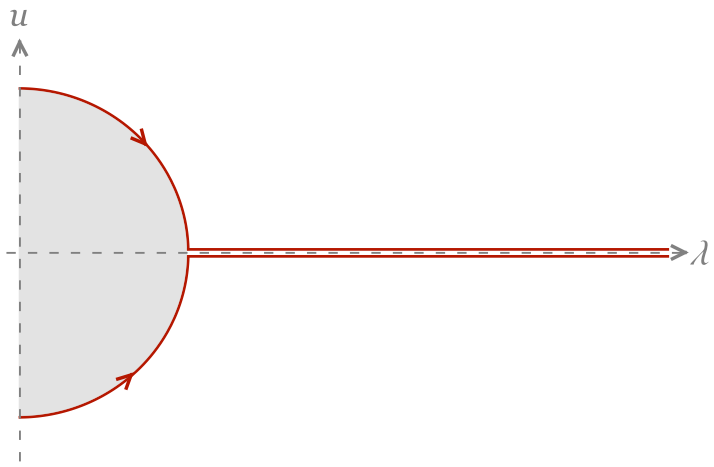

Figure 4.9: The two parity related maximal embeddings, corresponding to the highest energy solutions of the differential equation for the flavor brane profile.

- Most importantly, if $\tilde{u}(\lambda)$ is a solution, then also $-\tilde{u}(\lambda)$ is a solution (for this to hold it is crucial that the boundary condition $u(\lambda_\infty) = 0$ is parity-invariant). These solutions are related by a 3d parity transformation and have the same energy, simply because (4.7) is parity-invariant. This is the first achievement of holography: the fact that the effective potential for the eigenvalues of $\langle\bar{\psi}\psi\rangle$ has two degenerate minima at opposite non-vanishing values is an assumption in the large N description of QCD$_3$ [25]. Here instead, this is geometrically realized in a natural way.

Let us start discussing the solution in the asymptotic region where λ is close to the cutoff.[4] There $u(\lambda)$ is small and we will assume it to be slowly varying, so that the equation of motion becomes

$$\frac{d}{d\lambda}(\lambda^2\dot{u}) = -2u\,. \tag{4.12}$$

This equation is scale invariant, which reflects the absence of a scale in the theory in the far UV where r_0 is negligible (this QCD$_3$ UV-completion is $\mathcal{N} = 4$ SYM with 3d defect fermions, as in [133]). The characteristic polynomial has two complex conjugate roots $\alpha_\pm = (-1 \pm i\sqrt{7})/2$. The appearance of complex roots is because this equation describes the propagation of a field whose mass is below the Breitenlohner-Freedman bound, as already emphasized in [114, 133]. The violation of the BF bound corresponds to the instability of the embedding defined in eq. (4.10), which indeed does not represent the minimal energy configuration. This has been analyzed in detail in the case $r_0 = 0$ in [135], where it was shown that only the minimal energy configurations are free of tachyon instabilities. As we will discuss later, the instability of the maximal embedding is related to the loss of conformality of the dual field theory.

[4] An alternative regularization that does not require a cutoff consists in considering the full asymptotically flat D3-brane metric, and not only its near-horizon limit [134]. We prefer not to use this regularization since its holographic interpretation is less clear.

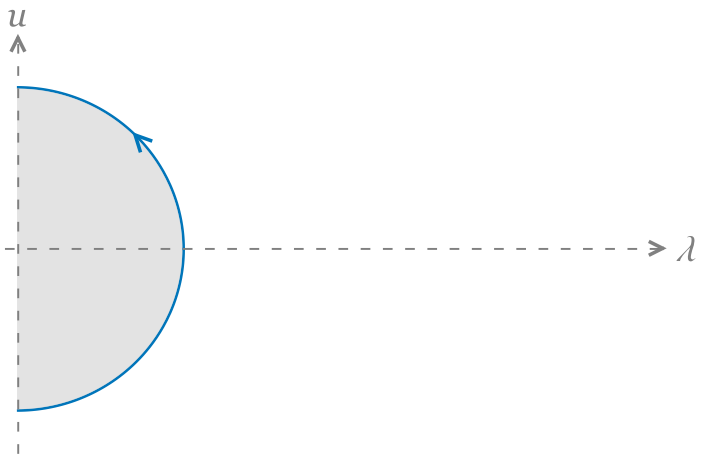

Figure 4.10: Chern-Simons branes are semicircles in the (λ, u) plane. A positive level correponds to the counterclockwise orientation.

The general form of the large λ behavior of the solution is

$$u(\lambda) = \pm\sqrt{\frac{\mu^3}{\lambda}}\sin\left(\frac{\sqrt{7}}{2}\log\frac{\lambda}{\mu} + \varphi\right), \tag{4.13}$$

where μ and φ are the two integration constants, being μ a positive quantity with the dimension of a length. As we will see later, this scale is related to the scale of the fermion condensate. The two signs are related to the two possible parity-related choices.

Requiring that $u(\lambda_\infty) = 0$, we can determine φ and the asymptotic solution reads

$$u(\lambda) = \pm\sqrt{\frac{\mu^3}{\lambda}}\sin\left(\frac{\sqrt{7}}{2}\log\frac{\lambda}{\lambda_\infty}\right). \tag{4.14}$$

We also get

$$\dot{u}(\lambda_\infty) = \pm\frac{\sqrt{7}}{2}\left(\frac{\mu}{\lambda_\infty}\right)^{3/2}. \tag{4.15}$$

Near the cutoff the global signs of the u and $\dot{u}$ are opposite: this means that the embedding with $\dot{u}(\lambda_\infty) > 0$ ($\dot{u}(\lambda_\infty) < 0$) approaches zero from negative (positive) values of u. The scale μ is fixed completely by the initial conditions at $\lambda = 0$ and it can be thought to be of the order of $u(0)$. Also, as a consistency check, we found $\dot{u}$ to be always numerically small (although non-vanishing) close to λ_∞, for any value of the cutoff.

Let us now discuss the solution in the other asymptotic region, where λ is small, $\dot{u}(\lambda) \sim 0$ and $\rho \sim u$. The behavior of $u(\lambda)$ for small values of λ is given by

$$u(\lambda) = u_0 - \frac{4(r_0^4 + u_0^4)}{5u_0(r_0^4 + 4u_0^4)}\lambda^2. \tag{4.16}$$

Note that the second derivative $\ddot{u}(0)$ has the opposite sign with respect to $u(0) = u_0$, meaning that the brane profile tends to bend towards the horizontal axis $u = 0$.

The asymptotic expansions of $u(\lambda)$ for large and small λ are given by (4.14) and (4.16), respectively. It is natural to make the following correspondence between the sign ambiguities of these formulas: if $u_0 > 0$ in (4.16) then the minus sign should be chosen in (4.14), and viceversa. This is confirmed by numerical analysis, as figure 4.11 shows. In this way, the D7-brane embedding interpolates from $u(0) = u_0$ to $u(\lambda_\infty) = 0$ monotonically without crossing the $u = 0$ axis. This zero-node embedding comes with two isoenergetic parity-related solutions, the 'up' with $u_0 > 0, \dot{u}_\infty < 0$ and the 'down' with $u_0 < 0, \dot{u}_\infty > 0$.

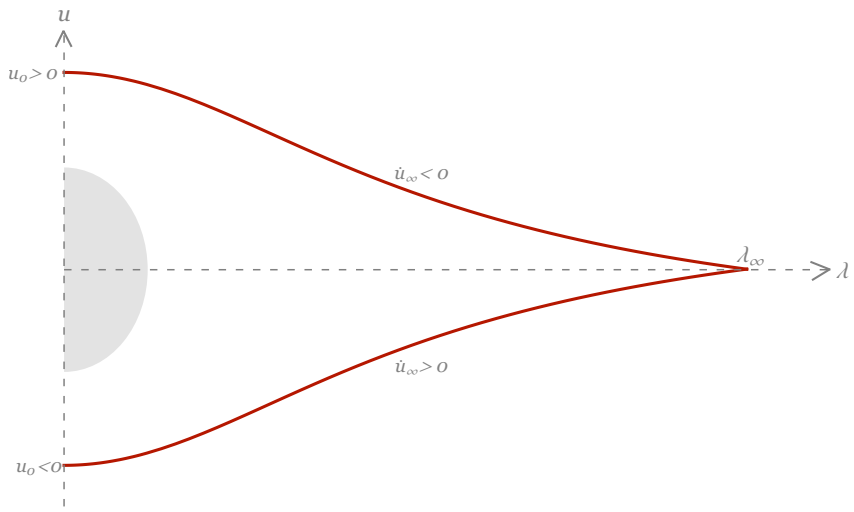

Figure 4.11: The two parity-related minimal embeddings in the massless case, numerical result with parameters $\mu = 1.34\, r_0$ and $\lambda_\infty = 5.73\, r_0$.

All other solutions of (4.8) are given by multiple-node functions $u(\lambda)$ and it is easy to show numerically that the associated energy is an increasing monotonic function of the number of nodes. In particular, we can regard the maximal embeddings (4.10) as the ones having the highest energy, since the constant behavior $u = 0$ for large values of λ can be seen as an embedding with infinite number of nodes.

Let us now compute the energy density associated to the flavor branes. For the maximal embedding it can be computed analytically and it reads, up to terms suppressed by $(r_0/\lambda_\infty)^4$

$$E_{D7}^{max} = -\frac{1}{V_3} S_{D7}^{max} = T_{D7} V_4 L^2 \left(\frac{\lambda_\infty^3}{3} + b_{max} r_0^3 \right) , \tag{4.17}$$

where

$$b_{max} = \frac{3\pi}{16} + \frac{1}{3}\left(2 + \sqrt{\frac{2}{\pi}} \Gamma\left(\frac{1}{4}\right) \Gamma\left(\frac{5}{4}\right) - \sqrt{2}\, {}_2F_1\left(-\frac{3}{4}, \frac{1}{2}; \frac{1}{4}; -1 \right) \right) \simeq 1.026\,. \tag{4.18}$$

The on-shell action includes a term which depends on the cutoff λ_∞, but this term is the same regardless of the particular solution of the equations of motion (i.e. it does not depend on the

number of nodes and, hence, on the scale μ). Since we are interested in comparing energies between different solutions with the same boundary conditions, we subtract (4.17) to the energy of a given embedding.

With this regularization the energy of the maximal embedding is clearly vanishing, whereas the energy of any other embedding is negative and monotonically increasing with the number of nodes. For the two parity-related minimal embeddings it reads

$$E_F^0 = -\frac{1}{V_3}(S_{D7} - S_{D7}^{max}) = -T_{D7}V_4L^2(br_0^3 + a\mu^3) \simeq -N(g_sN)(bM_{KK}^3 + aM_\mu^3) \ , \tag{4.19}$$

where a and b are order one dimensionless constant and the energy scale M_μ is related to the length scale μ through the holographic radius/energy relation [136], which we take here $\mu = M_\mu L^2/2$. This $\mathcal{O}(N)$ difference between the energy density of the maximal and the minimal embedding is related to the potential barrier that separates the degenerate vacua in field space.

One can consider a more general configuration, made of F D7-branes. As already noticed, the up and the down embeddings are energetically equivalent. Hence, in the large N limit in which flavor branes do not interact, one can choose p of them being up and $F-p$ being down. As p is varied from 0 to F all these configurations are energetically equivalent, with energy

$$E_{F,tot}^0 = pE_F^0 + (F-p)E_F^0 = FE_F^0 \ , \tag{4.20}$$

which, indeed, does not depend on p.

Massive case

Let us now consider the inclusion of a bare quark mass. The quark mass can be viewed as a source for the meson operator $\bar\psi\psi$, which is described by the flavor brane profile, whose bending introduces the characteristic length scale μ. We saw before that for large values of λ

$$u(\lambda) \sim \frac{1}{\sqrt{\lambda}} \, , \tag{4.21}$$

so a small mass m can be introduced by requiring that

$$\lim_{\lambda\to\lambda_\infty} \sqrt{\frac{\lambda}{\mu}}u(\lambda) = 2\pi l_s^2 m \, , \tag{4.22}$$

which amounts to interpret the bare quark mass as the spatial separation between the D3 and the D7-branes along the common transverse direction u in the ultraviolet regime of the theory. Indeed, quarks are the lightest modes of the open strings stretching between these branes, and get an energy proportional to their length.

We have seen that in the massless case there are two isoenergetic profiles for a flavor brane. Now we want to see if the inclusion of a small mass selects one of the two to be energetically favorite. This is to be expected, since the two different zero-node embeddings are not related anymore by a parity transformation $u \to -u$, because of the parity-breaking boundary condition

at infinity. Intuitively, a small positive (negative) mass will make the up (down) embedding favorite, thus lifting the large N vacuum degeneracy of the massless case. We now give a proof of this statement and, as a byproduct, we also derive the expression of the meson condensate for small quark mass.

Suppose to start from the massless case and perform a small change in the boundary condition of the flavor brane profile at the UV cutoff

$$\delta u_\infty = \sqrt{\frac{\mu}{\lambda_\infty}} 2\pi l_s^2 \delta m \,. \tag{4.23}$$

The corresponding variation of the on-shell action $S = \int d\lambda \mathcal{L}$ is given by

$$\delta S_{D7} = \frac{\partial \mathcal{L}}{\partial \dot{u}} \delta u \Big|_{\lambda=0}^{\lambda=\lambda_\infty} = -T_{D7} V_3 V_4 L^2 \left[(r_0^4 + 4\rho^4)^{3/2} \frac{\lambda^4}{8\rho^8} \frac{\dot{u}\ \delta u}{\sqrt{1+\dot{u}^2}} \right]_{\lambda=0}^{\lambda=\lambda_\infty} , \tag{4.24}$$

where in the first step we have used the equation of motion. Since $\dot{u}(0) = 0$, we get the following variation of the energy density

$$\delta E_F = T_{D7} V_4 L^2 \lambda_\infty^2 \dot{u}(\lambda_\infty) \delta u_\infty \simeq \pm N \sqrt{g_s N} M_\mu^2 \ \delta m \,. \tag{4.25}$$

Recall that $\dot{u}_\infty$ characterizes the massless embeddings and can have both signs. Now, if we give a positive (negative) mass, then the solution with $\dot{u}_\infty < 0$ ($\dot{u}_\infty > 0$) is preferred, i.e. the up (down) embedding is selected. This means that the quark mass lifts the degeneracy between the two embeddings. Thus, for the energetically favorite embedding we have that (up to quadratic corrections in the quark mass)

$$E_F(m) = E_F(0) - c|m| \simeq E_F^0 - N\sqrt{g_s N} M_\mu^2 |m| \,. \tag{4.26}$$

Note that this result implies that the fermion condensate is linear in N and it is negative for positive mass and viceversa, since

$$\langle \bar{\psi}\psi \rangle = \frac{dE_F}{dm} = -c\ \mathrm{sign}(m) \qquad \text{where} \qquad c \simeq N\sqrt{g_s N} M_\mu^2 \,. \tag{4.27}$$

It is now clear that the scale μ (or, equivalently, its energy counterpart M_μ) is related to the scale of symmetry breaking. The fact that there is a discontinuity in the first derivative of the on-shell action (which maps to the free energy of the dual field theory) signals the presence of a first-order phase transition whenever one switches from an up to a down embedding or viceversa. This observation will play a crucial role later.

Let us now consider a configuration of F flavor branes, with a common mass m. As discussed above, the degeneracy between up and down embeddings is lifted for $m \neq 0$. Indeed, in the large N limit where D7-branes do not interact, a configuration with p flavor branes in the up embedding and $F - p$ in the down one would have a total energy

$$E_F(m,p) = p(E_F^0 - cm) + (F-p)(E_F^0 + cm) = F E_F^0 + (F-2p)cm \,. \tag{4.28}$$

Clearly, if $m > 0$ the minimal energy configuration occurs for $p = F$, whereas if $m < 0$ for $p = 0$. In both cases, the total energy will just be F times $E_F(m)$, eq. (4.26). In the massless limit the degeneracy between up and down embeddings is regained, since the above equation reduces to eq. (4.20). This is insensitive to the value of p, and one recovers the degeneracy of all $F+1$ configurations obtained varying p from 0 to F.

4.2 Large N energetics of holographic QCD_3

In this section we want to derive the (large N) phase diagram of our holographic model. We will first discuss the generic structure of brane configurations describing its vacua. Then, using the results of the previous section, we will derive its full phase diagram and finally compare it with the pure QFT analysis. In section 4.3 we will instead discuss how this is modified by taking into account $1/N$ corrections.

4.2.1 Geometric structure of QCD_3 vacua

In the previous section we have discussed embeddings of flavor branes in the D3-brane cigar geometry. In section 2.3.3, we instead described the CS branes embedding in the same geometry. Here we would like to consider configurations having both CS and flavor branes, since a vacuum of holographic QCD_3 would in general include both.

Actually, one cannot displace flavor branes at will, i.e. independently of CS ones. Indeed, a CS/flavor brane configuration describing a vacuum of the theory should be compatible with UV data. The latter includes N, F, m and the axion monodromy measured at the spacetime location holographically dual to the UV of the field theory. On the (λ, u) plane (more precisely, it is the strip $0 \leq \lambda \leq \lambda_\infty$), this is clearly the point P_{UV} where all flavor branes intersect and the global symmetry is $U(F)$, i.e. $P_{UV} = (\lambda_\infty, 0)$ in the massless case.

We now show that in order to fix this monodromy to give a well-defined CS level $k \equiv k_b - F/2$, the number of CS branes must depend on p. The axion monodromy measures the effective CS level of the dual field theory as

$$\int_{S^1} F_1 = -k_{eff}\,, \tag{4.29}$$

where S^1 is a circle whose location in spacetime is specified, among all other coordinates, once we fix a point in the (λ, u) plane. Since C_0 couples magnetically to D7-branes, the Bianchi identity of F_1 is violated by source terms which are delta functions picked at the location of both flavor and CS branes. As usual, this can be easily seen by computing the equations of motion of the dual form C_8, which instead couples electrically to D7-branes.

Let us define as 'p sector' (with $p = 0, \ldots, F$) a brane configuration with p up branes (clockwise oriented), $F - p$ down branes (counterclockwise oriented) and k_0 counterclockwise oriented CS branes.[5] In order to determine k_0, we first compute k_{eff}, which is given by the following step function (we consider the massless case for definiteness)

$$k_{eff} = \begin{cases} k_0 - p & \text{in } \mathcal{R}_+\,, \\ k_0 & \text{in } \mathcal{R}_0\,, \\ k_0 + F - p & \text{in } \mathcal{R}_-\,, \end{cases} \tag{4.30}$$

where $\mathcal{R}_+$, $\mathcal{R}_0$ and $\mathcal{R}_-$ are the regions in the (λ, u) plane which are above, between and below flavor branes, respectively (see figure 4.12). At the intersection point P_{UV} both flavor branes

[5] When $k_0 < 0$, the number of counterclockwise CS branes being k_0 actually means to have $|k_0|$ clockwise CS branes.

count one-half and thus $k_{eff} = k_0 - p + F/2$ there. In order to have $k_{eff} = k$ at P_{UV} we fix the number of counterclockwise CS branes to be

$$k_0 = k + p - \frac{F}{2}\,. \tag{4.31}$$

As a result, we can rewrite

$$k_{eff} = \begin{cases} k - \frac{F}{2} & \text{in } \mathcal{R}_+\,, \\ k + p - \frac{F}{2} & \text{in } \mathcal{R}_0\,, \\ k + \frac{F}{2} & \text{in } \mathcal{R}_-\,. \end{cases} \tag{4.32}$$

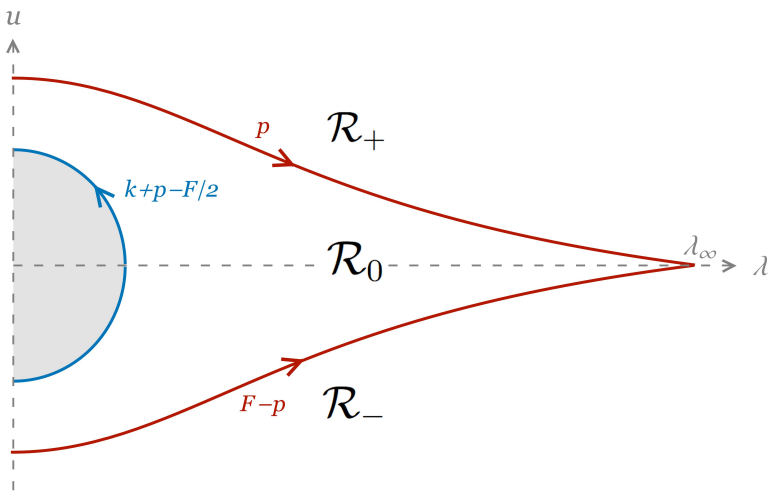

Figure 4.12: The configuration of flavor branes and (counterclockwise oriented) CS branes in a (massless) p sector. We interpret a negative number of counterclockwise branes as a positive number of clockwise branes.

This has a simple field theory interpretation. In region $\mathcal{R}_+$ ($\mathcal{R}_-$) it is as if all flavors have been integrated out with a negative (positive) mass. The effective CS levels read $k - F/2$ and $k + F/2$, respectively, consistently with $k_{eff} = k + \text{sign}(m)F/2$, as expected from field theory. In region $\mathcal{R}_0$ it is as if p flavors have been integrated out with a positive mass and $F - p$ with a negative one, and hence the effective level is $k + p - F/2$. In absence of flavor branes, when isotropy on the (λ, u) plane is recovered, the effective CS level coincides with the bare level k_b everywhere, as computed in eq. (2.74). Since k is the time-reversal odd CS level, we will take it to be non-negative without loss of generality.

Note that with the above argument we have recovered the number of CS branes k_0 in each p sector that we argued to be there with the mechanism of $F - p$ up branes 'pulled

down' and wrapping the S^5 before sitting in the down embedding, described around figure 4.3. These topological arguments, and in particular eq. (4.31), hold regardless of flavor branes being massless or massive, the only difference being that $P_{UV} = (\lambda_\infty, u_\infty)$ in the massive case.

In figure 4.12 the structure of a p sector is depicted. Its low-energy dynamics is as follows.

- Flavor branes break spontaneously the gauge $U(F)$ symmetry (associated to the F coincident branes in the UV) to $U(p) \times U(F-p)$. This happens since the F branes are spatially separated in the u direction, as soon as we move towards the bulk. By Higgs mechanism the gauge bosons corresponding to the broken part of the gauge group become massive. These correspond to the $2p(F-p)$ lightest modes of the open strings having one extremum on one down brane and the other on one up brane. Instead, the gauge bosons corresponding to the up/up and the down/down open strings are still massless, signaling the presence of an unbroken $U(p) \times U(F-p)$ gauge group. The longitudinal components of the massive gauge bosons are holographically associated with Goldstone bosons in the dual field theory, through massless poles which must appear in correlators involving currents. The global symmetry-breaking pattern is $U(F) \to U(p) \times U(F-p)$, leading to a number of Goldstone bosons which is indeed $F^2 - p^2 - (F-p)^2 = 2p(F-p)$. They parameterize a σ-model whose target space is

$$\mathrm{Gr}(p, F) = \frac{U(F)}{U(p) \times U(F-p)} \ . \tag{4.33}$$

  Note that the RR five-form flux induces on the flavor D7-branes a term that should match the level N Wess-Zumino term in the σ-model.

- The CS branes give, at low energy, a three dimensional $U(k + p - F/2)_{-N}$ theory (if $k + p - F/2 > 0$) or a $U(-k - p + F/2)_N$ theory (if $k + p - F/2 < 0$). These are pure three dimensional Chern-Simons theories, since the Yang-Mills sector decouples (gluons get a large tree-level mass and decouple well before the theory reaches strong coupling). In both cases, these theories are level/rank dual to $SU(N)_{k+p-F/2}$.

Thus, the IR dynamics of a p sector is described by

$$\mathrm{Gr}(p, F) \times SU(N)_{k+p-F/2} \, . \tag{4.34}$$

The Grassmannian and the topological field theory are mutually decoupled, since the branes do not interact at leading order in the large N expansion.

Finally, let us observe that the $F + 1$ sectors in (4.34) are the same which were found with in the large N limit of QCD_3, see section 1.6.4. However, it is worth noticing that in the field theory analysis only the Grassmannian of each sector was derived from the effective potential of the theory, whereas the topological part was conjectured to be there. In our construction both appear naturally in a simple geometrical way.

4.2.2 Phase diagram of holographic QCD_3

The $F+1$ sectors discussed above are all possible configurations that can describe holographic QCD_3 vacua. We now want to uncover the phase diagram of the theory as a function of the fermion mass m, by minimizing the (free) energy over p.

At large N, we have the contribution from the flavor branes, the CS branes and the mass deformation, neglecting any kind of brane interactions. We have already written in (4.28) the contribution from the flavor branes for each p sector. The CS contribution is just given by the number of CS branes in each sector times the energy density $E_{\rm CS}$ of each of them, eq. (2.76). The total (free) energy of the p sector is hence given by

$$E(p) = FE_F^0 - 2cmp + Fcm + \left|k + p - \frac{F}{2}\right| E_{\rm CS}\,, \tag{4.35}$$

where E_F^0, c and $E_{\rm CS}$ are all of order N. This formula is invariant under the transformation $p \to F-p$, $m \to -m$ and $k \to -k$, correctly implementing a time-reversal transformation. We now distinguish different cases (recall that we can take $k \geq 0$ and that $0 \leq p \leq F$). Let us define $m^* \equiv E_{\rm CS}/(2c)$ and neglect the irrelevant constant shift $FE_F^0 + Fcm$.

1. If $k \geq F/2$, the quantity inside the absolute value is positive $\forall p$. So we have

$$E(p) = (E_{\rm CS} - 2cm)p + \left(k - \frac{F}{2}\right) E_{\rm CS}\,, \tag{4.36}$$

whose minimum is for $p=0$ if $m < m^*$ and for $p=F$ if $m > m^*$. If $m = m^*$ all $F+1$ vacua are degenerate. The energy of the true vacuum as a function of m hence reads

$$E_{vac}(m) = \begin{cases} \left(k - \frac{F}{2}\right) E_{\rm CS} & \text{if } m < m^*\,, \\ -2cmF + \left(k + \frac{F}{2}\right) E_{\rm CS} & \text{if } m > m^*\,. \end{cases} \tag{4.37}$$

Since the derivative with respect to m is discontinuous at $m = m^*$, the phase transition is first order. The vacuum $p=0$ is the pure TQFT phase $SU(N)_{k-F/2}$ and the vacuum $p=F$ is the pure TQFT phase $SU(N)_{k+F/2}$, where the global symmetry of the UV theory is unbroken. The resulting phase diagram, depicted in figure 4.13, is the same as the one in the finite N case, but with the phase transition being first order.

2. If $k < F/2$, we have to see whether the quantity inside the absolute value is positive or negative. So we have to distinguish two subcases.

   (a) If $0 \leq F/2 - k \leq p \leq F$

$$E(p) = (E_{\rm CS} - 2cm)p + \left(k - \frac{F}{2}\right) E_{\rm CS}\,, \tag{4.38}$$

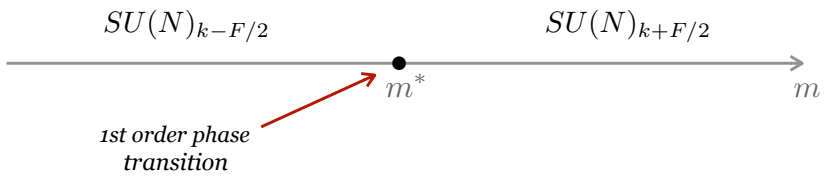

Figure 4.13: The phase diagram for $k \geq F/2$. At $m = m^*$ all $F+1$ vacua are degenerate.

whose minimum is for $p = F/2 - k$ if $m < m^*$ and for $p = F$ if $m > m^*$. If $m = m^*$ the vacua $p = F/2 - k, ..., F$ are degenerate. Note that

$$\begin{aligned} E(F/2-k) &= -2cm\left(\frac{F}{2}-k\right), \\ E(F) &= -2cmF + \left(\frac{F}{2}+k\right) E_{\rm CS}\,. \end{aligned} \tag{4.39}$$

(b) If $0 \leq p \leq F/2 - k \leq F$, then

$$E(p) = (-E_{\rm CS} - 2cm)p - \left(k - \frac{F}{2}\right) E_{\rm CS}\,, \tag{4.40}$$

whose minimum is $p = 0$ if $m < -m^*$ and $p = F/2 - k$ if $m > -m^*$, whereas if $m = -m^*$ the vacua $p = 0, ..., F/2 - k$ are degenerate. Note that

$$\begin{aligned} E(0) &= \left(\frac{F}{2}-k\right) E_{\rm CS}\,, \\ E(F/2-k) &= -2cm\left(\frac{F}{2}-k\right). \end{aligned} \tag{4.41}$$

Looking at the different energies it follows that: if $m < -m^*$ the true vacuum is $p = 0$, if $m = -m^*$ all the vacua $p = 0, ..., F/2 - k$ are degenerate, if $-m^* < m < m^*$ the true vacuum is $p = F/2 - k$, if $m = m^*$ all the vacua $p = F/2 - k, ..., F$ are degenerate, if $m > m^*$ the true vacuum is $p = F$. The energy of the true vacuum as a function of m hence reads

$$E_{vac}(m) = \begin{cases} \left(\frac{F}{2}-k\right) E_{\rm CS} & \text{if } m < -m^*\,, \\ -2cm\left(\frac{F}{2}-k\right) & \text{if } -m^* < m < m^*\,, \\ -2cmF + \left(\frac{F}{2}+k\right) E_{\rm CS} & \text{if } m > m^*\,. \end{cases} \tag{4.42}$$

Since the derivative with respect to m is discontinuous at $m = -m^*$ and $m = m^*$, the phase transitions are again first order. The vacua $p = 0$ and $p = F$ are the same as before. The vacuum $p = F/2 - k$ is described by the Grassmannian $\mathrm{Gr}(F/2-k, F)$ with no TQFT

sector, and the symmetry-breaking pattern $U(F) \to U(F/2-k) \times U(F/2+k)$ takes place. The resulting phase diagram, depicted in figure 4.14, is analogous to the small N case we reviewed in section 1.6.3. The two first-order phase transitions take place at opposite values of m. Hence, at leading order in the large N expansion, the point $m = 0$ sits always inside the so-called quantum phase $\forall k < F/2$. For $k = 0$ this is mandatory, as dictated by the VW theorem. Moreover, the width of the quantum phase in parameter space is given by

$$2m^* = \frac{E_{\rm CS}}{c} \sim \frac{r_0^3}{\mu^2 l_s^2} \sim \sqrt{g_s N}\frac{M_{KK}^3}{M_\mu^2} \ , \tag{4.43}$$

which is $\mathcal{O}(N^0)$ in the large N expansion.

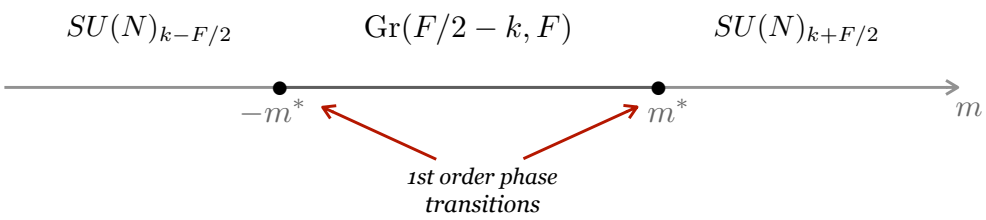

Figure 4.14: The phase diagram for $k < F/2$. At $m = -m^*$ the vacua with $p = 0, \ldots, F/2 - k$ are degenerate, at $m = m^*$ the vacua with $p = F/2 - k, \ldots, F$ are degenerate.

When translated in the asymptotic boundary condition for the embedding through (4.22), the critical value of the mass corresponds to

$$u^* = \sqrt{\frac{\mu}{\lambda_\infty}} 2\pi l_s^2 m^* \sim \sqrt{\frac{r_0}{\lambda_\infty}} \left(\frac{r_0}{\mu}\right)^{3/2} r_0 \ll r_0 \ , \tag{4.44}$$

so the brane embedding at the critical value is still very close to the massless one. Hence we are still well within the regime of small deviations from the latter and, as a consequence, also the Taylor expansion (4.25) is justified. One can consider next-to-leading order corrections to m^*, by computing the full mass dependence of the flavor brane energy. This gives a correction to (4.43), but clearly does not spoil the existence of first-order phase transitions and of a quantum phase whose width is $\mathcal{O}(N^0)$.

As opposite to what happens in the large N field theory description, in the holographic picture the quantum phase emerging for $k < F/2$ has a non-vanishing width already at leading order in the large N expansion. This implies that the phase diagram displays a different structure in the two regimes $k \geq F/2$ and $k < F/2$. Interestingly, our phase diagram is identical to the one conjectured for the same theory, but at finite N.

The apparent discrepancy between holography and large N field theory can be understood by pure field theory arguments, just recalling that our holographic set-up describes in fact a four dimensional gauge theory compactified on a (supersymmetry breaking) circle. This reduces to a pure three dimensional theory only in the limit where the radius of the compactified dimension

is sent all the way to zero, equivalently $M_{KK} \to \infty$. As we will show below, in such limit our results reconcile with the pure 3d analysis.

Let us first notice that taking $E_{\rm CS} = 0$, the two different phase diagrams displayed in figures 4.13 and 4.14 merge, both enjoying a single first-order phase transition at $m^* = 0$, where all vacua are degenerate. This scenario is exactly the one we reviewed in section 1.6.4 at the leading order in the large N expansion. In particular, eq. (4.35) reduces to (4.28), which exactly matches the effective potential computed with QFT techniques.

Large N QCD_3 with massless probe quarks has only one scale, which is $\Lambda_3 = g^2_{\mathrm{YM}_3} N$. All other quantities, such as the QCD-string tension (computed from the Wilson loop) and the fermion condensate, depend on Λ_3 in a way uniquely fixed by dimensional analysis (in particular both σ and $\langle\bar\psi\psi\rangle$ scale as Λ_3^2).

On the contrary, the four dimensional theory our holographic model describes is a $(\mathrm{S})\mathrm{YM}_4$ theory compactified on a circle, which is characterized by two parameters: the dimensionless 't Hooft coupling $\lambda_t = g^2_{\mathrm{YM}_4} N \sim g_s N$ and the circle radius $1/M_{KK}$. In units of M_{KK}, different physical quantities depend on different powers of λ_t. This is a common feature of several holographic theories realized through compactification on S^1 of a higher-dimensional gauge theory.

First of all recall that M_{KK} sets the scale of the supersymmetry breaking masses of the fermions (and subsequently of the scalars). Hence, from the point of view of the 4d theory, we can assume that for energies above M_{KK} the 't Hooft coupling is given by $\lambda_t \sim g_s N$ and it does not run, while at energies below M_{KK} it runs as in pure YM (since flavors are quenched), with a dynamical scale defined by

$$\Lambda_4 = M_{KK} e^{-\frac{1}{\beta\lambda_t}} \ , \tag{4.45}$$

with β an unimportant $\mathcal{O}(1)$ numerical positive factor. Note that the relation above implies that at the compactification scale M_{KK} the 4d theory is always in the deconfined phase, though for large λ_t very close to the confining scale Λ_4.

At energy scales below M_{KK} the theory becomes effectively three dimensional. Hence what is now relevant is the 3d dynamical scale. We first identify

$$g^2_{\mathrm{YM}_3} \sim g^2_{\mathrm{YM}_4} M_{KK} \ . \tag{4.46}$$

The above relation must be understood at the matching scale, i.e. at $E \sim M_{KK}$. The 3d dynamical scale is then

$$\Lambda_3 \sim g_s N M_{KK} \sim \lambda_t M_{KK} \ . \tag{4.47}$$

It is now obvious that the limits $\lambda_t \to 0$ and $\lambda_t \to \infty$ describe very different regimes. For $\lambda_t \to \infty$, the compactification scale is very close to the confining scale from the 4d point of view. Below that scale, from the 3d point of view one is already deeply in the confining regime. Thus one is never really in a 3d theory with perturbative degrees of freedom. When $\lambda_t \to 0$, instead, the theory compactifies when it is still in the perturbative regime, both in 4d and also in 3d. Hence the evolution can go on towards the IR, until the theory confines as a purely 3d theory. We will call the '3d limit' the latter, when one sends $M_{KK} \to \infty$ holding the 3d scale fixed.

From the 4d perspective, the non-vanishing CS level is obtained by turning on an x^3-dependent θ angle. Concretely, this is implemented as in eqs. (2.73)–(2.75). This would produce k equally spaced domain walls (more precisely, interfaces), i.e. each time $\theta = \pi \mod 2\pi$.[6] Deforming the varying θ to a step function can bring all domain walls together, and produce a level k CS term for the $SU(N)$ gauge field, when reduced to the domain wall (see [65,138,139]). The tension of such domain walls is given by $T_{DW} \sim N\Lambda_4^3$. In the 3d limit, this becomes

$$T_{DW} \sim N\Lambda_3^3 \frac{1}{\lambda_t^3} e^{-\frac{3}{\beta\lambda_t}} \to 0 \ . \tag{4.48}$$

We thus see that domain walls (which correspond to CS branes in our set-up) become tensionless in the 3d limit, so that the CS level becomes a feature of the 3d theory and is no longer associated to an object that has been added to the theory. Hence, it does not come as a surprise that as the energy of CS branes vanishes, $E_{\rm CS} \to 0$, our phase diagram becomes identical to the field theory one. In fact, our result can be regarded as an independent check for the validity of the analysis performed in the large N limit [25].

The consistency of this picture can be understood also from the point of view of the large N expansion. The finite width of the quantum phase in figure 4.14 is proportional to m^* and thus to $E_{\rm CS}$, suggesting that in the four dimensional theory compactified on a circle the large N expansion breaks down. This is actually the case and has a clear field theory origin. As we just emphasized, the 3d Chern-Simons term is implemented through a varying θ angle in the parent 4d theory. This generates k interfaces, described in the holographic set-up by wrapped D7-branes. These objects have tension proportional to N and this indeed spoils the large N counting rules of the four dimensional theory. In the 3d limit, where $E_{\rm CS} \to 0$, the consistency of large N counting is recovered.[7]

4.3 $1/N$ corrections

All what we have been discussing so far was at leading order in the large N expansion. Here we would like to consider the first next-to-leading order corrections. What we have to do is to compute $1/N$ contributions to the free energy and to minimize such contributions over the different p sectors. Since we are interested in the vacuum energy, we can safely neglect the contribution of the gauge fields on the probe branes, whose fluctuations describe instead the dynamical degrees of freedom of the theory.

Recall that at leading order we considered the sum of all contributions coming from the tensions of the probe branes, i.e. the DBI part of the on-shell action. Clearly, the presence of an axion introduces a term in the action given by

$$S_{RR} = -\frac{1}{2(2\pi)^7 l_s^8} \int d^{10}x \sqrt{-g} |F_1|^2 \ , \tag{4.49}$$

[6] Indeed, the D7-branes that engineer the CS level in the present set-up are straightforwardly related by T-duality to the D6-branes that holographically engineer the $\theta = \pi$ domain walls of YM_4 [137].

[7] We thank Zohar Komargodski for a discussion on this point.

where the integral has to be performed over the entire spacetime. This contribution is $1/N$ suppressed with respect to the DBI, since it has no explicit factor of g_s.
Given the result in (4.32), the only p-dependent part of the on-shell action is given when performing the integral in (4.49) over the region $\mathcal{R}_0$, where $k_{eff} = k_0$. Thus, neglecting p-independent terms we get

$$S_{RR} = -\frac{1}{2(2\pi)^7 l_s^8} V_3 V_4 L^2 \int_{\mathcal{R}_0} d\lambda\, du \int_{S^1} dx^3\, r^3\, |F_1|^2\,, \tag{4.50}$$

where r is expressed in terms of the radial coordinate $\rho^2 = u^2 + \lambda^2$ as in eq. (4.2). We can extract the $1/N$ correction to the free energy density as

$$E_{1/N}(p) = -\frac{S_{RR}}{V_3} = \Delta \left(k + p - \frac{F}{2}\right)^2\,, \tag{4.51}$$

where Δ is a positive constant given by

$$\Delta \sim (g_s N)^2 M_{KK} M_\mu^2\,. \tag{4.52}$$

As we are going to show below, the positiveness of Δ has important implications on the phase diagram. The corresponding field theory quantity was argued to be positive in the field theory analysis using consistency with the VW theorem, see section 1.6.4. In our holographic context, instead, we cannot use a similar argument, since the phase $p = F/2$ in the $k = 0$ massless case is already selected at leading order in large N and the VW theorem is surely satisfied regardless the sign of Δ.[8] Nicely, our geometric set-up encodes in a simple way the $1/N$ corrections and allows to determine the value of Δ in terms of the defining parameters of the model, besides showing its positivity. Similar arguments as the ones presented here were used in the Sakai-Sugimoto model to compute the Witten-Veneziano mass of the η' meson [89].
In our holographic set-up, having a positive Δ implies that at the microscopic level locally parallel probe branes effectively repel each other. The fact that the contribution of Δ to the free energy is a $1/N$ effect is consistent with brane interactions being next-to-leading order in g_s. This effective repulsion can be rephrased by saying that in our non-supersymmetric set-up, the effective tension of the probe branes is smaller than their effective charge. A similar effect was found in a different non-supersymmetric set-up, which allowed to perform such computations [140].
We can now sum the $1/N$ contribution in (4.51) to the leading order one in (4.35). Neglecting again p-independent contributions, one gets for the total energy

$$E = \left|k + p - \frac{F}{2}\right| E_{\rm CS} - 2\,c\,m' p + \Delta\, p(p - F)\,, \tag{4.53}$$

where $m' = m - k\Delta/c$ accounts for the expected $\mathcal{O}(1/N)$ shift of the fermion mass due to a non-vanishing CS level k. The important point is that the extremization problem is modified comparing to the leading order one by the addition of a subleading quadratic term, proportional to Δ. As we will see, the final phase diagram crucially depends on such quantity.

[8] Moreover, stricly speaking, the VW theorem does not necessarily apply to the gauge theory realized by our D-brane set-up, due to the presence of Yukawa couplings, which spoils the VW argument [62–64].

4.3.1 Phase diagram

We now establish the phase diagrams as the common flavor mass m is varied. Recall that at leading order (no p^2 term) we found one first-order transition at $m^* = E_{\rm CS}/(2c)$ when $k \geq F/2$ and two first-order transitions at $\pm m^*$ when $k < F/2$.

- $k \geq F/2$
  In this case $k + p - F/2 > 0$ so the expression (4.53) becomes

$$E = \Delta p^2 + p\,(E_{\rm CS} - 2\,m'c - \Delta F)\ , \tag{4.54}$$

  which we need to minimize as a function of p. Given that $\Delta > 0$ the function has a local minimum at

$$p_{min} = -\frac{E_{\rm CS} - 2\,m'c - \Delta F}{2\Delta}\ . \tag{4.55}$$

  The value of m' such that $p_{min} = p + \frac{1}{2}$ gives the mass for which a phase transition occurs between the phases labeled by p and $p+1$. A straightforward computation gives for the (shifted) mass the value

$$m_p = m^* + \frac{\Delta}{2c}(2p - F + 1)\ . \tag{4.56}$$

  As a check one can see that for the above value of the mass the vacua labeled by p and $p+1$ are degenerate in energy while all others have higher energy.

  This analysis holds for any of the $F+1$ values of p, so we get F first-order phase transitions at values m_p defined by (4.56). These are $\mathcal{O}(1/N)$ away from the leading order value m^*, at which all $F+1$ vacua were degenerate at large N. The resulting phase diagram is depicted in figure 4.15.

Figure 4.15: Phase diagram for $k \geq F/2$ at order $1/N$. All intermediate phases have $\mathcal{O}(1/N)$ widths. All masses m_p are positive. At each critical point a first-order phase transition occurs where two phases become degenerate.

- $k < F/2$
  In this case, the sign of $k + p - F/2$ is not fixed. We have two expressions for the energy, eq. (4.54) for $p \geq F/2 - k$ and

$$E = \Delta p^2 - p\,(E_{\rm CS} + 2\,m'c + \Delta F)\ , \tag{4.57}$$

  for $p < F/2 - k$. One can run the same argument as before and find the value of the mass for which a phase transition occurs between nearby phases. This is the expression (4.56) for $p \geq F/2 - k$ and

$$m_p = -m^* + \frac{\Delta}{2c}(2p - F + 1)\ . \tag{4.58}$$

for $p < F/2-k$. All in all we get again F phase transitions and a set of intermediate phases whose widths are $\mathcal{O}(1/N)$ suppressed but the one described by $p = F/2-k$, the quantum phase already present at leading order in the large N expansion. The corresponding phase diagram is reported in figure 4.16.

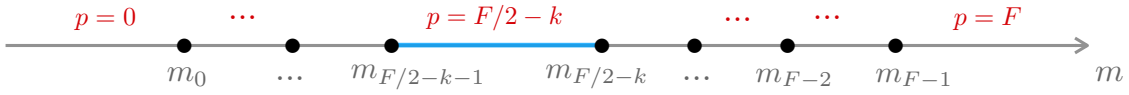

Figure 4.16: Phase diagram for $k < F/2$ at order $1/N$. The phase $p = F/2-k$, in blue, has $\mathcal{O}(1)$ width and it is the quantum phase already present at large N. All others intermediate phases have $\mathcal{O}(1/N)$ width. Masses on the right (left) of the quantum phase are positive (negative). At critical points the corresponding adjacent phases become degenerate.

The final result we get, figures 4.15 and 4.16, is a phase diagram similar to the one of section 1.6.4 at order $1/N$, the only difference being that the purely quantum phase $p = F/2 - k$ in the holographic set-up has an $\mathcal{O}(1)$ width. As for the leading order result, see the discussion in section 4.2.2, this originates from $m^* \propto E_{\rm CS}$ not being zero, which is a property of the four dimensional theory our holographic set-up describes, and which vanishes in the strict 3d limit.

4.4 Bosonization dualities from string theory

We saw in section 1.6.4 how the vacuum structure of QCD_3 can be described, in field theory, by the vacuum structure of two bosonic duals both in the small and large N limit, if accompanied by a appropriate potential. The holographic picture furnishes a simple geometric understanding on how dual bosonic theories for QCD_3 arise, similarly as it happens in the holographic description of QCD_4 domain walls [141].

Let us first consider the case $k \geq F/2$, when the $|k + p - F/2|$ CS branes in each p sector are always counterclockwise. Take the situation where this number is maximal, so that $p = F$ and all flavor branes are up. The lightest modes of the open strings stretching between CS D7-branes and flavor ones are scalars with one gauge index and one flavor index, i.e. F fundamental scalars of $U(k + F/2)$. The CS/CS open strings provide the gauge sector of the theory, while the masslessness of the up/up open strings signals the presence of an unbroken $U(F)$ global symmetry. Being the CS branes counterclockwise, the level of the theory is $-N$. All in all, we have the $U(F/2 + k)_{-N} + F\,\phi$ theory. All other configurations correspond to a partially Higgsed gauge group $U(k + p - F/2)$ and to a $U(F)$ global symmetry spontaneously broken to $U(p) \times U(F - p)$. The critical distance between the various brane embeddings should translate (though in a possibly complicated way) into the parameters of the scalar potential which guarantee such a vacuum structure.

In the case $k < F/2$, a single dual bosonic theory is not sufficient to describe all vacua, since the CS branes change orientation at $p = F/2 - k$. It is easy to realize that the same bosonic

theory described above includes all phases with $p = F, ..., F/2 - k$. To characterize all other phases, take the configuration where the number of clockwise CS branes is maximal, i.e. when $p = 0$ and all flavor branes are down. The gauge group is now $U(F/2 - k)$ at level $+N$ and the flavor symmetry $U(F)$ is unbroken. All the phases with $p = F/2 - k, ..., 0$ are described by moving up one by one the flavor branes, until one reaches the geometric configuration where there are no CS branes. This is described by $U(F/2 - k)_N + F\,\phi$ theory.

In our holographic picture, the fact that one of the two critical points stays at the same parametric value $m = m^*$, for both the $k \geq F/2$ and $k < F/2$ regimes, suggests that the same dual bosonic theory can describe the neighborhood of that critical point in both regimes. For $k < F/2$ a second critical point shows up, at exactly the time-reversed critical mass. This suggests that the dual bosonic description around $-m^*$ is indeed given by the time-reversal of the dual bosonic description of the critical point m^*. This observation supports our considerations above.

Nicely, in the string theory picture the shift of the CS level due to the integration of massive fermions can be equivalently interpreted as Higgsing of the gauge group of the dual bosonic theories. Consequently, the field theory assumption of maximal Higgsing is mapped into the requirement that the preferred vacua (in the massless case) are the ones with the minimal number of CS branes. In our set-up this fact is not an assumption, since it easily follows from the minimization of the on-shell energy density on the gravity side, at leading order in the large N expansion, as shown in section 4.2.2. Moreover, the holographic picture makes manifest the necessity of two mutually non-local dual bosonic theories in the case $k < F/2$, and gives an indirect check that the vacua of QCD_3 can be captured by a dual bosonic description even in the absence of a proper IR fixed point.
Let us finally comment on the scalar potential of the dual bosonic theory, as it emerges from the stringy description above. At leading order in N this is given by the sum of single trace operators up to a sextic term (higher order terms being irrelevant). This potential should guarantee the vacuum structure we discussed in section 4.2.2, including maximal Higgsing and the existence of first-order transitions. At subleading order in N double trace operators have to be included in the potential. In particular, a double trace quartic operator gives a contribution which has the same form as the Δ contribution in eq. (4.51). Hence, it is natural to identify Δ (up to a positive dimensionful constant) with the coupling of the double trace quartic operator of the dual bosonic theory. It is indeed the sign of Δ which fixes the topology of the phase diagram, once $1/N$ corrections are included.

4.5 Comments and outlook

In this concluding section, there are some aspects we would like to comment upon.
The first regards the large N expansion itself, see the discussion at the end of section 4.2.2. While the discrepancy between our phase diagram and field theory one of section 1.6.4 disappears in the 3d limit, since $E_{\mathrm{CS}} \to 0$, one cannot exclude that the holographic result contains more information than a mere contamination from the parent 4d theory. For instance, it is suggestive that a quantum phase, which is believed to exist in QCD_3 at finite N, naturally emerges in the

holographic set-up already at leading order, giving a phase diagram which is in fact identical to the one conjectured to hold at finite N. In principle, it is not guaranteed that the large N expansion strictly holds in CS QCD$_3$. In particular, the structure of the QCD$_3$ phase diagram at next-to-leading order in $1/N$ in section 1.6.4 was obtained under the assumption that the large N expansion works. Our holographic analysis provides some more evidence for the validity of this assumption, since the violating term is a pure 4d effect, but we believe it would be interesting to investigate this point further.

A second aspect we would like to comment upon regards the asymptotic solution of the equation of motion for the brane profile u admitting complex roots, see section 4.1. This is because the field u is below the Breitenlohner-Freedman (BF) bound. This is not uncommon in holographic models and has interesting implications. In particular, as originally discussed in [142], the violation of the BF bound can be associated to loss of conformality in the dual field theory (see also [143, 144]). This suggests a connection between the first-order nature of the phase transition in the large N, finite k and F regime we have investigated, and the nature of the scalar field u in the background (4.4).

Seemingly, as k is increased it is expected that the phase transition changes its nature and becomes second order for $k \sim N$, since, as we reviewed in section 1.6.3, for $k \gg N$ this was observed in [75–81]. As mentioned in section 1.6.4, we expect the F phase transitions of large N QCD$_3$ to coealesce at a multicritical point into a second order phase transition. In our model, the large k regime can be investigated by backreacting the CS branes, which in the present analysis were treated as probes instead. In a holographic model in which both the D3 and the CS branes are backreacted one should then expect the existence of a critical value $k_c = k_c(N)$ above which the roots for the characteristic polynomial for the (asymptotic) equation for u turn real. This is a compelling scenario worth being investigated.

Chapter 5

Aspects of five dimensional theories

Previously, we saw how three dimensional theories enjoy a rich dynamics in the IR and how this can be studied using properties that are peculiar to three dimensional physics. Some of these features, such as CS terms or parity anomaly, are present also in five dimensions. Moreover, similarly, we will gain more control over the dynamics of supersymmetric theories compared to four dimensions, thanks to some special features that are special to five dimensional physics.
In this Chapter, we review various aspects of five dimensional theories, with a particular focus on gauge theories. We start in section 5.1 discussing pure Yang-Mills theory in five dimensions. In section 5.2 we introduce CS terms in five dimensions, reviewing their quantization conditions and the relation with parity anomaly. Then, in section 5.3 we review fermions in five dimensions and discuss supersymmetric and superconformal field theories. In section 5.4 we focus on the perturbative dynamics of supersymmetric gauge theories and their UV fixed points. In the next section 5.5 we review the main string constructions of 5d theories, focusing on pq-web constructions in type IIB string theory. Finally, in section 5.6 we analyze the modern approach to classify superconformal fixed points and to describe the physics of their deformations in a more general framework.

5.1 Yang-Mills theory in five dimensions

Let us start writing the Yang-Mills Lagrangian for a gauge group G in five dimensions

$$\mathcal{L}_{\rm YM} = -\frac{1}{2g^2}{\rm Tr} F \wedge *F. \tag{5.1}$$

From dimensional analysis, we see that the gauge coupling is irrelevant since $[g] = M^{-1/2}$, so Yang-Mills theory is power counting non-renormalizable [145]. This is one of the main differences with three dimensional theories: the theory is IR free, while in the UV the coupling grows, and we expect to encounter a Landau pole. The physics at energies larger than $\sim \frac{1}{g^2}$ needs then to be UV completed. However, physics at energies smaller than the inverse gauge coupling square can be effectively described by the gauge theory itself. This is the main approach that we adopt in the next sections.

Standard parity in five dimensions $P : x^i \to -x^i$, $i = 1, .., 4$ belongs to the Lorentz group $SO(1, 4)$. To define an improper discrete parity transformation $\mathcal{P}$, we will take the reflection of one spatial direction [145]

$$\mathcal{P} : x^1 \to -x^1. \tag{5.2}$$

The gauge field A_μ transforms under this operation as

$$(A_0, A_1, ..., A_4) \to (A_0, -A_1, ..., A_4). \tag{5.3}$$

Time-reversal $\mathcal{T}$ acts on the coordinates as $(x^0, x^i) \to (-x^0, x^i)$ and correspondingly, the gauge potential transforms as

$$(A_0, \vec{A}) \to (A_0, -\vec{A}). \tag{5.4}$$

Finally, charge conjugation $\mathcal{C}$ acts on A_μ as

$$A_\mu \to -A_\mu. \tag{5.5}$$

We see that the pure Yang-Mills action is invariant under all the discrete symmetries $\mathcal{C}, \mathcal{P}, \mathcal{T}$.

Pure YM theory enjoys also additional global symmetries. As reviewed in section 1.1, in three dimensions we associate with any Abelian factor of the gauge group a topological symmetry j_T. In five dimensions, we can associate to any gauge group with field strength F a current [145]

$$j_I = \frac{1}{8\pi^2} * \mathrm{Tr}(F \wedge F). \tag{5.6}$$

This is identically conserved due to the Bianchi identities and defines a global zero-form $U(1)_I$ symmetry with charge

$$Q_I = \frac{1}{8\pi^2} \int_{\Sigma_4} *j_I = \frac{1}{8\pi^2} \int_{\Sigma_4} \mathrm{Tr}(F \wedge F) \tag{5.7}$$

where Σ_4 is a codimension one spacelike surface. The integral (5.7) is the instanton number of the gauge group. For this reason, states charged under this symmetry are denoted as instantons. These can be thought of as the five dimensional uplifts of four dimensional instantons. In the $SU(N)$ case, the charge assumes integer values, since the instanton number is always an integer. Its value is associated with the homotopy group $\pi_3(SU(N)) = \mathbb{Z}$. Also in the $U(1)$ case, the instanton number is quantized as an integer (on spin manifolds), as we saw in section 1.2. However, for generic compact groups, the instanton number can be non-integer, see [146]. Local operators charged under this symmetry are called instanton operators.
Analogously to the three dimensional monopole operators, these are disordered operators, defined by enforcing a boundary condition for the gauge field [147]. In particular, inserting an instanton operator $\mathcal{I}_m(x)$ of charge m in a correlation function amounts to introducing in the path integral a specific boundary condition for the gauge fields on a sphere S^4_x centered in x

$$\frac{1}{8\pi^2} \int_{S^4_x} \mathrm{Tr}(F \wedge F) = m. \tag{5.8}$$

These operators play a crucial role in the dynamics of gauge theories, determining their UV properties, as we will see in the next sections.
Finally, the theory is also invariant under a one-form symmetry, related to the center of the gauge group. Let us focus on $U(1)$ and $SU(N)$ gauge theories. In the first case, the symmetry is $U(1)$ and we can construct a conserved charge

$$Q = \frac{1}{g^2}\int_{\Sigma_3} *F \tag{5.9}$$

with Σ_3 a spacelike three-cycle. The symmetry acts on the gauge fields shifting it by a closed (but not exact) one-form β

$$A \to A + \beta. \tag{5.10}$$

This acts on a charged Wilson loops of charge m $W_m[\mathcal{C}] = e^{im\oint_{\mathcal{C}} A}$ as

$$W_m[\mathcal{C}] \to e^{im\oint \beta} W_m[\mathcal{C}] = e^{im\alpha} W_m[\mathcal{C}]. \tag{5.11}$$

In the $SU(N)$ case, the symmetry reduces to $\mathbb{Z}_N$. A fundamental Wilson loop will transform as $W_F \to e^{\frac{2\pi i}{N}} W_F$ under the generator of $\mathbb{Z}_N$. This symmetry is broken in presence of matter transforming in the, *e.g.*, fundamental representation.

5.2 CS terms

This section is dedicated to the analysis of CS terms in five dimensions. We first discuss CS terms for Abelian and non-Abelian gauge theories and their quantization. Then, we comment about instanton operators in presence of CS terms.

5.2.1 Abelian CS terms

Let us start discussing the quantization of CS terms in the Abelian case.
In five dimensions, we can add to the Maxwell Lagrangian a cubic term in the gauge field, the five dimensional CS Lagrangian

$$S_{\text{CS}} = \frac{k}{24\pi^2}\int_{M_5} AdAdA. \tag{5.12}$$

We refer to the theory in (5.12) as $U(1)_k$ pure Chen-Simons (CS) theory.
Under an infinitesimal gauge transformation $A \to A + d\lambda$, $e^{iS_{\text{YM}}}$ is gauge-invariant (neglecting boundary terms). However, as happens in three dimensions, this term depends explicitly on the gauge potential, which is a connection over the bundle, so it is only defined locally in general.
To define this term globally, we should extend the field to a six dimensional manifold, with boundary M_5.
Independence on the extension at the path integral level requires [148, 149] the quantization of the CS level

$$k \in \mathbb{Z}. \tag{5.13}$$

The same quantization condition holds in presence of multiple $U(1)$ fields for mixed CS term

$$\mathrm{CS}(A^a) = \frac{k_{abc}}{24\pi^2}\int_{M_5} A^a dA^b dA^c \tag{5.14}$$

with $k_{abc} \in \mathbb{Z}$ for any a, b, c.
Looking at the transformations of the gauge field of section 5.1, we see that the CS term changes sign under parity and charge conjugation, while it is invariant under $\mathcal{CP}$ and $\mathcal{T}$. Finally, notice that, in contrast to three dimensions, the CS term is cubic in the gauge potential. So, in presence of a Maxwell term, the gauge field does not acquire a topological mass. However, in the UV the kinetic term appears suppressed with respect to the CS term, having a smaller number of derivatives. This can be then neglected in this regime and the dynamics is described by a pure CS theory. This, although topological, has equations of motion

$$\epsilon^{\mu\nu\rho\sigma\delta}F_{\nu\rho}F_{\sigma\delta} = 0 \tag{5.15}$$

which admit solutions with local degrees of freedom [150–152].
Finally, as in three dimensions, the CS term breaks the $U(1)$ one-form symmetry of the Abelian theory down to $\mathbb{Z}_k$, since the CS term is not invariant under generic shifts of the gauge field.

5.2.2 Non-Abelian CS terms

The previous discussion is easily generalized to non-Abelian gauge fields.
To ensure invariance under infinitesimal gauge transformations, the cubic term in (5.12) should be improved by two additional quartic and quintic terms [149]

$$S_{\mathrm{CS}} = \frac{k}{24\pi^2}\int \mathrm{Tr}\left(AF^2 + \frac{i}{2}A^3F - \frac{1}{10}A^5\right). \tag{5.16}$$

This is gauge-invariant under infinitesimal gauge transformations (in absence of boundaries).
From (5.16), we see that the CS term is proportional to the cubic index of the representation R [153]

$$d_{abc} = \frac{1}{2}\mathrm{Tr}T_a^R(T_b^RT_c^R + T_c^RT_b^R). \tag{5.17}$$

This is different from the three dimensional case, where the CS term was proportional to the Dynkin index of the representation, see (1.138). In particular, we see that a non-Abelian CS term exists only if $d^R_{abc} \neq 0$ for some representation R. So, this exists only for a gauge group $SU(N)$ with $N \geq 3$.
Although (5.16) is invariant under infinitesimal transformations, it is not under large gauge transformations. If we consider a large gauge transformation

$$A \to g^{-1}Ag + ig^{-1}dg \tag{5.18}$$

with g a non-trivial element of $\pi_5(SU(N)) = \mathbb{Z}$ with winding number m, the CS term in 5.16 transforms as

$$\frac{k}{240\pi^2}\int \mathrm{Tr}\left(g^{-1}dgg^{-1}dgg^{-1}dgg^{-1}dgg^{-1}dgg^{-1}dg\right) = 2\pi mk. \tag{5.19}$$

So, the level needs to be an integer to ensure gauge invariance

$$k \in \mathbb{Z}. \tag{5.20}$$

Finally, the CS term breaks the $\mathbb{Z}_N$ one-form symmetry of the non-Abelian theory down to $\mathbb{Z}_{\text{gdc}(k,N)}$, see [154].

5.2.3 Instantons and CS terms

In Chapter 1, we saw that in three dimensions the CS term couples the topological current to the gauge field. Due to this coupling, monopoles become charged under the gauge group with a charge proportional to the value of the CS term. The same happens in five dimensions. The CS term is cubic in the gauge field and defines a coupling between the gauge field and the topological current. Schematically, the coupling reads

$$S_{\text{CS}} = \frac{1}{24\pi^2}\int AdAdA \sim \int A \wedge *j_I. \tag{5.21}$$

Indeed, instantonic configurations of the gauge field are electric sources of the equations of motion [147]

$$D_i F_a^{0i} = \frac{g^2 k}{32\pi^2} d_{bca}\epsilon^{ijkl} F_{ij}^b F_{kl}^c. \tag{5.22}$$

So, when $k \neq 0$, instantons are charged under the gauge group. The same conclusion can be drawn by studying disordered operators. When a disordered operator $\mathcal{I}_m(x)$ is inserted in a correlation function of some local gauge-invariant operators $\mathcal{O}_i(x_i)$, the path integral representation of the correlation function is modified as

$$\langle \mathcal{I}_n(x)\mathcal{O}_1(x_1)...\mathcal{O}_k(x_k)\rangle = \int_{\frac{1}{8\pi^2}\text{Tr}\oint F\wedge F = n} [DXDAD\psi]\mathcal{O}_1(x_1)...\mathcal{O}_k(x_k)e^{iS}. \tag{5.23}$$

Under an infinitesimal gauge transformation $A \to A + D\lambda$, the CS term induces a variation of the correlation function

$$\delta\langle \mathcal{I}_n(x)\mathcal{O}_1(x_1)...\mathcal{O}_k(x_k)\rangle = \frac{k}{8\pi^2}\text{Tr}\left[\lambda(x)\oint_{S^4_x} F\wedge F\right]\langle \mathcal{I}_n(x)\mathcal{O}_1(x_1)...\mathcal{O}_k(x_k)\rangle \tag{5.24}$$

and so

$$\delta\mathcal{I}_n(x) = k d_{abc} Q_I^{ab}\lambda^c \mathcal{I}_n \tag{5.25}$$

where $Q_I^{ab} = \frac{1}{8\pi^2}\oint F^a \wedge F^b$. So, in presence of a single Abelian factor, we see that instantons acquire an electric charge n_e proportional to the CS level k and their instanton charge m

$$n_e = km. \tag{5.26}$$

5.3 Fermions in five dimensions

In this section, we first discuss generalities about fermions in five dimensions, such as their transformation properties under discrete symmetry and their parity anomaly. Then, we construct the minimal supersymmetry algebra in five dimensions and we review its main representations. Finally, we analyze some general aspects of superconformal field theories (SCFT) and their deformations.

5.3.1 Fermions in five dimensions

Let us start by discussing the representations of the five dimensional Clifford algebra

$$\{\gamma_\mu, \gamma_\nu\} = 2\eta_{\mu\nu}. \tag{5.27}$$

In general, in odd dimensions there exist two inequivalent representations of the Clifford algebra [148]. In five dimensions, these are identified by the product of all the gamma matrices $\gamma_0\gamma_1\gamma_2\gamma_3\gamma_4 = \pm i$. Choosing the minus sign in the product, we can employ the following representation [155]

$$\gamma^0 = \begin{pmatrix} 0 & 1 \\ -1 & 0 \end{pmatrix},\ \gamma^1 = \begin{pmatrix} 0 & 1 \\ 1 & 0 \end{pmatrix},\ \gamma^2 = \begin{pmatrix} \sigma_1 & 0 \\ 0 & -\sigma_1 \end{pmatrix},\ \gamma^3 = \begin{pmatrix} \sigma_3 & 0 \\ 0 & -\sigma_3 \end{pmatrix},\ \gamma^4 = \begin{pmatrix} -\sigma_2 & 0 \\ 0 & \sigma_2 \end{pmatrix}. \tag{5.28}$$

We can introduce a charge conjugation matrix C satisfying $C\gamma^\mu C^{-1} = (\gamma^\mu)^T$, which in our representation reads $C = \gamma^0\gamma^4$. Since we are in odd dimensions, chirality is absent, so we cannot impose a Weyl condition. The spinor representation is four dimensional and pseudo-real, so we cannot impose a Majorana condition neither [155, 156].
Instead, we can introduce two Dirac spinors ψ^i_α label by the index i, forming a doublet under an $SU(2)$ global symmetry. Since the doublet representation of $SU(2)$ is pseudo-real, we can introduce a symplectic Majorana condition [157, 158]

$$\psi^i = \epsilon^{ij} C \bar{\psi}^T_j \tag{5.29}$$

that halves the number of degrees of freedom. Spinors satisfying these conditions are called symplectic-Majorana fermions. This representation has the same number of degrees of freedom of a Dirac fermion, but it has a manifest $SU(2)$ symmetry.
In both cases, we can construct mass terms. For a Dirac fermion, we have the standard mass $im\bar{\psi}\psi$ with $m \in \mathbb{R}$ [153], while for the symplectic-Majorana formulation, we can construct a symplectic Majorana mass term $im^A(\bar{\psi}\sigma^A\psi)$ at the price of breaking the $SU(2)$ symmetry , where A is an index of the adjoint representation of $SU(2)$ [155].

The little group of massive particles has two inequivalent representation [148, 159]. These correspond to the dotted and undotted spinors of $SO(4) \simeq SU(2) \times SU(2)$, associated with the first and the second $SU(2)$ subgroups. These representations are distinguished by the sign of

the mass and are physically inequivalent.[1] However, changing the sign of the mass in the Dirac equation

$$(i\gamma^\mu D_\mu - m)\psi = 0 \tag{5.31}$$

has the same effect as changing the representation of the Clifford algebra $\gamma^\mu \to -\gamma^\mu$, so the inequivalent representations of the little group are related by a change of the Clifford representation.

Discrete symmetries act on Dirac fermions as

$$\mathcal{P} : \psi \to i\gamma^1\psi, \;\; \mathcal{T} : \psi \to -i\gamma^0\gamma^4\psi, \;\; \mathcal{C} : \psi \to \psi^C = \gamma^4\psi^*. \tag{5.32}$$

We see then that a mass term for a Dirac fermion breaks both $\mathcal{C}$ and $\mathcal{P}$, but preserves $\mathcal{CP}$. On the contrary, a Majorana mass term breaks both $\mathcal{C}$ and $\mathcal{P}$ and preserves always a subgroup of $SU(2)$ and $\mathcal{T}$, denote as $\mathcal{T}'$. The mass term breaks also charge conjugation. Only a subgroup of $SU(2)$ and $\mathcal{C}$, denoted by $\mathcal{C}'$, together with $\mathcal{P}$ is preserved [155].

CS terms induced by fermions

As in three dimensions, CS terms are generated in presence of fermions charged under the gauge group. This is a manifestation of a mixed anomaly[2] between parity symmetry and gauge invariance, namely the five dimensional analog of three dimensional parity anomaly [153, 161]. In some cases, as in three dimensions, we are then forced to introduce classical CS terms to preserve gauge invariance at the quantum level.
Let us take a Dirac fermion of mass m charged with charge q under a $U(1)$ gauge group. Since the fermion is massive, we can integrate it out for energies smaller than the mass of the fermion. This operation generates a CS level for the $U(1)$ gauge field. As in the three dimensional case, the shift is one-loop exact and it is generated by the parity-violating contribution [148] coming from the diagram in figure 5.1. The resulting shift is proportional to the cube of the charge and to the sign of the mass

$$\Delta k = -\frac{q^3}{2}\mathrm{sgn}(m). \tag{5.33}$$

As in three dimensions, this is consistent with the common properties of k and m under the discrete symmetries. We see that the CS term in (5.33) is not correctly normalized for generic

[1] Indeed, the Pauli-Lubanski operator in five dimensions is a tensor $W^{\mu\nu} = \frac{1}{2}\epsilon^{\mu\nu\rho\sigma\delta}L_{\rho\sigma}P_\delta$, with $L_{\mu\nu}$ the Lorentz generators. The Casimirs of the Poincaré group are $W^2 \equiv W^{\mu\nu}W_{\mu\nu}$ and $H \equiv W^{\mu\nu}L_{\mu\nu}$, together with P^2. The irreducible massive representations are then characterized by the conditions

$$\frac{1}{8}(W^2 + mH) = m^2 j_1(j_1+1), \;\; \frac{1}{8}(W^2 - mH) = m^2 j_2(j_2+1) \tag{5.30}$$

where j_1, j_2 are the eigenvalues associated to the Cartan generator of the two $SU(2)$ groups in $\mathrm{SO}(4) \simeq SU(2) \times SU(2)$, the little group of massive states. The spinor representations $s_1 = 0$, $s_2 = \frac{1}{2}$ and $s_1 = \frac{1}{2}$, $s_2 = 0$ are physically inequivalent [160]

[2] CS terms indeed appear, as a contact term in the three-point function of the gauge currents, see [153].

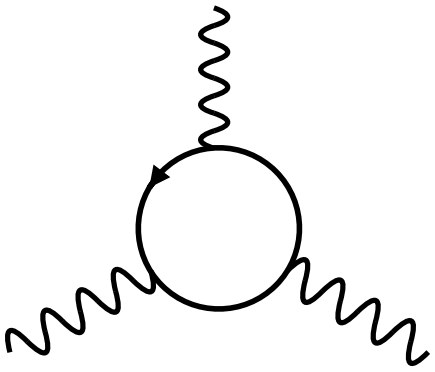

Figure 5.1: One-loop diagram generating a CS term.

charges. This is the manifestation of parity anomaly [149]. A half-integer CS term k needs then to be introduced in the Lagrangian.[3] The CS level obeys the following quantization condition

$$k - \frac{F}{2} \in \mathbb{Z}. \tag{5.34}$$

As in three dimensions, in presence of an odd number of fermions, k cannot be set to zero and so $\mathcal{P}$ cannot be preserved together with gauge invariance.
When we have massive fermions charged under multiple gauge fields, mixed CS terms can be generated by integrating them out. In particular, taking a theory of r $U(1)$ fields with F Dirac fermions charged under the i-th gauge group with charges q_i^f and mass m_f, we generate a mixed CS term of the form

$$\Delta k_{lmn} = -\frac{1}{2}\sum_{f=1}^{F}(q^f)_l(q^f)_m(q^f)_n \mathrm{sgn}(m_f). \tag{5.35}$$

The analysis can be generalized to the non-Abelian case. CS terms can be generated by integrating out fermions charged under the gauge group. For fermions in a representation R, the shift is proportional to the third Casimir of the representation R. For $SU(N)$, integrating out F fundamental fermions of mass m generates a shift

$$\Delta k = -\frac{F}{2}\mathrm{sgn}(m). \tag{5.36}$$

Again, the level k respects the quantization condition

$$k - \frac{F}{2} \in \mathbb{Z} \tag{5.37}$$

so it is half-integer for an odd number of fermions. We see then that, to ensure gauge invariance, a CS term must be added to the theory whenever F is odd.

[3]Here the convention for k is analogous to [31], so it is related to the bare level k_b as $k = k_b - F/2$. This is also denoted as the $-1/2$ convention in [153].

5.3.2 Supersymmetry

Having defined fermions in five dimensions, we can construct the minimal supersymmetry algebra. The antisymmetric product of two spinors contains the vector representation of $SO(1,4)$. The minimal ($\mathcal{N}=1$) algebra is then generated by a single symplectic Majorana fermion Q^i_α. Its components are eight supercharges, so $\mathcal{N}=1$ in five dimensions equivalent to $\mathcal{N}=2$ supersymmetry in four dimensions. The global symmetry of the symplectic Majorana fermion is then identified with the automorphism of the algebra $SU(2)_R$. As happens in four dimensions, we can preserve supersymmetry only if also $SU(2)_R$ is preserved.
The anticommutator[4] between two supercharges gives [163]

$$\{Q^i_\alpha, \bar{Q}^\beta_j\} = -2i\delta^i_j P_\mu (\gamma^\mu)^\beta_\alpha + \delta^i_j Z \delta^\beta_\alpha. \tag{5.38}$$

So, we see that even though this is the minimal supersymmetry algebra, we have a central charge Z, as in $\mathcal{N}=2$ in four dimensions. As in four dimensions [2, 164, 165], any Abelian charge contributes to Z linearly. We will review these aspects in detail in section 5.3.4.
From the algebra, we can construct massless and massive representations. Here we focus on massless multiplets that we will encounter in our discussion on five dimensional SUSY theories, namely the hyper and the vector multiplets.

- Hypermultiplet: on shell, a hypermultiplet contains four real scalars and a Dirac fermion ψ. Off-shell, we have additional auxiliary fields F^i, which are complex scalars in the fundamental of $SU(2)_R$. The four scalars are charged under the R-symmetry and form a complex doublet H^i [166]. We will denote this multiplet as $\mathcal{H} = (H^i, \psi, F^i)$. Since the doublet of $SU(2)_R$ is a pseudo-real representation, we can always describe a single hypermultiplet as a collection of two half hypermultiplets satisfying a pseudo-reality condition [165]. The same can be done for r hypermultiplets [166], which can be written as $2r$ half hypermultiplets subjected to a pseudo-reality condition

$$(H^i_a)^* = \Omega^{ab}\epsilon_{ij} H^j_b, \;\; (\psi_{a\alpha})^* = \Omega^{ab} C^{\alpha\beta}\psi_{b\beta}, \;\; (F^i_a)^* = \Omega^{ab}\epsilon_{ij} F^j_b \tag{5.39}$$

  where $\alpha, \beta = 1, ..., 4$ are the Lorentz indices of the spinor. The global symmetry of r free hypermultiplets is then $Sp(r)$ instead of $U(r)$. This is explicit in the half hypermultiplet formulation in (5.39) since the condition is imposed using Ω^{ab} with $a, b = 1, ..., 2r$, the antisymmetric invariant tensor of the $Sp(r)$ group.

- Vector multiplet: on-shell, the content of a vector multiplet is a real scalar ϕ, a symplectic-Majorana fermion λ^i and a gauge boson A_μ. Off-shell, we have also an auxiliary scalar $D^{(ij)}$ in the triplet of $SU(2)_R$. We will denote the multiplet as $\mathcal{A} = (\phi, \lambda^i, A_\mu, D^{(ij)})$. This is (Hodge) dual to a tensor multiplet, whose content is given by a two-form, a real scalar, and a spinor [145].
  The real scalar ϕ can be interpreted as the fifth component of the gauge field A_5 coming from the compactification of a six dimensional vector multiplet. As a consequence, parity $\mathcal{P}$ together with the transformation $\phi \to -\phi$ is a symmetry of the massless vector theory,

[4] Here we omit the brane charges associated with the algebra [162].

since in six dimensions the transformation on $A_5 \to -A_5$ together with parity implements a Lorentz transformation. For the same reason, ϕ is also odd under charge conjugation $\mathcal{C}$.

$\mathcal{N} = 1$ SUSY constrains the mass spectrum of the theory. To respect unitarity, the physical mass M of any state should respect the BPS bound defined by the central charge Z of the state[5]

$$M \geq |Z|. \tag{5.40}$$

We can then divide multiplets into two categories: the BPS or short ones, which saturate the bound (5.40), and the long ones, which do not saturate the bound. BPS multiplets are protected by supersymmetry and will be extensively employed in the next sections. The relevant ones for our analysis are [167]:

- Hypermultiplet: it has the same content as a massless hypermultiplet. Looking at its mass term, we see that the global symmetry of a single hypermultiplet reduces to $U(1)$, while for r hypermultiplet, this reduces to $U(r)$.

- Vector multiplet: it has the same content as a massless vector multiplet. This acquires a mass via self-Higgsing, namely giving a VEV to the real scalar of the vector multiplet.

5.3.3 Field theory parameters

Supersymmetry restricts the possible couplings that appear in a generic Lagrangian. In particular, when we have eight supercharges, these are constrained by the global symmetries of the theory.[6]. In five dimensions, massive parameters can be only introduced as VEVs of vector multiplet scalars. This allows us to introduce parameters in the Lagrangian of mass dimension one, since $[\phi] = M$. So, massive parameters can be introduced by coupling the theory to the background vector multiplet associated with the global symmetry of the theory and giving a VEV to its scalar component. The maximal number of parameters that we can add is then equal to the rank of the global symmetry group $\mathcal{G}$. For example, when we have F massless hypermultiplets, the global symmetry is $Sp(F)$. We can then introduce r different mass parameters at the cost of breaking the global symmetry to its maximal torus $U(1)^r$. These are nothing but the r independent masses that we can assign to each hypermultiplet. This explains why mass terms and scalars of the vector multiplet ϕ share the same transformations under discrete symmetries. When the scalar associated with the global symmetry takes a VEV $\langle\phi\rangle = m$, parity is broken since the VEV is odd under its action.
As we saw in section 5.1, pure SYM possesses a topological symmetry $U(1)_I$. A parameter of rank 1 can be then introduced in the theory. This is nothing but the inverse gauge coupling square of the theory $\frac{1}{g^2}$, which has mass dimension 1. This can be seen directly by coupling the topological conserved current in (5.6) to the vector superfields [145].

[5] In the bound, we reabsorbed a constant $\sqrt{2}$ factor.
[6] In 4d $\mathcal{N} = 2$, this was used for example to prove some relevant non-renormalization theorems, see [168]

5.3.4 Central charge

As in 4d $\mathcal{N} = 2$ SUSY, the algebra possesses a central charge. This is an operator of the algebra whose expression in terms of field content of the theory can be obtained from Noether's theorem [163]. In particular, since this is a central element of the algebra, it commutes with the Hamiltonian and it is conserved. The eigenvalues of this operator, obtained by acting on a SUSY multiplet with it, are nothing but a linear combination of all the Abelian charges of the multiplet. When we consider a gauge theory with some hypermultiplets, the central charge is a linear combination of the Cartan generators of the global symmetry (including the topological one), as well as the Cartan generators of the gauge symmetry. We denote the parameters associated with these symmetries as m_i and ϕ_i respectively. These multiply the Abelian charge operators that together form the central charge. Acting on a state with global charge q^i and electric charges n^j, the central charge assumes the form

$$Z = \sum_i q^i m_i + \sum_j n^j \phi_j. \tag{5.41}$$

In the following, we separate the instantonic contribution to the central charge from the contribution coming from the symmetry of the hypermultiplets, namely the flavor symmetry of the theory. The charge of the instantonic symmetry will be denoted as I and its parameter as $\frac{1}{g^2}$. The charge and parameter associated with the Cartan generators of the flavor symmetry are denoted as q^f, m_f respectively. BPS states in the theory then saturate the BPS bound

$$M = \Big|\frac{1}{g^2} I + \sum_f q^f m_f + \sum_j n^j \phi_j\Big|. \tag{5.42}$$

5.3.5 Superconformal field theories

In this section, we introduce the superconformal multiplets and comment on their classification and their unitarity bounds. Then, at the end of the discussion, we analyze all the possible supersymmetric deformations of SCFTs in five dimensions.

Let us start by reviewing the construction of representations of the conformal group. In generic d spacetime dimensions, the conformal algebra contains the Lorentz algebra $\mathfrak{so}(1, d-1)$ as subalgebra together with the dilation transformations D and the special conformal ones K_μ. They all together form an $\mathfrak{so}(2, d)$ algebra. Representations of $\mathfrak{so}(2, d)$ are denoted as conformal multiplets. Each operator $\mathcal{O}$ of the multiplet is identified by its eigenvalue under the dilation operator $\Delta_\mathcal{O}$, called the weight, and its representation under the Lorentz group R_L. In Euclidean signature, the Lorentz group in 5d reads $\mathfrak{so}(5) \simeq \mathfrak{sp}(4)$, and its representations are identified by two Dynkin labels. A conformal multiplet is a lowest weight representation. This can be constructed starting from an operator $\mathcal{O}$ in some Lorentz representations R_L which is annihilated by the special conformal transformations K_μ and then acting with the other generators of the algebra. The operator $\mathcal{O}$ is then a primary field, while all other operators in the multiplet are its descendants, obtained as derivatives of $\mathcal{O}$ [50]. To ensure unitarity, the weight of the conformal primary should satisfy the bound

$$\Delta_\mathcal{O} \geq f(d, R_L) \tag{5.43}$$

which depends on the spacetime dimension and the Lorentz representation through the function f. For example, a scalar in generic dimensions satisfies

$$\Delta_{\mathcal{O}} \geq \frac{d-2}{2} \tag{5.44}$$

while a vector satisfies

$$\Delta_{\mathcal{O}} \geq d-1. \tag{5.45}$$

In both cases, something peculiar happens when the operator saturates the bound. In the first case, the scalar is free, while in the second case the vector is conserved, $\partial_\mu \mathcal{O}^\mu = 0$.

Supersymmetry enlarges the conformal algebra to a superconformal one. In five dimensions, only one superalgebra is allowed and preserves eight supercharges.[7] This is the $\mathfrak{f}(4)$ algebra. The bosonic subalgebra contains the conformal algebra $\mathfrak{so}(2,5)$ and the R-symmetry algebra $\mathfrak{R}$, which is $\mathfrak{su}(2)_R$. We have also additional supercharges, denoted by S^i, which are necessary to close the superalgebra.
An operator $\mathcal{O}$ is identified by its R-symmetry Dynkin label r, its Lorentz representation R_L and its weight $\Delta_{\mathcal{O}}$. Operators organize in representations of the superconformal group, known as superconformal multiplets (SCM). These are lowest weight representations and are generated starting from an operator $\mathcal{O}$ which is annihilated by all supercharges S^i and special conformal transformations K_μ. Operators satisfying this condition are denoted as superconformal primaries (SCP). Acting on these operators with the remaining elements of the superalgebra, we construct the superconformal multiplet. Some of the operators obtained in the constructions are conformal descendants of the SCP. All other operators are conformal primaries. Defining a superconformal multiplet, we will indicate only its content in terms of its conformal primaries. This is equivalent to the expansion of a superfield in terms of its components.
Superconformal multiplets are also distinguished by their shortening properties. Some of the multiplets can be short if their SCPs are also annihilated by some of the Qs. The anti-commutator of two supercharges is proportional to the momentum operator, so when this acts on an operator cannot generate conformal primaries but only descendants. Then, due to Fermi statistic, we can in general act on the superconformal primaries with a string of N supercharges and obtain a conformal primary for any $N \leq N_Q$ where N_Q is the total number of supercharges. When N saturates the bound, the multiplet is long and it is denoted by the letter L. The highest component of the multiplets is $Q^{N_Q}\mathcal{O}$ and it is invariant under SUSY transformations. If instead $N < N_Q$, as it happens when the SCP is annihilated by a subset of supercharges, the multiplet is short.
Also in the superconformal case, we have unitarity bounds for SCPs. However, due to the presence of supercharges, the number of superconformal descendants is larger than the one of conformal ones, leading to stringent conditions. These bounds were calculated in [169–175] and depend on the Lorentz and R- charges as

$$\Delta_{\mathcal{O}} \geq f(j_1, j_2) + g(r) + \delta_A \equiv \Delta_A \tag{5.46}$$

[7] Here, we are considering only the total number of Poincaré supercharges.

$$\Delta_{\mathcal{O}} = f(j_1, j_2) + g(r) + \delta_{B,C,D} \equiv \Delta_{B,C,D},\ \delta_A > \delta_B > \delta_C > \delta_D. \tag{5.47}$$

The first inequality looks like the usual unitarity constraint, but $f(j_1, j_2)$ is different from the bosonic case. Multiplets satisfying the bound have generic Lorentz and R-symmetry Dynkin labels. The bound is saturated by short multiplets, the A-multiplets. When the weight is smaller than Δ_A, unitarity is lost unless weights satisfy one of the equalities in (5.47). This happens only for specific values of the Lorentz and R-symmetry Dynkin labels. The multiplets that satisfy these equalities are denoted as B, C, D multiplets. This establishes a hierarchy for the weights in the spectrum of an SCFT, since $\Delta_A > \Delta_B > \Delta_C > \Delta_D$. Finally, each type of multiplet will be also classified by the level l of its first null state, equivalent to the number of supercharges that are needed to reach it acting on the SCP. Denoting collectively the labels L, A, B, C, D as T, a generic multiplet with SCP $\mathcal{O}$ in the representation $[j_1, j_2]$ of the Lorentz group, with weight $\Delta_{\mathcal{O}}$ and Dynkin label r is identified by the following notation

$$T_l[j_1, j_2]^{(r)}_{\Delta_{\mathcal{O}}}. \tag{5.48}$$

Multiplets of SCFTs were constructed and classified in [176, 177]. This classification is useful to see which deformations are allowed in a SCFT. A SCFT can be deformed either by sourcing an operator $\mathcal{O}$ or by giving a VEV to it. Focusing on the first type of deformations, to preserve supersymmetry $\mathcal{O}$ must be annihilated by all the supercharges Qs and be neutral under the R-symmetry. This is the case when we consider the highest components of superconformal multiplets which are scalars and singlets under R-symmetry. These operators can then be sourced without breaking supersymmetry. The corresponding deformation is irrelevant when $\Delta_{\mathcal{O}} > d$, marginal if $\Delta_{\mathcal{O}} = d$ and relevant if $\Delta_{\mathcal{O}} < d$. Turning on an irrelevant deformation, we come back to the fixed point and superconformal symmetry remains preserved. Turning on a marginal deformation, instead, we preserve superconformal symmetry and the source associated with the operator parametrizes a conformal manifold. Finally, relevant deformations break conformal symmetry and trigger an RG-flow. Focusing on the two latter deformations, it is possible to show [177] that in five dimensions no marginal deformation is allowed (namely, we cannot have a supersymmetric conformal manifold). Moreover, relevant deformations are highly constrained. In particular, only one relevant deformation is allowed and comes from sourcing the highest component of the $C_1[0, 0]^{(2)}_3$ short multiplet

$$[0, 0]^{(2)}_3 \to [1, 0]^{(1)}_{7/2} \to [0, 1]^{(0)}_4 \oplus [0, 0]^{(0)}_4 \tag{5.49}$$

where $[0, 1]$ is the vector representation of $\mathfrak{sp}(4)$ and $[1, 0]$ the spinorial one. One of the highest components is a vector $J_{\mu,A}$, which is then conserved. This is nothing but the multiplet containing the conserved current of the global symmetry $\mathcal{G}$ of the SCFT

$$\mathcal{J}_{\mathcal{G}} = (\mu^A_{(ij)}, \psi^A_i, J^A_\mu, M^A) \tag{5.50}$$

where $\mu^A_{(ij)} \equiv [0, 0]^{(2)}_3$, $\psi^A_i \equiv [1, 0]^{(1)}_{7/2}$ and $M^A \equiv [0, 0]^{(0)}_4$ and A is an adjoint representation index of $\mathcal{G}$. Sourcing the highest component M^A we generically break the global symmetry to its Cartan torus. To this deformation, we associate then $\mathrm{rk}(\mathcal{G})$ parameters. The breaking of

conformal invariance via this relevant operator triggers an RG-flow from the SCFT to some IR phase with smaller global symmetry. Modifying the values of the parameters, we span the low-energy phase diagram of the SCFT and, tuning them in a specific way, we can hope to reach another non-trivial SCFT in the IR.

5.4 SUSY gauge theories: perturbative dynamics

In this section, we discuss the perturbative dynamics of supersymmetric gauge theories. We start reviewing their prepotential and the most general supersymmetric Lagrangian of a vector multiplet coupled to F hypermultiplets. Then, we discuss moduli spaces of five dimensional gauge theories. At the end of the section, we review their dynamics on the Coulomb branch, introducing the criterion of convexity and analyzing in detail the $U(1)$ and $SU(N)$ cases.

5.4.1 Prepotential and $\mathcal{N} = 1$ Lagrangians

Lagrangians are strongly constrained by supersymmetry and so is their moduli space $\mathcal{M}$. When we have eight supercharges in four dimensions, $\mathcal{M}$ is a direct product of the manifold $\mathcal{M}^V$ of the (complex) scalars of the vector multiplets $\mathcal{A}^a$ and the manifold $\mathcal{M}^H$ of the hyper scalars H^i_f. The former space is denoted in literature as the Coulomb branch (CB), while the latter is denoted as the Higgs branch (HB). Moreover, SUSY constraints also the properties of these manifolds. The manifold $\mathcal{M}^H$ is hyperKähler[8], while $\mathcal{M}^V$ is special Kähler. In particular, a special manifold is Kähler with a Kähler potential coming from derivatives of a holomorphic function, called the prepotential. We denote the superfield hosting this function as $\mathcal{F}(\mathcal{A})$. The entire SYM Lagrangian is then completely determined (up to two derivatives) by this holomorphic function.

Similar constraints are found also in five dimensions. The moduli space parameterized by the hypermultiplet scalars is again hyperKähler. On the other hand, five dimensional vector multiplets contain real scalars. The corresponding manifold is then no more special Kähler. This is very special real [157] and its metric is still determined by a prepotential $\mathcal{F}(\mathcal{A})$.
Let us consider the case of N $U(1)$ vector multiplets $\mathcal{A}^a$. The lowest component of the prepotential is a real function of the scalars $\mathcal{F}(\phi^a)$ associated with the vector multiplet $\mathcal{A}^a$. The metric on the moduli space reads

$$ds^2 = t(\phi)_{ab}\, d\phi^a\, d\phi^b \tag{5.51}$$

with $t(\phi)_{ab} = \frac{\partial \mathcal{F}}{\partial \phi^a \phi^b}$. This is nothing but the gauge coupling constants of the "photons" $\mathcal{A}^a$.
Moreover, SUSY restricts further the form of the prepotential in five dimensions. Indeed, this can be at most cubic in the scalar fields [145]. Indeed, let us consider the case of a single gauge field. Under compactification, the fourth component of the gauge field A_4 becomes the imaginary part of the scalar of the four dimensional vector multiplet and the gauge symmetry

[8] This is a Kähler manifold with a quaternionic structure, i.e. with three different complex structures satisfying quaternionic identities.

acting on it reduces to a shift symmetry $\mathcal{A}_4 \to \mathcal{A}_4 + ia$. This symmetry is violated by more than cubic terms in the prepotential, leading to inconsistency. For example, if we add a quartic term $\mathcal{F} = \frac{1}{4!}\phi^4$ to the five dimensional prepotential, we introduce in the four dimensional Lagrangian a coupling

$$\mathcal{L} \sim (\phi^2 - A_5^2)F^2 \tag{5.52}$$

which breaks the shift symmetry.
Let us now restrict the analysis to a local patch of the moduli space. The prepotential then reads

$$\mathcal{F} = c_0 + c_a\mathcal{A}^a + \frac{1}{2}h_{ab}\mathcal{A}^a\mathcal{A}^b + \frac{k_{abc}}{6}\mathcal{A}^a\mathcal{A}^b\mathcal{A}^c. \tag{5.53}$$

Since only the metric (and its derivatives) enters in the Lagrangian, c_0 and c_a can be set to zero. Reality properties of the Lagrangian and invariance under shift symmetry restrict h_{ab}, k_{abc} to be real. The prepotential reduces on the local patch to

$$\mathcal{F} = \frac{1}{2}h_{ab}\mathcal{A}^a\mathcal{A}^b + \frac{k_{abc}}{6}\mathcal{A}^a\mathcal{A}^b\mathcal{A}^c. \tag{5.54}$$

For a single gauge field, this is

$$\mathcal{F} = \frac{1}{2g^2}\mathcal{A}^2 + \frac{k}{6}\mathcal{A}^3 \tag{5.55}$$

with $k, g \in \mathbb{R}$. The metric for the vector multiplet reads

$$h = \frac{1}{g^2} + k\phi \tag{5.56}$$

leading to an effective coupling for the gauge field on the CB.
The same analysis can be done for non-Abelian gauge theories with gauge group G. The prepotential is gauge-invariant and has locally the same structure

$$\mathcal{F}(\phi) = \frac{1}{2g^2}\mathrm{Tr}\phi^2 + \frac{k}{6}\mathrm{Tr}\phi^3. \tag{5.57}$$

Expanding the scalar field in a basis of generators T_a in the fundamental representation of G as $\phi = \phi^a T_a$, we see that the cubic term in the prepotential is proportional to the cubic Casimir of the fundamental representation d^F_{abc}. Then, as for CS terms, also the cubic term in the prepotential is present for non-Abelian theories only when G is $SU(N)$ with $N \geq 3$.

We can now construct the most general Lagrangian preserving $\mathcal{N} = 1$ supersymmetry in five dimensions. The quadratic term in the prepotential (5.57) generates respectively the kinetic term of the fields of the vector multiplet and the Yukawa interactions required by supersymmetry. The off-shell Lagrangian obtained from the quadratic term reads [158, 178]

$$\mathcal{L}_{\mathrm{SYM}} = \frac{1}{g^2}\left(-\frac{1}{2}\mathrm{Tr}F^2 - \mathrm{Tr}(D_\mu\phi)^2 - i\mathrm{Tr}(\bar{\lambda}\gamma^\mu D_\mu\lambda) + \mathrm{Tr}D^2 + i\mathrm{Tr}(\bar{\lambda}[\phi,\lambda])\right). \tag{5.58}$$

On the other hand, cubic term in the prepotential leads to the couplings [178]

$$\mathcal{L}_{cubic} = \frac{k}{24\pi^2}\mathrm{Tr}\left[AF^2 + \frac{i}{2}A^3F - \frac{1}{10}A^5 - 3\bar{\lambda}\gamma^{\mu\nu}\lambda F_{\mu\nu} + 6i\bar{\lambda}D\lambda\right] + \frac{k}{2\pi^2}\mathrm{Tr}[\phi\mathcal{L}_{\mathrm{SYM}}]. \quad (5.59)$$

The cubic term in the prepotential introduces then a CS term and its SUSY completion (5.59). We can also write the most general Lagrangian of a hypermultiplet in some representation R of the gauge group [178]

$$\mathcal{L} = (D_\mu H)^\dagger(D^\mu H) - i\bar{\psi}\gamma^\mu D_\mu\psi + F^\dagger F - i\bar{\psi}\phi\psi + H^\dagger DH + H^\dagger\phi^2 H - (\sqrt{2}\bar{\psi}\lambda H + \mathrm{h.c.}). \quad (5.60)$$

Notice that, as expected, in (5.60) there is no dependence on the prepotential.
The dimension of the real scalar of the vector multiplet is $[\phi] = M^1$, while the dimension of the hyperscalars is $[H^i] = M^{3/2}$, due to the different normalizations of the kinetic terms.
Having introduced the classical prepotential, we can now consider the classical properties of the moduli space and its quantum corrections.

5.4.2 Moduli space

We now review some basic properties of the classical moduli space of gauge theories in five dimensions, distinguishing between the Coulomb and the Higgs branch.

- Coulomb branch:
  Taking a generic gauge group G of rank N, a generic point on the CB is identified by a VEV for the scalar $\phi = \phi^a T^a$ of the vector multiplet. At this point, the gauge group is generically broken to its Cartan torus $U(1)^N$. The inequivalent vacua are parametrized by the coordinates ϕ^a with $a = 1, ..., N$. These belong to the weight space of the gauge algebra $\mathfrak{g}$. However, a leftover redundancy comes from the Weyl group $\mathcal{W}$ of G, acting on the coordinates ϕ^a. The inequivalent vacua (and so the CB) describe then a wedge subspace of $\mathbb{R}^N$ obtained from the action of the Weyl group $\mathbb{R}^N/\mathcal{W}$. In the following, we take as representative of this equivalence class the fundamental Weyl chamber of the corresponding weights ϕ^a, defined as the space of weights ϕ^a satisfying the condition

  $$C_0 = \{\phi^a | (\phi^a, \alpha_i) \geq 0,\ i = 1, ..., N\} \quad (5.61)$$

  with α_i the simple roots of $\mathfrak{g}$. At the edges of the chamber, the gauge group admits non-Abelian enhancement. At any point of the CB, the original R-symmetry of the theory remains preserved, since ϕ is a singlet under $SU(2)_R$.

  The classical analysis can be modified due to quantum corrections, which change the metric of the moduli space, as we will see next section.

- Higgs branch:
  On the HB, the scalars associated with the hypermultiplets take a VEV. At a generic point, the rank of the gauge group is reduced due to Higgsing. As in four dimensions,

the manifold is hyperKähler. At weak coupling, non-renormalization theorems protect the structure of the HB, which is classical exact. However, in absence of a Lagrangian description, as we will see, the HB can get corrections.
On the Higgs branch, both the global symmetry and the R-symmetry of the theory act as isometries. As a consequence, this branch can be distinguished from the CB by the breaking of the global and the R-symmetries. In particular, the original $SU(2)_R$ is broken at a generic point as well as part of the global symmetry. A subgroup of the two represents then an emergent R-symmetry $SU(2)_{R'}$, which is preserved at any point of the HB. This property can be used as a non-perturbative definition of the Higgs branch.

Higgs branches of five dimensional theories are extensively studied in the literature, in particular in strong coupling limits of gauge theories [179–205]. Although we will review some of these aspects in section 5.5.6, we refer the reader to the literature for a more complete treatment of the subject.

5.4.3 Coulomb branch dynamics

On a generic point of the CB, the gauge group G is broken to its Cartan torus and the theory is effectively Abelian, parametrized by the vector multiplets $\mathcal{A} = \sum_{i=a}^{N} \mathcal{A}^a T_a$ with T_a the Cartan generators. The Higgsing gives masses to the vector multiplets charged under the Cartan generators with charge q_a. In the following, these multiplets will be denoted as W multiplets, in analogy with electro-weak symmetry breaking in the Standard Model. Fermions get a mass through the Yukawa coupling in (5.58). The multiplets are BPS, being the result of self-Higgsing and get a physical mass M equal to their central charge

$$M = |q_a \phi^a| = |Z|. \tag{5.62}$$

At sufficiently low-energy and away from the origin, these multiplets can be integrated out, and the low-energy effective theory reduces to a theory of N Abelian vector multiplets. However, massive gauginos inside these multiplets are expected to shift the CS level of the theory. Being this related to the cubic potential, gauginos are then expected to give corrections to the prepotential [145, 148]. In particular, the CS term shifts as

$$\Delta k_r = \frac{1}{2} \sum_a \text{sgn}(q_a^r \phi^a) \tag{5.63}$$

due to the contribution coming from the r-th massive multiplet. The charges q_a^r of this multiplet define the Dynkin label of a root of the gauge algebra. We indicate this root as a vector $\mathbf{R}_r = (q_1^r, ..., q_N^r)$. Summing the contributions coming from all the massive vectors, the shift reads

$$\Delta k = \frac{1}{2} \sum_{\mathbf{R} \in \text{roots}} \text{sgn}(\mathbf{R} \cdot \phi). \tag{5.64}$$

The cubic term of the prepotential shifts then as

$$\Delta \mathcal{F} = \frac{1}{12} \sum_{\mathbf{R} \in \text{roots}} |\mathbf{R} \cdot \phi|^3. \tag{5.65}$$

This modifies the metric on the CB and the corresponding effective coupling. Moreover, the process introduces singularities on the CB. At a point at the boundary of the Weyl chamber, for some $\mathbf{R}$ we have $\mathbf{R}\cdot\phi = 0$, signaling the enhancement of the gauge symmetry to a non-Abelian subgroup of G. The metric, however, is not smooth at this point, due to the modulus. This is physically meaningful: at that point, the multiplet that we integrated out is massless and the low-energy description breaks down. To recover a low-energy description, we have to include the new massless multiplet and consider an effective field theory in presence of the non-Abelian gauge group.

When we add matter, the low-energy dynamics on the CB enriches. Let us consider a single hypermultiplet in a representation R of the group G. On a generic point of the CB, this acquires a mass due to the interaction terms with the scalar of the vector multiplet in (5.60). The physical mass equals the central charge

$$m^r = |q_a^r \phi^a + m| = |Z| \tag{5.66}$$

where again q_a^r is the charge under the a-th Cartan of the r-th massive hypermultiplet and m is a bare mass for the hypermultiplet. As in the vector case, fermions induce a shift of the level

$$\Delta k = -\frac{1}{2}\sum_a \mathrm{sgn}(q_a^r \phi^a + m). \tag{5.67}$$

Notice that this is opposite in sign with respect (5.63). This comes from the fact that only short multiplets contribute to the level [145]. We associate the r-th weight $\mathbf{w}_r$ of the representation R to the r-th hypermultiplet. The prepotential gets quantum corrected as

$$\Delta\mathcal{F} = -\frac{1}{12}\sum_{\mathbf{w}_r\in\text{weights}} |\mathbf{w}_r\cdot\phi + m|^3. \tag{5.68}$$

Also in this case the metric develops a singularity at $\mathbf{w}_r\cdot\phi + m = 0$. This again coincides with the point on the CB at which the hypermultiplet becomes massless and needs to be included in the low-energy description.
In the most general case, the prepotential for a gauge group G and $f = 1, ..., F$ hypermultiplets in the representation R_f with a CS term k reads

$$\mathcal{F} = \frac{1}{2g^2}h_{ab}\phi^a\phi^b + \frac{k}{6}d_{abc}\phi^a\phi^b\phi^c + \frac{1}{12}\left(\sum_{\mathbf{R}\,\in\,\text{roots}} |\mathbf{R}\cdot\phi|^3 - \sum_f \sum_{\mathbf{w}_r\in\mathbf{W}_R} |\mathbf{w}_r\cdot\phi + m_f|^3\right) \tag{5.69}$$

with $h_{ab} = \mathrm{Tr}(T_a T_b)$ and d_{abc} both evaluated for the Cartan's and $\mathbf{W}_R$ are the weights of the R representation of G. This quantum corrected prepotential is dubbed in the literature as the Intrilligator-Morrison-Seiberg (IMS) prepotential [149]. This is exact at one-loop, as expected by the one-loop exactness of the shift of the CS term, resulting from the five dimensional version of the Coleman-Hill theorem [148].

BPS states on the CB

On top of perturbative states, also non-perturbative ones charged under the gauge group acquire additional contributions to their mass on the CB. Moreover, also their properties get modified, as we review in this section.
We know from section 5.1 that to each gauge group of a five dimensional theory we can associate a topological zero-form symmetry $U(1)_I$, under which instanton states are charged. The parameter associated with this symmetry is the inverse gauge coupling square $\frac{1}{g^2}$, which enters the central charge formula as in (5.41). We can then ask what happens to instantons on a generic point on the CB. These are singlets under the gauge group in absence of a CS term. On a generic point of the CB, however, the gauge group is broken to its Cartan torus and a CS term is generated. Instantons acquire then a charge under the Cartan generators.
Let us take for simplicity the case $G = SU(2)$. No classical CS term can be introduced in this case and instantons are singlets under the gauge group.
On the CB, however, $SU(2)$ is broken to its Cartan $U(1)$, and a CS term k is generated by quantum corrections, as we can see from the IMS formula (5.69). Instantons then get an electric charge kI on the CB. This tells us that the naive central charge of the theory

$$Z^{\text{naive}} = q_e\phi + \frac{1}{g^2}I \tag{5.70}$$

actually acquires an additional contribution due to the CS term

$$Z = (q_e + kI)\phi + \frac{1}{g^2}I. \tag{5.71}$$

So, the true electric charge is not only the charge under the Cartan of $SU(2)$, but an additional contribution comes from the global charge I. This phenomenon is dubbed electric/instanton mixing [145]. This has a simple physical interpretation. In presence of a CS term, the gauge coupling is shifted by a contribution linear in ϕ

$$\frac{1}{g^2_{eff}} = \frac{1}{g^2} + k\phi. \tag{5.72}$$

We expect instantons to be massive with mass $\sim \frac{1}{g^2_{eff}}$. So, to the instanton charge I we should associate, due to the BPS property, a mass parameter $\frac{1}{g^2_{eff}}$ instead of $\frac{1}{g^2}$. Inserting this parameter in the naive central charge (5.70), this is modified as

$$Z = q_e\phi + \frac{1}{g^2_{eff}}I = (q_e + kI)\phi + \frac{1}{g^2}I \tag{5.73}$$

reproducing the mixing.
Also, the properties of instanton states are modified on the CB of the $SU(2)$ theory. At the origin $\phi = 0$, we can construct solitonic configurations of the gauge field which are non-singular. These are labeled by a continuous modulus ρ, which parametrizes the size of the

instanton [145, 206, 207]. On the other hand, on a generic point of the CB, instantons tend to shrink to $\rho = 0$ and become singular. Their detailed properties depend on the short distance physics, which depends on how we regularize the theory. This is a signal of the lack of renormalizability of the theory [145].

We finally discuss monopole strings in five dimensions. Again, let us specialize to the $SU(2)$ case. We know that monopoles in four dimensions are BPS particles [2]. The mass parameter associated with the dual magnetic gauge group ϕ_D

$$\phi_D = \frac{\partial \mathcal{F}}{\partial a} \tag{5.74}$$

appears in the central charge as

$$Z = n_e \phi + n_m \phi_D \tag{5.75}$$

where n_m is the magnetic charge of the monopole.
In five dimensions, monopoles are actually strings [145]. Indeed, a vector multiplet can be dualized (in absence of a CS term) to a tensor multiplet. The corresponding mass parameter ϕ_D of mass dimension $[\phi_D] = M^2$ reads

$$\phi_D = \frac{\partial \mathcal{F}}{\partial \mathcal{A}}(\phi) = \frac{\phi}{g^2} + \frac{k}{2}\phi^2. \tag{5.76}$$

This represents the tension of the associated monopole string. Monopoles charged under the two-form field are then strings. BPS strings satisfy the BPS bound given by the corresponding central charge [9]

$$T = Z_m = n_m(\phi_D + c_m). \tag{5.77}$$

When the theory is compactified to four dimensions, monopole strings wrapped around the compactification circle become the corresponding monopoles in four dimensions [207].
Notice that ϕ_D (as well as the metric itself) cannot change discontinuously between open sets as $1/g^2$ and k do. Moreover, from (5.76) we see that by integrating the tension of the BPS string, we obtain the prepotential of the gauge theory. This will be useful when we will deal with string constructions of five dimensional theories in section 5.5.

Prepotential convexity

As we saw in the previous section, the metric on the CB and the effective gauge coupling are obtained from derivatives of the prepotential. Singularities for the metric are allowed at some points on the CB, where particles that have been integrated out become massless. However, to have a well-defined kinetic term for the gauge field, the metric on the CB must be positive definite at any point. This is ensured only when the prepotential is convex on the entire moduli space.
The quadratic piece is always convex whenever $\frac{1}{g^2} h_{ab} > 0$. So this piece is convex when $\frac{1}{g^2} >$

[9] This enters in the supersymmetry algebra as a brane charge [162, 163].

0. The cubic piece, on the other hand, is not always convex. Cubic contributions coming from hypermultiplets reduce in general the convexity of the prepotential. On the other hand, contributions coming from vectors are always convex on the entire CB. Away from the origin of the CB, the metric can then stop to be positive definite and the effective description can break down. This tells us that additional information is needed to describe the entire CB. As we will see next, this can be an indication of the non-renormalizability of the theory, as for the $U(1)$ theories, or the signal that some non-perturbative states must be considered in the effective description of the CB.
In general, the theory can be made sensible at best in a subspace near the origin taking the classical part $\frac{1}{g^2}h_{ab} > 0$. However, when the metric is well defined on the entire CB, a scale-invariant fixed point $1/g^2 = 0$ can be reached. Although these theories are power counting non-renormalizable, we will see that some of them admit SCFTs as UV completions. The gauge theory description is then interpreted as an effective field theory (EFT) describing the endpoint of an RG-flow started from a UV SCFT triggered by the inverse gauge coupling squared mass parameter $\frac{1}{g^2}$. We see then that a necessary condition (at the perturbative level) for the theory to reach a strong coupling fixed point is to have a positive definite metric over the entire CB.
Equipped with this criterion, we can classify gauge theories based on their prepotential. Let us start with pure non-Abelian gauge theories in absence of a CS term. On top of the classical quadratic term, massive vectors contribute to the prepotential on the CB. This contribution of the form $|\mathbf{R}\cdot\phi|^3$ is always purely convex. We see that all these theories fulfill the criterion since the prepotential is convex at any point of the CB.
This is no more true in presence of matter. Hypermultiplets introduce pure concave terms $-|\mathbf{w}_R\cdot\phi + m|^3$, which can spoil convexity. This depends then on the number of flavors we add and on their representations under the gauge group. Indeed, integrating out matter makes the prepotential more convex [149], so the prepotential behaves better the smaller the number of hypermultiplets. However, in some cases, this is always concave, regardless of the number of matter fields. For example, any representation R containing a weight $\mathbf{w}_R$ larger or equal length than a root leads to a concave prepotential, since gauge bosons cannot compensate for the concavity at large values of the CB parameter.
When classical CS terms are added, the convexity of the prepotential needs to be studied in detail, as we will see in the next sections when discussing the $SU(N)$ case.
We finish this section by discussing in detail the CB dynamics of $U(1)$ and $SU(N)$ gauge theories and their convexity conditions.

$U(1) + F$ flavors

Let us start considering a $U(1)$ gauge theory with F electrons with charge one. The CB of $U(1)$ is $\mathbb{R}$ and it is parameterized by a single coordinate $\phi \in \mathbb{R}$. We can choose the quadratic coefficient $\frac{1}{g^2}$ to be positive definite. In absence of hypermultiplets, the prepotential is then well-defined but the metric is trivial $\frac{1}{g^2}$, so the CB cannot be described at the putative fixed point $\frac{1}{g^2} = 0$.
Adding F massless electrons, the global symmetry of the theory is $SU(F)\times U(1)_I$. Being the electrons charged under the gauge field, they take a mass on the CB proportional to ϕ, namely

$M = |\phi|$. The gauge coupling is modified at one-loop as

$$\frac{1}{g^2_{eff}} = \frac{1}{g^2} - \frac{F}{2}|\phi|. \tag{5.78}$$

The metric is not smooth, signaling the presence of massless fermions at $\phi = 0$, as expected. Of course, if F is odd, we should equip the theory with a CS level k. This is neither a concave nor a convex contribution and can be interpreted as coming from the decoupling of some additional electrons with a positive mass. As a consequence, we can reabsorb this contribution in the value of F.
The metric in (5.78) is not positive anywhere on the CB. In fact, for any positive $1/g^2$, the effective coupling diverges at a finite point of the moduli space $\phi_s = \pm\frac{2}{Fg^2}$. The cutoff scale $\sim \frac{1}{g^2}$ signals the non-renormalizability of the theory and the necessity of a UV completion.
The $SU(F)$ symmetry can be broken explicitly by adding different masses for the electrons. The most generic mass term breaks $SU(F)$ to its Cartan torus $U(1)^{F-1}$. Also $\mathcal{C}$ and $\mathcal{P}$ are broken, and only $\mathcal{CP}$ is preserved. The values of the masses m_f, $f = 1, ..., F$ parametrize the VEV [10] of the scalar ϕ of the background vector multiplet associated with the global symmetry. Hypermultiplets induce a CS level

$$\Delta k = -\frac{1}{2}\sum_{f=1}^{F} \text{sgn}(\phi + m_f). \tag{5.79}$$

and the effective coupling reads

$$\frac{1}{g^2_{eff}} = \frac{1}{g^2} - \frac{1}{2}\sum_f |\phi + m_f|. \tag{5.80}$$

Some comments are in order. First of all, we see that $\frac{1}{g^2}$ is further constrained by masses. This should respect the inequality

$$\frac{1}{g^2} \geq \frac{1}{2}\sum_f |m_f| \tag{5.81}$$

in order for the metric to be well-defined at the origin of the CB.
Secondly, at $\phi = -m_f$ an electron becomes massless and, as expected, a singularity appears on the CB metric. When $\tilde{F}$ masses are equal, the effective theory at the singularity is a $U(1)$ theory with $\tilde{F}$ massless electrons with flavor symmetry $SU(\tilde{F})$.
The presence of masses does not cure the non-renormalizability of the theory, since at some point of the CB the prepotential stops again to be convex.

$SU(2) + F$ fundamentals

Let us start by considering pure $SU(2)$ SYM. Since the gauge group has rank one, the CB of the theory is one dimensional and parametrized by a single coordinate ϕ. On a generic point,

[10] Note that they sum to $\sum_f m_f = 0$ or, alternative, the sum is non-physical, since the flavor group is special unitary.

the gauge group is broken to its Cartan $U(1)_c$. Since the $SU(2)$ Weyl group is the permutation group S_2 (namely $\mathbb{Z}_2$), we can restrict the value of $\phi \in \mathbb{R}^+$ in the fundamental chamber. At its edge, $\phi = 0$ and the gauge symmetry enhances to $SU(2)$.
At a generic point of the CB, the adjoint representation **3** decomposes as $\mathbf{2} + (-\mathbf{2}) + \mathbf{0}$ under the Cartan. Massive vectors induce a CS term for $U(1)_c$ and the effective coupling reads

$$\frac{1}{g^2_{eff}} = \frac{1}{g^2} + 8\phi. \tag{5.82}$$

Note that, as expected from the previous discussion, this theory fulfills the convexity requirement for a UV fixed point at $1/g^2 = 0$. So, even in absence of matter, this theory is expected to possess a UV completion.

Let us now introduce flavors. In particular, we consider F massless quarks in the fundamental representation. The flavor symmetry is $SO(2F)$, since the gauge group is symplectic $SU(2) \simeq Sp(1)$. On the CB, the fundamental representation decomposes into two representations of the Cartan group of charges $\mathbf{1} + (-\mathbf{1})$. From the central charge formula (5.41), the corresponding electrons acquire a mass

$$M = |\phi|. \tag{5.83}$$

Both states, in particular, generate the same CS terms, since their charges compensate the signs of the masses. The effective coupling changes as

$$\frac{1}{g^2_{eff}} = \frac{1}{g^2} + (8 - F)\phi. \tag{5.84}$$

The coupling in (5.84) shows an interesting behavior. If $F > 8$, this becomes negative at

$$\phi = \frac{1}{g^2(F-8)}. \tag{5.85}$$

The convexity requirement is not full-filled, signaling that a new description is needed at these scales. This is analogous to the $U(1)$ case.
On the other hand, if $F < 8$, the effective coupling is positive definite for any value of ϕ. These theories are then expected to have a fixed point for $1/g^2 = 0$. As we will see later, string theory constructions [145, 207] give us substantial evidence of the presence of these UV completions!
The case $F = 8$ is more subtle since the coupling trivializes as for $U(1)$ with no electrons. However, recent evidence suggests that also $SU(2)$ with $F = 8$ possesses a UV completion, but in terms of a six dimensional SCFT [208–210].

Since the flavor symmetry is $SO(2F)$ in the massless case, we can introduce F different physical masses m_f, $f = 1, ..., F$ for each fundamental. This breaks, in general, $SO(2F) \to U(1)^F$. When all masses m_f are equal and we are the origin of the CB, the symmetry reduces, instead, to $U(F)$. On a generic point of the CB, the physical mass can be obtained from the central charge

$$M_{f,\pm} = |\phi \pm m_f| \tag{5.86}$$

for the electron of positive (resp. negative) charge coming from the f-th quark. Due to the mass splitting in (5.86), the two electrons associated with this quark contribute differently to the effective gauge coupling

$$\frac{1}{g_{eff}^2} = \frac{1}{g^2} + 8\phi - \frac{1}{2}\sum_f |\phi - m_f| - \frac{1}{2}\sum_f |\phi + m_f|. \tag{5.87}$$

Close to the singularities at $\phi = m_f > 0$, the effective coupling reduces to the coupling of a $U(1)$ theory with a single electron. This is indeed the corresponding effective theory at this point of the CB. If M masses coincide, the theory reduces to $U(1) + M$ massless electrons with $SU(M)$ global symmetry. As in the $U(1)$ case, the gauge coupling should be chosen to be larger than the sum of the masses of the quarks, $\frac{1}{g^2} \geq \sum_f |m_f|$, to have a well-defined metric at the origin of the CB.

Finally, let us comment on a peculiarity of the $SU(2)$ group. Since $\pi_4(Sp(N)) = \mathbb{Z}_2$ and $Sp(1) \simeq SU(2)$, we can in principle add to the theory a (discrete) θ term with values $\theta = 0, \pi$. As for the four dimensional θ term, this labels the instantonic configurations of the gauge field belonging to the corresponding homotopy class. The perturbative physics of the theory is unchanged by this term, so the prepotential is the same as $SU(2)$ SYM. Moreover, the angle is non-physical in presence of fermions [149]. However, as we will see, the θ angle changes drastically the non-perturbative physics of the theory for pure $SU(2)$ SYM. For this reason, we will label differently the pure $SU(2)$ theory equipped with a non-zero θ angle, which will be denoted as $SU(2)_\pi$ SYM.

$SU(N) + F$ fundamentals

The CB of the $SU(N)$ theory is parameterized by the VEV of the scalar field $\phi = \text{diag}(\phi_1, ..., \phi_N)$ in the adjoint of $SU(N)$, obeying the condition $\sum_a \phi_a = 0$. The Weyl group is the permutation group of N elements S_N. The CB is then the wedge $\mathbb{R}^{N-1}/S_N$, and we restrict to the fundamental chamber choosing $\phi_1 \geq \phi_2 \geq ... \geq \phi_N$. At a generic point, the gauge group breaks to its Cartan torus $U(1)^{N-1}$. At the edges of the Weyl chamber, where two or more ϕ_as become equal, a non-Abelian subgroup of $SU(N)$ is indeed preserved.
Classical CS terms k can be also introduced in this theory. Since the decoupling of a fundamental flavor of mass m gives rise to a CS contribution of the form

$$\Delta k = -\frac{1}{2}\text{sgn}(m) \tag{5.88}$$

we can interpret this classical term as coming from integrating out massive fundamentals. Taking care of the contribution coming from the vector multiplets, the prepotential reads

$$\mathcal{F} = \frac{1}{2g^2}\phi_a\phi^a + \frac{1}{6}\sum_{a<b}(\phi_a - \phi_b)^3 + \frac{k}{6}\sum_a \phi_a^3. \tag{5.89}$$

The metric $g_{ab}^{-2} = \frac{\partial \mathcal{F}}{\partial\phi_a\partial\phi_b}$ is then positive definite for any N satisfying the inequality [149]

$$N \geq |k|. \tag{5.90}$$

These theories are then expected to enjoy a UV fixed point. In presence of F massless fundamental quarks, the flavor symmetry is $U(F)$. As usual, when the number of flavors is odd, a CS term k needs to be added for consistency, since the quantization condition in presence of fundamentals reads

$$k + \frac{F}{2} \in \mathbb{Z}. \tag{5.91}$$

Massless fundamentals contribute to the prepotential as

$$\mathcal{F}_{fund.} = -\frac{F}{12} \sum_a |\phi_a|^3. \tag{5.92}$$

So, if the number of fermions is small enough, the prepotential is convex on the entire CB. This happens if and only if

$$F \leq 2N - 2|k| \tag{5.93}$$

When this bound holds, the theory is expected to admit a UV fixed point. This expectation is confirmed by string theory constructions [207, 211] and field theory analysis [208].

5.5 String constructions

One of the main tools to study five dimensional theories comes from string constructions. Some five dimensional theories, such as $Sp(N)$ SYM, can be constructed in type I'. Moreover, the majority of these theories can be realized via compactification of M-theory on CY_3 [149, 153, 212–244] and via pq-web constructions [207, 245, 246]. The inter-twin between these constructions and the localization calculations of the partition functions [178, 247–249] unveiled interesting properties of gauge and non-Lagrangian theories in five dimensions, such as global symmetry enhancement at their UV fixed points [178, 246–249], Higgs branch enhancement and the tight connection with three dimensional theories through magnetic quivers [179–205].

In this section, we discuss two specific string constructions: the type I' and the pq-web construction. We first review the former, describing the construction for $SU(2)$ theories with F fundamentals, and how this gives us substantial evidence of the existence of UV fixed points for $F < 8$. Then, we discuss the latter construction, first reviewing type IIB supergravity, its branes, and how we can construct BPS string junctions, and then discussing the generalities of the pq-web construction with and without 7-branes. For sake of brevity, we do not review applications of type I' constructions to holography [250–256], neither pq-webs in presence of orientifolds [193, 210, 216, 257–262] nor the magnetic quiver program [179–205].

Type I' construction

Let us start by discussing type I' constructions.
Type I' string theory is T-dual to type I. In particular, compactifying type I on a circle of radius R, we obtain type I' on a circle of radius $\frac{\alpha'}{R}$. After T-duality, the 16 D9 branes of the

first theory become the 16 D8 branes of type I'. These can be distributed at some generic point of the S^1 and their positions are related to a specific VEV for the Wilson line associated with the $SO(32)$ gauge theory of the type I D9 branes. The O9 orientifold of type I reduces to an O8-, so the circle is orbifolded to an interval $\mathfrak{I} = {}^{S^1}\!/_{\mathbb{Z}_2}$. The orientifold and its copy lie then at the endpoints of the interval $\mathfrak{I}$. In type I, we can then add a D5 brane and wrap it around the circle. After T-duality, this becomes a D4 brane localized at a point of the interval. On this brane lives a 5d $\mathcal{N} = 1$ $U(1)$ gauge theory. However, when the D4 sits on top of one orientifold, the gauge group gets enhanced to $Sp(1) \simeq SU(2)$. This describes the low-energy physics of the brane system. The distance ϕ of the brane from the orientifold parametrizes the CB of the $SU(2)$ theory.

From the D4 viewpoint, the theory on the D8 branes is weakly coupled and its gauge group represents a global symmetry. Strings stretching between the D4 and the D8 branes give rise to hypermultiplets in the fundamental representation of $SU(2)$. A mass for these hypermultiplets is given by separating the D8 branes from the D4. On a generic point of the interval, when F D8 branes are on top of the D4, the theory reduces at low-energies to $U(1)$ with F electrons. If, on the other hand, the branes sit at one orientifold, the theory is $SU(2)$ with F massless quarks. In the first case, we have an $SU(F)$ flavor symmetry, while in the latter the symmetry is $SO(2F)$. This agrees with the gauge theory on the D8: when these are on top of the orientifold, the theory on their worldvolume is special orthogonal, due to the orientifold projection.

The system has four mixed Neumann Dirichlet directions with all Neumann directions of the D4 in common with the D8. The D4 behaves then as an instanton for the D8 worlvolume theory [97, 263]. The moduli space of the D4 dissolved in the D8 woldvolume is the HB of the five dimensional theory. It is then simple to read the Higgs branch of $SU(2)$ theories with F flavors: this is nothing but the moduli space of one $SO(2F)$ instanton in $\mathbb{R}^4$.

The presence of the D8 branes located at points m_i, $i = 1, ..., 16$ on the interval $\mathfrak{I}$ introduces a background for the F_0 field of type I' (since C_9 couples to the D8 branes)

$$F_0 = \frac{1}{4\pi}\begin{cases} 16 & 0 < \phi < m_1 \\ 16 - 2i & m_i < \phi < m_{i+1}. \end{cases} \tag{5.94}$$

On the D4 worldvolume, the background generates a non-trivial CS term from the coupling $F_0 A F^2$, see (2.24). The instantonic symmetry $U(1)_I$ is associated with the circle of compactification. In particular, the gauge coupling $1/g^2$ of the theory on the probe brane in type I is related to the string coupling as

$$\frac{1}{g^2} \sim \frac{R M_s^2}{g_I} \sim \frac{M_s}{g_{I'}} \tag{5.95}$$

with $g_I(g_{I'})$ the dimensionless type I (type I') coupling constant, R the radius of S^1 and M_s the string scale. So, the coupling changes when the radius R does. This is nothing but the scalar superpartner of the $U(1)$ symmetry coming from the RR potential A_1 of type I' [264].

The D8 branes introduce also a non-trivial geometry for the D4 probe. Considering a configuration with n_L D8 at one orientifold, $n_R = 16 - p - n_L$ at the other orientifold and the remaining ones p in the middle of the interval at m_i, $i = 1, ..., p$, the background generated by the D8

branes reads [250, 264]

$$ds^2 = H_8^{-1/2}(-dt^2 + dx_1^2 + ... + dx_8^2) + H_8^{1/2} dz^2, \;\; e^{-\phi} = g_{I'}^{-1} H_8^{5/4} \tag{5.96}$$

where H_8 is the usual harmonic function in (2.23) and z is the coordinate of the interval. Expanding the DBI on the D4 brane, the effective gauge coupling reduces to the $SU(2)$ one

$$1/g_{eff}^2(\phi) = \frac{1}{g^2} + 8\phi - n_L\phi - \frac{1}{2}\sum_{i=1}^{p} |\phi - m_i| - \frac{1}{2}\sum_{i=1}^{p} |\phi + m_i|, \tag{5.97}$$

being the CB parameter $\phi \equiv \frac{z}{l_s^2}$. Looking at (5.97), we see that for sufficiently large R, the coupling remains finite. However, diminishing the radius to a value $R_0(g, n_L, m_i)$, the effective coupling diverges at the right orientifold. Taking $p = 0, \; n_L > 8$, this happens at

$$R_0 = g^2(n_L - 8). \tag{5.98}$$

If we place the D4 brane at the left orientifold, (5.98) tells us that the effective coupling diverges at the point of the CB associated with the right orientifold, as expected for $SU(2)$ theories with $F > 8$.

Since $\frac{1}{g^2} \sim \frac{1}{g_{I'}}$, the effective coupling diverges when $\frac{1}{g_{I'}} \sim n_L - 8$. This remains valid also if $p \neq 0$.

If we place the D4 at the right orientifold, the theory is now $SU(2)$ with $F = n_R < 8$ flavors and its bare gauge coupling is $\tilde{g} = g_{eff}(1/R)$. Rewriting the CB parameter as $\tilde{\phi} = 1/R - \phi \geq 0$, the effective coupling reduces to

$$\frac{1}{\tilde{g}_{eff}^2(\tilde{\phi})} = \frac{1}{\tilde{g}^2} + (8 - F)\tilde{\phi}. \tag{5.99}$$

We see then that for $R = R_0$ the bare coupling $\frac{1}{\tilde{g}^2}$ goes to zero and the theory at the orientifold is strongly coupled.[11] However, we know that the long-distance dynamics on the brane is always a local QFT. Since its coupling goes to infinity, this theory must be at a fixed point of the RG-flow. We can then ask what are the properties of these fixed points. Surprisingly, we can show that at these points the global symmetry of the theory enhances to a larger group. To see how this works, we should do a little step back and discuss type I/heterotic duality.

Type I is dual to $SO(32)$ heterotic string theory and the parameters g_I, R_I of the first theory map to the parameters g_h, R_h of the latter as

$$R = R_I = R_h g_h^{-1/2}, \;\; g_I = g_h^{-1}. \tag{5.100}$$

Via T-duality between type I and type I', we can map the parameter of the latter to the parameter to the heterotic ones as

$$R_{I'} = \alpha' R_h^{-1} g_h^{1/2}, \;\; g_{I'} = g_h^{-1/2} M_s^{-1} R_h^{-1}. \tag{5.101}$$

[11] If $n_L < 8$, the opposite happens: the theory at the left orientifold becomes strongly coupled, while the coupling of the theory at the right orientifold diverges at some point of the CB.

The expectation values of the Wilson lines in heterotic string theory are mapped to the position of the D8 branes of type I'. So, giving some expectation value to the Wilson lines, the $SO(32)$ heterotic gauge group is broken down to some subgroup. In type I', the same result is obtained by tuning in a specific way the positions of the D8 branes. However, since the heterotic theory is compactified on a circle of radius R_h, some winding states can become massless at some self-dual radius, leading to enhancement of the gauge symmetry. Let us choose a Wilson line breaking $SO(32)$ down to $SO(14) \times SO(18)$, at the self-dual radius

$$R_h = \sqrt{\alpha'/8} \tag{5.102}$$

The left movers of heterotic string introduce an additional $U(1)_L$. At the self-dual radius (5.102), additional winding states become massless and enhance $SO(14)\times U(1)_L$ to[12] E_8. To this configuration, it corresponds a particular brane setup in type I'. To respect the $SO(14)\times SO(18)$ algebra, 7 D8 branes are placed at an orientifold (say the left one), and the remaining 9 are placed at the other. The corresponding dilaton profile can be read from (5.96). The additional $U(1)_L$ coming from the left movers maps to the instantonic symmetry of the theory [266]. Although the two theories are dual to each other, it seems that their gauge symmetry does not match at the self-dual radius of heterotic string. However, at this point, in type I' the dilaton diverges at the right orientifold. So the enhancement is not visible in type I' (and neither in type I), since perturbation theory breaks down. However, the duality tells us that, due to the heterotic enhancement, the global symmetry of the five dimensional theory enhances from $SO(14) \times U(1)$ to E_8 [145]. We see then that $SU(2)$ with 7 flavors has an SCFT in the UV with global symmetry enhanced from $SO(2F) \times U(1)_I$ to E_8. Note that this is a purely non-perturbative effect: the flavor and the topological symmetry mix at the fixed point and they both contribute to the enhancement.

The same analysis can be performed also for lower F. In the heterotic framework, we can lower the value of F by giving different VEVs to the Wilson lines to break $SO(14) \times SO(18)$ down to a subgroup. In type I', this is equivalent to moving some D8 branes away from the orientifold. The symmetry enhances to E_{F+1} for $F < 8$ when the radius is equal to (5.98) for $n_L = 16 - F$ or equivalently when the heterotic radius $R_h = \sqrt{\frac{\alpha'_h(8-F)}{8}}$ [266, 267]. This is precisely the point at which the dilaton diverges and our description at the right orientifold is strongly coupled!

As in the $F = 7$ case, also for lower F the instantonic symmetry $U(1)_I$ and the flavor symmetry mix at the fixed point, leading to the global enhancement.

When $F = 0$, no D8 brane is placed at the orientifold where the D4 sits and the low energy theory is $SU(2)$ SYM. We then see that this theory admits an SCFT at which the instantonic symmetry $U(1)_I$ enhances to $SU(2)_I$!

More exotic fixed points can be obtained by considering other expectation values for the Wilson lines of the heterotic group. In particular, the moduli space of heterotic string theory admits the existence of $SU(18)$ and $SO(34)$ enhancements. In type I', this is equivalent to having more than 16 D8 branes. In the first case, we have 18 D8 branes inside the interval, while in the latter we have 17 branes at one orientifold. When this happens, the theory at the orientifold

[12] Note that, however, the enhancement is associated with the Wilson lines of heterotic string, so we cannot infer the global structure of the gauge group. This motivated the analysis of [154, 265].

is believed to be non-Lagrangian with no global symmetry. This is denoted in literature as the E_0 theory. The existence of this non-Lagrangian theory can be inferred by looking at the phase diagram of the E_2 theory, i.e. the UV completion of $SU(2)$ SYM with a single fundamental flavor [212, 245].
The Higgs branches of these gauge theories change at the strong coupling fixed point. This becomes the moduli space of E_{F+1} instantons. This is surprising if we consider pure $SU(2)$ SYM. At the perturbative level, the Higgs branch is zero dimensional, since there are no perturbative hypermultiplets. However, at the fixed point, this enhances to the moduli space of $SU(2)$ instantons $\mathbb{C}^2/\mathbb{Z}_2$. This is possible due to the presence of massless instantons at the fixed point, which are, in fact, responsible for the parametrization of the Higgs branch of the SCFT [179]. This matches the enhancement in the heterotic theory: this originates from winding states becoming massless at the self-dual radius, which in type I' are mapped to D0 branes. The left $U(1)_L$ is mapped to the RR field which couples to the D0s [268]. These are nothing but instantons for the D4 worldvolume theory, as we can see from the mixed Neumann Dirichlet directions of the D0/D4 system. So, when winding states become massless, instantons on the D4 worldvolume become light, and perturbation theory breaks down. Then, additional massless vectors described by the D0 branes contribute to the global symmetry enhancement on the D8 worldvolume at the self-dual radius [266, 267].
Notice that the previous reasoning does not hold in presence of a θ term. This can be introduced in the construction as a background for the A_1 field [249]. Superconformal index computations [249], field theory results [208] and pq-web techniques [207] can be used to show that the global $U(1)_I$ symmetry of $SU(2)_\pi$ in absence of flavor does not enhance to $SU(2)_I$ in the UV. The corresponding fixed point is denoted as $\tilde{E}_1$.

pq-web constructions

Below, we review the pq-web construction of five dimensional gauge theories. In sections 5.5.1 and 5.5.2, type IIB supergravity and its solitons, its bound states, and corresponding junctions are discussed. In section 5.5.3, we construct gauge theories using brane webs. In sections 5.5.4 and 5.5.5, we give the tools to extract information about gauge theories from the pq-web, such as their prepotential and their BPS states. In the last section, we add 7-branes to the webs and we discuss how the global symmetries, the HB, and continuation past infinite coupling of the gauge theories can be understood in terms of these improved pq-webs.

5.5.1 Type IIB supergravity, $SL(2,\mathbb{Z})$ invariance and bound states

In this section, we review bound states and string junctions in type IIB string theory. The main part of the analysis is based on [97, 269, 270].
Let us start by discussing branes in type IIB. As mentioned in Chapter 2, these are electric (or magnetic) sources of the RR and NSNS fields of type IIB supergravity.
The RR fields of type IIB are $C_0, C_2, C_4, C_6, C_8, C_{10}$ and, we have D(-1), D1, D3, D5, D7, and D9 branes in the spectrum. In particular, by Hodge duality, D7 (resp. D5) branes are magnetic

sources of C_0 (resp. C_2).
The NSNS fields are the dilaton ϕ, the two-form field B_2, and the metric g_{MN}. The VEV of e^{ϕ} is the type IIB string coupling g_s. The fundamental strings F1 couples electrically to B_2, while NS5 branes couple to it magnetically.
Type IIB SUGRA possesses $SL(2,\mathbb{R})$ invariance. This descends from self-duality of type IIB string theory $SL(2,\mathbb{Z})$. This is a weak-strong coupling duality, acting on the states of type IIB. In supergravity, this reduces to $SL(2,\mathbb{R})$, since we do not require charge quantization [97]. The most general $SL(2,\mathbb{Z})$ transformation reads

$$\Lambda = \begin{pmatrix} a & b \\ c & d \end{pmatrix}, \quad ab - cd = 1, \quad a, b, c, d \in \mathbb{Z} \tag{5.103}$$

and the group has two generators, the S and T transformations

$$S = \begin{pmatrix} 0 & 1 \\ -1 & 0 \end{pmatrix}, \quad T = \begin{pmatrix} 1 & 1 \\ 0 & 1 \end{pmatrix}. \tag{5.104}$$

This remains true also for $SL(2,\mathbb{R})$, where now $a, b, c, d \in \mathbb{R}$.
Under an $SL(2,\mathbb{R})$ transformation in supergravity, fields transform as follows

- The axio-dilaton field $\tau \equiv C_0 + ie^{-\phi}$ transforms as

$$\tau \to \frac{a\tau + b}{c\tau + d}. \tag{5.105}$$

  In particular, S relates weakly coupled to strongly coupled string theory, since it sends $\tau \to -\frac{1}{\tau}$;

- The fields B_2 and C_2 combine into a doublet of $SL(2,\mathbb{R})$ and transform as

$$\begin{pmatrix} B_2 \\ C_2 \end{pmatrix} \to \Lambda^{-T} \begin{pmatrix} B_2 \\ C_2 \end{pmatrix}; \tag{5.106}$$

- The four form C_4 is invariant under $SL(2,\mathbb{R})$;

- The metric in the Einstein frame $g_E = e^{-\phi/2} g_S$ is also invariant.

We can then write a manifestly invariant Lagrangian under $SL(2,\mathbb{R})$ for supergravity. Defining the covariant fields

$$\mathcal{M} = e^{\phi} \begin{pmatrix} |\tau|^2 & C_0 \\ C_0 & 1 \end{pmatrix}, \quad G_3 = \begin{pmatrix} H_3 \\ F_3 \end{pmatrix} = \begin{pmatrix} dB_2 \\ dC_2 \end{pmatrix}, \quad F_5 = dC_4 - \frac{1}{2} C_2 H_3 + \frac{1}{2} B_2 dC_2 \tag{5.107}$$

with transformation properties

$$\mathcal{M} \to \Lambda \mathcal{M} \Lambda^T, \quad \begin{pmatrix} H_3 \\ F_3 \end{pmatrix} \to \Lambda^{-T} \begin{pmatrix} H_3 \\ F_3 \end{pmatrix}, \quad F_5 \to F_5. \tag{5.108}$$

This reads

$$S_{IIB} = \frac{1}{2\kappa^2}\int d^{10}x\sqrt{-g_E}\left(R + \frac{1}{4}\mathrm{Tr}[\partial_\mu\mathcal{M}\partial^\mu\mathcal{M}] - \frac{1}{12}G_3^T\mathcal{M}G_3 - \frac{1}{480}F_5^2\right) - \frac{\epsilon_{ij}}{4\kappa^2}\int C_4\wedge G_3^i\wedge G_3^j \tag{5.109}$$

with $2\kappa^2 = (2\pi)^7\alpha'^4 g_s^2$ is the Newton's constant $G_N = \frac{\kappa^2}{8\pi}$.
Since type IIB string theory is self-dual under $SL(2,\mathbb{Z})$, BPS states organize in representations of this transformation group. D3 branes are singlets of $SL(2,\mathbb{Z})$, while branes that source electrically or magnetically (B_2, C_2) with charges (p_e, q_e) and (p_m, q_m) respectively transform as

$$\begin{pmatrix} p_e \\ q_e \end{pmatrix} \to \Lambda \begin{pmatrix} p_e \\ q_e \end{pmatrix}, \quad \begin{pmatrix} q_m \\ p_m \end{pmatrix} \to \Lambda \begin{pmatrix} q_m \\ p_m \end{pmatrix}. \tag{5.110}$$

We see then that an F1 string is mapped to a D1 brane and a D5 brane to an NS5 by S-duality. These are said to be S-dual. Of course, we can act with a more general transformation on branes. In particular, the most general $SL(2,\mathbb{Z})$ matrix maps an F1 string into a state with (p,q) charges under (B_2, C_2), with p, q relatively prime. The same happens for 5-branes. Due to self-duality, these solutions are non-perturbative BPS states of type IIB string theory. This agrees with the existence of bound states of p F1 and q D1 strings of charges (p,q) relatively prime, as well as of p D5 and q NS5 branes [97, 271] with relatively prime charges. Conventionally, bound states of strings with p B_2 and q C_2 charges are called (p,q) strings, while bound states of p D5 and q NS5 branes are called (p,q) 5-branes. Being all these states BPS, their tensions are related to their charges by the BPS bound [207, 270]

$$T_{p,q} = |p + q\tau|T_s, \;\; T_{p,q} = |p + q\tau|T_{(1,0)} \tag{5.111}$$

for a (p,q) string and a (p,q) 5-brane respectively. In (5.111) T_s is the string tension $\frac{1}{2\pi\alpha'}$ while $T_{(1,0)}$ is the D5 brane tension $g_s^{-1}(2\pi)^{-5}(\alpha')^{-3}$.
Finally, $SL(2,\mathbb{Z})$ duality acts non-trivially on the D7 branes also. These are magnetically charged under C_0, so we expect them to transform under $SL(2,\mathbb{Z})$. The resulting object, called a $[p,q]$ 7-branes, couples magnetically to both C_0 and $e^{-\phi}$.
As we will see later, these branes are peculiar: being magnetically charged under C_0 and ϕ, they introduce branch cuts for the axio-dilaton via their monodromies, together with a non-trivial metric [211, 272–277].

5.5.2 String junctions and brane webs

From (p,q) strings (resp. 5-branes), we can construct more complicated BPS states, called string junctions (resp. brane webs). These are states defined by a set of (p_i, q_i), $i = 1, ..., n$ strings (resp. 5-branes) that join together at a single point. To see under which conditions these states preserve supersymmetry, we first review which supercharges are preserved by (p,q) strings (resp. 5-branes) in general.
Let us focus on a generic Dp brane aligned along the first $p+1$ directions $x^0, ..., x^p$. This is a 1/2 BPS state preserving 16 out of 32 type IIB supercharges. The Majorana-Weyl spinors $\epsilon_{L,R}$ defining the preserved supersymmetries $\epsilon_L Q^L + \epsilon_R Q^R$ satisfy the equation [271]

$$\epsilon_L = \beta^\perp \epsilon_R \tag{5.112}$$

where $\beta^\perp$ is the product of all the gamma matrices $\gamma^0...\gamma^p$ aligned along the Neumann directions of the brane. For example, the $\beta^\perp$ of a D1 extended along 01 reads $\beta^\perp = \gamma^0\gamma^1$. The condition (5.112) halves the number of conserved supercharges of type IIB. When multiple Dp branes are present, only the supercharges compatible with all the conditions (5.112) associated with each brane are preserved. In particular, it can be shown that some supersymmetry remains whenever the mixed Neumann Dirichlet boundary conditions $\#_{ND}$ are a multiple of four [271]. In particular, 8 supercharges are conserved if $\#_{ND} = 4, 8$ and 16 if $\#_{ND} = 0$.
States charged under the NSNS field B_2 do not preserve the supercharges (5.112). In fact, the condition for both F1 strings[13] and NS5 branes is modified as

$$\epsilon_L = \beta^\perp \epsilon_L, \;\; \epsilon_R = -\beta^\perp \epsilon_R. \tag{5.113}$$

We see that when a Dp brane and an F1 (resp. NS5 brane) are present, 8 supercharges are preserved if $\#_{ND} = p+1$ (resp. $\#_{ND} = 7-p$). Then, for example, the following system preserves 8 supercharges (taking p < 5): an F1 string along 01 and a Dp along 02...p, a D5 along 012345 and an NS5 along 012346, or a generic Dp brane ending on an NS5 along 012346 with p common Neumann directions. Denoting $(x^1, x^2) \equiv (x, y)$, we see that an F1 string perpendicular to a Dp brane in the (x, y) plane preserves eight supercharges. We can then wonder if an F1 string that terminates on this brane perpendicularly, forming a junction, preserves this same amount of supersymmetry.
First, let us notice that the F1 can terminate on a Dp brane only if its charge can be absorbed by some field configuration on the brane worldvolume [269]. This is dictated by charge conservation and it is a general feature of a brane ending on another brane: a brane can terminate on another if the latter has a worldvolume field able to compensate for the charge of the former.[14] In our case, the endpoint of the string on the Dp brane is a charged particle for the gauge field A_μ on the Dp worldvolume. A Coulomb field is generated by the charge and reads

$$A_0 = \frac{Q}{r^{p-2}} \tag{5.114}$$

where $r = x^m x_m$ with $m = 2, ..., p$ is the radial coordinate associated with the spatial direction of the Dp woldvolume. In particular, the endpoint of the string is located at $r = 0$. The behavior of the Coulomb potential at infinity then depends only on the codimension of the string endpoint in the worldvolume of the Dp brane.
A background of the form (5.114), however, is not a BPS solution of the equations of motion of the worldvolume theory. The background is BPS only if also a bosonic field $X^1(r)$ parametrizing the position of the brane in the transverse direction y is turned on. The BPS equation for this field reads

$$\nabla^2 X^1 = Q\delta(r) \tag{5.115}$$

where ∇^2 represents the Laplacian in p dimensions. This leads to a bending of the Dp brane as

$$X^1 = \frac{Q}{r^{p-2}}. \tag{5.116}$$

[13] Actually, for an F1 string $\epsilon_R = \pm\beta^\perp \epsilon_R$, where the sign depends on its orientation.

[14] A simple way to verify the endability comes from T- and U-duality. If our brane system is dual to a system of a string ending on a Dp brane, then the first brane is endable on the latter [269].

Note that Q is quantized in the worldvolume gauge theory as

$$Q = n g_{\rm SYM}^2 = n g_s l_s^{p-3}, \;\; n \in \mathbb{Z} \tag{5.117}$$

so, in the $g_{\rm SYM} \to 0$ limit, the bending is suppressed [278].
The same reasoning applies in the case of a Dq brane ending on a D(q+p) brane. The D(q+p) brane is bent by the Dq endpoint and the bending depends only on the codimension of the endpoint, which is still p. In general, the X^2 profile in (5.116) receives quantum corrections [279] in the vicinity of the endpoint. However, at large r, the bending (5.116) correctly describes the asymptotic shape of the D(p+q) brane.

Let us now focus on the case of an F1 string ending on D1 brane. Let us take $g_s = 1$ for definiteness. The codimension of the string endpoint is one. The one dimensional Laplace equation

$$\nabla^2 x = \delta(y) \tag{5.118}$$

describes how the D1 brane bends. The most general solution reads

$$x = \frac{1}{2}|y| + cy + d. \tag{5.119}$$

We can tune c and d to have a D1 brane asymptotically aligned along y in the limit $y \to -\infty$. The bending reduces to

$$x = \frac{1}{2}|y|(1 + \mathrm{sgn}(y)) \tag{5.120}$$

and it is shown in figure 5.2. For negative y, we see the F1 string ending perpendicularly on

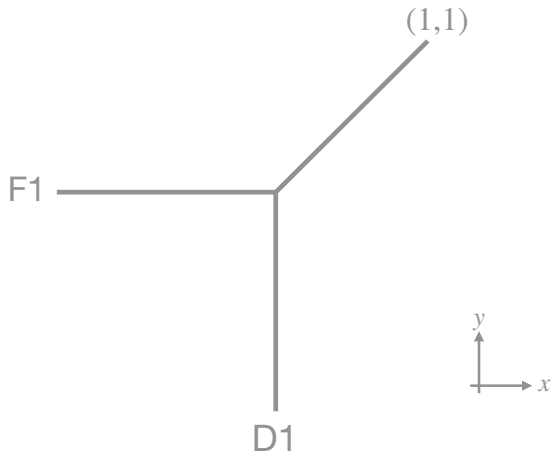

Figure 5.2: Bending of D1 brane by an F1 string.

the D1 brane. For positive y, however, the D-brane bends at an angle $\pi/4$ with respect to the x axis. This apparently violates supersymmetry. However, the D-brane bent at 45° is not a D1. Indeed, the F1 and the D1 actually merge and become a $(1,1)$ bound state. The whole

system is then compatible with supersymmetry. Indeed, a (p,q) string along $0x$, in presence of a non-trivial axio-dilaton τ, preserves the following supercharges [270]

$$\epsilon_L + i\epsilon_R = e^{i\phi(p,q,\tau)}\gamma^2...\gamma^9(\epsilon_L - i\epsilon_R) \tag{5.121}$$

where $\phi(p,q,\tau) = \arg(p+q\tau)$. So, when we consider a (p,q) string at angle $\phi(p,q,\tau)$ with respect to x together with the F1/D1 system, the following supercharges

$$\epsilon_L = \gamma^2...\gamma^9\epsilon_L,\ \ \epsilon_R = -\gamma^2...\gamma^9\epsilon_R,\ \ \epsilon_L = \gamma^1\gamma^3...\gamma^9\epsilon_R \tag{5.122}$$

are still preserved. These are the same eight supercharges preserved originally by the F1/D1 system. In particular, any system of (p_i,q_i) strings oriented along a $(p_i + q_iC_0, q_ig_s^{-1})$ vector preserves the same supercharges as the F1/D1 system. In the $\tau = i, (p=1,q=1)$ case, the angle is 45°. So, the junction preserves eight supercharges!
Notice, moreover, that SUSY forbids any possible corrections to the bending (5.120). So the formula remains valid also close to the intersection point [245].
More generally, we see that N (p_i,q_i) strings oriented along $(p_i + q_iC_0, q_ig_s^{-1})$ vectors preserve 1/4 supercharges by virtue of (5.121). Many strings emanating from the same point with this orientation and respecting charge conservation form a BPS junction and this happens when

$$\sum_{i=1}^{N} p_i = \sum_{i=1}^{N} q_i = 0,\ \ (p_i,q_i) \parallel \vec{T}_{p_i,q_i} \equiv (p_i + q_iC_0, q_ig_s^{-1}). \tag{5.123}$$

These conditions can be recast in an equation of conservation of "momentum"

$$\sum_{i=1}^{N} \vec{T}_{p_i,q_i} = 0 \tag{5.124}$$

with $\vec{T}_{p_i,q_i} = (p_i + q_iC_0, q_ig_s^{-1})$ the "momentum" associated to the (p_i,q_i) brane. Since the preserved supercharges in (5.122) depend only on the orientation of the strings at the junction, we can connect different junctions respecting the previous rules without breaking supersymmetry. The corresponding systems are denoted as string networks, see figure 5.3.
The same reasoning applies also for 5-branes junctions. A D5 can end on an NS5 and the bending of the NS5 caused by the D5 is linear. This can still be interpreted as the formation of $(1,1)$ 5-brane bound state. Any corrections to this bending would break the remaining SUSY [245]. Connecting different 5-brane junctions we can construct brane webs (denoted also as pq-webs), namely the equivalent of string networks for five branes. When each junction of the web conserves the momentum

$$\sum_{i=1}^{N} \vec{T}_{p_i,q_i} = 0 \tag{5.125}$$

this is 1/4 BPS.

In the next section, we see how using these webs we can embed five dimensional gauge theories in type IIB and how information on these theories can be extracted.

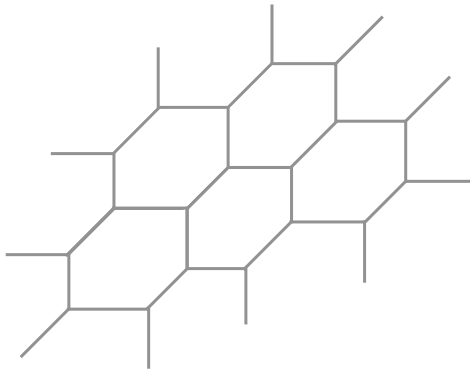

Figure 5.3: Example of string network at $\tau = i$.

5.5.3 Gauge theories from brane webs

In the previous section, we saw how to construct 1/4 BPS webs of 5-branes. Their low-energy physics should be described by the open strings ending on them. In particular, some of the branes composing the web are finite dimensional. The low-energy dynamics is then expected to be described by a five dimensional theory living on the finite branes. This idea parallels general brane constructions, such as Hanany-Witten (HW) constructions [280]. For these reasons, in this section, we first review the HW construction of three dimensional gauge theories, and then we adapt the acquired knowledge to understand constructions of five dimensional theories via brane webs.

The Hanany-Witten construction was first introduced in [280] to describe $\mathcal{N} = 4$ three dimensional theories. These were described through systems composed of D3 branes along 012x direction, NS5 branes along 01234y, and D5 branes along 012789, where $(x, y) \equiv (x^5, x^6)$. In the (x, y) plane, the D3s (resp. NS5s) are extended along x (resp. y), while the D5s are pointlike. All the branes in the system have three common Neumann directions. Moreover, it is possible to show that the system preserves eight supercharges.
The worldvolume theory on the D3 brane, in absence of other branes, is $\mathcal{N} = 4$ SYM in 4d. However, this is endable on the D5s/NS5s. In the following, we will consider the classical $g_s = 0$ limit, to discard bending effects. A D3 brane can be then suspended between two straight 5-branes of generic type. When this happens, the theory on its woldvolume gets modified as follows.
Firstly, the fields on the D3 branes are subject to boundary conditions given by the 5-branes. Scalars parametrizing the position of the D3 brane in the $34y$ (resp. 789) directions have a fixed value $\vec{z}$ (resp. $\vec{w}$) at the endpoint of the D3 brane at D5 (resp. NS5) position. As a consequence, these scalars are subject to Dirichlet boundary conditions at the endpoints, while the remaining ones are subject to Neumann boundary conditions. These breaks supersymmetry and the woldvolume theory preserves only eight supercharges, as expected. Analogously, the gauge fields F_{MN} with $M, N = 0, 1, 2, x$ satisfies Neumann (resp. Dirichlet) boundary conditions

at the endpoint where the D3 end on the D5 (resp. NS5) brane. These read [281]

$$F_{\mu\nu}\big|_{\vec{z}} = 0 \text{ (resp. } F_{\mu x}\big|_{\vec{w}} = 0). \tag{5.126}$$

Boundary conditions on fermions are obtained from the remaining supersymmetry.
Secondly, the theory on the worldvolume of the D3 is three dimensional for low enough energies, since the x direction is compact of length L. In the reduction, scalars satisfying Dirichlet boundary conditions acquire a Kaluza-Klein mass $\sim \frac{1}{L}$ and can be integrated out at low-energies. On the other hand, scalars satisfying Neumann conditions survive the reduction. The same thing happens when we deal with the gauge field. We can then distinguish three cases: when the D3 is suspended between two NS5 branes, two D5 branes, and a D5 and an NS5 one.
In the first case, a gauge boson and three scalars survive the reduction. Since the theory is $\mathcal{N} = 4$ SUSY in 3d, the quantum field theory on the D3 worlvolume is $\mathcal{N} = 4$ $U(1)$ SYM. When N D3 branes are suspended between the two NS5 and are on top of each other, the gauge group theory enhances to $U(N)$.
When a D3 is suspended between two D5 branes, three scalars survive, together with the third component of the gauge field A_x. This is the content of a $\mathcal{N} = 4$ hypermultiplet.
Finally, when a D3 is suspended between a D5 and an NS5 brane, all scalars and gauge bosons are lifted and the three dimensional theory is gapped with a unique vacuum [280].

The same analysis applies to 5-brane webs in the $g_s = 0$ limit [207, 282]. When a D5 is suspended between two NS5, a single scalar survives the reduction. This parametrizes the position of the D5 in the worldvolume of the NS5 since all other transverse directions are Dirichlet for the NS5 branes. Moreover, the gauge field in the tangent directions survives the reduction and the five dimensional content of the theory reduces to a single vector multiplet. When N D5 branes are suspended between the NS5, the five dimensional theory is $U(N)$ $\mathcal{N} = 1$ SYM. The gauge coupling on the D5 brane is dimensionful and proportional to the length L_x of the compact direction x, namely $\frac{1}{g_{5d}^2} = \frac{L_x}{g_s l_s^2}$. This is irrelevant, as expected for five dimensional gauge theories. Quantum corrections modify the previous system. The D5 bends the NS5 on which it ends to preserve supersymmetry and charge conservation. When a single brane is considered, all its scalars are lifted by the bending, since the D5 is stuck at the two junctions and cannot move, see figure 5.4. As a consequence, the vector multiplet is lifted [245]. On the contrary, when the gauge group is non-Abelian, the brane web has $N - 1$ moduli, as we will see in the next section. So the theory on the D5 reduces to $SU(N)$. This holds also for a generic stack of (p, q) 5-branes, since, as we mentioned in section 5.5.1, $SL(2, \mathbb{Z})$ duality relates the theory on these branes to the $SU(N)$ theory living on a stack of N D5 branes. The theory on these branes does not decouple at strong string coupling. Indeed, this can be seen naively from the fact that at $\tau = i$ the NS5 brane mass and the gauge coupling of the corresponding field theory are the same as those of a D5 brane. In particular, if the NS5 are compact themselves, the gauge coupling on an NS5 stack becomes proportional to their length L_y. So the couplings on the two different stacks are of the same order, and we then expect both stacks to contribute to the field theory dynamics. As we will see, this aspect is crucial to understanding the electric/instanton charge mixing in the pq-web context [207].
The theory on the 5-branes reduces to a five dimensional gauge theory only at low enough

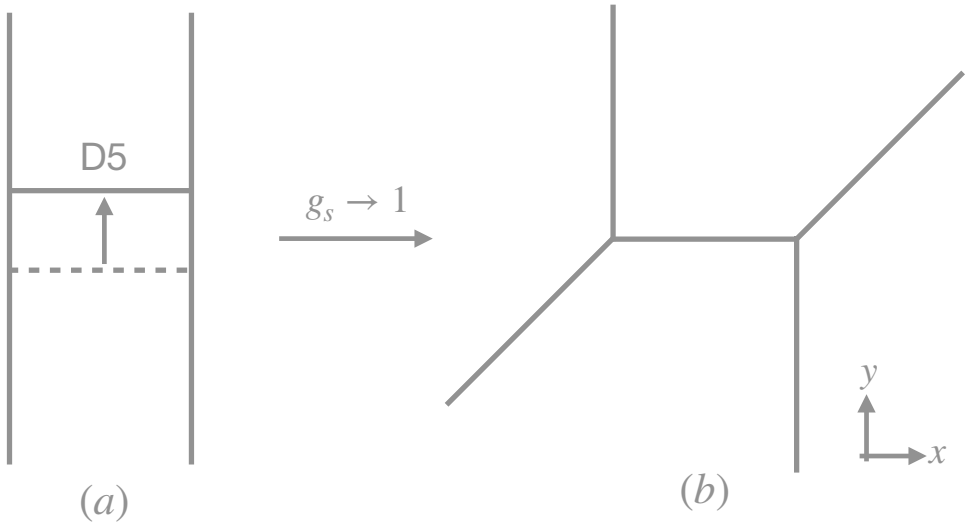

Figure 5.4: A D5 brane suspended between two NS5 before (a) and after (b) quantum corrections.

energies. Indeed, for this to hold gravity and the KK modes coming from the compactification of the theory need to decouple. This happens for energies smaller than the Planck mass M_p and the KK modes mass $\sim \frac{1}{L_x}, \frac{1}{L_y}$, where L_x, L_y are the largest length scales in the configuration. So in the low energy limit

$$E \ll M_p, \ E \ll \frac{1}{L_x}, \frac{1}{L_y} \tag{5.127}$$

the physics of the web is described by a five dimensional $\mathcal{N} = 1$ gauge theory.
We have now all the tools to describe five dimensional gauge theories using pq-webs. We start building the simplest possible five dimensional gauge theory, namely pure $SU(2)$ SYM. This will be our playground to construct more complicated theories, as we will do next.

$SU(2)$ example

Let us start from the web in figure 5.5(a). Fix, for definiteness, $\tau = i$. The web has two three-junctions of a $(1,1)$, $(1,-1)$, and two D5 branes which are suspended between the junctions themselves. Having in mind the previous discussion, it follows that the theory on the D5 branes is five dimensional pure $SU(2)$ SYM. The corresponding gauge coupling $\frac{1}{g^2}$ is proportional to the length of the compact direction along which the D5 extends. Changing this length changes the gauge coupling of the theory. In the process, we move the $(1,1)$ and $(1,-1)$ branes, as we can see in figure 5.5(b). Being these branes semi-infinite the amount of energy necessary to move these objects is infinite from the five dimensional point of view. This agrees with the field theory interpretation of this length: the gauge coupling represents an external parameter of the theory, not a modulus.
All other moves of the semi-infinite branes are either trivial or not allowed by supersymmetry.

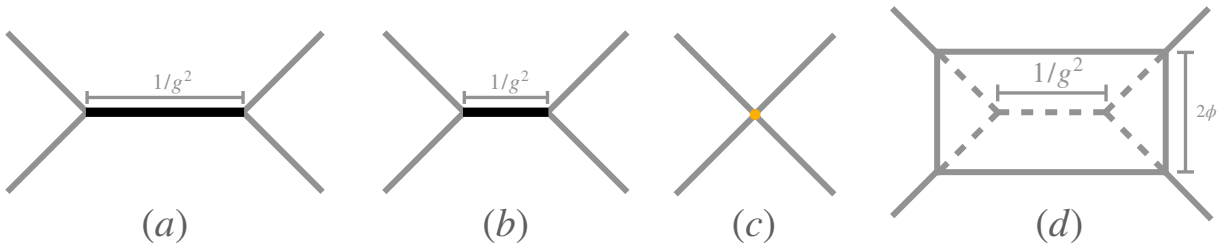

Figure 5.5: The $SU(2)$ theory (a), its global deformation (b), its fixed point (c) and its moduli space (d).

This matches the field theory expectation: the theory has a rank one global symmetry, to which we can associate a single massive parameter $1/g^2$.
Note that in the web we can send $\frac{1}{g^2} \to 0$ by collapsing the three junctions into a four junction, see figure 5.5(c). This non-trivial four junction represents the SCFT associated with the $SU(2)$ SYM theory, namely the E_1 theory. The strong coupling fixed point of this theory is then easily accessible in this construction.

We now want to describe the CB of the theory in the pq-web context. Going to the CB is naturally interpreted in the web by separating the D5 branes in the vertical direction y. In this way, the states of the strings connecting the two D5s become massive, and the $SU(2)$ gauge symmetry is broken to its Cartan. However, this operation by itself is not allowed by supersymmetry. What we can do, instead, is to separate the D5 at the cost of producing NS5 branes in the process, as we see in figure 5.5(d).
The resulting web is supersymmetric. In the process, we moved only finite branes. This corresponds to a modulus from the field theory point of view. So, the opening of figure 5.5 can be interpreted as going on the CB of the $SU(2)$ theory. The non-Abelian symmetry is restored only when the D5 branes are on top of each other, so the distance between the two branes is proportional to the CB parameter. In particular, the fundamental string stretched between the horizontal D5s describes a vector multiplet W becoming massive, with mass $M_W = |\phi|$. The mass of the lowest excitation of the string is

$$m_W = L_y T_s. \tag{5.128}$$

Then, we reproduce the field theory result by identifying $L_y T_s = \phi$. In the following, we will measure lengths of branes web in units of string tension, so $L_y = \phi$ and $L_x = \frac{1}{g^2}$.
In the previous analysis, we kept the axio-dilaton fixed to i and we matched the parameter of the field theory with lengths of the brane web. We can ask if this is too restrictive. It turns out [207] that the axio-dilaton is in general a redundant parameter for the low-energy theories of brane webs.[15] This is compatible with the absence of possible additional independent parameters for the gauge theory. So, from now on, we will always fix $\tau = i$.

[15]Namely, we can always compensate a change of the string coupling with a change of lengths of the web to maintain the same physical parameters m_W, m_I fixed. The same happens with a non-zero axion [207]

Let us comment on the realization of the $SU(2)_R$ symmetry and $SL(2,\mathbb{Z})$ duality in the pq-web. We know from section 5.3.2 that any $\mathcal{N}=1$ SUSY theory preserves an $SU(2)_R$ R-symmetry. In the pq-web context, the symmetry is realized geometrically: this is nothing but the $SO(3)$ isometry of the three Dirichlet directions (x^7, x^8, x^9) common to all the branes. This agrees also with our previous interpretation of the pq-web deformations: all operations that we did acted on the plane and so they preserved the R-symmetry, as expected from the changing of an external parameter or a CB modulus. In the same vein, from the discussion of section 5.4.2, we expect the Higgs branch to be described by some deformation involving finite branes outside the (x,y) plane. We address this issue later when we add 7-branes to the web.
String theory is $SL(2,\mathbb{Z})$ self-dual. An $SL(2,\mathbb{Z})$ transformation Λ acts on both τ an the 5-branes. Since, to preserve supersymmetry, we assigned to a (p,q) brane a (p,q) direction in the (x,y) plane, we see that the transformation reduces to a coordinate transformation on the (x,y) plane (since we can always set $\tau = i$ after). So the duality maps pq-webs into pq-webs via a coordinate transformation

$$\begin{bmatrix} x' \\ y' \end{bmatrix} = \Lambda \begin{bmatrix} x \\ y \end{bmatrix}, \quad \Lambda \in SL(2,\mathbb{Z}). \tag{5.129}$$

So, for example, applying S duality to our $SU(2)$ pq-web at a generic point on the CB, we obtain another $SU(2)$ pq-web, with different parameters. We will comment extensively on this map in the following sections.
Since $SL(2,\mathbb{Z})$ is a symmetry of type IIB string theory, the physics of the pq-webs mapped by the duality should be related. In particular, moduli and parameters are mapped between the two theories. This establishes UV dualities between five dimensional gauge theories, as we will see in section 5.5.6.

5.5.4 Deformations

With the $SU(2)$ discussion in mind, we can now generalize the previous analysis to more complicated pq-webs.
We denote generically as deformations of a pq-web any deformation of the web which respects supersymmetry and does not change the charges or the orientation of the external branes (like instead $SL(2,\mathbb{Z})$ duality does). These deformations can change the position of the external legs. If this happens, the deformation is denoted as global, while if not as local. The two types of moves have the following properties.

- Global deformations:
  A global deformation changes the asymptotics of the web, moving the external semi-infinite branes. From the viewpoint of the five dimensional theory, this is associated with a change of a parameter. Since all parameters in a supersymmetric theory are related to the Cartan of the global symmetry group $\mathcal{G}$, the number of independent deformations equals the rank of $\mathcal{G}$. In the E_1 case, for example, we have a $SU(2)_I$ topological symmetry to which we associated a single parameter $\frac{1}{g^2}$.

This gives us a way to calculate the rank of the global symmetry from the number of independent global deformations of the web n_G. Taking a pq-web with E external branes, their number reads

$$n_G = E - 3. \tag{5.130}$$

Note that this formula holds both at weak and strong coupling: the rank of the symmetry remains the same along the RG-flow and so does the number of external branes.

- Local deformations:
  Local deformations involve only finite branes. They are CB moduli from the viewpoint of the five dimensional theory. Their number n_L is then equal to the rank of the gauge group.[16]
  Let us take a pq-web with I internal edges and V vertices and with a single connected component. The number of local deformations reads

$$n_L = I - V + 1 = F \tag{5.131}$$

  where F is the number of faces of the web and in the second equality we used the Euler formula $I - V + 1 = F$. Indeed, in the $SU(2)$ case, the diagram has a single face, in agreement with the CB being one dimensional. Again, this holds both for $SU(2)$ SYM and for the E_1 theory, which inherits the SYM Coulomb branch.

Let us consider some examples.
The brane web describing $SU(N)_k$ gauge theories with $|k| \leq N$ is shown in figure 5.6. The web

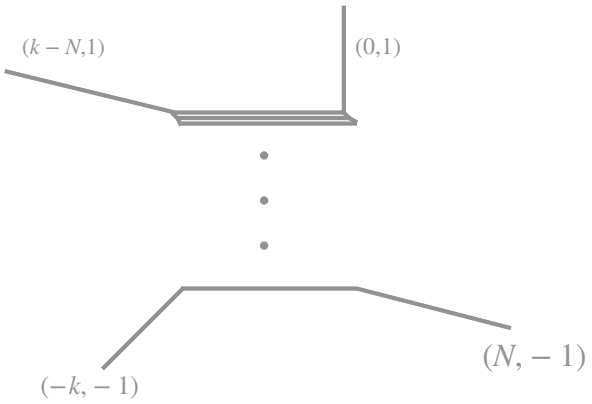

Figure 5.6: $SU(N)_k$ theory.

has $n_L = N - 1$, $n_G = 1$, as expected from a theory of rank $N - 1$ and global symmetry $U(1)_I$. All these theories admit a fixed point, due to the convexity condition (5.93).
All the webs (up to $SL(2,\mathbb{Z})$ duality) of $SU(2)$ gauge theories with a single mass parameter are shown in figure 5.7. The θ angle is the only parameter that distinguishes the three theories.

[16] Actually, this holds if the theory is Lagrangian. As we will see later, some non-Lagrangian theories can admit a CB, which cannot be interpreted in terms of VEVs of a scalar field of a vector multiplet.

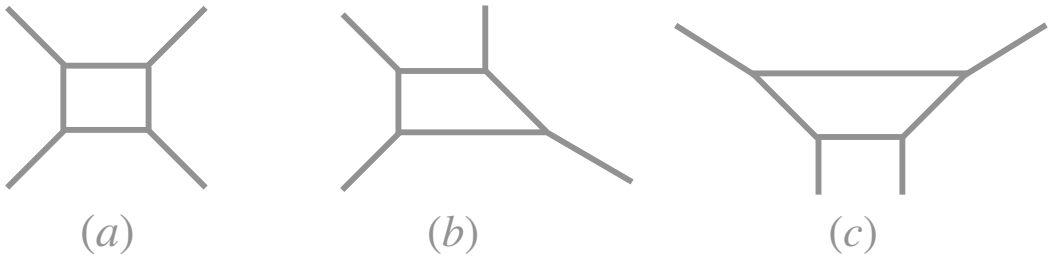

Figure 5.7: $SU(2)$ theories with θ angle 0 (a), (c) and π (b)

In particular, the web (a) corresponds to $SU(2)$ SYM, while (b) corresponds to $SU(2)_\pi$ SYM. The former (resp. latter) diagrams can be obtained from the E_2 diagram by integrating out the quark with a positive (resp. negative) mass. The diagram (c) instead can be shown to be an $SU(2)$ SYM theory, as that corresponding to web (a) [207, 211, 283]. We will come back to this point when discussing symmetry enhancement and HW transitions in section 5.5.6.

Determining n_L can be subtle when one sits at the origin of the CB. Let us take the example of the E_0 junction in figure 5.8 and one of the junctions in figure 5.4(b). Both are three junctions of branes. However, in the first case, the junction can be opened, while in the second case the junction cannot be resolved and so we cannot associate a CB to it. The theory of figure 5.8

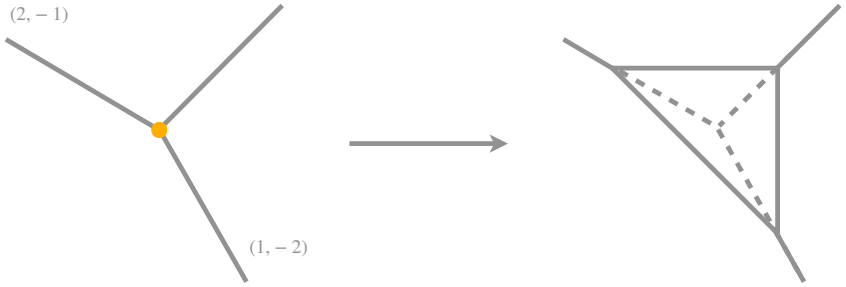

Figure 5.8: E_0 theory.

is rather peculiar. This has no parameters, so the web has no gauge theory interpretation and no global symmetry. However, it has a CB of dimension 1, since $n_L = 1$. This theory can be identified with the E_0 theory we discussed above. In particular, this can be obtained from a series of deformations of the E_2 pq-web [245], as expected from the field theory analysis of the E_2 fixed point [212]. The theory is believed to be non-Lagrangian. The analysis of its BPS spectrum will be elucidated in the next section.
A simple way to understand the resolvability of a web comes from the analysis of its grid diagram. Although this technique is rather powerful, we will not discuss it in detail and we refer the reader to [207] for a clear description of this method.

5.5.5 BPS Spectrum

The BPS spectrum of gauge theories can be studied in detail thanks to brane web constructions. This allows us to understand the phenomena of Higgs branch and symmetry enhancements in the pq-web context, as we will see in the next sections. Here, we first review the BPS spectrum of the $SU(2)$ theory and we introduce string networks in the context of the pq-web. Then, we generalize the analysis to more complicated webs. Finally, we introduce flavors and discuss pq-webs of quiver gauge theories, analyzing their BPS spectrum.

$SU(2)$ case

We already mentioned in section 5.5.3 that massive W bosons are realized in the $SU(2)$ pq-web as fundamental strings stretching between the two D5 branes at some point of the CB. The mass of their lowest excitation is equal to the CB parameter $|\phi|$. However, this is not the only BPS state of the $SU(2)$ theory. From the field theory analysis, we know that also instantons and monopole strings belong to the BPS spectrum and we expect them to be described in the pq-web construction. Indeed, in the following, we will construct all these states in terms of strings and branes of type IIB string theory.
The simplest case comes from massive vectors. An F1 string stretching perpendicularly between the two D5 describes a massive W boson. Looking at its preserved supercharges, this string breaks 1/2 of the pq-web supersymmetries. This is then a 1/2 BPS object of the five dimensional theory, as expected. Analogously, D1 branes stretching perpendicularly between NS5 branes are responsible for the enhancement of the gauge theory on the NS5 worldvolume [97]. As the W bosons, these are 1/2 BPS objects. Moreover, they can be interpreted as instantons of the five dimensional theory. This can be understood by looking at the mixed ND direction between the D1 and the D5: these are four, all Neumann for the D5. We see that the D1 can be then interpreted as an instanton of the five dimensional gauge theory.[17] At the origin of the CB, instantons of the gauge theory have an additional modulus related to their size, as mentioned in section 5.4.3, leading to a continuous spectrum. Away from the origin, the gauge symmetry is Abelian and the instantons are pointlike and singular. Looking at the D1, a single compact modulus remains on the CB and parametrizes the position of the D1 inside the face of the web. Then, these states are vector multiplets of the five dimensional theory[18]. Indeed, S duality maps an F1 stretching between two D5 with a D1 stretching between two NS5 [207]. The mass of this state, calculated from the tensions of branes, is equal to the central charge of an instanton particle of charges $(n_e = 2, I = 1)$

$$M_I = 2\phi + \frac{1}{g^2}. \tag{5.132}$$

In particular, the electric charge of the instanton comes entirely from the mixing: the D1 has no CP factor associated with the D5 branes, so it is a singlet of the $SU(2)$ gauge group. Its electric charge comes entirely from the CS term induced on the CB. From the pq-web point of view, the mixing can be interpreted as a contribution to the electric charge coming from all

[17] Actually when $C_0 \neq 0$ there are some additional subtleties, see [207].
[18] Also the W boson possesses the same zero mode.

the 5-branes composing the face. Whenever the D1 or the F1 end on a D5 or an NS5, to each endpoint we associate a contribution $n_e = 1$ to the total electric charge of the state.
Taking the W boson and the instanton, we can ask if there exist also BPS bound states composed of a W bosons and b instantons, namely with charge $(n_e = 2a + 2b, I = 2b)$. From the central charge, their corresponding mass is $\left|(2a + 2b)\phi + 2b\frac{1}{g^2}\right|$. This is at threshold with the sum of the masses of their constituents, so it is not clear if these states are stable or not.[19] However, bound states of this kind have a simple interpretation in the brane web context: these are junctions of F1 and D1 strings. Due to charge conservation, these bound states should end on the various branes composing the faces of the web. So, to these states, we associate a string junction of a F1 strings and b D1 branes. The basic example with $a = 1, b = 1$ is shown in figure 5.9(c). The state preserves the (p, q) charges since any (p, q) string is ending on the corresponding (p, q) 5-branes and it is also 1/2 BPS since it breaks half of the supercharges preserved by the brane web. Moreover, the mass of the junction matches the central charge formula. Using the refined techniques of [280, 284], it is easy to show that actually only string junctions associated with states of charges $(n_e, I) = (2n, m)$ for $n, m \geq 1$ or $n = 1, m = 0$ are actually BPS. This is a strong result: thanks to the pq-web, we gained information about the stability of the non-perturbative BPS states of $SU(2)$ SYM!

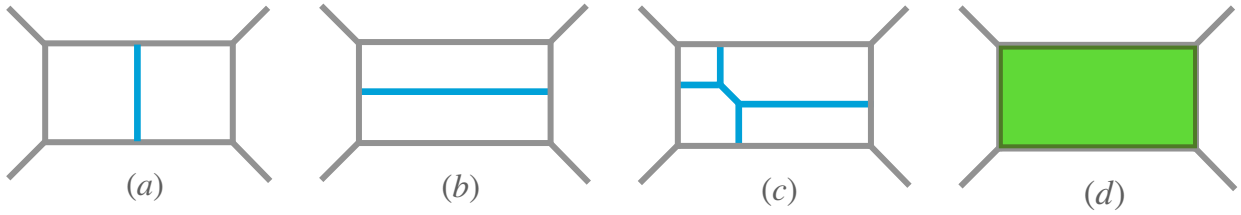

Figure 5.9: BPS states of $SU(2)$ SYM. W boson (a), instanton (b), generic bound state (c) and magnetic string (d).

Finally, we can also construct magnetic strings. These are described by D3 branes wrapping the face of the web, see figure 5.9(d). Indeed, a D3 brane is endable on both an NS5 and D5 brane and preserves 1/2 of the original supersymmetries of the web. Moreover, it has two Neumann directions in common with the whole brane system, so it is a string from the five dimensional point of view. This is BPS and carries charge, so it is actually a five dimensional monopole string. Its tension equals the area of the wrapped face (in units of T_s^2). This matches the expected formula

$$T_m = 2\phi\left(\frac{1}{g^2} + 2\phi\right) = \frac{\partial \mathcal{F}}{\partial \phi} \tag{5.133}$$

coming from the $SU(2)$ prepotential[20]

$$\mathcal{F} = \frac{1}{g^2}\phi^2 + \frac{4}{3}\phi^3. \tag{5.134}$$

[19] This is a feature of five dimensions since the central charge Z is real.
[20] Here, we rescaled the value of $1/g^2$ to adapt to the conventions of [155].

General case

The previous analysis can be generalized to more complicated webs.
A generic 1/2 BPS bound state is described by a string junction ending on some internal branes. In the pq-web, any (p, q) string is oriented in the (x, y) plane along a $(q, -p)$ vector, in order to end on a (p, q) 5-brane perpendicularly and to respect supersymmetry. Each endpoint of the junction ending on either internal branes contributes to the electric charge of the BPS state associated with the corresponding face of the web. This is the result of the mixing of all Abelian charges of the branes composing the web. On the other hand, the state is in a non-trivial representation of the gauge group only when the endpoints lie on the D5 branes realizing the gauge theory. Finally, its mass can be calculated from the tension of the junction, and its charges are obtained by comparing the corresponding lowest mass excitations with the central charge formula.

D3 branes wrapping faces are associated with monopole strings of the five dimensional theory. Labeling each face of the web by $a = 1, ..., N$ with N the total number of faces, we associate a CB parameter ϕ_a to the a-th face. The tension T_a of the brane wrapping it equals the derivative of the prepotential with respect to the ϕ^a CB parameter

$$T_a = \frac{\partial \mathcal{F}}{\partial \phi^a} \tag{5.135}$$

The prepotential of the theory can be then obtained directly from the geometric lengths of the web!

As an example, we can now construct the BPS spectrum and obtain the prepotential of the E_0 theory. Although there is no gauge theory parameter, the web has a modulus to which we can associate a charge coming from the endpoints of string junctions on the internal branes. The basic BPS state is identified by the string junction of figure 5.10. This has $n_e = 3$ and it is the

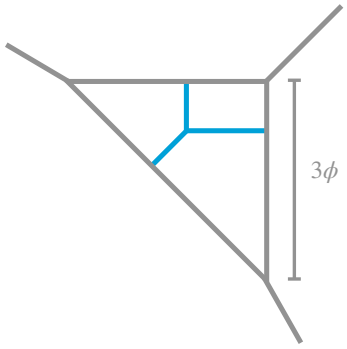

Figure 5.10: BPS states for E_0 theory.

state of lowest charge. This is again the signal of a lack of gauge theory interpretation since no BPS junctions can be associated with massive W bosons on the CB (these would have $n_e = 2$).

We can also obtain the prepotential of the theory by looking at the D3 brane wrapping the face of the web. The tension of this string and the corresponding prepotential read

$$T = \frac{9}{2}\phi^2 \to \mathcal{F} = \frac{3}{2}\phi^3 \tag{5.136}$$

This matches the prepotential obtained in field theory from the decoupling of the E_2 theory in [246].

Adding flavors: hypermultiplets

Let us now consider gauge theories with fundamental hypermultiplets. As for HW brane setups [280], semi-infinite D5 branes introduce flavors in the field theory described by the web [207]. Strings connecting these branes and the finite length ones hosting the gauge theory have CP factors associated with the fundamental representation of both gauge groups. Their lowest excitations are hypermultiplets. The distance of the semi-infinite branes from the gauge theory branes corresponds to a mass for the flavors. When F semi-infinite branes are considered, strings ending are in the fundamental representation of their gauge group, which reduces to a flavor symmetry from the five dimensional point of view.
Let us consider the simplest possible case, $SU(2)$ with one flavor. The theory has an $SO(2)_F \times U(1)_I$ global symmetry. The mass of the quark m represents the parameter associated with the flavor group $SO(2)_F$. The pq-web at the origin of the CB is shown in figure 5.11(a). The

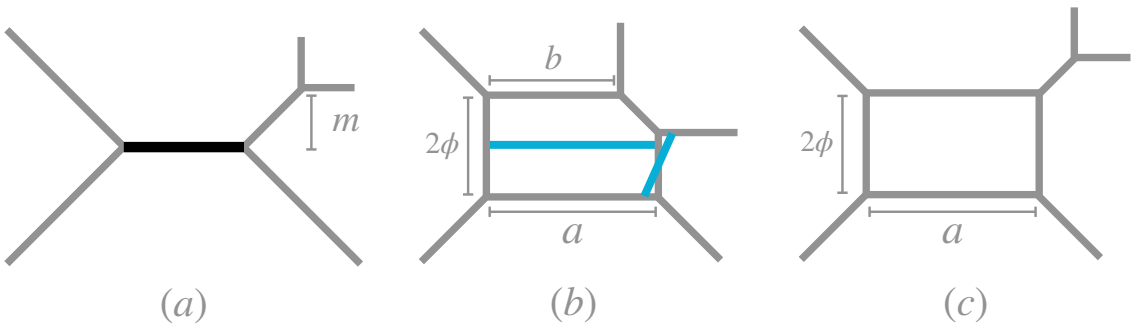

Figure 5.11: The pq-web at the origin of the CB with a mass m turned on (a). An electron and an instanton can be constructed as an F1 string between two D5 branes or a D1 between two NS5 branes respectively (b). No quark state can be constructed in terms of strings (c).

central charge reads

$$Z = n_e\phi + \frac{I}{g^2} + q^f m \tag{5.137}$$

where q^f is the charge of the state under the flavor group. On top of the usual W-boson ($n_e = 2, I = 0, q^f = 0$), also flavors are BPS states of the theory. At a generic point on the CB, a quark splits into two electrons of opposite charge $n_e = \pm 1$ with physical masses

$$M_\pm = |\phi \pm m|. \tag{5.138}$$

We can then ask how these quarks are described in the pq-web. First, notice that the bottom a and the upper b edges of the web are fixed to

$$a = 1/g^2 + 2\phi - m/2,\ b = 1/g^2 + \phi + m/2 \tag{5.139}$$

in order to reproduce the $SU(2)$+1 flavor prepotential for $|m| \leq \phi$.
If $|m| \leq \phi$, we see that one electron is realized in figure 5.11(b) as an F1 string connecting the gauge and the flavor branes. Its mass matches M_+, as expected from the BPS formula. On the other hand, the other quark cannot be constructed as a string in the pq-web, since no F1 string connects the upper gauge brane with the flavor one respecting supersymmetry[21], see figure 5.11(b).
When $m > \phi$ as in figure 5.11(d), both flavors cannot be realized as string junctions.
As we will see later, this problem is solved by introducing 7-branes in the pq-web.
From the web, we immediately recognize an instanton coming from a D1 stretching between two NS5 figure 5.11(b). Looking at its mass

$$M = \left|\frac{1}{g^2} + 2\phi - \frac{m}{2}\right| \tag{5.140}$$

we see that the instanton, of charges $n_e = 2, I = 1$, acquires also a flavor charge $q^f = -1/2$. As we will see later, this comes from mixing between flavor and instantonic symmetries.

Quivers

The semi-infinite D5s associated with the flavor symmetry can be made finite by ending them on additional junctions. In this way, the theory on their worldvolume becomes effective five dimensional, and the flavor symmetry is gauged. This realizes a five dimensional quiver theory, as happens for the $SU(2) \times SU(2)$ theory in figure 5.12(a). The original flavors become bi-fundamental fields arising from strings connecting D5 branes associated with the two different gauge groups. Let us focus, for simplicity, on the $SU(2) \times SU(2)$ case. From the viewpoint of the first node described by the D5 branes on the left, the branes of the other node introduce two flavors, associated with an $SO(4)$ flavor symmetry. However, this symmetry is partially gauged by the $SU(2)$ group of the second node. The two parameters associated with the $SO(4)$ symmetry are then the CB parameter of the second node ϕ_2 and the mass of the bifundamental field m_B, coming from separating vertically the two D5 stacks. The first deformation is shown in figure 5.12(b) and the latter in figure 5.12(c). So, to a single bifundamental corresponds an $SU(2)_{BF}$ symmetry at $m_B = 0$, which is broken to $U(1)_{BF}$ when $m_B \neq 0$.
As in the E_2 case, only for some values of the CB parameters ϕ_1, ϕ_2 bifundamentals are realized as strings of the pq-web, see figure 5.12(b). When this is so, to each endpoint of the string, it is associated an electric charge (n_e^1, n_e^2) for the Cartan of each node.
An additional flavor charge q^B is associated with the $U(1)_{BF}$ symmetry. The central charge then reads

$$Z = n_e^1\phi_1 + n_e^2\phi_2 + q_B m_B. \tag{5.141}$$

Finally, the perturbative prepotential of the quiver can be obtained by looking at the tensions

[21] This state can be realized as an instanton living in the $(1, -1)$ brane woldvolume [207].

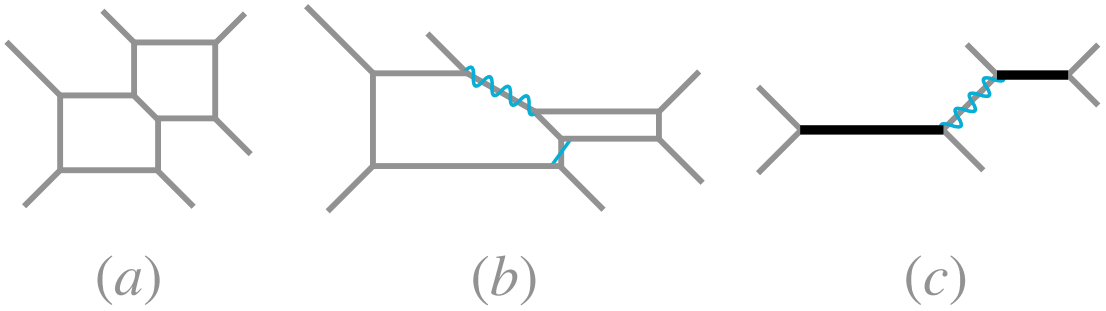

Figure 5.12: $SU(2) \times SU(2)$ quiver theory (a), its bifundamentals on the CB with no mass (b) and the bifundamental at the origin of the CB with $m_B \neq 0$ (c).

of the D3 branes wrapping the various faces of the brane web. For the brane web in figure 5.12, this reads

$$\mathcal{F} = \frac{1}{g_1^2}\phi_1^2 + \frac{1}{g_2^2}\phi_2^2 + \frac{4}{3}(\phi_1^3 + \phi_2^3) - \frac{1}{12}|\phi_1 \pm \phi_2 \pm m_B|^3. \tag{5.142}$$

5.5.6 pq-web with 7-branes

As we saw above, pq-web constructions are useful to understand many perturbative and non-perturbative properties of five dimensional gauge theories. However, some others are missing in this formulation.

First of all, from the pq-web, we can only extract the rank of the global symmetry group. So, the enhancement at the UV fixed point is in general difficult to analyze. In some cases, as for $SU(2)$ SYM in the configuration in figure 5.7(c), this can be inferred from the superposition of the external branes [207]. Alternatively, this can be seen looking at the degeneracy of the BPS states at a point of the CB of the SCFT [245]. However, these information are hard to extract in more general cases.

Moreover, all local deformations of these webs that we analyzed preserve $SU(2)_R$, since they act on the (x, y) plane. So, a parametrization of the Higgs branch of the theory in terms of local deformations is missing. All these problems are solved by the introduction of 7-branes.

A generic $[p, q]$ 7-brane transverse to the (x, y) plane preserves the same supercharges of the pq-web, see (5.112). Naively, 7-branes seem to play the same role performed by the D5 branes in the HW systems. In the latter constructions, D5 branes are introduced to add flavors to the theory. This is an alternative way with respect to introducing flavors via semi-infinite D3 branes, see figure 5.13(a), as we did in the previous section. Strings stretching between D3 brane and D5 brane describe a flavor in the three dimensional theory, as we can see in figure 5.13(b). The mass of the corresponding flavor is proportional to the distance between the D3 brane and the semi-infinite D3 (resp. the infinite D5) brane. The theory on the finite D3 brane is then $\mathcal{N} = 4$ $U(1)$ plus one flavor. The only physical parameter associated with the D5 in this theory is its distance from the D3, namely the mass of the flavor. So, when we move the D5

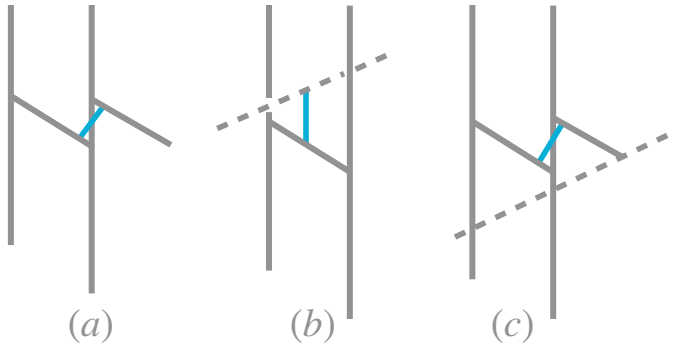

Figure 5.13: $U(1)$ gauge theory with one flavor with semi-infinite D3 branes (a), D5 brane (b) and after HW transition (c).

horizontally (say to the right) no parameter nor modulus changes. Moreover, we do not expect any change from the field theory point of view also when the D5 hits the NS5 branes on the right and moves towards it. Indeed, in the process an additional D3 brane is created [280] and emanates from the point where the D5 hit the NS5, see figure 5.13(c). The transition between the two configurations is denoted in the literature as Hanany-Witten (HW) transition. In this new framework, the flavor is now described by a string connecting the finite and the semi-infinite brane. No parameters in the theory depend on the length of the D3 brane stretching between the D5 and the NS5 (this is expected, since the theory on this brane is gapped). Then, the D5 can be pushed towards infinity, and we end up with the configuration figure 5.13(a).
What is the analog of this operation in the pq-web?
As in the HW case, we can naively add a D7 brane to the system to introduce a flavor: this comes from the string stretching between D5 branes and D7 in figure 5.14(a). We can then try

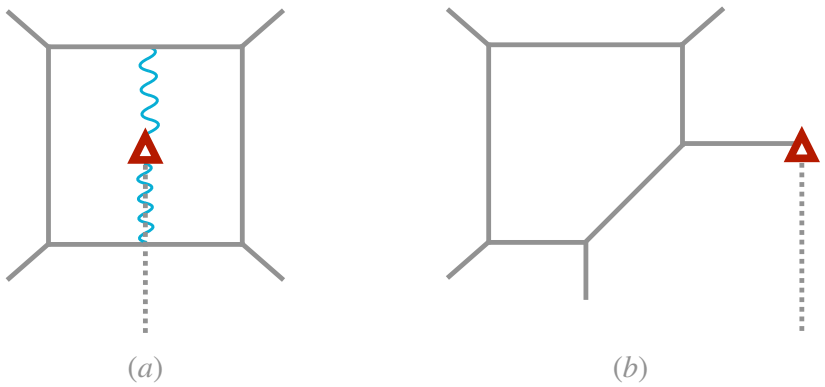

Figure 5.14: Brane creation in the E_1 case with a D7.

to perform the same operation, moving to the right the D7 brane and making it pass through the NS5. However, we encounter an obstacle: the operation needs to modify also the original pq-web, to preserve supersymmetry, see figure 5.14(b). This is related to the peculiar properties

of 7-branes, which will be the topic of the next section.

Properties of 7-branes

A 7-brane sources a non-trivial axio-dilaton background, being magnetically charged under it. This background introduces a branch cut going from infinity to the brane. The axio-dilaton is transformed crossing the cut counterclockwise by an $SL(2,\mathbb{Z})$ monodromy transformation

$$K_{p,q} = \begin{pmatrix} 1+pq & -p^2 \\ q^2 & 1-pq \end{pmatrix}. \tag{5.143}$$

Moreover, 7-branes introduce a non-trivial metric [273], which in complex coordinates $z = x+iy$ reads on the plane

$$ds^2 = \tau_2 \eta(\tau)^2 \bar{\eta}(\bar{\tau}) \prod_i (z-z_i)^{-1/12} (\bar{z}-\bar{z}_i)^{-1/12} dz d\bar{z} \tag{5.144}$$

where z_i defined the position of the i-th brane on the plane. BPS states then change passing the cut accordingly to the $SL(2,\mathbb{Z})$ monodromy (5.143). In particular, an (m,n) 5-brane passing counterclockwise the branch cut of a $[p,q]$ 7-brane transforms as

$$\begin{pmatrix} m \\ n \end{pmatrix} \to \begin{pmatrix} m' \\ n' \end{pmatrix} = K_{[p,q]} \begin{pmatrix} m \\ n \end{pmatrix}, \tag{5.145}$$

A generic (m,n) string passing the cut changes as $M_{p,q}$ as well [272]. Since a generic (r,s) string (resp. 5-brane) is oriented along a $(s,-r)$ (resp. (r,s)) direction in the (x,y) plane, the change of charges can be interpreted as a change of direction of the string (resp. brane) passing the cut.
On top of this change of direction, 5-branes do not follow any more straight geodesics, due to the non-trivial metric (5.144). The form of these geodesics is hard to determine in general, so, as it is usual in literature, sometimes we will keep (p,q) 5-branes as straight lines along (p,q) vectors, to identify them in the web, while in some other cases we will schematically indicate the geodesics followed by the 5-branes as some smooth curve on the (x,y) plane.
A 7-brane passing through a 5-branes leads to a generalized HW transition, where additional branes are created. More precisely, let us take an (m,n) 5-brane passing a cut of a $[p,q]$ 7-brane, as in figure 5.15. Before the transition, the 5-brane changes charges as it passes the cut, becoming a $K_{[p,q]}(m,n)$ 5-brane. After the transition, $(qm-pn)$ (p,q) 5-branes are created and connect the 5-brane to the 7-brane, as in figure 5.15. In this way, we performed an Hanany-Witten transition in the pq-web context. As similar transition happens for a $[p,q]$ 7-branes passing an (m,n) string [272].

In the previous analysis, we had the freedom of positioning the cut to lie vertically from the 7-branes down to infinity, since we were dealing with a single 7-brane. However, when we have multiple branes, we have multiple branch cuts. So, we have still the freedom of moving a branch cut until we hit the cut of another 7-brane. This happens when, for example, we want to exchange two 7-branes $X_{[p,q]}$ and $X_{[m,n]}$, as figure 5.16(b). Making the left brane passing the right

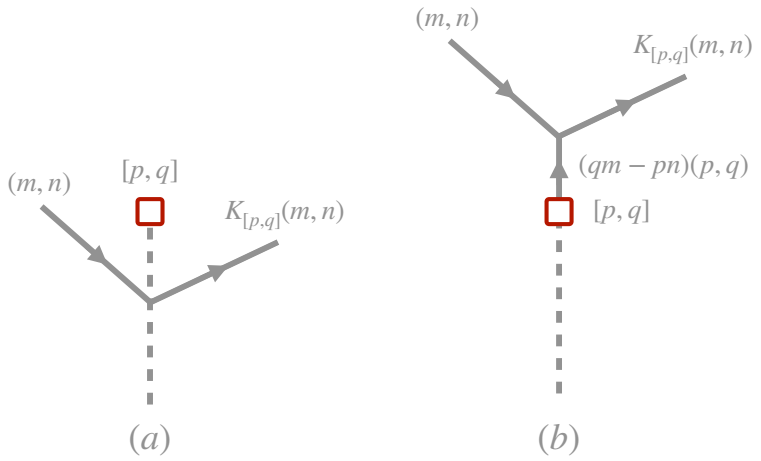

Figure 5.15: A (m,n) brane passing the branch cut of a $[p,q]$ 7-branes (a) and after HW transition (b).

one, the former becomes a $X_{[p,q]+(pn-qm)[m,n]}$ in order to conserve the total monodromy

$$X_{[p,q]}X_{[m,n]} = X_{[m,n]}X_{[p,q]+(pn-qm)[m,n]}. \tag{5.146}$$

The resulting system of 7-branes is then shown in figure 5.16(c) and it is equivalent to the initial one in figure 5.16(a).
Similarly, if we exchange the two branes by moving the right one on the left, the right brane becomes $X_{[m,n]+(pn-qm)[p,q]}$.

5-branes ending on 7-branes

Having specified the properties of 7-branes, we can introduce them into the pq-web.
Let us start by adding D7 branes in the E_1 pq-web, figure 5.14(a). As we mentioned, a D7 introduces a flavor: on the CB, the two corresponding electrons are strings stretching between the D7 and the two D5 branes. The distance between the D7 and the D5s is associated with the mass m of the flavor. We already see a large improvement from the original setup: both flavors can be constructed in terms of string states. The horizontal position of the D7, as for the D5s in the HW case, is not a parameter nor a modulus of the theory, since the only parameter associated with the flavor comes from the vertical distance from the D5 branes. We can then move the D7 horizontally to the right and cross the NS5 branes. The crossing produces, via HW effect, a single D5 brane[22] connecting the NS5 with the D7. The branch cut can be now moved to avoid intersection with the pq-web and the D7 can be pushed to infinity. This reduces the web to the $SU(2)$ plus one flavor one, see figure 5.14(b). As in the HW setup, now electrons are described by strings connecting the semi-infinite and the finite D5s (or instantons of the $(1,-1)$ brane).

[22]Moreover, moving the branch cut, the junction is modified accordingly to the rules in (5.146).

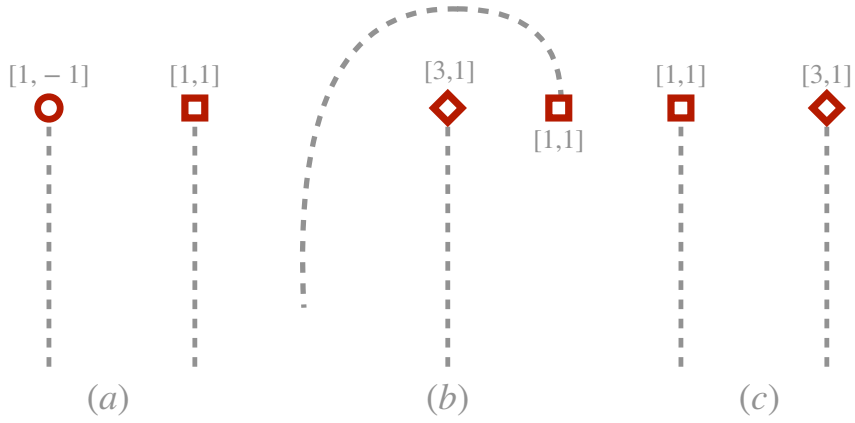

Figure 5.16: Exchange of a $[1,-1]$ and a $[1,1]$ brane.

Similarly, a (p,q) 5-branes can end[23] on a $[p,q]$ 7-brane. We can then make all 5-branes of the system finite by ending them on the appropriate 7-branes, see figure 5.17. As in the D7 case,

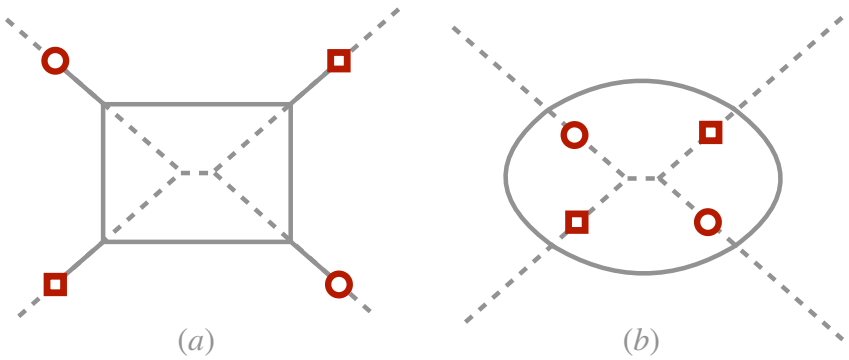

Figure 5.17: E_1 theory where the semi-infinite 5-branes are replaced by segments (a). E_1 theory after the D7s are shifted inside the web, creating a brane loop (b).

moving the 7-branes along the 5-prong does not change any parameter or modulus of the theory. Then, adding 7-branes or not is irrelevant from the field theory point of view. Of course, due to their branch cuts and the non-trivial metric, 7-branes change instead the pq-web. These effects, in many cases, can be neglected when 7-branes are very far away from the web.[24]
However, when the 7-branes are close to the web, the 5-branes follow curved geodesics, as shown in figure 5.17(b) and close into a brane loop [285].

[23] Due to charge conservation, (p,q) 5-branes are the only branes endable on $[p,q]$ 7-branes [211].
[24] This happens when their distance from the faces of the web is larger than any physical scale of the system.

Global symmetry

Previously, we saw how $SU(2)$ theories with $F < 8$ flavors admit UV fixed points with enhanced global symmetry. This enhancement was first observed in type I' constructions [145], and calculations from instantonic zero modes [208] and the superconformal index [247–249] gave independent evidence of this enhancement and revealed, in addition, a plethora of theories admitting fixed points with enhanced global symmetry.
The main advantage of adding 7-branes comes from the possibility of making the global symmetry of the five dimensional theory manifest. The corresponding algebra comes from the algebra of 7-branes. These algebras were intensively studied in [272–277] and in this section, we review only some basics properties that can be useful in the brane web context.

First of all, we remind that quark states were constructed in the pq-web alternatively as strings connecting two D5 branes (when this parametrization is possible) and as strings connecting a D5 to the D7. The same behavior applies to any BPS state: a state can be described, due to HW brane creation, as a 5-5 or a 5-7 string junction. For example, we can consider the F1 string connecting two D5 branes in the $SU(2)$ theory, see figure 5.18(a). This corresponds to the massive W boson. We can now continuously move[25] it as in figure 5.18(b). When the F1

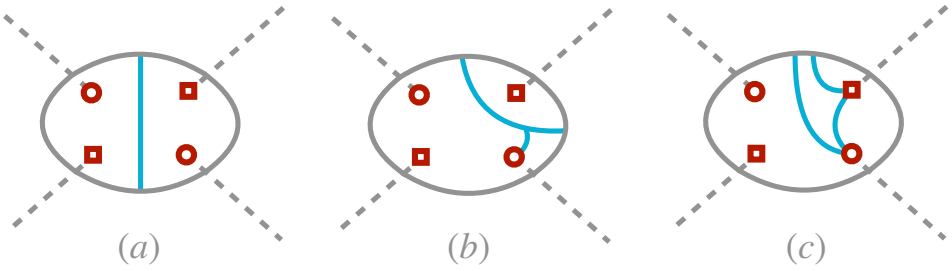

Figure 5.18: W boson states changing passing the 7-brane cut.

passes the cut of the $(1,-1)$ brane, additional strings are created via the HW effect, see figure 5.18(b). Passing also the $(1,1)$ cut, we arrive to figure 5.18(c). In this configuration, the W boson is represented by a 5-7 string junction. The same result holds for any BPS state [211]. These string junctions fall then into representations of the 7-brane algebra. These were studied in [277] and the properties of corresponding string junctions were analyzed in [276]. The main results of the analysis are listed below.

- A generic string junction $\mathbf{J}$ is uniquely identified by the number of prongs ending on the various 7-branes (the invariant charges of the junction [273]) and by its (p,q) charges. On the space of junctions, we can introduce a scalar product between two networks $\mathbf{J}$ and $\mathbf{J}'$,

[25] This operation does not change the corresponding state of the field theory, see [211].

defined as the intersection form $(\mathbf{J}, \mathbf{J}')$. This form is uniquely determined by the invariant charges and the (p, q) charges of the networks, together with the type of 7-branes of the system. The corresponding square norm for the junction $\mathbf{J}$, namely its self-intersection, is denoted as $(\mathbf{J}, \mathbf{J}) \equiv \mathbf{J}^2$;

- A necessary condition for a generic junction $\mathbf{J}$ to be BPS is that its self-intersection satisfies the bound
$$\mathbf{J}^2 \geq -2 + \gcd(p, q). \tag{5.147}$$
The corresponding state in the five dimensional theory is then 1/2 BPS;

- BPS junctions $\mathbf{J}$ with no external charges saturating the previous bound $\mathbf{J}^2 = -2$ belong to the adjoint representation of the algebra of 7-branes. Their mutual intersection form determines the Cartan matrix of the algebra of the system of 7-branes;

- BPS junctions $\mathbf{J}$ with external charges (p, q) belong to some representation R of the 7-branes algebra. This representation is completely determined by the invariant and the (p, q) charges.

Thanks to the previous results, it is possible to prove [211] that the algebra of 7-branes associated with a generic pq-web is at least an affine algebra[26], as opposed to global symmetries of these theories that are associated with finite Lie algebras. However, it can be shown that all BPS states of the five dimensional theory do not see the affine structure and fall into representations of the corresponding finite subalgebra. So, looking at the 7-brane system, we can read off the global symmetry of the five dimensional theory and the representations of the BPS states!
Let us consider, for example, the E_1 theory. The 7-brane system is composed of two $[1, -1]$ and two $[1, 1]$ branes. In the literature, these are labeled as $\mathbf{B}$ and $\mathbf{C}$ branes respectively. The total monodromy of the system is $\mathbf{BCBC}$. Its affine algebra is $\widehat{\mathfrak{su}(2)} \equiv \hat{E}_1$ [276] and its finite subalgebra is nothing but $\mathfrak{su}(2)$, as expected for the E_1 theory!
All BPS states fall into representations of the global symmetry group. For example, one can show that the W-boson and the instanton of the $SU(2)$ theory form a doublet of $SU(2)_I$!
Although this seems surprising, these states are actually degenerate on the CB of the E_1 theory, since their masses are both equal to 2ϕ. Moreover, they are both vector multiplets and they are exchanged by S-duality at the fixed point, see figure 5.19.

The states become non-degenerate only when the gauge coupling is turned on. This breaks $SU(2)_I \to U(1)_{q_I}$. However, the masses of the BPS states are not split as expected for a $SU(2)_I$ doublet. This is due to the mixing phenomenon: the Cartan $U(1)_{q_I}$ associated with the global symmetry group is not the instantonic symmetry of the gauge symmetry $U(1)_I$. In particular, the charge q_I associated with the former is related to the instantonic charge I associated with the latter as
$$I = \frac{1}{2}\left(\frac{n_e}{2} + q_I\right) \tag{5.148}$$
with n_e the electric charge of the state.
A similar mixing happens for $SU(2)$ with one flavor. All BPS states fall into representations

[26] For example, the 7-brane system of the pq-web of $SU(2)$ with 8 flavors is a non Kac-Moody loop algebra [211].

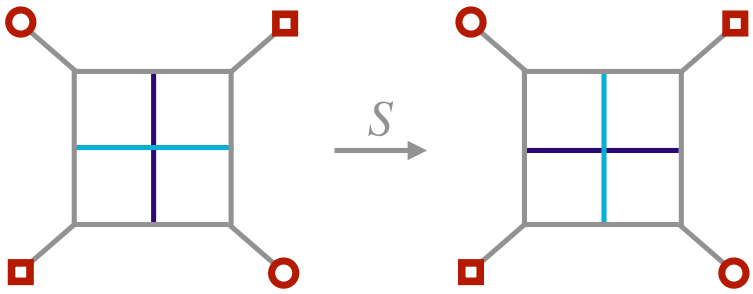

Figure 5.19: W boson (dark blue) and instanton I (light blue) exchanged by S-duality.

under the global symmetry $SU(2)_I \times SO(2)_F$ at the fixed point. Also in this case, however, the Cartan of $SU(2)_I$ differs from the $U(1)_I$ instantonic symmetry as

$$q_I = \frac{7}{4}I - \frac{n_e}{2} - \frac{q^f}{2} \tag{5.149}$$

The mixing involves also the UV flavor symmetry $U(1)_{Q_f}$, whose charge Q_f is related to the charge q_f of the IR symmetry $U(1)_F$ as $Q_f = q^f + I/2$.

Although string junctions fall into representations of $SU(2)_I$, we know that the global symmetry is broken at weak coupling. We can then ask how the enhancement can be seen from the 7-branes viewpoint.
As mentioned above, moving 7-branes along 5-prongs does not change any parameter (or modulus) of the gauge theory. However, at weak coupling branes of the same type **B** or **C** cannot meet at the same point of the (x, y) plane, since their minimal distance equals the inverse gauge coupling squared, see figure 5.20(a). At infinite coupling, instead, branes of the same type, for example, the **C**s, can be superimposed at the same point, as in figure 5.20(b). The string connecting the **C** (resp. **B**) branes becomes massless at this point, leading to a gauge symmetry enhancement on the worldvolume of the 7-branes. This is nothing but the realization of the $SU(2)_I$ symmetry enhancement since the string that becomes massless is associated with the root of the finite algebra of 7-branes.
Note that the enhancement appears only when we superimpose a couple of **B** or **C** branes. Indeed, the **BCC** system of brane is non-collapsible [286], so the associated branes cannot be superimposed at the same point. Then, once the **C** (resp. **B**) branes are placed in the middle of the face, the other branes must remain at a finite distance due to non-collapsibility. The symmetry then enhances at most to $SU(2)_I$.

The same mechanism is responsible for the global symmetry enhancement of the E_{F+1} theories for $F < 7$ at the corresponding fixed point.
Note that, adding F flavors to the system, the axio-dilaton in presence of the corresponding

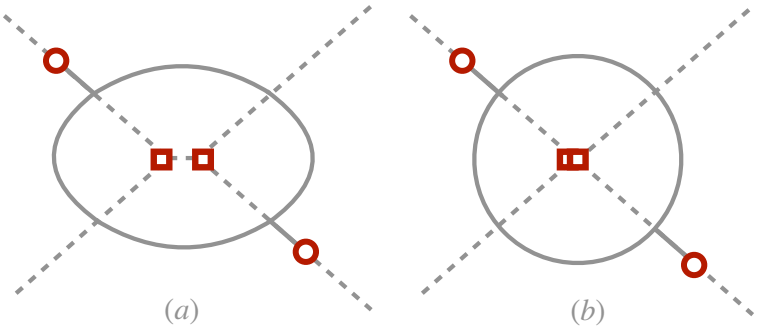

Figure 5.20: **C** branes at minimal distance $1/g^2$ at weak (a) and strong (b) coupling.

monodromy reads

$$\tau(z) = \frac{i}{2\pi}(8-F)\log(z) + \tau_0 \tag{5.150}$$

where τ_0 is a constant. So the axio-dilaton and the metric (which is proportional to its imaginary part) remain positive definite if and only if $F < 8$. If $F > 8$, the metric becomes negative, leading to inconsistency. This explains why for $F > 8$ we cannot have UV fixed points. If $F = 8$, the metric trivializes, and the corresponding algebra of 7-branes becomes the loop algebra $\hat{E}_9$. Both these aspects are related to the six dimensional nature of the UV completion of $SU(2)$ theory with $F = 8$ [208, 287].

Flow past infinite coupling

In the previous section, we saw how we can infer symmetry enhancement from 7-branes. In particular, the fixed point of $SU(2)$ SYM can be reached by tuning to zero the inverse gauge coupling squared of the gauge theory. To this parameter, it is associated with the mutual position between some of the external branes (for example, this was the length of the D5 branes in the pure $SU(2)$ case). In field theory, this parameter has to be positive, to have a well-defined metric at the origin of the CB. However, in the brane web, this can take any real value. We can then ask what happens from the field theory perspective when we deform the pq-web past infinite coupling.

Let us consider again the $SU(2)$ theory and the corresponding web, figure 5.21. The gauge theory lives on the parallel D5 branes. Their distance is proportional to the CB parameter and their length is proportional to the inverse gauge coupling squared. However, also the parallel NS5 branes host an $\widehat{SU(2)}$ gauge theory at a point of the CB. This has a CB parameter $2\hat{\phi}$ proportional to the distance between the two NS5 branes $2\hat{\phi} \equiv 2\phi + \frac{1}{g^2}$ and a gauge coupling $\frac{1}{\hat{g}^2}$ proportional to the difference between their length and the CB parameter, namely $\frac{1}{\hat{g}^2} \equiv -\frac{1}{g^2}$. Surely, if $1/g^2 > 0$, the NS5 gauge theory is not a valid description, since they have negative coupling. In this case, only the D5 brane theory is well-defined. However, when we start approaching the fixed point the coupling of both theories goes to zero and both descriptions become strongly coupled. The face of the web reduces to a square, describing the CB of the E_1 theory, see figure 5.21(c). Passing this point, we can keep squashing the web vertically. In

this way, the length of the D5 branes $\frac{1}{g^2} + 2\phi$ becomes smaller than the CB parameter 2ϕ, the gauge coupling $\frac{1}{g^2}$ becomes negative and the description in terms of D5 branes is no more valid. However, now, the description of the NS5 branes is well-defined, having a positive gauge coupling. Moreover, by keeping squashing we can make the NS5 coincide, see figure 5.21(d). Their gauge group enhances to $\widehat{SU(2)}$. The NS5 branes describe then the five dimensional

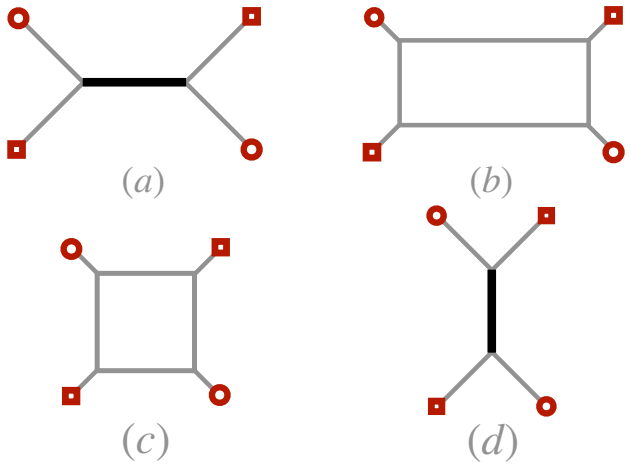

Figure 5.21: Continuation past infinity of the $SU(2)$ theory.

physics after continuation past infinite coupling. BPS states are mapped between one another within the two descriptions: W-bosons for the D5 brane theory become instantons of the NS5 theory and vice-versa. This mapping is realized precisely by S-duality: the gauge theory on the NS5 branes is S-dual to the gauge theory description of two D5 branes and the parameters $(1/\hat{g}^2, \hat{\phi})$ of the former are mapped by S-duality to the parameters $(1/g^2, \phi)$ of the latter as

$$\frac{1}{\hat{g}^2} = -\frac{1}{g^2}, \quad \hat{\phi} = \phi + \frac{1}{2g^2} \tag{5.151}$$

In conclusion, away from the FP, there is only one gauge theory interpretation with a positive coupling, while the other has no physical meaning. Deforming the FP by the parameter $1/g^2$, we flow to the first or the second description, depending on the sign of $\frac{1}{g^2}$.
This is an example of UV duality: two theories share the same UV fixed point and are related by a past infinite coupling limit. Moreover, being $1/g^2$ related to the VEV of the scalar field of the $SU(2)_I$ global symmetry multiplet, the two descriptions are mapped one another by the Weyl group of $SU(2)$, which sends $\frac{1}{g^2} \to -\frac{1}{g^2}$. This is the reason why $SU(2)$ gauge theory is mapped into another $SU(2)$ theory under S-duality.[27]

[27]This can be also seen from the discussion in [288] regarding fiber-base duality. For $SU(2)$ with $F \leq 7$, the flavor symmetry $SO(2F)$ together with the fiber-base duality generates the E_{F+1} symmetry. In more general cases, however, fiber-base duality does not belong to the Weyl group of the enhanced global symmetry and it does not act as a self-duality for the theory.

Dualities

UV dualities are rather common in five dimensions. These relations can hold among different gauge theories, see [247,256] or between gauge theories and non-Lagrangian ones [207]. In many cases, the two IR descriptions have different global symmetries. However, at the fixed point, the global symmetry can enhance in both descriptions and matches across the duality. We can think about this process starting from the SCFT in the UV: we can leave the fixed point turning on a SUSY preserving flavor current deformation. In doing so, we break the global symmetries of the SCFT to a subgroup. As a consequence, deforming in different ways, we arrive at different IR phases preserving (potentially) different subgroups of the UV flavor symmetry. So, from the point of view of the IR theories, the global symmetry enhances flowing backward along the RG flow.

In general, we can establish a map among parameters and moduli of the two descriptions, and, at least when we are sufficiently close to the fixed point, also the BPS spectrum matches.

Many of these dualities, obtained from the pq-web, can be tested via superconformal index calculations, as was done in [247, 256]. In particular, from the IR phases, we can infer the symmetry enhancement by looking at BPS protected operators. Indeed, as we saw in the examples treated above, instantonic operators can provide the broken currents in the IR necessary to enhance the global symmetry in the UV [208], and can parametrize the additional directions coming from the enhancement of the Higgs branch [179]. So, studying these operators in the IR yields important information about the UV physics of the theory.

We can also invert the logic. Thanks to UV dualities, we can infer the existence of fixed points and symmetry enhancement for some gauge theory descriptions. In this way, we can see that many theories, which fail the convexity condition, admit a fixed point, being UV dual to theories with convex prepotentials. This was the case for quiver theories [256].

We finish this section by reviewing an example of UV duality, namely the correspondence between the $+_{M,N}$ and $+_{N,M}$ theories [207].

The $+_{M,N}$ fixed point consists of N NS5 and M D5 branes intersecting at a single point. We can flow away from the fixed point separating the NS5 branes, as in figure 5.22. The field theory lives on the finite D5 branes of the web and it is an $SU(M)^{N-1}$ quiver theory. On top of the $N-2$ bifundamentals $(\mathbf{M},\mathbf{M})$ stretching between each pair of adjacent gauge groups, we have a pair of M fundamentals charged under the first and the last nodes of the quiver, see figure 5.23. The global symmetry of the quiver is $SU(M)^2 \times U(1)_F^2 \times U(1)_B^{N-2} \times U(1)_I^{N-1}$. This is expected to enhance at the fixed point to $SU(N)^2 \times SU(M)^2 \times U(1)$, since the N (resp. M) D5 (resp. NS5) branes coincide at the fixed point.[28]

Alternatively, we can stretch the web vertically. All gauge couplings of the quiver (5.23) are continued past infinity, so the field theory now lives on the finite NS5 branes. This can be seen by S-dualizing the web, obtaining the quiver theory associated with the $+_{N,M}$ theory. The quiver is $SU(N)^{M-1}$ with $M-2$ bifundamentals $(\mathbf{N},\mathbf{N})$ and N hypermultiplets charged under the first and last node, see figure 5.24. The global symmetry is $SU(N)^2 \times U(1)_F^2 \times U(1)_B^{M-2} \times U(1)_I^{M-1}$. However, at the fixed point the symmetry enhances again to $SU(N)^2 \times SU(M)^2 \times U(1)$, match-

[28] Actually when N or M is small, the global symmetry gets enhanced to a larger group. For example, if $N=2$, the symmetry enhances to $SU(2M) \times SU(2)^2$ [288].

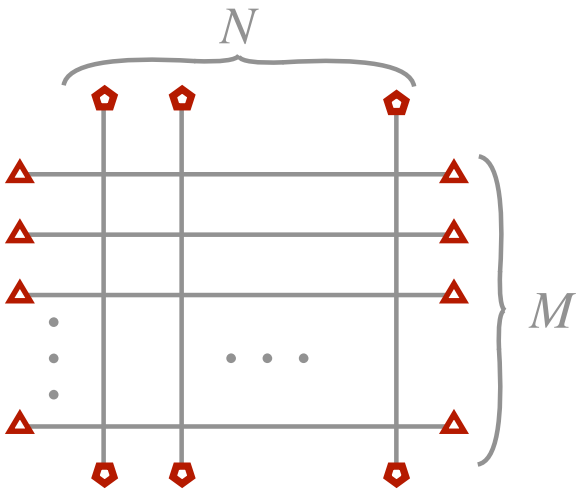

Figure 5.22: The brane web of $+_{M,N}$ theory.

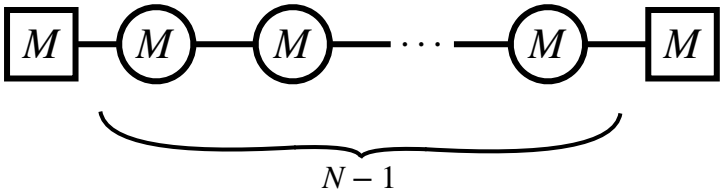

Figure 5.23: Quiver of $+_{M,N}$ theory.

ing across the duality.
The dimension of the CB matches across the duality [207] as well as the number of parameters. Indeed, gauge couplings of one theory are mapped to masses of the other and vice-versa. The same happens for the BPS states of the two theories [256].
Dualities were also employed recently to calculate the complete prepotentials for quiver theories [246] and were also related to the lifting of known 4d IR dualities to five dimensions [4].

Higgs branches

Finally, let us comment on the parametrization of the Higgs branch in presence of 7-branes. As we mentioned earlier, in absence of 7-branes, all local deformations lie on the (x, y) plane and are associated with the CB of the theory.
On the other hand, 7-branes are localized on the plane and extended in its transverse directions. The 789 directions, which are common Dirichlet directions for all the 5-branes of the web, are Neumann directions for the 7-branes. So, when a finite 5-brane is suspended between two 7-branes, we can detach it from the web and slide it along the 789 directions, respecting charge conservation and supersymmetry. The dynamics at low-energies of the corresponding five brane

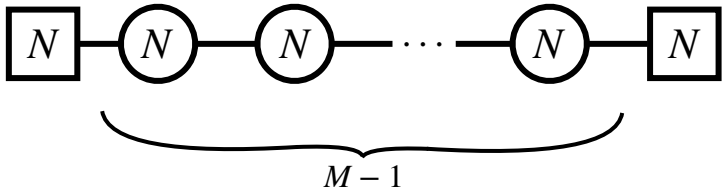

Figure 5.24: Quiver of $+_{N,M}$ theory.

is described by a theory of a hypermultiplet. The position of the D5 suspended between the two D7 is parametrized by three scalar fields in the adjoint representation of the R-symmetry acting in the 789 space. The A_6 component of the gauge field survives boundary conditions [289] and adds up to form the hypermultiplet. So, sliding the D5 along the D7, we give a VEV to the hypermultiplet and this parametrizes one direction of the HB. This parallels the HB description in the HW setups, where a D3 suspended among two D5s parametrizes a quaternionic direction of the HB [280].
The same reasoning applies whenever we have a (p, q) branes suspended between two $[p, q]$ 7-branes or more generally, whenever our system possesses a subweb that can be detached from the rest of the web [187, 207]. Then, the dimension of the HB equals the number of possible detachable webs, namely the number of zero-sum subsets of (p, q) labels of the external legs.

In the weak coupling limit, when we have a gauge theory description, the Higgs branch is parametrized by VEVs of the gauge invariant operators of the theory. Take for example the $SU(N)$ theories with n_L flavors on the left of the web and n_R on the right, see figure 5.25(a). To enter the Higgs branch, we can give a VEV to a meson or a baryon. To do so, we need to tune some parameters to have massless quarks to form the gauge-invariants. In the pq-web, this is equivalent to performing a series of global and local deformations to obtain a brane detachable from the main web. Examples of this kind are shown in figure 5.25(b) and (c). In the first case, the gauge-invariant operator parametrizing the HB is a meson, in the second it is a baryon [207]. The D5 (resp. NS5) brane is now detachable and parametrizes a quaternionic direction of the mesonic (resp. baryonic) branch.
In the process, part of the gauge group is broken by the VEV of the operator, as can be seen from the smaller number of faces of the remaining web. Moreover, the global symmetry is spontaneously broken, as well as the original R-symmetry. Both act on the HB moduli space as isometries [179]. However, to preserve supersymmetry, at each point of the HB an emergent $SU(2)_{R'}$ symmetry, coming from the subgroup of $SU(2)_R$ and the global symmetry itself, is preserved.
In presence of multiple 5-branes ending on some common 7-branes, things are more subtle. Indeed, it is not always possible to detach a subweb that is apparently detachable, see figure 5.26(a). The obstruction to this operation is known as the s-rule [280, 283, 289]. The rule was first analyzed in [280] and was later found to be associated with the Pauli exclusion princi-

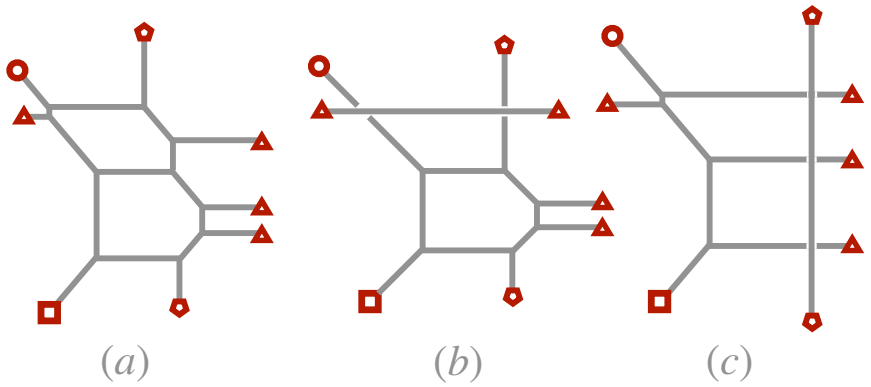

Figure 5.25: Higgs branch. We can start from (a) and pull up the top left and right flavor branes, make them coincide with the top finite D5 brane, and arrive at the web (b). The horizontal line is detachable and parametrizes one direction of the mesonic branch. The same happens for (c) for the baryonic branch.

ple [290]. In five dimensions, the s-rule states that the number of (p, q) 5-branes that can be suspended between a $[p, q]$ 7-branes and a (r, s) 5-brane must be smaller or equal than $|ps - qr|$. If this condition is not fulfilled, we break supersymmetry. This excludes, for example, the possibility of detaching the D5 segment in figure 5.26.

At the fixed point, the HB enhancement corresponds to a larger number of detachable webs

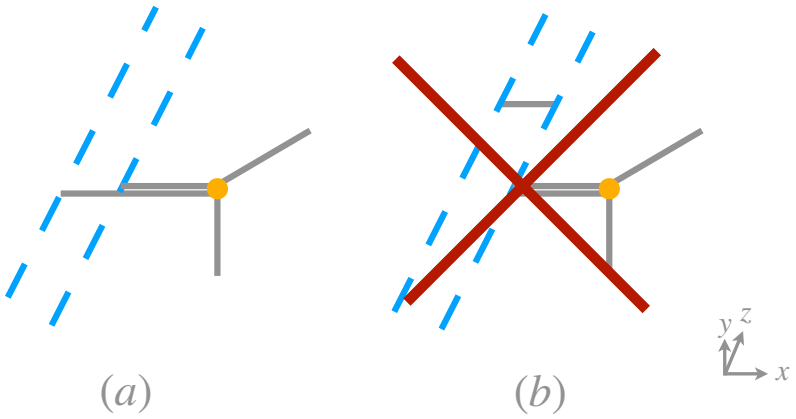

Figure 5.26: Non-detachable web.

with respect to the weak coupling brane web. There is a huge literature regarding the study of the HB at infinite coupling [186–205] which is mainly related to the possibility of describing these as the quantum Coulomb branches of some $\mathcal{N} = 4$ three dimensional theory, via the so-called magnetic quiver program. These techniques are behind the scope of this thesis and so we will not discuss them in detail. In this last part of the section, we only limit ourselves to studying the HB of the E_1 theory from its pq-web diagram.

At weak coupling, we know that $SU(2)$ SYM possesses a zero dimensional HB, since the theory has no hypermultiplets. At the fixed point, the HB is known to enhance to $\mathbb{C}^2/\mathbb{Z}_2$. This is visible from the E_1 pq-web in figure 5.27(a). At the fixed point, the $(1,1)$ brane between the $[1,1]$

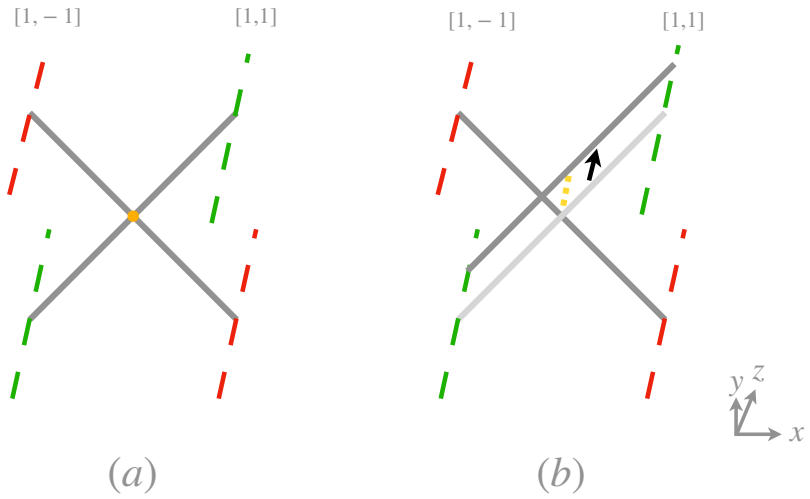

Figure 5.27: Higgs branch of the E_1 theory.

7-branes can detach and move in the 789 space. This parametrizes the single quaternionic HB direction at infinite coupling. The existence of this branch can be confirmed by analyzing the contribution of instantons to the chiral ring [179, 208]. From the pq-web, we can also construct the corresponding magnetic quiver [187] which is nothing but $U(1)$ plus two flavors.
In field theory terms, the HB of the E_1 theory is parametrized by a current $\Phi_{(ij)}$ in the adjoint of $SU(2)_R$ obeying the condition

$$(\Phi_{(12)})^2 = \Phi_{(11)}\Phi_{(22)}. \tag{5.152}$$

This is chargeless under the Cartan of $SU(2)_I$ and it can be identified as the lowest component of the flavor current multiplet of the E_1 theory $\mu^{(12)}_{(ij)}$. This shows the non-perturbative nature of this HB, being this described by a current multiplet of an instantonic symmetry.

5.6 Complete prepotential

In the previous sections, we saw how five dimensional gauge theories are highly constrained by supersymmetry and how their perturbative dynamics on the CB is encoded in their prepotential. Originally [149] it was thought that theories could be classified by the convexity of their prepotential, which was supposed to give a necessary (but not sufficient) condition for the existence of UV fixed points. However, string constructions showed that many theories with non-convex prepotentials possess UV completions in five dimensions, being often UV dual to field theories with convex prepotentials. So, the convexity of the IMS prepotential (5.69) does

not give us a good criterion to classify five dimensional theories. Moreover, this is also blind to symmetry enhancement, being this a purely non-perturbative effect. This suggests the necessity of generalizing the description of five dimensional gauge theories to include these properties.
In this section, we first review the modern criterion to classify five dimensional gauge theories admitting a UV fixed point. Then, we introduce the complete prepotential, which generalizes the IMS formula in (5.69) to include non-perturbative effects. Armed with this toolkit, we conclude this discussion with some interesting examples.

5.6.1 New criterion for UV fixed points

As we reviewed in section 5.4.3, particles contribute to the prepotential via concave terms. Depending on the sign of their mass, the CB is divided into subchambers and the prepotential takes different expressions in each subchamber. However, the prepotential depends only on masses of perturbative particles, through its cubic terms. These are only a subset of the BPS states of the theory. In particular, non-perturbative BPS particles are expected to modify the physics of the theory when they become light.
Let us consider the central charge of a generic gauge theory

$$Z_e = \sum_a n_e^a \phi_a + \sum I_i/g_i^2, \;\; Z_m = \sum_a n_m^a \phi_{Da} \tag{5.153}$$

where $\phi_{Da} = \partial_a \mathcal{F}(\phi)$ and $1/g_i^2$ the gauge coupling associated with the i-th gauge group. Tensions of monopole strings must be positive and we expect r of them to be independent

$$T_i(\phi) \equiv \partial_a \mathcal{F}(\phi) = \phi_{D,\,a}, \;\; a = 1, ..., r. \tag{5.154}$$

Non-perturbative objects become massless on the CB whenever the central charge (5.153) is zero. When this happens, the perturbative theory described by the prepotential breaks down and a new description is mandatory. How we can extend the description past this point?
To answer this question, let us start by considering, for definiteness, the $SU(2)_\pi \times SU(2)_\pi$ quiver, see figure 5.28(a). The prepotential of this quiver is reported in (5.155). This theory does not fulfill the convexity requirement. However, this is S-dual to $SU(3)$ with two flavors [247], which admits a UV fixed point, figure 5.28(b). This tells us that the perturbative description of the prepotential of the quiver fails at some point of the CB. After this value, a non-perturbative description is needed, and the theory is UV completed by the fixed point of $SU(3) + 2F$. This expectation is actually fulfilled if we look at the prepotential of the quiver

$$\mathcal{F}(\phi) = \frac{1}{g_1^2}\phi_1^2 + \frac{1}{6}(8\phi_1^3 + 8\phi_2^3 - (\phi_1 + \phi_2)^3 - (\phi_1 - \phi_2)^3) + \frac{1}{g_2^2}\phi_2^2. \tag{5.155}$$

Here we restrict the analysis to the chamber $\phi_1 > \phi_2 > 0$ and we have set to zero the bifundamental mass m_B. Looking at (5.155), we see that the metric becomes negative near $\phi_2 \sim 0.255\phi_1$ for $1/g_{1,2}^2 \ll 1$. However, before reaching this point, the monopole strings with tension

$$T_1 = 2\phi_2/g_2^2 - 2\phi_1\phi_2 + 4\phi_2^2 \tag{5.156}$$

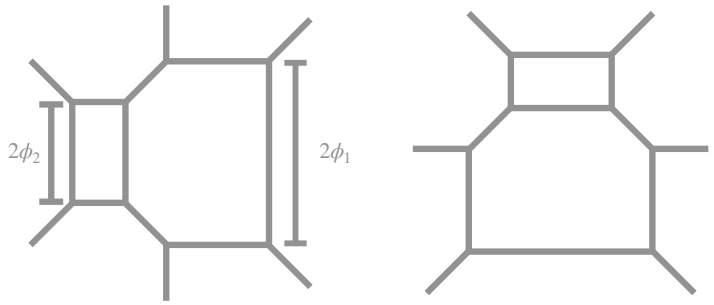

Figure 5.28: $SU(2)_\pi \times SU(2)_\pi$ quiver gauge theory (a) and its S-dual $SU(3) + 2F$ in (b).

associated with the first gauge group becomes massless at $\phi_2 \sim \phi_1/2$ for $1/g^2_{1,2} \ll 1$. At this point, the perturbative dynamics breaks down and we cannot trust anymore the perturbative prepotential. This is only valid in a subwedge $\phi_1 > \phi_2 > \phi_1/2$ of the chamber $\phi_1 > \phi_2 > 0$. So the prepotential is already non-trustable before reaching the non-convexity point!
We can then ask if, including this non-perturbative effect, we can describe completely the CB of the quiver theory. This is indeed the case. When we pass the massless point, the new light states are taken into account by the description through the $SU(3)$+2F prepotential!
In this other description, the point at which the string becomes tensionless coincides with a boundary of the Weyl chamber of the $SU(3)$ gauge theory, at which a non-Abelian $SU(2)$ subgroup is preserved. As a consequence, the CB past this point is merely a Weyl copy of the original CB wedge.

The previous analysis suggests a new criterion to classify five dimensional theories. Looking at the positivity of the metric on the entire CB is too stringent: some of the regions of this "naive" CB can be impossible to describe using the perturbative prepotential. However, if no non-perturbative state becomes massless on the CB, the prepotential of well-behaved theories (namely, theories that admit a fixed point) needs to be convex. The subregion of the CB where all non-perturbative BPS states have a positive mass/tension is denoted as the physical CB $\mathcal{C}_{phys}$ of the theory and it is defined as

$$\mathcal{C}_{phys} = \{\phi \in \mathcal{C} |\, T(\phi) > 0, \;\; M_I^2(\phi) > 0\} \tag{5.157}$$

where M_I and T are respectively any possible masses and tensions of non-perturbative BPS states. The metric should be then positive definite along the entire physical CB to reach a UV fixed point. Indeed, when this condition holds we can safely take the limit $1/g^2 \to 0$ and reach the fixed point by tuning $\phi = 0$.
The type of hyperplanes that enclose the physical CB (and so the corresponding BPS states that becomes massless) can be classified by looking at the CY realization of these theories [218]. These are nothing but boundaries of Weyl chambers (so, past this plane, the theory is a Weyl copy of the original one), superconformal fixed points (where we have tensionless monopole

strings interacting with massless electric particles), and flops (where BPS particles become massless). At these points, their central charges vanish. In particular, it is sufficient to focus on the Coulomb branch of the SCFT, turning off all mass parameters. Since the charges of the states n_e^a and n_m^a are quantized, the hyperplanes are identified only by the vanishing of rational linear combinations of the mass parameters ϕ_a, namely $\sum n_e^a \phi_a = 0$ with $n_e^a \in \mathbb{Q}$ (and similarly for the monopole strings). This hyperplane is denoted as a rational boundary. The physical CB reads then

$$\mathcal{C}_{phys} = \mathcal{C}_{T\geq 0} = \{\phi \in \mathcal{C}\ T(\phi) \geq 0\}, \text{ and } \partial\mathcal{C}_{phys}, \text{ is rational.} \tag{5.158}$$

The existence of a physical CB identified by (5.158) is conjectured to be a necessary (although not sufficient) condition for the existence of a non-trivial fixed point [218, 219]. However, verifying the existence of a physical CB can be quite involved for higher rank theories. The classification of five dimensional theories (at rank smaller or equal than two) was obtained by looking for theories fulfilling one of the following three requirements

- If the metric is positive somewhere in the naive CB $\mathcal{C}$ (possibly including unphysical regions), then there exists a physical CB.
- If $T(\phi) > 0$ in some region $\mathcal{C}_{T>0} \subseteq \mathcal{C}$, the metric is positive in this region.
- If the prepotential is positive everywhere in the CB $\mathcal{C}$ (possibly including unphysical regions), there exists a physical CB.

All above conditions are conjectured to hold whenever the physical CB $\mathcal{C}_{\text{phys}}$ exists and the metric of the theory is positive on it [218, 219] Using the previous conditions, a classification of rank one and rank two theories has been performed and generalized in [153, 220, 221, 226]. In particular, the analysis of this classification suggested an origin of all five dimensional SCFTs from compactification of six dimensional SCFTs [219, 227].

5.6.2 Prepotential with enhanced symmetry

We saw in section 5.5.6 how we can continue a gauge theory past infinite coupling and how the physics after the continuation is described by another, UV dual, five dimensional theory (either Lagrangian or not). This is related to the original descriptions, but in general, it has a different prepotential and a different global symmetry. This comes from the perturbative nature of the IMS prepotential: this does not take into account continuation past infinite coupling, nor non-perturbative physics, such as instantons becoming massless for some values of the parameters. Both problems can be overcome by the construction of the so-called complete prepotential that takes care of these issues.

Let us consider, for example, pure $SU(2)$ SYM. When the θ angle is zero, its perturbative global symmetry $U(1)_I$ is known to enhance to E_1 at the UV fixed point. On the contrary, if $\theta = \pi$, the UV fixed point is the $\tilde{E}_1$ theory and the global symmetry does not enhance.
Despite these differences, the perturbative dynamics of the two theories is the same and it is

described by the IMS prepotential

$$\mathcal{F} = 2h\phi^2 + \frac{4}{3}\phi^3 \tag{5.159}$$

with $h = \frac{1}{2g^2}$. The theories differ only at the non-perturbative level.
When the θ angle is zero, at the fixed point the Weyl group of $SU(2)_I$ acts on the gauge coupling as $h \leftrightarrow -h$ and relates the UV dual descriptions of the E_1 fixed point at positive and negative couplings. In the pq-web construction, it is S-duality that relates the two descriptions. The IMS prepotential of the $SU(2)$ theory is blind to this symmetry, as we can see from (5.159). To implement a duality invariant description, we need to re-express the prepotential in terms of S-invariant parameters. Since the CB parameter ϕ gets mapped by the duality to $\phi + h$ and $h \to -h$, the invariant CB parameter

$$\tilde{\phi} = \phi + \frac{h}{2} \tag{5.160}$$

is left unchanged by the S-transformation.[29] The effective coupling can be expressed as a function of $\tilde{\phi}$ only

$$\frac{1}{g^2_{eff}} = 8\tilde{\phi} \tag{5.161}$$

and it is well-define for any values of the parameters. The corresponding prepotential reads

$$\mathcal{F}^{\text{compl.}}_{E_1} = -h^2\tilde{\phi} + \frac{4}{3}\tilde{\phi}^3 \tag{5.162}$$

which is manifestly invariant under the Weyl group. The expression (5.162) represents the complete prepotential of the E_1 theory. The invariant CB parameter makes manifest the representation of the W-boson and the instanton of E_1 theory under the $SU(2)_I$ global symmetry, since in this parametrization their masses

$$M_W = |2\tilde{\phi} - h|, \;\; M_I = |2\tilde{\phi} + h| \tag{5.163}$$

are exchanged by the Weyl group.

As mentioned above, the complete prepotential should also take care of flops coming from non-perturbative states. These become important considering, for example, $SU(2)_\pi$ SYM.
Its fixed point $\tilde{E}_1$ has no enhanced symmetry, so we do not need to introduce an invariant CB parameter in this case. However, past infinite coupling, the description via the perturbative prepotential breaks down. Indeed, from both field theory [212] and pq-web [245] analysis, we know that past infinite coupling the theory flows to the E_0 fixed point, see figure 5.29(c). Its prepotential (5.136) can be written in terms of the $SU(2)$ SYM parameters as

$$\mathcal{F} = \frac{3}{2}\phi^3 + 3\phi^2 + \frac{1}{2}h^2\phi \tag{5.164}$$

[29] This transformation is interpreted as a fiber/base duality in the CY construction of the $SU(2)$ SYM theory [288].

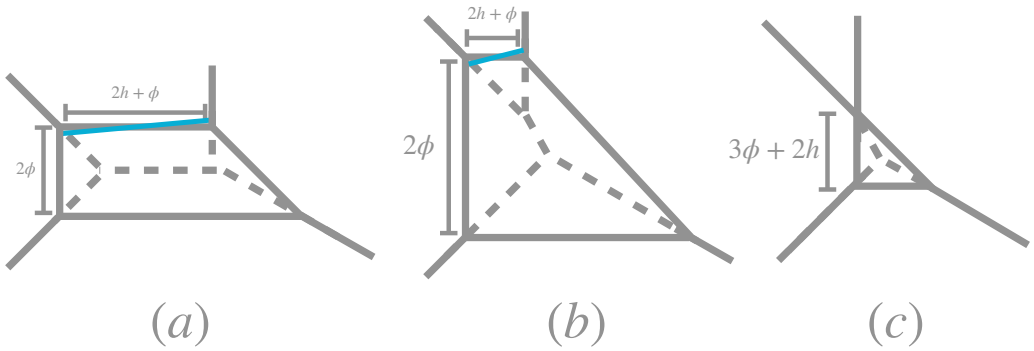

Figure 5.29: $\tilde{E}_1$ with positive coupling (a), negative coupling with $\phi+2h>0$ (b) and $\phi+2h<0$ (c) leading to the E_0 theory.

where the Coulomb branch is bounded $\phi \geq -\frac{2}{3}h$ to ensure the positivity of the monopole string tension. The two prepotentials (5.159) and (5.164) differ by a contribution

$$\Delta\mathcal{F} = \frac{1}{6}(\phi + 2h)^3. \tag{5.165}$$

This difference can be explained by a flop of an instantonic hypermultiplet. Indeed, looking at the $\tilde{E}_1$ theory in figure 5.29(a), we can go past infinite coupling (b) and start decreasing the value of the CB parameter in order to reach the E_0 description. At $\phi + 2h$, the hypermultiplet becomes massless, see figure 5.29(b). Being this instanton charged under the gauge group on the CB, the prepotential jumps by a term proportional to the cube of its mass, which is exactly the difference (5.165). The complete prepotential of the $\tilde{E}_1$ theory

$$\mathcal{F}_{\tilde{E}_1} = 2h\phi^2 + \frac{4}{3}\phi^3 + \frac{1}{6}[[\phi + 2h]]^3, \quad [[x]] = \theta(-x)x \tag{5.166}$$

is then valid in the whole range of the parameters!

The previous arguments can be generalized to more complicated theories. The complete prepotential of a generic theory can be obtained from the IMS one following the procedure listed below:

- Writing the IMS prepotential in a certain Weyl subchamber;
- Rewriting it in terms of the invariant CB parameters $\tilde{\phi}_a$, by shifting the original ϕ_as by some linear combination of the mass parameters. For example, for $SU(2) + F$ flavors, the invariant CB parameter reads [246, 288]

$$\tilde{\phi} = \phi + \frac{4}{8 - F}h. \tag{5.167}$$

- Applying the Weyl reflection associated with the global symmetry of the SCFT to the resulting prepotential. In this way, cubic terms generated by BPS states come into representations of the global symmetry group and the prepotential is manifestly invariant under the action of the Weyl group.

Adopting this strategy, we can obtain the complete prepotential with manifest enhanced global symmetry. This was done, for example, for $SU(2) + F < 8$ flavors and $Sp(2) + 1AS + F \leq 7$ flavors in [246].

Chapter 6

Searching for non-supersymmetric CFTs in five dimensions

In the previous Chapter, we focused on the study of $\mathcal{N} = 1$ supersymmetric field theories. Thanks to supersymmetry, we unveiled a plethora of SCFTs, many of which were obtained as UV completions of gauge theories. These are quite well-studied and we have also a (conjectured) method to classify them.

In spite of this knowledge, we know very little about the existence of non-supersymmetric conformal field theories in five dimensions. This comes from the fact that five dimensional Gaussian fixed points do not admit relevant deformation, contrary to lower dimensions. So there is no hope to find a CFT by deforming a Gaussian fixed point in the UV. Many strategies were employed to search for non-supersymmetric fixed points in five dimensions, such as ϵ-expansion, bootstrap, or lattice techniques (see [291–301] for some recent works). Although these analyses provided hints for the existence of these theories, it is fair to say that we are still far from having a clear understanding of the existence of interacting CFT in five dimensions without supersymmetry.

Another possible strategy comes by starting from a known SCFT and deforming it via a soft SUSY breaking deformation. Although the fixed point that we deform is still strongly coupled, thanks to supersymmetry we have much more handle on its properties. In this way, some characteristics of the endpoint of the RG-flow, where we can hopefully find a non-SUSY CFT, can be actually inferred from the ones of the original SCFT. This way of thinking motivated the construction of [155], which we briefly review in section 6.1. The remaining part of the Chapter, which is based on the original works in [302, 303], is organized as follows. Section 6.2 contains a recap of the properties of the moduli space of 5d $SU(2)$ SYM and the E_1 theory. In particular, we also offer some improvements of the 5-brane web description of the E_1 theory and its moduli space, characterizing the hypermultiplets describing the Higgs branch. These will play a crucial role for what comes in section 6.3, where we discuss the supersymmetry breaking mass deformation reviewed in section 6.1, its description in terms of 5-brane web and its effects on the IR dynamics. In section 6.4 the resulting phase diagram as a function of the deformation parameters is discussed. In the remaining part of the Chapter, we study the nature of this phase transition by looking directly at the corresponding pq-web construction. In section 6.5, we show

that neglecting brane interactions, the phase transition looks first order for any value of the parameters. While brane interactions are difficult to compute for this system, this can be done if we consider a generalization of the E_1 theory, known as $X_{1,N}$ theory, which admits a similar supersymmetry breaking deformation. In section 6.6 we review the main aspects of this class of theories and in section 6.7 we analyze the deformation at large N looking at their pq-web. In this case, the effect of brane interactions can be reliably computed, and we show that there exists a region of the parameter space where the corresponding phase transition is in fact second order. Our result provides concrete evidence for the existence of non-supersymmetric CFTs in five dimensions. We conclude in section 6.8 with a summary of our results and a discussion on some open questions.

6.1 Non-SUSY CFTs from E_1 theory?

From section 5.3.5 we know that SCFTs admit only one relevant class of SUSY preserving deformations, coming from sourcing the top component of the flavor current multiplet $\mathcal{J}_{\mathcal{G}}$ as

$$\delta\mathcal{L} = \phi_A M^A, \tag{6.1}$$

see eq. (5.50). Generically, this breaks the global symmetry to its Cartan torus, since the source ϕ_A comes from the VEV of the scalar of the background vector multiplet associated with the global symmetry.
In the $SU(2)$ case, the operation triggers an RG-flow to $SU(2)$ SYM with the gauge coupling $\phi_{(ab)} = h\hat{v}_{(ab)}$, where a is an index of the fundamental representation of $SU(2)_I$ and $\hat{v}$ is the versor indicating the Cartan direction preserved by the deformation. The identification between the UV deformation and the IR gauge coupling is possible since the current multiplet is an operator protected along the RG-flow, being short. The Weyl group of $SU(2)_I$ relates the two $SU(2)$ gauge theory descriptions at positive and negative couplings, as encoded in the complete prepotential (5.162) of the theory. At the fixed point, BPS states charged under both $SU(2)_I \times SU(2)_R$ become massless, leading to a strongly interacting superconformal field theory, the E_1 theory itself.

Looking at the current multiplet, another Lorentz preserving relevant deformations comes from sourcing the lowest component $\mu^{(ab)}_{(ij)}$ of the current multiplet

$$\delta\mathcal{L} = Y^{(ij)}_{(ab)}\mu^{(ab)}_{(ij)}, \;\; Y^{(ij)}_{(ab)} = \tilde{m}^{(ij)}\hat{v}_{(ab)} \tag{6.2}$$

where we choose two Cartan directions $\hat{v}$ (resp. $\tilde{m}$) for $SU(2)_I$ (resp. $SU(2)_R$). This is interpreted as giving a VEV to the auxiliary field $Y^{(ij)}_{(ab)}$, belonging to the background vector multiplet associated with the global symmetry.
This deformation breaks SUSY and $SU(2)_I \times SU(2)_R \to U(1)_I \times U(1)_R$. Moreover, this triggers an RG-flow. To understand the endpoint of this flow, we can start looking at the effect of the deformation on the $SU(2)$ SYM theory. This is equivalent to studying the RG-flow triggered by both the SUSY and the SUSY breaking deformations of the E_1 theory

$$\delta\mathcal{L} = \phi_{(ab)}M^{(ab)} + Y^{(ij)}_{(ab)}\mu^{(ab)}_{(ij)}, \;\; \phi_{(ab)} = h\hat{v}_{(ab)}, \text{ and } Y^{(ij)}_{(ab)} = \tilde{m}^{(ij)}\hat{v}_{(ab)} \tag{6.3}$$

in the weak coupling limit $h^2 \ll \tilde{m}$. Again the subgroup $U(1)_I \times U(1)_R$ is preserved by the deformations, having chosen the Cartan directions $\tilde{m}^I = (0, 0, \tilde{m})$, $\hat{v}_A = (0, 0, 1)$, with I an index of the adjoint representation of $SU(2)_R$. In the limit $h^2 \ll \tilde{m}$, we can study the SUSY breaking deformation by looking at its effect on $SU(2)$ SYM. This is nothing but a VEV for the D-term of the background $U(1)_I$ vector multiplet. The deformation can be written in terms of the SYM fields as

$$\delta\mathcal{L} = \tilde{m}\mathrm{Tr}\left(\frac{i}{4}\bar{\lambda}\sigma^3\lambda + \sigma D^i\right) \tag{6.4}$$

where we denoted the scalar of the $SU(2)$ SYM vector multiplet as σ to avoid confusion with ϕ, while σ^3 is the third Pauli matrix. The term (6.4) gives a mass to the scalar and the gauginos of the vector multiplet, upon integrating out the auxiliary fields. The CB is then lifted and, integrating out massive matter, we end up with pure $SU(2)$ YM in the IR, see figure 6.1. The same deformation at negative gauge coupling $h < 0$ leads again to pure $SU(2)$ YM. The $\tilde{m}$ axis separates the two $SU(2)$ YM phases, as shown in figure 6.1. Although these theories appear the same, they actually differ by topological invariants, the CS level of the global $U(1)_I \times U(1)_R$ symmetry, as we now review.

By introducing the background fields A_R for $U(1)_R$ and A_I for $U(1)_I$ and choosing $h > 0$, the CS terms of $SU(2)$ YM theory with positive coupling read

$$k_R = -\frac{3}{2}\mathrm{sgn}(m), \;\; k_I = -2. \tag{6.5}$$

The former level in (6.5) comes from integrating out the massive gauginos, which have a mass $\sim \tilde{m}g^2$ and are charged under the R-symmetry. Since they are in the triplet of $SU(2)$ group, they contribute with a $\frac{3}{2}$ coefficient in (6.5).

The second level can be obtained by looking at the complete prepotential in (5.162). This is nothing but the coefficient of the cubic term in h, that, although it is a constant in the field σ, it cannot be put to zero without spoiling the invariance of the prepotential under the Weyl group of $SU(2)_I$. The CS levels for the $h < 0$ phase can be then obtained using the residual Weyl groups $\mathbb{Z}_2^I \times \mathbb{Z}_2^R$ coming from the breaking of $SU(2)_I \times SU(2)_R$. These act rotating the vector associated with the Cartan directions $\hat{v}_{(ab)}$ and $\tilde{m}^{(ij)}$ to minus themselves. So, the first group sends

$$(h, \tilde{m}) \to (-h, -\tilde{m}), \;\; A_I \to -A_I, \;\; (k_I, k_R) \to (-k_I, k_R) \tag{6.6}$$

being A_I the gauge potential associated with the Cartan of $SU(2)_I$, while the second sends

$$(h, \tilde{m}) \to (h, -\tilde{m}), \;\; A_R \to -A_R, \;\; (k_I, k_R) \to (k_I, -k_R). \tag{6.7}$$

Combining the two operations, the resulting transformation $\mathbb{Z}_2^h$ sends

$$(h, \tilde{m}) \to (-h, \tilde{m}), \;\; (k_I, k_R) \to (-k_I, -k_R). \tag{6.8}$$

This is a symmetry of the theory at $h = 0$. As we cross the $\tilde{m}$ axis, both levels jump

$$\Delta k_I = 4, \;\; \Delta k_R = 3. \tag{6.9}$$

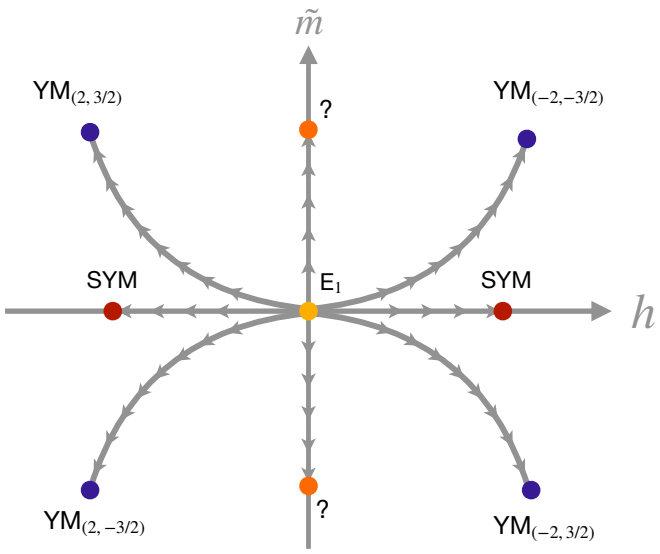

Figure 6.1: Phase diagram of E_1 theory.

The corresponding phase diagram is shown in figure 6.1.

We can now ask what is the physical meaning of this jump of CS levels.
The jump of k_R across the h axis is easily understood: the gauginos, charged under the R-symmetry, become massless when the $SU(2)_R$ symmetry (and supersymmetry) is restored. The jump of both levels across the $\tilde{m}$ axis, on the other hand, cannot be explained by a flop of some perturbative state. On this axis, the non-perturbative level jumps and separates two distinct phases, leading to a phase transition. Three possibilities are then in order:

- Spontaneous symmetry breaking of a continuous symmetry: the Abelian global symmetries $U(1)_R \times U(1)_I$ can be spontaneously broken to a subgroup on the axis. The transition is then second order and it is described by a gapless theory of Goldstone bosons;

- Spontaneous symmetry breaking of $\mathbb{Z}_2^h$: the discrete symmetry $\mathbb{Z}_2^h$ can be spontaneously broken on the axis. At the phase transition, we have two different degenerate vacua with different CS levels exchanged by the discrete symmetry. Turning on h, one of the two vacua has lower energy while the other becomes metastable. The vacua exchange under flipping the sign of h, realizing a first-order phase transition.

- Symmetries conservation: all symmetries are preserved. The jump of the level comes from massless modes, charged under the global $U(1)_I \times U(1)_R$ symmetry. Since both k_I and k_R jump, non-perturbative states (namely instantons) and states charged under $U(1)_R$ become massless at the same point.[1] This is the hallmark of an interacting conformal field theory describing the phase transition.

[1] A similar thing happens, for example, at the E_1 point, where both non-perturbative and perturbative particles, such as instantons and W-bosons respectively, become massless at that point.

It is then natural to ask if the last possibility is realized and we have found a non-supersymmetric conformal field theory in the phase diagram of softly broken $SU(2)$ SYM. Answering this question will be the main goal of this Chapter. However, to do so, we need first to understand how the deformation acts on the moduli space on the E_1 theory. For this reason, in the next section, we will briefly expand the discussion of section 5.5.6 on the HB of the E_1 theory.

6.2 Moduli space and supersymmetric deformations

Let us focus on the moduli space of the E_1 theory and on its supersymmetric deformation. We first summarize known field theory results and then show how they can be described in (p,q)-brane web brane language.

The E_1 theory admits both a Coulomb branch and a Higgs branch. The former is present also in $\mathcal{N}=1$ $SU(2)$ pure SYM while the latter is peculiar to the E_1 theory only. The Higgs branch is a one dimensional hyper-Kähler sigma model $\mathbb{C}^2/\mathbb{Z}_2$ parametrized, locally, by a complex hypermultiplet $\mathcal{H}$ with scalar components H_i, where i is an index in the fundamental of $SU(2)_R$. At a generic point on the Higgs branch the global symmetry is broken to $D[SU(2)_I \times SU(2)_R] = SU(2)_{R'}$, which is still an R-symmetry. This gives rise to three Goldstone modes which, together with the scaling modulus, describe the one dimensional quaternionic sigma model.

This parametrization hides the action of the instantonic symmetry on the Higgs branch and of the aforementioned symmetry breaking pattern. To make this action manifest, the complex hypermultiplet can more conveniently be described as two real half hypers $\mathcal{H}^a$ with a an index in the fundamental representation of $SU(2)_I$ and $\mathcal{H}^a = \overline{\mathcal{H}}_a$.

Using real half hyper parametrization, one can easily see the lifting of the Higgs branch at finite gauge coupling. This is done by introducing background vector fields of the instantonic $SU(2)_I$ symmetry. The $SU(2)_I$ current multiplet can be described in terms of the real half hypermultiplets $\mathcal{H}^a$. The hypermultiplet scalars H_i^a transform in the bi-fundamental of $SU(2)_I \times SU(2)_R$ global symmetry. Since the $SU(2)_I$ instantonic symmetry acts on the Higgs branch, and hence on H_i^a, the bottom component $\mu_{(ij)}^{(ab)}$ of the $SU(2)_I$ current multiplet can reliably be tracked on the Higgs branch:[2] it is simply the tri-holomorphic moment map of the $SU(2)_I$ symmetry and reads

$$\mu_{(ij)}^{(ab)} \sim H_{(i}^{(a} H_{j)}^{b)} \ , \tag{6.10}$$

which in turn implies, for instance, that

$$M^{(ab)} \sim \Omega^{\alpha\beta} Q_\alpha^i Q_\beta^j \mu_{(ij)}^{(ab)} \ , \tag{6.11}$$

where $\Omega^{\alpha\beta}$ is the $Spin(5)$ symplectic invariant tensor and Q_α^i are the supercharges.

$\mathcal{N}=1$ supersymmetry couples the background gauge field with the $SU(2)_I$ current multiplet $\mathcal{J}^{(ab)}$ and by (6.10) and (6.11) to the hyperscalars H_i^a as

$$Y_{(ab)}^{(ij)} \cdot H_{(i}^{(a} H_{j)}^{b)} \quad \text{and} \quad \phi_{(ab)} \cdot \Omega^{\alpha\beta} Q_\alpha^i Q_\beta^j H_{(i}^{(a} H_{j)}^{b)} \ . \tag{6.12}$$

[2] We thank Thomas Dumitrescu for clarifying this to us.

A VEV for the scalar operator $\phi_{(ab)}$ corresponds to a massive deformation proportional to the inverse gauge coupling squared, $1/g^2$ [145]. This brings the E_1 theory down to $SU(2)$ SYM and breaks the global $SU(2)_I$ symmetry to $U(1)_I$ while leaving the $SU(2)_R$ symmetry untouched, as expected for $\mathcal{N}=1$ $SU(2)$ SYM.

In fact, via (6.12), $\langle\phi_{(ab)}\rangle$ provides a mass also to the hypermultiplets $\mathcal{H}^a$

$$\phi_{(ab)}\, M^{(ab)} \;\longrightarrow\; \Delta\mathcal{L} = \langle\phi_{(12)}\rangle M^{(12)} = \frac{1}{g^2} M^{(12)} = \frac{1}{g^2}\Omega^{\alpha\beta} Q^i_\alpha Q^j_\beta\, H^{(1}_{(i} H^{2)}_{j)}\ , \tag{6.13}$$

where we have chosen a specific Cartan direction, for definiteness.[3] We hence see that the Higgs branch is lifted at weak coupling, as anticipated. This is a supersymmetric mass deformation since $M^{(ab)}$ is a highest component operator of the $SU(2)_I$ current multiplet and so the full hypermultiplet becomes massive, i.e. both H^a_i and its fermionic superpartner ψ^a_H, with a mass $m_{\text{SUSY}} = 1/g^2$.

The E_1 theory and $SU(2)$ SYM admit also a Coulomb branch. This is parametrized in terms of the VEV of a scalar operator σ (which at weak coupling corresponds to the scalar component in the Cartan of the $SU(2)$ vector multiplet). This scalar operator does not carry any global index, hence along the Coulomb branch the full global symmetry $SU(2)_I \times SU(2)_R$ (or $U(1)_I \times SU(2)_R$ at finite coupling) is preserved. Further, the hypermultiplet parametrizing the Higgs branch gets a mass proportional to $\langle\sigma\rangle$, showing that the E_1 theory does not admit a mixed branch. One reason for this to be expected is that the Higgs branch is singular at its origin and it is known that the Coulomb branch of the E_1 theory is smooth for any finite value of $\langle\sigma\rangle$ [145, 212]. Another way to see that the Higgs branch is lifted on the Coulomb branch comes from the BPS bound for instantonic particles. At weak coupling, the breaking of the $SU(2)$ gauge symmetry on the Coulomb branch generates a CS level k for the Cartan surviving the breaking. As we reviewed in Chapter 5, the effect of this CS level consists, in giving a net additional electric charge $n_e = kI$ to particles charged under the instantonic symmetry, with I the $U(1)_I$ charge. If the particle is BPS, its mass then reads

$$M = |n_e\langle\sigma\rangle + hI|\ . \tag{6.14}$$

Since this bound remains true also in the strong coupling limit, particles charged under the instantonic symmetry, as the hypermultiplet $\mathcal{H}^a$, obtain a mass proportional to $\langle\sigma\rangle$ on the Coulomb branch.

Brane web description

Let us consider the Higgs branch, which is a property of the E_1 theory, only, in the pq-web context. This is described in figure 6.2 and it is obtained by displacing the $(1,1)$ 5-brane in the space transverse to the (x,y) plane. As we discussed in section 5.5.6, the complex hypermultiplet $\mathcal{H}$ parametrizing the Higgs branch can be identified as the lowest energy excitations of the $(1,1)$ strings on the $(1,1)$ 5-branes across the $(1,-1)$ 5-branes, which is a free hypermultiplet when the $(1,1)$ and $(1,-1)$ 5-branes do not intersect.

[3] Note that, for later purposes, we changed the convention for h, denoting $h \equiv 1/g^2$.

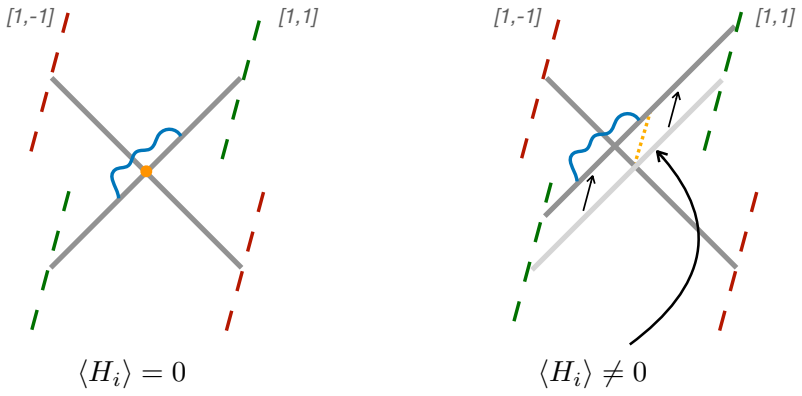

Figure 6.2: The E_1 theory at the origin (left) and at an arbitrary point (right) of the Higgs branch. The blue wiggles represent the hypermultiplet $\mathcal{H}$. The $(1,1)$ 5-branes slides along the $[1,1]$ 7-branes, giving rise to a free hypermultiplet (a finite 5-brane stretching between two 7-branes). The VEV of H_i is proportional to the distance between the $(1,1)$ and $(1,-1)$ 5-branes in the transverse space.

This process describes a symmetry breaking pattern $SU(2)_R \to U(1)_R$: the brane separation occurs in the transverse directions of the 5-brane system, which is $\mathbb{R}^3$, and hence only $SO(2)$ rotations, corresponding to a $U(1)_R$ symmetry, survive in the transverse space. It is worth noticing that one cannot display the full Higgs branch symmetry breaking pattern $SU(2)_I \times SU(2)_R \to SU(2)_{R'}$. This is because the two symmetries, the R-symmetry and the instantonic symmetry, have different realizations in the brane web. The former is realized geometrically, in terms of rotations in the three dimensional transverse space the 5-brane system shares. The latter is instead realized in terms of string degrees of freedom, namely the $(1,1)$ strings living on the $[1,1]$ 7-branes. These two symmetries have different origins and cannot mix, so the web diagram is not manifestly invariant under the unbroken group.

Let us now consider the supersymmetric mass deformation (6.13) which makes the E_1 theory flow to pure $SU(2)$ SYM. This is described by the global deformation depicted in figure 6.3. We see from the figure that the Higgs branch is lifted, as expected. Indeed, as soon as $1/g^2 \neq 0$ the $(1,1)$ and $(1,-1)$ 5-branes cannot anymore be moved apart since the quadruple brane junction splits into two triple ones. At the same time, the $(1,1)$ strings describing the hypermultiplet $\mathcal{H}$ get stretched and get a mass proportional to $1/g^2$, in agreement with field theory expectations.

An important comment is worth at this point. Although from figure 6.3(b) we do see that $\mathcal{H}$ gets a mass at finite gauge coupling, this description is inaccurate. The hypermultiplet parametrizing the Higgs branch is a BPS state but a $(1,1)$ string connecting two separated $(1,1)$ branes as in figure 6.3(b) is not. A similar problem arises when adding flavors on a brane web [207,211]. As in that case, a simpler and more direct description can be obtained performing a HW transition on the original brane web, as described in figure 6.4 (see appendix of [283]). After the transition, a $(1,1)$ string stretching between the $(1,1)$ 5-brane and the $[1,1]$ 7-brane

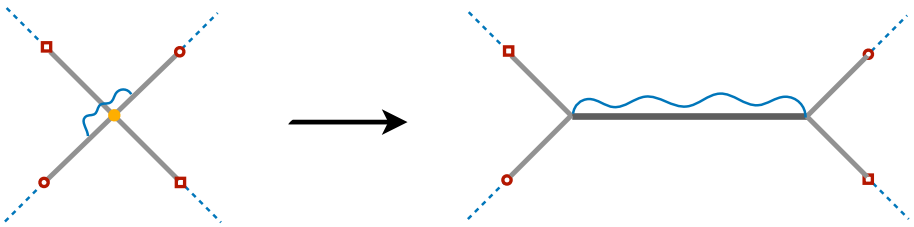

$\mathrm{m}_{\mathcal{H}} = 0$ $\qquad$ $\mathrm{m}_{\mathcal{H}} \sim 1/g^2$

(a) $\qquad$ (b)

Figure 6.3: Higgs branch lifting and (a naive description of) hypermultiplet mass generation at finite gauge coupling.

can be constructed and correctly represents the hypermultiplet degrees of freedom.

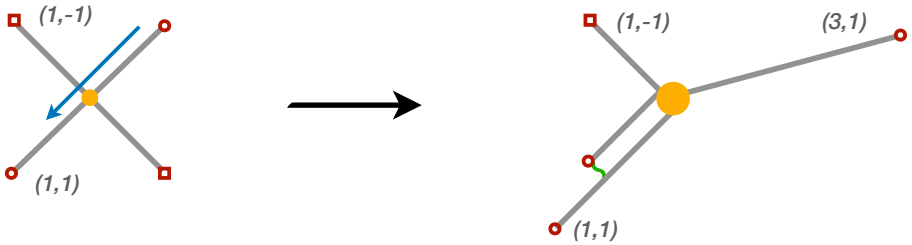

Figure 6.4: Hanany-Witten transition. In the resulting 5-brane web the string representing the hypermultiplet is now a $(1,1)$ string stretched between the $(1,1)$ 7-branes and 5-branes (green wiggle). The two $(1,1)$ 5-branes on the bottom left are displaced just to visualize the hypermultiplet degrees of freedom.

As illustrated in figure 6.5, at finite gauge coupling this string acquires a mass which, in units of the fundamental string tension T_s, is

$$m_{\mathcal{H}} = 1/g^2 \ , \tag{6.15}$$

which is the same of an instanton with unit charge. As it is clear from the figure, the $(1,1)$ string length is suppressed by a $\sqrt{2}$ factor with respect to that of the D1-brane on the D5-brane which is an instanton of the $SU(2)$ theory, but its tension is $\sqrt{2}$ larger and the two factors compensate. This shows that this state is BPS and at threshold with an instanton with $I = 1$, see eq. (6.14).[4]

[4]This agrees with the fact that all BPS saturated states in the $\mathcal{N} = 1$ $SU(2)$ theory can be viewed as bound states of two basic states, an instanton and, when the Coulomb branch opens-up, a massive W-boson (see [207] for a detailed discussion).

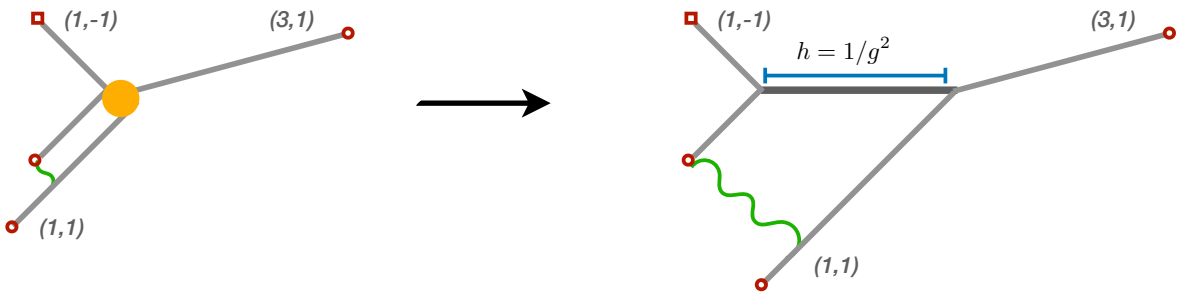

Figure 6.5: Supersymmetric mass deformation. The $(1,1)$ string representing the hypermultiplet $\mathcal{H}^a$ gets a mass proportional to the inverse coupling squared.

In this dual frame, the hypermultiplet degrees of freedom are naturally described in terms of the real half hypermultiplet $\mathcal{H}^a$, which are nothing but the $(1,1)$ strings connecting 5 and 7-branes in figure 6.4. The Higgs branch is obtained by displacing a $(1,1)$ 5-brane segment in the transverse space, as shown in figure 6.6. The free hyper parametrizing the Higgs branch is a $(1,1)$ string living on the finite $(1,1)$ 5-brane (blue wiggles in the figure), which is in fact a complex hyper, as in figure 6.2.

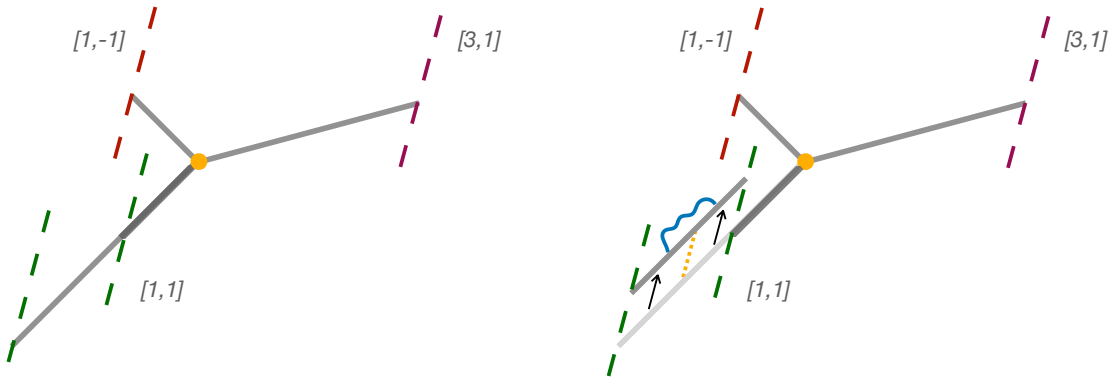

Figure 6.6: Higgs branch description in the HW dual frame. Displacing a finite $(1,1)$ 5-brane in the transverse space provides a VEV to the hyperscalars H_i^a [304]. The blue wiggles on the 5-brane describe the complex hypermultiplet parametrizing the Higgs branch.

Let us now see how the brane web captures the correct symmetry breaking pattern induced by the mass deformation. From figure 6.3 one can also see the correct symmetry breaking pattern $SU(2)_I \times SU(2)_R \to U(1)_I \times SU(2)_R$. From the brane web perspective, the $SU(2)_I$ group is realized as the gauge group of the 7-branes. The low energy excitations of the $(1,1)$ strings living on the $[1,1]$ 7-branes are a vector multiplet in eight dimensions. Once reduced to 5 dimensions, in terms of $\mathcal{N} = 1$ representations this corresponds to a (free) hypermultiplet and a vector multiplet (at zero coupling). The latter represents the background vector multiplet of the

flavor symmetry of the five dimensional E_1 theory. At finite gauge coupling, the $[1,1]$ 7-branes get displaced due to the finite length $(2,0)$ 5-brane, and the $(1,1)$ strings connecting the 7-branes get stretched and acquire a minimal length of order $1/g^2$, see figure 6.7. This is Higgsing for the $SU(2)_I$ theory living on the $[1,1]$ 7-branes, which is broken to $U(1)_I$, and corresponds to give a VEV $\sim 1/g^2$ to the lowest component of the (background) vector multiplet, $\phi_{(ab)}$. The $SU(2)_R$ symmetry is instead preserved since the deformation does not involve the transverse space.[5]

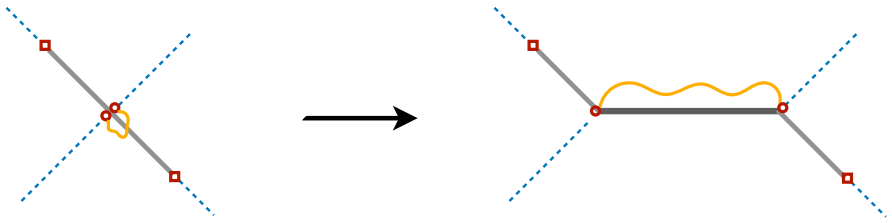

Figure 6.7: Geometric description of the symmetric breaking $SU(2)_I \to U(1)_I$ induced by the mass deformation (6.13). At $1/g^2 \neq 0$ the two $[1,1]$ 7-branes cannot anymore be put on top of each other, the $(1,1)$ strings living on them (yellow wiggles) get stretched and the instantonic symmetry is broken to $U(1)_I$. The R-symmetry remains untouched.

Let us finally discuss the Coulomb branch, which exists both for the E_1 theory and for $\mathcal{N}=1$ $SU(2)$ SYM. We report in figure 6.8 its description both at weak coupling and at infinite coupling. As for the latter, one easily sees that the Higgs branch is lifted, since the $(1,1)$ 5-brane cannot anymore be moved apart along the transverse space, in agreement with field theory analysis. The $(1,1)$ strings describing the hypermultiplet $\mathcal{H}$ becomes massive and saturates the BPS mass formula (6.14) with $n_e = 4$ and $I = 1$. It is then at threshold with a bound state of a W-boson ($n_e = 2, I = 0$) and an instanton with unit instantonic charge ($n_e = 2, I = 1$ – recall that on the Coulomb branch an instanton acquires an effective $U(1)$ charge).

Finally, in agreement with field theory expectations, one can see that on the Coulomb branch the full global symmetry is preserved, $SU(2)_I \times SU(2)_R$ and $U(1)_I \times SU(2)_R$ at infinite and finite couplings, respectively. The $SU(2)_R$ symmetry is preserved since the deformation does not involve transverse directions, as opposed to the Higgs branch deformation described in figure 6.2. Also, the instantonic symmetry is preserved. In particular, as shown in figure 6.9, in the E_1 theory the $[1,1]$ 7-branes can still be freely moved on the $(1,1)$ 5-branes prong, preserving the full $SU(2)_I$ symmetry.

6.3 Supersymmetry breaking mass deformation

In this section, we discuss the supersymmetry breaking deformation reviewed in section 6.1, provide its geometric realization via brane webs, and discuss its effects on the low energy

[5] An identical argument can be done in the dual setup of figure 6.5.

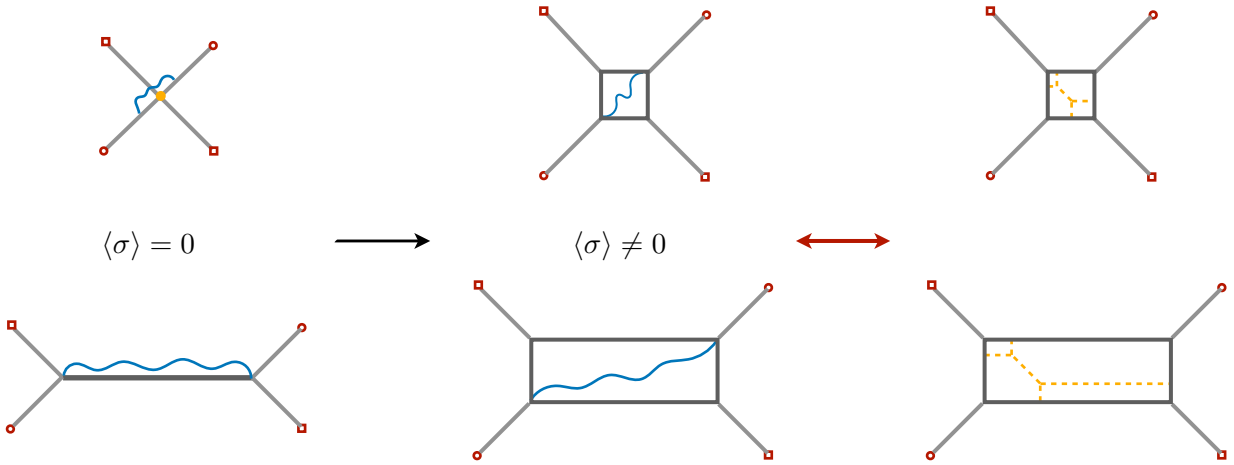

Figure 6.8: Coulomb branch description for the E_1 theory (up) and at weak coupling (down). The E_1 theory Higgs branch is lifted since the $(1,1)$ 5-brane cannot anymore be displaced in the transverse space. The hypermultiplet (blue wiggles in the figure) becomes massive. The corresponding BPS state has $n_e = 4$ and (at finite gauge coupling - bottom figures) instantonic charge $I = 1$. It is at threshold with a bound state of an instanton and a W-boson, whose (p,q)-brane web description is depicted in the most right figures.

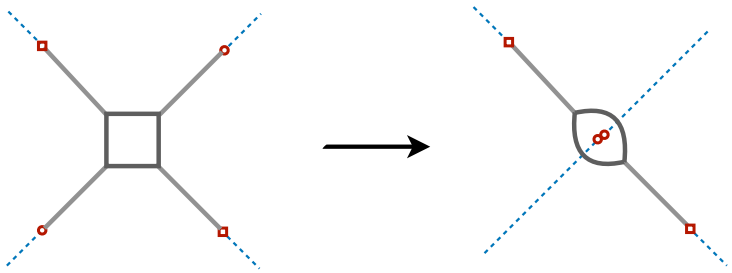

Figure 6.9: On the Coulomb branch of the E_1 theory the $[1,1]$ 7-branes can still be moved on top of each other and the full $SU(2)_I$ global symmetry is preserved. The presence of 7-branes creates a non-trivial metric so the 5-branes follow curved geodesics. The curved 5-branes in the right figure are just a pictorial way to mimic this effect (which does not change the nature of the 5-branes, namely their charges).

dynamics.
Let us look at the supersymmetry breaking deformation (6.2) more closely and start considering deforming the E_1 fixed point just with

$$\Delta\mathcal{L} = \widetilde{m}\mu^{(12)}_{(12)} \,, \tag{6.16}$$

namely at infinite coupling, $h = 0$. One can easily show that this deformation induces an instability on the Higgs branch, which in the E_1 theory is instead a flat direction. More precisely,

under (6.16) a mass term is generated for the hyperscalars H_i^a parametrizing the Higgs branch but this mass term always has a positive and a negative eigenvalues. To see this, let us rewrite (6.16) using (6.10) as

$$\Delta\mathcal{L} = \widetilde{m}\left(H_1^1 H_2^2 + H_1^2 H_2^1\right) \ . \tag{6.17}$$

Recalling that $H^{ia} = \overline{H}_{ia}$, with little algebra the above equation can be recasted as

$$\Delta\mathcal{L} = \widetilde{m}\left(|H_1^1|^2 - |H_1^2|^2\right) \ , \tag{6.18}$$

which shows that regardless of the sign of $\widetilde{m}$ there always exists a tachyonic mode and hence an instability.[6] Considering the more general deformation (6.3) we then see that there are two competitive contributions to scalar masses, one weighted by $\widetilde{m}$ and one by h (the latter, being a supersymmetric mass deformation, always gives positive mass squared contribution for the hyperscalars H_i^a)

$$\Delta\mathcal{L} = (h^2 + \widetilde{m})|H_1^1|^2 + (h^2 - \widetilde{m})|H_1^2|^2 \ . \tag{6.19}$$

This implies that, unlike the regime $|\widetilde{m}| \ll h^2$, the regime $|\widetilde{m}| \gg h^2$ describes a region of instability. Before discussing what the fate of this instability could be, let us see how this discussion translates in brane-web language.

The supersymmetry breaking deformation (6.16) has (at least) the following properties:

1. Break supersymmetry.
2. Break $SU(2)_I \times SU(2)_R$ to $U(1)_I \times U(1)_R$.
3. Lift the Higgs branch of the E_1 theory.
4. Lift the Coulomb branch.

Starting from the E_1 theory, figure 6.10(a), let us consider a rigid rotation of the two (semi-infinite) right 5-branes along the x-axis, as shown in figure 6.10.

This deformation satisfies all the above requirements. First, the rotation along the x-axis changes the angles between the 5-branes of the E_1 fixed point, and therefore the supersymmetric condition for brane junctions is not anymore satisfied. Supersymmetry is then broken. The R-symmetry is broken to $U(1)_R$ since only $SO(2)$ rotations are still allowed in the transverse space. The rotation by an angle α also misaligns the $[1,1]$ 7-branes on which the $(1,1)$ 5-branes end which get rotated one another by the very same angle. Therefore, the 7-branes are not anymore parallel and the $SU(2)_I$ instantonic symmetry is broken to $U(1)_I$.[7] The Higgs branch is lifted since the possibility to displace any of the 5-branes along transverse directions at no cost, as in figure 6.2, is now geometrically obstructed. Finally, also the Coulomb branch is lifted. The four 5-branes describing the string junction cannot undergo a process as the one described in figure

[6] We thank Thomas Dumitrescu for pointing this out to us.

[7] This also signals the instability. The tilt, besides Higgsing the $SU(2)_I$ gauge theory on the 7-branes, makes open strings connecting the two 7-branes becoming tachyonic, one mode getting a positive mass squared and the other one getting a negative mass squared [305, 306]. This can be seen as the D-term of the $SU(2)_I$ vector multiplet on the 7-branes getting a VEV along a Cartan direction.

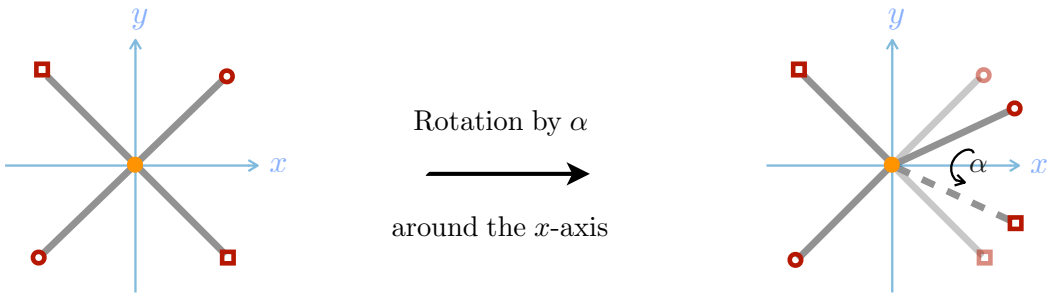

Figure 6.10: The supersymmetry breaking deformation: a rigid rotation around the x-axis of the right $(1,1)$ and $(1,-1)$ 5-branes.

6.8 because the finite length D5 and NS5 branes would now be misaligned and it costs energy to open up the string junction. So the modulus σ parametrizing the Coulomb branch is lifted. We then propose the deformation in figure 6.10 to be the one we are looking for.

A further check for the validity of our proposal comes from computing the resulting low energy spectrum at weak coupling, namely at large $|h|$. Field theory analysis shows that the supersymmetry breaking deformation lifts the whole $\mathcal{N}=1$ vector multiplet of $SU(2)$ SYM but the vector field and the theory flows to pure YM in the IR. So, if our proposal is correct, not only the real scalar σ but also the gaugini should be lifted by rotating the brane system as in figure 6.10. To show that this is the case it is easier to work in the limit $g_s \to 0$ (this makes the analysis simpler but does not change the end result). In this regime the supersymmetric brane system depicted in figure 6.10(a) becomes a system of two parallel NS5-branes with two D5-branes stretched between them. The D5s extend along $(01234x)$ and the NS5s along $(01234y)$, which are separated in the x direction by the finite length D5-branes. Standard analysis of the boundary conditions of the low energy modes on the D5-branes shows that a full 5d $\mathcal{N}=1$ vector multiplet survives.

In this regime, our supersymmetry breaking deformation amounts to rotating the right NS5-brane by an angle α around the x direction, as shown in figure 6.11.

The boundary conditions for a massless vector of section 5.5.3 are still satisfied, in particular, is still true that

$$F_{\mu x} = 0 \quad , \quad F_{\mu\nu} \text{ unconstrained} \tag{6.20}$$

where $\mu,\nu = 0,\ldots,4$, which are Neumann directions for both the D5 and the NS5-branes. On the contrary, the boundary condition for getting a massless gaugino is violated. In the supersymmetric configuration, the following conditions are satisfied at both ends of the finite D5-branes

$$\lambda_- \equiv (1-\Gamma)\lambda = 0 \quad , \quad \lambda_+ \equiv (1+\Gamma)\lambda \text{ unconstrained} \, , \tag{6.21}$$

where λ is the spin 1/2 field of the D5-brane theory and $\Gamma = \Gamma_x\Gamma_7\Gamma_8\Gamma_9$ is a product of Dirac matrices with indices on the NS5-brane transverse directions. The mode λ_+ is the gaugino, partner of the gauge field A_μ. Upon rotating one NS5-brane by an arbitrary angle in, say, the $(y7)$ plane, the condition which is satisfied at the corresponding intersection is the same as

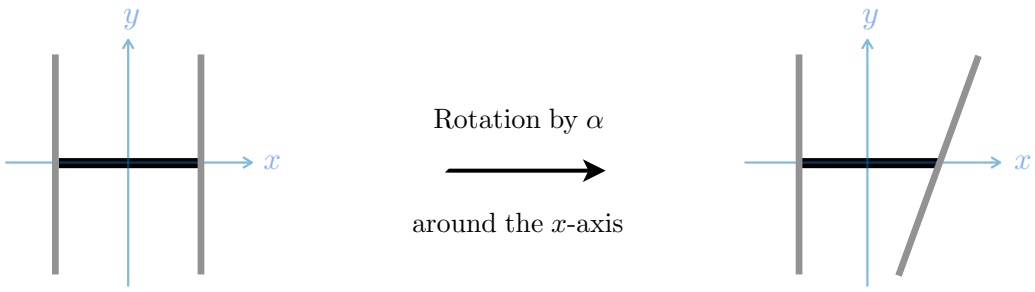

Figure 6.11: The supersymmetric and the supersymmetry breaking configurations at $g_s = 0$ and finite $h = 1/g^2$. The grey lines are NS5-branes. In the right figure, the NS-brane on the extreme right is rotated around the x-axis on the $(y7)$ plane.

(6.21) but implemented by a different Γ matrix, namely $\Gamma' = \Gamma_x\Gamma_{7'}\Gamma_8\Gamma_9$ where $7'$ is a transverse direction for the rotated NS5-brane, together with $x, 8, 9$. This mixes the $+$ and $-$ modes so that an unconstrained one, compatible with both boundary conditions at the right and left NS5-branes, does not exist anymore. Hence, the gaugino is lifted.

The analysis of the boundary conditions at the D5/NS5 intersections provides also another way to see that after the supersymmetry breaking rotation the modulus σ is lifted. On the D5-branes there are four scalars, $\phi^{y,7,8,9}$, associated with the possibility for the D5s to move in the directions transverse to their worldvolume. The NS5 branes fix to zero all scalars transverse to both the D5 and the NS5 branes. So, for an NS5 along $01234y$, we get

$$\phi^{7,8,9} = 0 \ . \tag{6.22}$$

In the supersymmetric case, the D5s are suspended between two identical NS5, so ϕ^y survives the boundary conditions and is nothing but the scalar field σ in the vector multiplet of the five dimensional gauge theory living on the finite length D5-branes. Upon rotating the right NS5-brane as in figure 6.11 the boundary conditions there change, fixing now to zero the modes

$$\phi^{7',8,9} = 0 \ . \tag{6.23}$$

As a consequence, imposing the two conditions at once, all scalar modes are lifted.

The origin of the instability in the rotated brane web can be seen as follows. Under a rotation by an angle α around the x-axis the $[1,1]$ and $[1,-1]$ 7-branes on which the 5-branes end get twisted by the same angle. This implies, in turn, that the two $[1,1]$ 7-branes where the $(1,1)$ strings describing the background vector multiplet live become a system of branes at angles with 2 mixed Neumann-Dirichlet boundary conditions. This provides a VEV to the D-term component of the (background) vector multiplet described by the 7-7 strings, $Y^{(ij)}_{(ab)}$. More precisely, we have

$$\langle Y^{(ij)}_{(ab)} \rangle = \hat{m}^{(ij)}\hat{v}_{(ab)}\frac{1}{\pi\alpha'}\tan\frac{\alpha}{2} \tag{6.24}$$

with $\hat{m}^{(ij)}$ and $\hat{v}_{(ab)}$ being unit vectors indicating the Cartan's directions, which we choose along (12) in both, as discussed in section 6.1. Via the coupling (6.12) this generates a mass

deformation in the E_1 theory

$$Y^{(ij)}_{(ab)}\,\mu^{(ab)}_{(ij)} \;\longrightarrow \Delta\mathcal{L} = \langle Y^{(12)}_{(12)}\rangle \mu^{(12)}_{(12)} = \widetilde{m}\,\mu^{(12)}_{(12)} = \widetilde{m}(|H^1_1|^2 - |H^1_2|^2)\ , \tag{6.25}$$

which is nothing but eq. (6.18).[8] The operator $\mu^{(ab)}_{(ij)}$ is a lowest component operator of the $SU(2)_I$ current multiplet and therefore the deformation above breaks supersymmetry explicitly.

The scalar operator $Y^{(ij)}_{(ab)}$ is in the adjoint of both $SU(2)$'s of the global symmetry group and a VEV breaks them to their Cartan generators, $SU(2)_I \times SU(2)_R \to U(1)_I \times U(1)_R$. As already noticed, this is matched geometrically: the angle between the $[1,1]$ 7-branes breaks $SU(2)_I \to U(1)_I$ and at the same time leaves only a two dimensional plane transverse to both the (x,y) plane and to the plane spanned by the two 7-branes at angles, hence breaking the R-symmetry as $SU(2)_R \to SO(2) \simeq U(1)_R$. Note that unlike the symmetry breaking pattern on the Higgs branch we discussed previously, in this case, we have a complete description of the symmetry breaking pattern, $SU(2)_I \times SU(2)_I \to U(1)_I \times U(1)_R$. This is because in this case, the breaking pattern does not mix the two symmetries. Moreover, everything depends on a VEV for $Y^{(ij)}_{(ab)}$ which is a fundamental degree of freedom for the $[1,1]$ 7-branes theory.

Let us end with an important remark about the range of validity of the above brane description. In order for the brane-web after the deformation to describe a five dimensional field theory, we need to decouple the Kaluza-Klein (KK) six dimensional modes. Being the supersymmetry breaking scale $M_{SB} = \tilde{m}g^2$ and the KK mass $\sim \frac{1}{\Delta x} = g^2/l_s^2$, with l_s the string length, the following inequality should hold, $M_{SB} \ll g^2/l_s^2$. So, if the supersymmetry breaking deformation is sufficiently smaller than the gauge coupling squared in string units (which is a weaker and weaker constraint the larger the gauge coupling), the brane-web still describes a five dimensional field theory and the KK modes do not mix.

6.4 Phase diagram of softly broken SYM

The picture emerging from our analysis is that the parameter space is divided into two qualitatively different regions. One region, which includes the weak coupling regime, where at low energy the mass deformed E_1 theory reduces to pure $SU(2)$ YM. A second region, symmetrically displaced around the $\widetilde{m}$-axis, where the global symmetry is spontaneously broken due to the condensation of the hyperscalar H^a_i, with a symmetry breaking pattern $U(1)_I \times U(1)_R \to D[U(1)_I \times U(1)_R] \equiv U(1)$. This implies that a phase transition should occur between them.

The response of the brane web in the two regimes seems to confirm this picture. For any fixed angle α, for small enough h so that an open string tachyon is generated, the $(1,1)$ semi-infinite branes are expected to recombine and separate from the $(1,-1)$ recombined brane in the transverse direction, in analogy with what happens with systems of branes at angles in flat space, see e.g. [307]. Space separation induces a VEV for the hyperscalars, as discussed in section 6.2, and the global symmetry is spontaneously broken. On the contrary, for large enough h the tachyon disappears from the spectrum and brane recombination is disfavored (notice, further, that the larger h the heavier is the $(2,0)$ 5-brane which keeps the half $(1,1)$

[8] One can reach the same result also looking directly at the 5-brane theory.

and $(1,-1)$ 5-branes apart, working against brane recombination). Hence in this regime, the brane web does not break and the VEV of the Higgs field vanishes.

A concrete handle on the fate of the instability may come from an effective field theory approach. Clearly, by breaking supersymmetry, the exact scalar potential is expected to contain more terms than just quadratic ones, eq. (6.19). While we cannot find its complete expression, there are two regimes where we can be quite safe about its form.

Let us start from the E_1 supersymmetric fixed point and sit at a point of the Higgs branch where the hyperscalar field VEV is very large. In this regime the low energy dynamics is described by the massless hypermultiplet $\mathcal{H}$ only, since all other degrees of freedom have masses of order $\langle H \rangle$.

Let us now switch on the non-supersymmetric mass deformation. This lifts the modulus and a potential is generated. Requiring that no singularities arise as $\widetilde{m} \to 0$, one can easily conclude by dimensional analysis that, besides the quadratic term, only operators with negative powers of H can appear. This ensures that the absolute minimum at $\langle H \rangle \to \infty$ predicted by the leading order analysis survives. Hence we conclude that on the $\widetilde{m}$-axis the global symmetry is indeed spontaneously broken and the potential is unbounded from below.[9]

Let us now consider the other extreme regime, $\widetilde{m} = 0, h \neq 0$. In this regime, the hypermultiplet is a massive BPS state at threshold and so we expect no corrections to the potential other than the supersymmetric mass term

$$V(H,h) = h^2 H^2 \ . \tag{6.26}$$

In particular, and more relevant to us, the minimum of the potential is at $\langle H \rangle = 0$ (as dictated by $\mathcal{N}=1$ SYM, which is in an unbroken phase). So, as anticipated, there should exist a curve in the $(h, \widetilde{m})$ plane where a phase transition occurs, separating a region where the $U(1)_I \times U(1)_R$ global symmetry is preserved from a region where it is spontaneously broken.

For both $\widetilde{m}$ and h non-vanishing, the potential should interpolate between the above regimes. Computing its exact expression is a daunting task (in brane-web language this would correspond to computing the full tachyon potential). Moreover, as soon as $h \neq 0$ it is not at all guaranteed that the only light field is the hypermultiplet $\mathcal{H}$. So, in principle, the potential could depend on more scalar fields than just the hyperscalars. Still, even under the restrictive assumption of one light field only, some lessons can be learned, just using continuity arguments and consistency of various limits. In particular, one can show that as soon as $h \neq 0$ the instability may disappear, and global minima at finite distance in field space may arise, corresponding to a stable symmetry broken phase out of the $\widetilde{m}$-axis. On the other hand, without further insights, one cannot be conclusive about the order of the phase transition separating the symmetry broken and the symmetry preserving phases. This depends on the exact form of the potential, which we do not know. A qualitative picture of the phase diagram is reported in figure 6.12.

[9] Depending on the specific form of the higher order corrections local minima can appear at finite distance in the moduli space, but these do not change our conclusions. In principle, it is also possible that a competitive unstable vacuum shows up at vanishing VEV for H. This cannot be excluded, but the brane-web description of the supersymmetry breaking deformation, figure 6.10, suggests this not to be the case. As already emphasized, for vanishing h the 5-branes tend to recombine and separate in the transverse space, hence providing a non-

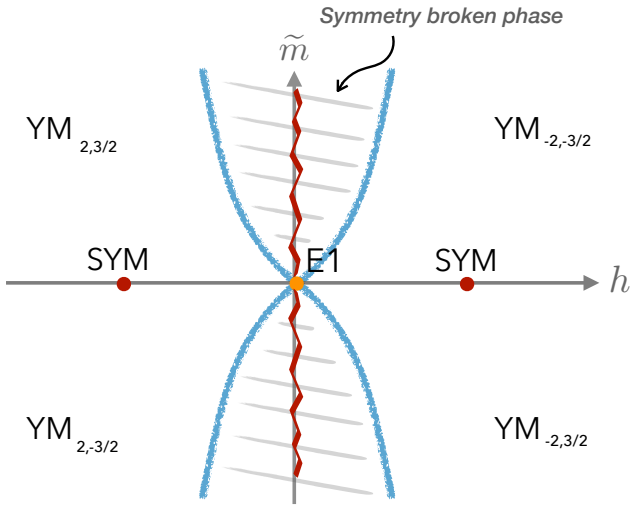

Figure 6.12: Phase diagram of softly broken E_1 SCFT. The four regions described by pure $SU(2)$ YM enjoy different $U(1)_I$ and $U(1)_R$ background CS levels, as indicated. The instability region (red wavy line) can be confined on the $\widetilde{m}$-axis or extend in part or all the symmetry broken phase, depending on the exact form of the potential. Along the blue thick lines, a phase transition occurs, which can be first or second order. In the latter case, note that the critical line does not represent a non-supersymmetric one dimensional conformal manifold. The deformation out of the E_1 fixed point is a relevant one, which is seen as irrelevant from the IR theory point of view. The ratio $h^2/\widetilde{m}$ is a marginal parameter but its value is tuned on the critical line. Hence, if a CFT actually exists, it is unique.

If the phase transition is second order and the corresponding CFT an interacting one, this could be viewed as a UV-completion of pure YM $SU(2)$. Upon integrating out the massive gaugini and the real scalar at one loop, the effective YM coupling reads

$$1/g^2_{\rm YM} = 1/g^2 - ag^2|\widetilde{m}| \ , \tag{6.27}$$

with a positive and $1/g^2 = h$. This suggests that the theory becomes strongly coupled at finite h, where the YM coupling diverges. Past infinite coupling the theory enters a different phase where one could expect, on general ground, an instantonic operator to condense. This nicely agrees with the phase diagram described in figure 6.12, which was obtained looking at the Higgs branch dynamics and which shows that in the confining phase an instantonic operator does condense, in fact.

vanishing VEV for H. That the end-point of this process is a reconnected, stable non-supersymmetric brane web is very unlikely and we exclude such possibility.

6.5 Phase transition from brane web

Another way to analyze this phase transition, as we mentioned in the previous section, comes from the analysis of the pq-web of the E_1 theory. For generic values of h and $\widetilde{m}$ there exist two brane webs compatible with charge conservation, a recombined smooth configuration after tachyon condensation and the original connected one, as described qualitatively in figure 6.13. Following the discussion above, we expect the former to dominate for $h^2 < \widetilde{m}$ and the latter for $h^2 > \widetilde{m}$. At $h^2 \sim \widetilde{m}$ a phase transition between these topological distinct configurations is expected and one could wonder whether using brane web dynamics the order of such phase transition can be determined.

Figure 6.13: On the left the recombined brane web after tachyon condensation. The $(1,1)$ and $(1,-1)$ 5-branes are separated in a direction transverse to the (x,y) plane. On the right the connected supersymmetry breaking configuration. Each three junction is supersymmetric but the whole system breaks supersymmetry since the boundary conditions of the D5-branes (dark grey line) on the two three junctions are mutually non-BPS.

The energy of the two configurations and, in turn, the way the transition between the two brane webs occurs depends on the interaction between the constituent branes. This is hard to compute, in particular in a non-supersymmetric setup as the one we are interested in. Let us then analyze the brane system by neglecting brane interactions, first.

In this limit, the energies of the two configurations are nothing but the tensions of the various branes shaping them. In the calculation, the 7-branes on which the 5-branes end furnish a regulator, since this way the otherwise semi-infinite 5-branes become finitely extended and their energy finite.

The 5-brane constituting the brane webs are of different kinds and so are their tensions. In particular, recall that the tension of a (p,q) 5-brane is

$$T_{(p,q)} = \sqrt{p^2+q^2}\, T_{(1,0)} \ , \tag{6.28}$$

where $T_{(1,0)}$ is the D5-brane tension and the complexified Type IIB string coupling has been set to its self-dual point, $\tau = i$. With this in mind, let us start considering the connected configuration in the supersymmetric limit, as shown in figure 6.14. The energy of this configuration is easily computed to be

$$E_{\text{con.}}(h,L) = 4\sqrt{2}L + 2h \tag{6.29}$$

in units of $T_{(1,0)}$. If we now rotate the right junction by an angle $\alpha \leq \pi$ around the x-axis as in

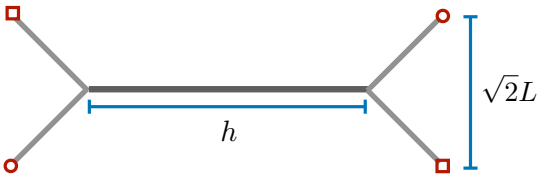

Figure 6.14: The connected configuration for $\alpha = 0$. The $(1,1)$ and $(1,-1)$ 5-brane segments have all length L.

the right figure 6.13, keeping the angle between the $(1,1)$ and the $(1,-1)$ 5-brane fixed,[10] the energy remains the same since all lengths remain fixed. Hence, the total energy of the connected configuration in the limit in which brane interactions are neglected equals (6.29) for any α.

In this same limit, the reconnected configuration compatible with charge conservation is nothing but the straight brane version of the brane web on the left of figure 6.13. This comes from merging of the $(1,1)$ 5-brane prongs into a unique straight $(1,1)$ 5-brane suspended between the $[1,1]$ 7-branes, and similarly for the $(1,-1)$ 5-branes, as shown in figure 6.15. The energy

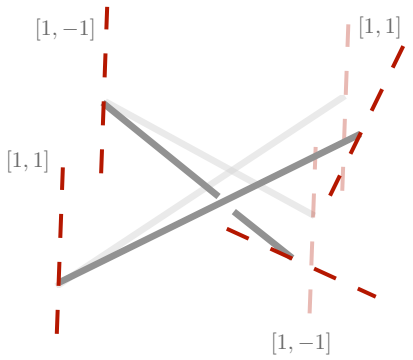

Figure 6.15: Recombined configuration neglecting brane interactions. Fixing the boundary conditions, that is the positions of the 7-branes, the minimal energy configurations are straight lines, as indicated.

$E_{\text{rec.}}$ of the configuration depends now on the rotation angle α and reads

$$E_{\text{rec.}}(h, L, \alpha) = 2\sqrt{2}\sqrt{(h+\sqrt{2}L)^2 + 2L^2\cos^2\frac{\alpha}{2}}\ . \tag{6.30}$$

Comparing eqs. (6.29) and (6.30) we see that the connected configuration is the one with minimal energy and hence is the true vacuum of the theory for $h > h^*$, while the reconnected one has minimal energy for $h < h^*$, where

$$h^* = \sqrt{2}L\sqrt{1-\cos\alpha}\ . \tag{6.31}$$

[10] This can be shown to be the configuration minimizing the energy.

At $h = h^*$ the two configurations, which exist and remain distinct for any value of h, are degenerate in energy and there is a phase transition between them (in the supersymmetric limit, $\alpha = 0$, the transition occurs at $h^* = 0$ and, consistently, the connected configuration is always dominant). The corresponding phase diagram is similar to figure 6.12 and suggests that the phase transition, at least at this level of the analysis, is actually first order.[11] In particular, in both cases the transition depends on the angle α. However, in the phase diagram of figure 6.12, the transition point h^* is proportional to the string length l_s, while in our configuration, which is completely semi-classical, there is no dependence on this parameter.[12]

One might wonder if anything could change once brane interactions are taken into account. In fact, it is expected brane interactions to affect the order of the phase transition, as it was shown to be the case in *e.g.* [308], where four dimensional gauge theories were studied using rather similar brane models. One of the key ingredients of the analysis of [308] was the possibility of selecting a regime where few constituent branes could be studied as probes in the background of many others, and take advantage of the gravitational background generated by the latter. This is something we cannot achieve in our case since our brane web is composed of one $(1,1)$, one $(1,-1)$ and, once $h \neq 0$, two $(1,0)$ 5-branes and none of them can be treated as a probe in the background of the others. So, in order to take advantage of an approach as in [308] a generalization of the E_1 theory is required. A natural such candidate is the so-called $X_{1,N}$ theory [256], whose structure will be reviewed in the next section.

6.6 Generalizations of E_1: the $X_{1,N}$ theory

The brane web of N $(1,1)$ branes intersecting M $(1,-1)$ branes at a 90 degrees angle realizes the so-called $X_{M,N}$ fixed point [256]. Specializing to the case $M = 1$, the web reduces to the

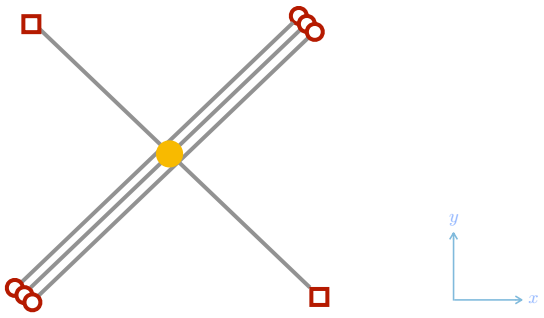

Figure 6.16: $X_{1,N}$ fixed point ($N = 3$ in the figure).

one in figure 6.16.

[11] The same result was found independently by Oren Bergman and Diego Rodriguez-Gomez.

[12] We find here a spurious dependence on the parameter L that we used to regulate. We will further comment about it when considering the effects of brane interactions, in section 6.7.

Similarly to the E_1 theory, one can switch on (the now several) supersymmetric relevant deformations. These trigger an RG-flow and drive the theory to a supersymmetric gauge theory in the IR. This corresponds to opening-up the brane web as shown in figure 6.17, while figure 6.18 is the quiver diagram describing such low energy effective theory. This is a $SU(2)^N$

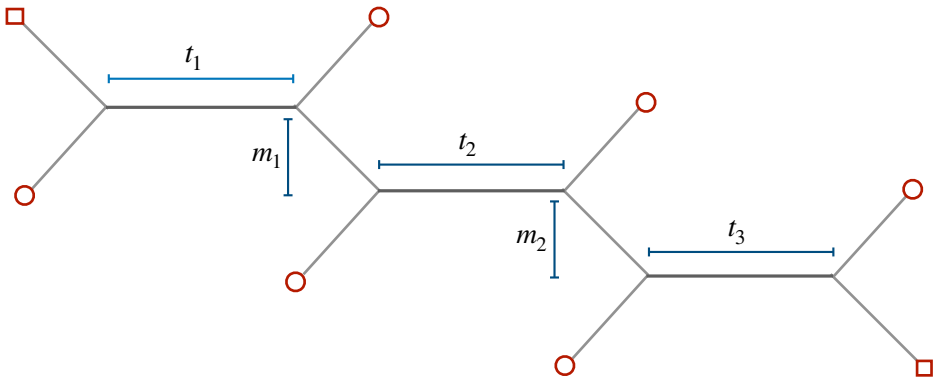

Figure 6.17: The $X_{1,N}$ brane web in the $SU(2)^N$ limit.

supersymmetric gauge theory with matter in the bifundamental.

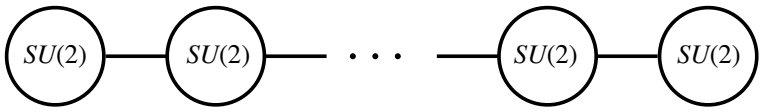

Figure 6.18: $SU(2)^N$ quiver.

The lengths of the $(1,0)$ branes, that we dub t_i in the following, correspond to the square of the inverse (effective) gauge couplings of the $SU(2)$ gauge factors. The vertical distance between the D5-branes associated with the $i-$th and the $(i+1)-$th groups defines instead the mass m_i of the corresponding bifundamental.

For generic values of t_i and m_i the global symmetry of the system is $U(1)_I^N \times U(1)_F^{N-1}$. Similarly to what happens for E_1, when $t_i = 0$ the instantonic $U(1)_I$ associated with the $i-$th node enhances to $SU(2)_I$. This is manifest from the brane web: when $t_i = 0$ one can make two 7-branes of the same type (either $[1,1]$ or $[1,-1]$) to lie on top of each other, hence enhancing the 8-dimensional gauge symmetry living on their world-volume, which corresponds to an instantonic symmetry in the five dimensional theory [211,302]. Similarly, when $m_i = 0$, two $(1,1)$ 5-branes become aligned, inducing an enhancement of the corresponding flavor symmetry from $U(1)_{BF}$ to $SU(2)_{BF}$.

At the fixed point, the global symmetry is believed to get enhanced to $SU(2N)$ [247]. This can be understood from the brane web by the possibility of superimposing the $2N$ $[1,1]$ 7-branes

at the fixed point, see figure 6.16.[13] This also implies that the Higgs branch, parametrized at weak coupling by the massless bifundamentals, gets enhanced. At the fixed point, this is the $2N$-dimensional minimal nilpotent orbit $\overline{\mathcal{O}_{[2^N]}(\mathfrak{su}(2N))}$, as can be shown by drawing the corresponding magnetic quiver. This is nothing but the space of $2N \times 2N$ complex matrices M with $M^2 = 0, \mathrm{Tr}M = 0$ or the Higgs branch of four dimensional $U(N)$ supersymmetric gauge theory with $2N$ flavors.[14]

In the following, we will consider a supersymmetry breaking deformation of the $X_{1,N}$ theory very similar to the one we discussed previously for the E_1 theory. Again, the existence of a phase transition in the space of parameters will be manifest. However, very much like what was done in [308], in this case, the possibility to play with the large N limit will let us get some insights on the nature of this phase transition. In particular, we will show that in a certain range of parameters the phase transition is actually second order, and a non-supersymmetric fixed point is then expected to exist in the phase diagram.

6.7 Phase transitions in the $X_{1,N}$ theory

Let us consider a deformation of the $X_{1,N}$ theory with parameters $t_i = -2m_i = h$ for all i. This makes the single junction of the fixed point theory to separated into two, as shown in figure 6.19: the $(1,1)$ 5-branes remain perpendicular to the $(1,-1)$ ones while $(N+1, N-1)$ represents the intermediate (p,q) 5-brane, whose length equals h. The $SU(2N)$ flavor symmetry is broken to $SU(N)_L \times SU(N)_R \times U(1)_B$ while the $SU(2)$ R-symmetry remains unbroken since the deformation takes place in the (x, y) plane, only.

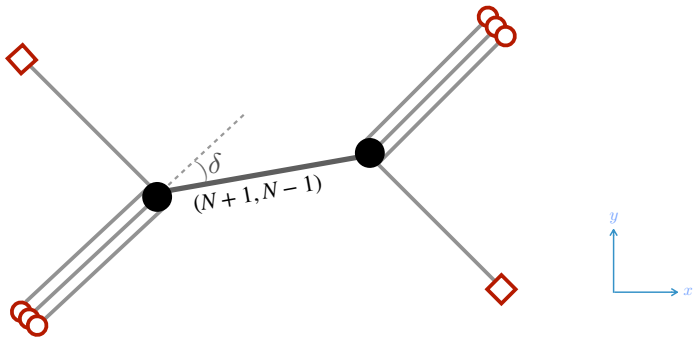

Figure 6.19: Opening the fixed point via a supersymmetric deformation with parameters $t_i = -2m_i = h$. The $(1,-1)$ 5-branes remain at a 90 degrees angle with the $(1,1)$ 5-brane stack, while the larger N the smaller the angle δ between the stack and the $(N+1, N-1)$ 5-brane of length h.

[13] Strictly speaking, this argument is a bit naive since no affine extension of the A_{N-1} algebra can be constructed from systems of 7-branes [277]. So the standard methods used in presence of exceptional symmetries [211] cannot be applied.

[14] We thank Antoine Bourget for elucidating this point to us.

It is worth noting that, for generic N, this deformation does not give any simple five dimensional field theory, but rather a limit in which some of the gauge couplings of the N $SU(2)$ gauge factors diverge[15]. An exception is the case $N = 1$ for which the mass deformation leads to pure $SU(2)$ SYM.

Exactly as we did for E_1, we can now break supersymmetry by rotating the right brane junction by an angle α around the axis along which the $(N+1, N-1)$ 5-brane is aligned. The deformation involves the transverse directions to the (x, y) plane and hence affects now also the $SU(2)$ R-symmetry, which gets broken to its Cartan. This has a natural field theory counterpart. The supersymmetry preserving deformation corresponds to giving a non-vanishing VEV to the lowest component of the background vector multiplet associated with the global symmetry current, which is a singlet under the $SU(2)$ R-symmetry. Here, instead, we give a VEV to a highest component which, as such, breaks supersymmetry. This is a triplet under $SU(2)$ and so the R-symmetry is broken to $U(1)$, very much like what happens for the E_1 theory [155, 302].

From the structure of the brane web, and comparing with figure 6.13, one could argue the effects of the supersymmetry breaking deformation to be qualitatively similar to what happens for the E_1 theory [302]. A scalar mode is expected to become tachyonic for small enough h and the brane web wants to recombine. The two competing configurations, compatible with brane charge conservation, are shown in figure 6.20. Their energies, in the limit in which brane interactions are neglected, are a generalization of eqs. (6.29)-(6.30) and read

$$\begin{aligned} E_{\text{rec.}} &= \sqrt{2}\,[f(\sin\delta) + N f(\cos\delta)] \quad , \quad f(a) \equiv \sqrt{(h+2La)^2 + 4L^2(1-a^2)\cos^2\frac{\alpha}{2}}\,, \\ E_{\text{con.}} &= \sqrt{2}\left[2NL + 2L + \sqrt{N^2+1}\,h\right] \quad , \end{aligned} \tag{6.32}$$

where the reconnected configuration is the natural generalization to $N > 1$ of the straight brane configuration of figure 6.15. It is possible to show that also in this case there exists a (single)

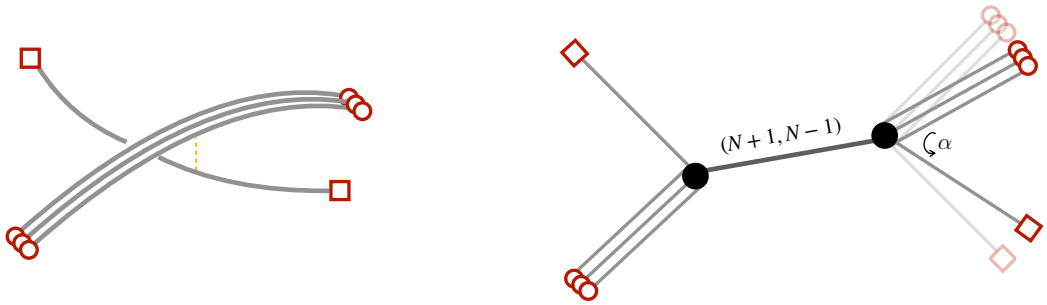

Figure 6.20: The two competing brane webs after the supersymmetry breaking deformation. The recombined system consists of one $(1, -1)$ 5-brane and N $(1, 1)$ 5-branes, separated in a direction transverse to the (x, y) plane.

[15]For instance, for $N = 2$ after the deformation $t_1 = t_2 = -2m$, we get a theory where both gauge couplings of the two $SU(2)$ nodes diverge.

critical value h^* that separates two regions in the space of parameters where one brane web dominates against the other, and viceversa.

So far this is no different from what we discussed in section 6.5, and neglecting interactions the phase transition looks again first order. The point, now, is that we can consider N to be parametrically large. This has two effects. The first is that it makes easier to compute brane interactions in the recombined brane system, left of figure 6.20, since in the large N limit this can be treated as a probe $(1,-1)$ 5-brane in the gravitational background of N $(1,1)$ 5-branes. The second effect is that it makes the angle δ between the two stacks of N $(1,1)$ 5-branes and the $(N+1,N-1)$ 5-brane, see figure 6.19, going to zero

$$\cos\delta = \frac{N}{\sqrt{N^2+1}} \quad , \quad \lim_{N\to\infty} \delta = 0 \ , \tag{6.33}$$

while the $(N+1,N-1)$ 5-brane are indistinguishable from a stack of N $(1,1)$ 5-branes. Hence, in the strict $N\to\infty$ limit the system in figure 6.19 reduces to that in figure 6.21. Physically, in this limit brane charge conservation at brane junctions does not force the N stack to bend anymore (and to change its nature) due to the $(1,-1)$ branes which end on it. In this regime, the energies (6.32) of the two configurations simplify as

$$\begin{aligned} E_{\text{rec.}} &= \sqrt{2}\left[N(h+2L)+\sqrt{h^2+4L^2\cos^2\frac{\alpha}{2}}\right]+\mathcal{O}\left(1/N\right) \ , \\ E_{\text{con.}} &= \sqrt{2}\left[N(h+2L)+2L\right]+\mathcal{O}\left(1/N\right) \ . \end{aligned} \tag{6.34}$$

The transition point h^* reads then $h^* = 2L\sin\alpha/2$.

We note, in passing, that in this limit our system becomes very similar to the one considered in [308], yet in one dimension higher. This will be useful later.

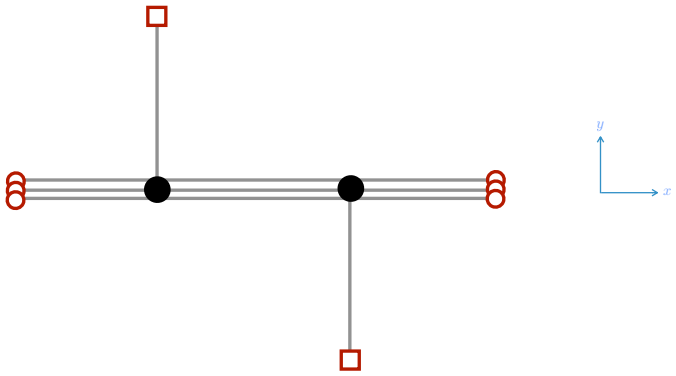

Figure 6.21: The deformed $X_{1,N}$ theory in the large N limit. The system becomes that of N $(1,1)$ 5-branes on which two $(1,-1)$ 5-branes ends.

6.7.1 Phase transitions in the backreacted $X_{1,N}$ brane-web

In this section we will take brane interactions into account and see how the nature of the phase transition discussed previously may change.

As already noticed, in the large N limit the original supersymmetric configuration simplifies to the one depicted in figure 6.21. Rotating by an angle α the non-supersymmetric connected and reconnected brane webs look instead as in figure 6.22.

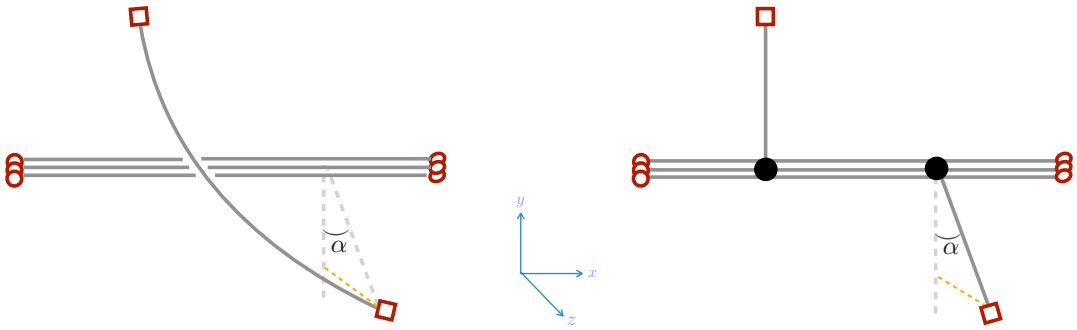

Figure 6.22: The two competing brane webs after the supersymmetry breaking deformation, in the large N limit. The difference in energy depends only on that of the $(1,-1)$ 5-brane, since that of the (rigid, in this limit) $(1,1)$ 5-brane stack contributes equally to the two webs.

The difference in energy between the two configurations depends on the $(1,-1)$ 5-brane only, since the $(1,1)$ 5-brane stack is unperturbed in this limit, as in the non-interacting case. Hence, its contribution will be factored out in what follows, and we will just compute the $(1,-1)$ 5-branes energy. The system can be treated as a probe $(1,-1)$ 5-brane in the gravitational background of N $(1,1)$ 5-branes which can exert a force on (and hence bend) the probe brane. Note, however, that by the very geometry of the problem, this does not happen for the connected brane web, right of figure 6.22, whose energy is then the same as when interactions are neglected, eq. (6.32). In what follows, we will hence compute the effects of brane interactions on the left brane web of figure 6.22.

Let us start considering the background generated by the $(1,1)$ branes stack. We can align these branes along the $01234x$ directions, while the $(1,-1)$ branes, in the supersymmetric configuration, are aligned along $01234y$. It is useful to introduce cylindrical coordinates as

$$(x,y,z) = (x,\rho\cos\phi,\rho\sin\phi)\,. \tag{6.35}$$

In these coordinates the N $(1,1)$ 5-branes are located along $(x,0,0)$ while the $(1,-1)$ 5-brane, after the supersymmetry breaking deformation, has boundary conditions on the $[1,-1]$ 7-branes it ends on $P_1 \equiv (x_1,\rho_1,0)$ and $P_2 \equiv (x_2,\rho_2\cos\varphi,\rho_2\sin\varphi)$, where

$$\varphi = \pi - \alpha\ . \tag{6.36}$$

The supersymmetric limit corresponds to $\varphi=\pi$. In these cylindrical coordinates, the backreacted metric of the N $(1,1)$ 5-branes takes the form[16]

$$ds_{10}^2 = H^{-1/4}ds^2_{\mathbb{R}_{1,4}} + H^{-1/4}dx^2 + H^{3/4}(d\rho^2+\rho^2d\phi^2+ds^2_{\mathbb{R}_2})\,,\quad H = 1+\frac{\ell^2}{\rho^2}\,, \tag{6.37}$$

[16]We present the metric in Einstein frame, and take asymptotic values of the axio-dilaton to equal $\tau_0 = i$, as before.

where $\ell = 2^{1/4} l_s \sqrt{N}$. To simplify notations we will set measure quantities in units of ℓ, and reïnstate the correct factors through dimensional analysis when needed. The axio-dilaton equals

$$\tau = \frac{1+H}{1-H} + 2\,i\frac{\sqrt{H}}{1+H}\,, \tag{6.38}$$

while the three forms have support on the S^3 sphere surrounding the stack

$$\frac{1}{(2\pi l_s)^2}\int_{S^3} F_3 = N, \quad \frac{1}{(2\pi l_s)^2}\int_{S^3} H_3 = N. \tag{6.39}$$

The brane action of the $(1,-1)$ 5-brane consists of a DBI term and a WZW term, given by [309]

$$S_{(1,-1)} = -T_{(1,0)}\int d^6\xi\,\Delta(\tau,\bar\tau)\sqrt{-\det\left(P[g_{\mu\nu}] + \frac{P[C_2 - B_2]}{\Delta(\tau,\bar\tau)}\right)} + T_{(1,0)}\int (C_6 - B_6)\ . \tag{6.40}$$

where

$$\Delta(\tau,\bar\tau) = \sqrt{\frac{2i(1-\tau)(1-\bar\tau)}{\tau-\bar\tau}}\ . \tag{6.41}$$

Note that the two-form gauge potentials are transverse to the $(1,-1)$ 5-branes, and the six-form gauge potentials are equal, thus the brane action will only depend on the ten-dimensional metric and axio-dilaton.

Filling in the metric pull-back and the value of τ one finds that

$$S_{(1,-1)} = -\sqrt{2}T_{(1,0)}\int dx\sqrt{H^{-1} + \dot\rho^2 + \rho^2\dot\phi^2}\ , \tag{6.42}$$

where we have denoted derivatives with respect to x with a dot. Modulo an overall normalization, the DBI (6.42) is the same as for a D5 brane in the background of a NS5 brane [308]. Indeed, the two configurations are $SL(2,\mathbb{R})$ dual. Since the corresponding Lagrangian, $\mathcal{L}_{(1,-1)}$, does not explicitly depend on x and ϕ we find the following two constants of motion

$$\mathcal{I} = H\mathcal{L}_{(1,-1)}\,, \tag{6.43}$$

$$\mathcal{Q} = H\rho^2\dot\phi\ . \tag{6.44}$$

We search for brane configurations ending on the points P_1 and P_2. These develop a minimum x_m at which $\dot\rho(x_m) = 0$. This represents the turning point of the solution, namely the minimal distance of the probe from the brane stack. Taking $\rho_m = \rho(x_m)$, we find that

$$\sqrt{1 + \rho_m^2 + \mathcal{Q}^2} = \rho_m\mathcal{I}\,. \tag{6.45}$$

To solve the full equations of motion we split the solution into two branches $x \in [x_i, x_m]$, where $i = 1, 2$ and, as mentioned below eq. (6.35), x_i labels the positions of the $[1,-1]$ 7-branes along

the x direction. We can then use eqs. (6.44) and (6.45) to solve eq. (6.43) through separation of variables

$$\begin{aligned}\sqrt{1+\mathcal{Q}^2}(x_m - x_1) &= \int_{\rho_m}^{\rho_1} d\rho \frac{H}{\sqrt{H_m - H}} = \rho_m \sqrt{\rho_1^2 - \rho_m^2} + \theta_1 \ , \\ \sqrt{1+\mathcal{Q}^2}(x_2 - x_m) &= \int_{\rho_m}^{\rho_2} d\rho \frac{H}{\sqrt{H_m - H}} = \rho_m \sqrt{\rho_2^2 - \rho_m^2} + \theta_2 \ ,\end{aligned} \tag{6.46}$$

where, for later convenience we have defined $\theta_i = \arccos(\rho_m/\rho_i)$. Similarly, we find, using the equation of motion for ρ, that

$$\sqrt{1+\mathcal{Q}^2}\phi_m = -\mathcal{Q}\,\theta_1 \ , \quad \sqrt{1+\mathcal{Q}^2}(\phi_m - \varphi) = \mathcal{Q}\,\theta_2 \ , \tag{6.47}$$

To further analyze the system we will assume the simplification $\rho_1 = \rho_2 \equiv L$, and thus $\theta_1 = \theta_2 \equiv \theta$, such that

$$\sqrt{1+\mathcal{Q}^2}h = L^2 \sin 2\theta + 2\theta \, , \quad \sqrt{1+\mathcal{Q}^2}\varphi = 2\mathcal{Q}\,\theta \, , \tag{6.48}$$

where $h \equiv x_2 - x_1$. Solving the second equation in (6.48) for $\mathcal{Q}$ we can rewrite the first equation as (reinstating the appropriate factors of ℓ defined below eq. (6.37))

$$\ell h(\theta) = \sqrt{1 - \left(\frac{\varphi}{2\theta}\right)^2}(L^2 \sin 2\theta + 2\ell^2\theta) \ , \tag{6.49}$$

which is transcendental and does not have a closed-form expression when solving for θ. Since the constant of motion $\mathcal{Q}$ is real, and $0 \leq \varphi \leq \pi$ we conclude that $\varphi \leq 2\theta \leq \pi$. In the supersymmetric limit, this equation trivializes and one has a solution only for $h = 0$. This is consistent since in this regime the reconnected and the connected brane webs become the same, while for $h \neq 0$ the reconnected one does not exist.

The energies for the reconnected and connected configurations can be now easily computed as (minus) their evaluated brane actions and read

$$\ell E_{\text{rec.}} = 2\sqrt{2}T_{(1,0)}\sqrt{H_m - \left(\frac{\varphi}{2\theta}\right)^2}\rho_m L \sin\theta \ , \ E_{\text{con.}} = 2\sqrt{2}T_{(1,0)}L \ , \tag{6.50}$$

where, as already noticed, the energy of the connected configuration is unaffected by brane interactions and hence equals that in eq. (6.32). This implies that

$$\left(\frac{E_{\text{rec.}}}{E_{\text{con.}}}\right)^2 = \left(1 - \frac{\varphi^2}{4\theta^2 H_m}\right)\left(1 + \frac{\rho_m^2}{\ell^2}\right)\left(1 - \frac{\rho_m^2}{L^2}\right) \ . \tag{6.51}$$

The natural variables of interest are the distance between the two $[1,-1]$ 7-branes along the x direction, h, the relative rotation between them φ, and their distance from the $(1,1)$ 5-branes stack, L. To rewrite the ratio of energies in terms of these physical variables one must solve eq. (6.49) to find $\theta(h,\varphi,L)$. This requires a combination of analytical and numerical methods and will be dealt with below.

We will first focus on the case $\alpha = \pi$, that can be studied almost completely analytically. This will be important when we move on studying the system for general values of α, which will turn out to be qualitatively similar, albeit one must resort to numerical methods.

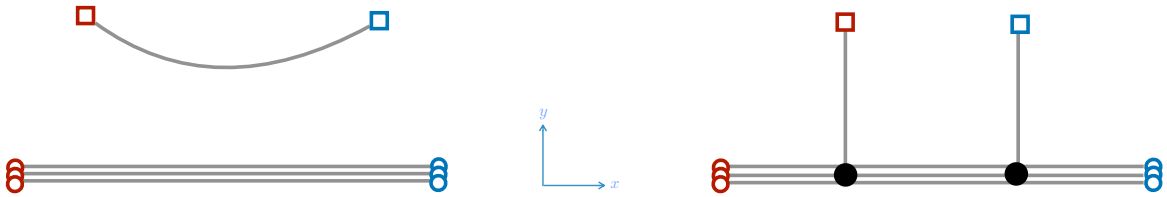

Figure 6.23: The reconnected and connected brane webs for $\alpha = \pi$. In this case, everything happens on the (x, y) plane only. Blue squares and circles refer to 7-branes orthogonal to the (x, y) plane which look however as anti-branes compared to unrotated ones.

The $\alpha = \pi$ case

Taking $\alpha = \pi$, the brane setup is $SL(2, \mathbb{R})$ dual to a D5-NS5 system that is T-dual to the D4-NS5 brane system studied in [308]. Following a completely analog analysis as in [308] we will give strong evidence that, in a certain range of parameters, the $X_{1,N}$ brane-web undergoes a second order phase transition. Even though the computation is cognate to the one in [308] we will go through it in detail since it will provide a good intuition for the physics in the situations that $\alpha \neq \pi$.

First, notice that taking $\alpha = \pi$ several quantities simplify. The transcendental eq. (6.49) now becomes Kepler's equation[17]

$$\ell h(\theta) = L^2 \sin 2\theta + 2\ell^2 \theta \,, \tag{6.52}$$

where $0 \leq \theta \leq \pi/2$. A maximum for h is reached at

$$\ell h_0 = L^2 \sin 2\theta_0 + 2\ell^2 \theta_0 \,, \quad \text{with} \quad L^2 \cos 2\theta_0 = -\ell^2 \,, \tag{6.53}$$

which can only be solved when $L \geq \ell$. In the following, we will split the analysis into two cases, $L \leq \ell$, and $L > \ell$, which will turn out being qualitatively different.

- $L \leq \ell$: We find that h monotonically increases from $h(0) = 0$ to $h(\pi/2) = \pi\ell$. In the regime $0 \leq h \leq \pi\ell$ there are thus two solutions to the brane action, the reconnected and the connected ones, whose brane webs are depicted in figure 6.23. The ratio of their respective energies is given by

$$\left(\frac{E_{\text{rec.}}}{E_{\text{con.}}}\right)^2 = \left(1 + \frac{\rho_m^2}{\ell^2}\right)\left(1 - \frac{\rho_m^2}{L^2}\right) < 1 \,. \tag{6.54}$$

  This ratio is always smaller than one, so we find that the energetically favorable configuration is the reconnected one. At $h = \pi\ell$ we find that $\rho_m = 0$, the ratio goes to one and, consistently, the reconnected and the connected brane webs become degenerate. For

[17] This equation can actually be solved analytically for θ, in terms of a series of Bessel functions, within the range $-\ell\pi < h < \ell\pi$.

$h > \pi\ell$ eq. (6.52) ceases to have a solution, and thus only the connected configuration solves the equations of motion.

Schematically we depict the distinct phases of the brane configurations through a potential in figure 6.24. Whenever $h < \pi\ell$, the potential has a minimum coinciding with the

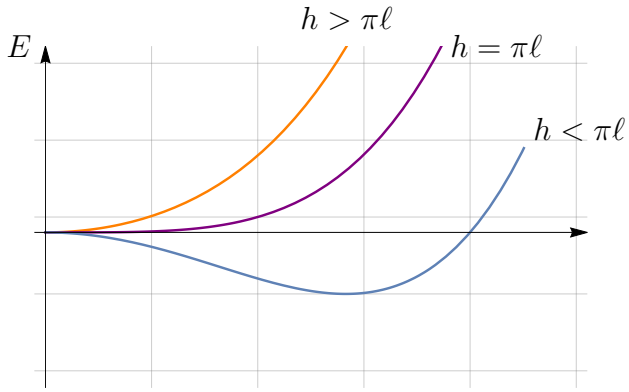

Figure 6.24: The potential energy as a function of the configuration space of the web as h is varied, for $L \leq \ell$.

reconnected configuration and a maximum coinciding with the connected one. As the value h increases, the minimum of the potential does as well, until $h = \pi\ell$, at which point the two extrema merge and the potential has a single minimum corresponding to the connected configuration. We thus find that the system undergoes a second order phase transition when h passes the value $\pi\ell = \pi\, 2^{1/4}\ell_s\sqrt{N}$. We note, for future purposes, that this value is independent of L.

- $L > \ell$: the function $h(\theta)$ has a maximum, h_0, given by eq. (6.53). This maximum decreases whenever L does, until $L = \ell$, at which it is at $\theta_0 = \pi/2$. Whenever $h > h_0$ there is no solution to eq. (6.52), and therefore only the connected configuration exists. Instead, in the region

$$h_0 \geq h \geq \pi\ell \ , \tag{6.55}$$

Kepler's equation has two solutions labeled by θ_S, θ_L, denoting the previous angles as, respectively, the smallest and the largest ones associated with the same value of h. These solutions are associated with two distinct reconnected 5-brane configurations.

For $h < \pi\ell$ one can show that

$$\left(\frac{E_{\text{rec.}}}{E_{\text{con.}}}\right)^2 = \left(1 + \frac{\rho_m^2}{\ell^2}\right)\left(1 - \frac{\rho_m^2}{L^2}\right) = \left(1 + \frac{L^2\cos^2\theta}{\ell^2}\right)\sin^2\theta \leq 1\,. \tag{6.56}$$

The reason is that the ratio is monotonically increasing in θ and smaller than or equal to 1 for

$$\theta \leq \theta^*\,, \quad \text{where} \quad \theta^* = \arcsin\ell/L < \theta_0\,, \tag{6.57}$$

where $h^* = h(\theta^*) > \pi\ell$. Hence for $h < \pi\ell$ the reconnected brane configuration is always energetically favorable with respect to the connected one.

When $h > \pi\ell$ the analysis is slightly more involved. There are now three brane configurations whose energies $(E_{\text{con.}}, E^S_{\text{rec.}}, E^L_{\text{rec.}})$ we have to compare, where the energies $E^S_{\text{rec.}}$, $E^L_{\text{rec.}}$ are associated with the smooth solutions with θ_S, θ_L respectively. Since $\pi/2 > \theta_L > \theta_0$, and the ratio of energies decreases in this region, we have that

$$\left(\frac{E^L_{\text{rec.}}}{E_{\text{con.}}}\right)^2 > \left(\frac{E_{\text{rec.}}(\pi/2)}{E_{\text{con.}}}\right)^2 = 1\,, \tag{6.58}$$

with $E_{\text{rec.}}(\pi/2)$ represents the energy of the reconnected configuration with $\theta = \pi/2$. This tells us that connected configuration is always energetically favorable compared to the reconnected one with $\theta = \theta_L$. Moreover, it can be shown that $E^L_{\text{rec.}} > E^S_{\text{rec.}}$, using the fact that the sum and differences of θ_L and θ_S are bounded by

$$0 \leq \theta_L + \theta_S \leq \pi\,, \quad \text{and} \quad 0 \leq \theta_L - \theta_S \leq \pi/2\,, \tag{6.59}$$

and that $h(\theta_L) = h(\theta_S)$. The discussion above shows that $E^S_{\text{rec.}}/E_{\text{con.}}$ can be either bigger or smaller than 1, depending on the value of $h(\theta_S)$. We denote with $h^* = h(\theta^*)$ the value of $h(\theta_S)$ for which $E^S_{\text{rec.}}/E_{\text{con.}} = 1$. Schematically the different phases are depicted through a potential in figure 6.25.

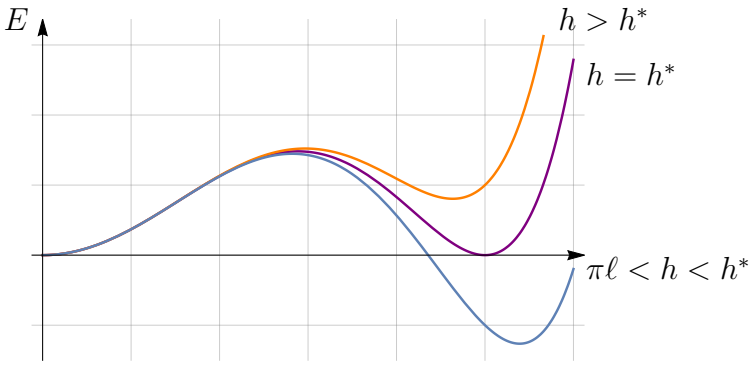

Figure 6.25: The potential energy as a function of the configuration space of the web for some values of h, for $L > \ell$.

The connected configurations correspond to the left minimum of the potentials, the smooth reconnected solutions with $\theta = \theta_L$ correspond to the maxima of the potentials, and the smooth reconnected solutions associated with θ_S correspond to the right minima. Depending on h, these minima can be either local or global, showing that the brane configuration undergoes a first order phase transition when h passes through h^*. Note that contrary to the case $L \leq \ell$, the point at which the phase transition occurs, h^*, now depends on L through eq. (6.57).

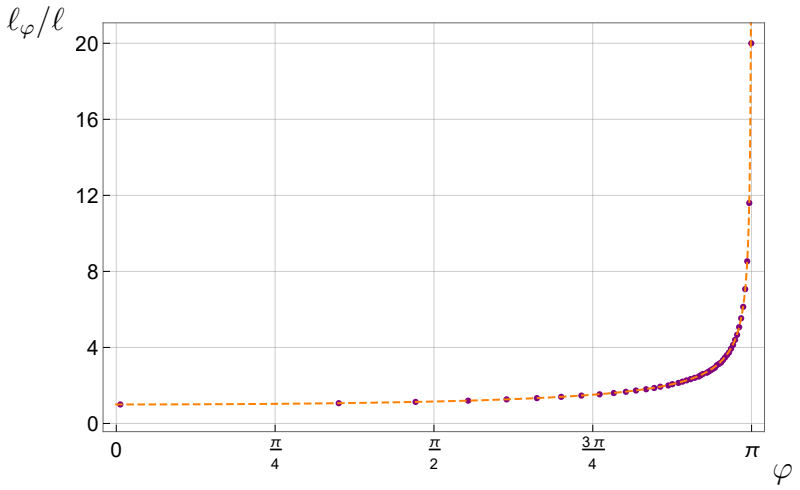

Figure 6.26: Plot of ℓ_φ/ℓ as a function of φ. The yellow dotted line represents the analytical function $\pi/\sqrt{\pi^2-\varphi^2}$, and the purple dots show the numerical results.

Generic values of α

We now want to generalize the previous analysis to generic values of α. The transcendental equation is now

$$\ell h = \sqrt{1-\left(\frac{\varphi}{2\theta}\right)^2}\left(L^2\sin 2\theta + 2\ell^2\theta\right), \tag{6.60}$$

and h has an extremum at

$$L\cos 2\theta\left[2\theta(4\theta^2-\varphi^2)+\varphi^2\tan 2\theta\right] = -8\ell\theta^3\,. \tag{6.61}$$

Eq. (6.60) is not solvable analytically, so we will have to resort partly to numerical analysis. In this way, one can show that this equation has a zero only for

$$L \geq \ell_\varphi = \frac{\pi\ell}{\sqrt{\pi^2-\varphi^2}} \geq 1\,, \tag{6.62}$$

where ℓ_φ plays the same role as ℓ of previous section ($\ell_{\varphi=0}=\ell$). The function h has at most one extremum, which is a maximum when $L \geq \ell_\varphi$. This follows from the fact that for $\pi/2 > \theta > \theta_0$, where θ_0 is the value for which h reaches its maximum h_0, the second derivative of h with respect to θ is strictly negative.

Qualitatively, h behaves similarly to the case $\alpha=\pi$, just replacing $\ell \to \ell_\varphi$. In the following, we then distinguish the case $L \leq \ell_\varphi$ from the case $L > \ell_\varphi$.

- $L \leq \ell_\varphi$: There are two brane configurations, a connected configuration and a reconnected one. Additionally, since the reconnected energy is monotonically increasing in h and h itself is monotonically increasing in L, we find that

$$\left(\frac{E_{\text{rec.}}}{E_{\text{con.}}}\right)^2 \leq \left[1+\frac{\theta^2-4\varphi^2}{(\pi/2)^2-4\varphi^2}\frac{(\pi/2)^2}{\theta^2}\cos^2\theta\right]\sin^2\theta \leq 1\,. \tag{6.63}$$

The ratio only saturates the bound at $\theta = \pi/2$. Therefore, when $L \leq \ell_\varphi$ there are two possible brane configurations, the connected and reconnected one and the latter is energetically favorable. When h increases and crosses the value $\tilde{h} = \ell\sqrt{\pi^2 - \varphi^2}$, a second order phase transition occurs, after which only the connected brane configuration remains. We thus find a behavior that is qualitative the same as in the case $\alpha = \pi$.

The minimal distance ρ_m between the recombined $(1, -1)$ brane and the stack decreases continuously from $\rho_m = L\cos\varphi/2$ at $h = 0$ down to $\rho_m = 0$ at the transition $h = \tilde{h}$. In the process, the reconnected brane comes closer and closer to the stack and flattens along the direction of the latter, until ρ_m reaches zero. At this point, the reconnected configuration becomes indistinguishable from the connected one, as it can be shown taking the $\rho_m \to 0$ limit in the equations of motion (6.43)-(6.44), realizing the second order phase transition.

- $L > \ell_\varphi$: the function h does have a maximum h_0, and when

$$h_0 \geq h \geq \tilde{h}\,, \quad \text{with} \quad \tilde{h} = \ell\sqrt{\pi^2 - \varphi^2}\,, \tag{6.64}$$

there exist two reconnected configurations, together with the connected one. The two reconnected configurations are again associated with two values $\theta_S \leq \theta_L$, for which $h(\theta_S) = h(\theta_L)$. Analogously to the $\alpha = \pi$ case, we denote the energies of the three configurations as $E_{\text{con.}}$, $E^S_{\text{rec.}}$, and $E^L_{\text{rec.}}$. Numerically, it is possible to show that

$$\left(\frac{E^L_{\text{rec.}}}{E^S_{\text{rec.}}}\right) \geq 1\,, \qquad \left(\frac{E^L_{\text{rec.}}}{E_{\text{con.}}}\right) \geq 1\,, \tag{6.65}$$

and that $E^S_{\text{rec.}}/E_{\text{con.}}$ can be either bigger or smaller than 1, depending if $h(\theta_S)$ is above or below a critical value h^*. In figure 6.27 we show the generic behavior of the ratio of energies in function of h, here specifically at values $L/\ell = 2$, and $\varphi = \pi/16$, illustrating the behavior mentioned above.

Whenever $h < \tilde{h}$, one can argue, in a similar way as we did in the $L \leq \ell_\varphi$ case, that there is only one reconnected configuration, and that its energy is always favored over the connected one. Therefore we can conclude that if $L > \ell_\varphi$, the brane system undergoes a first order phase transition when h increases and crosses a value h^*, as in the $\alpha = \pi$ case.

All in all, we then see that the brane system behaves qualitatively the same, independent of the value of α. For the ease of the reader, we summarize below the different cases and the associated phase transitions.

Summary

When $L \leq \ell_\varphi$ and $h < \tilde{h} = \ell\sqrt{\pi^2 - \varphi^2}$, there are two brane configurations, a reconnected configuration and a connected one, and the former is always energetically favorable compared to the latter. As the value of h increases and passes $\tilde{h}$, the two configurations become the same and a second order phase transition occurs at $h = \tilde{h}$.

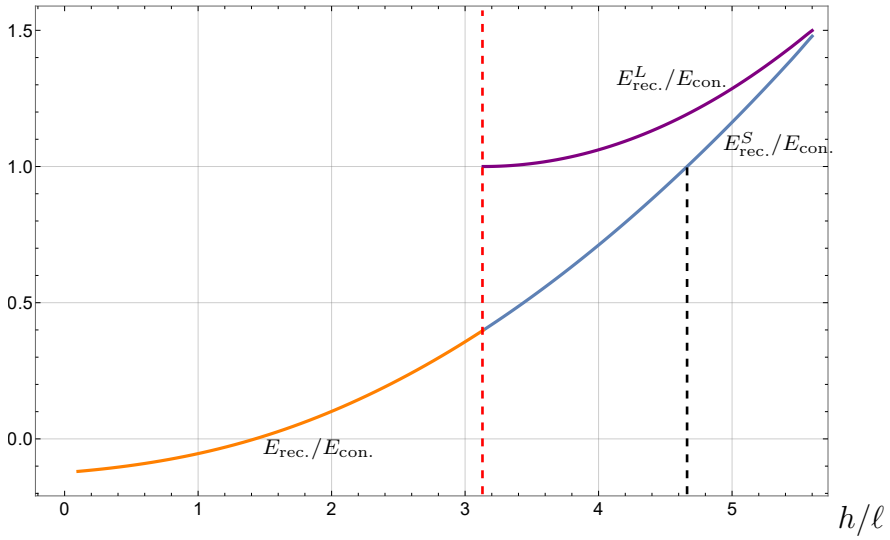

Figure 6.27: Ratio of energies for the different configurations as a function of h/ℓ, for the values $L = 2\ell$ and $\varphi = \pi/16$. The red dashed line represents the value $\tilde{h}/\ell = \sqrt{\pi^2 - \varphi^2}$ above which two reconnected configurations exist. The black dashed line represents the value h^*/ℓ, where $E^S_{\text{rec.}}/E_{\text{con.}} = 1$ and the first order phase transition occurs.

When $L > \ell_\varphi$ and $h < \tilde{h}$ there is one reconnected configuration that is always energetically favorable with respect to the connected one, as for $L \leq \ell_\varphi$. However, when $h \geq \tilde{h}$, there are three brane configurations: two reconnected and one connected. The θ_L reconnected configuration is unstable, having maximal energy. The θ_S and the connected configurations represent a global and a local minimum, respectively, whenever $h < h^*$. For $h > h^*$, the role of the two solutions exchange and the connected one becomes an absolute minimum. So, as h increases, the brane configurations undergo a first order phase transition at $h = h^*$.

It is worth noting that for small supersymmetry breaking parameter, $\alpha \sim 0$, one gets that $\ell_\varphi \sim \alpha^{-1/2} \to \infty$ and the range in which the phase transition is second order, *i.e.* $L \leq \ell_\varphi$, can be made parametrically large.

6.7.2 On the tachyonic origin of the phase transition

In section 6.7.1, by computing energies of brane webs in the limit of a large number N of $(1,1)$ 5-branes, we have shown that a phase transition of first or second order occurs between a connected and a reconnected configuration, as one varies h, at fixed L. As in the simplest setup of the E_1 theory [302], the instability of the connected brane web against decay to the reconnected one is expected to originate from a tachyonic mode of an open $(1,-1)$ string stretched between the $(1,-1)$ 5-branes which develops for small enough h.

Let us start considering two D5 branes at an angle α. At weak string coupling, the spectrum of the strings ending on the branes can be explicitly calculated and the modes localized at the intersection are tachyonic with mass $m_T^2 \sim -2\pi\alpha\, \ell_s^2 T_s^2$. This holds both at small angles α and at large angles $\alpha \sim \pi$. Separating the D5 at a distance h, the lowest excitations develop an

additional positive mass $\sim h^2 T_s^2$ since the minimal length of these strings is now h. So, when $h^2 = \tilde{h}^2_{\text{flat}} \sim 2\pi\alpha\ell_s^2$, the lowest mode becomes massless and the system is locally stable. This is expected to remain true also at strong g_s coupling, as was argued in [308] in the case of two D4 branes at angles.

Since this brane system is $SL(2,\mathbb{Z})$ dual a system of two $(1,-1)$ 5-branes, one can argue that also in this latter system a tachyonic mode is present at small enough distance between the branes, while for $h^2 \sim \alpha\ell_s^2$ the configuration should become locally stable.

Our previous analysis shows that this is what actually happens for $L \leq \ell_\varphi$:[18] there is a phase transition at $h = \tilde{h}$ and, for $h > \tilde{h}$, the connected configuration becomes an absolute minimum of the energy system. At this point, $\tilde{h} \sim \sqrt{\alpha}$ for both $\alpha \sim 0$ and $\alpha \sim \pi$, so we expect the tachyon to condense and to be responsible for the second order phase transition.

For $L > \ell_\varphi$, the connected configuration ceases to be a maximum at $h \sim \tilde{h}$ but remains globally unstable until $h = h^*$. At that point, this is energetically favorable and becomes the absolute minimum of the configuration energy. So at $h \sim \tilde{h}$, the local instability is resolved when the tachyon becomes massless, but a non-perturbative one remains until $h \sim h^*$. This realizes the first order phase transition we saw in section 6.7.1.

Note that our transition point $\tilde{h}$ is of order $\sqrt{N}$, while the tachyonic mass between the branes is expected to be $\sim \mathcal{O}(1)$. The same mismatch was found in [308] in the case of two D4 branes at an $\alpha = \pi$ angle in a background of N NS5 branes. This apparent tension of the parameters was related to the presence of the NS5 stack[19] which was found to modify the tachyonic contribution to the mass as

$$m_T^2 \sim -\pi\alpha\,\ell^2 T_s^2. \tag{6.66}$$

Again, this was argued to remain true also at strong g_s coupling.

Although the system in [308] is only $SL(2,\mathbb{R})$ dual to ours, we find the same behavior for our brane set-up at $\alpha = \pi$ and a similar transition at $\alpha \neq \pi$. We are then led to conclude that also in our case the second order phase transition is mediated by a tachyon becoming massless at $h \sim \tilde{h}$. Figures 6.24 and 6.25 provide a qualitative behavior of the tachyon potential whose minimum, the tachyon VEV, goes smoothly to zero as h is varied or jumps abruptly when the transition is, respectively, second order, figure 6.24 or first order, figure 6.25.

6.8 Discussion

At the beginning of this Chapter, we first studied the phase diagram of the E_1 theory as a function of the two deformation parameters h and $\tilde{m}$. A phase transition was found to separate a symmetry broken phase, where the symmetry $U(1)_I \times U(1)_R$ is spontaneously broken to a diagonal subgroup $U(1)$, from a symmetry preserving phase. However, we were not able to have satisfactory control of the dynamics of this point, neither via field theory nor via pq-web techniques, due to its strongly coupled nature. As a consequence, it was not possible to understand

[18] Remind that $\ell_\varphi = \frac{\pi\ell}{\sqrt{\pi^2-\varphi^2}}$ with $\ell = 2^{1/4}\ell_s\sqrt{N}$.

[19] In their case, the angle was fixed to $\alpha = \pi$.

the order of this phase transition.
More control was gained starting from section 6.6, by studying a generalization of this supersymmetry breaking deformation considering a similar setup for the $X_{1,N}$ theory. The response of the system upon this supersymmetry breaking deformation is qualitatively similar to the E_1 case. In particular, turning on both the supersymmetry preserving and the supersymmetry breaking deformations at once, it was shown that the parameter space is divided into two different regions separated by a phase transition. In the $X_{1,N}$ case thanks to the possibility of taking N large, it was possible to characterize the phase transition, which, in a certain regime of parameters, was shown to be second order. This gives evidence for the existence of non-supersymmetric fixed points in five dimensions.

One could wonder whether finite N corrections could change the state of affairs. Following arguments similar to those in [308], whose brane system is similar to ours in section 6.7, one could argue that no qualitative difference is expected. Note, however, that while finite N corrections modify both brane systems, an advantage of the system considered in [308] is that a small string coupling limit can be taken in which $1/N$ corrections can in principle be computed. This is not the case for the $X_{1,N}$ web, whose structure changes as the string coupling is modified.

Another aspect which deserves attention has to do with the dependence of our result on the fixed length L of the 5-brane prongs. In particular, as L crosses ℓ_φ from the bottom, the phase transition turns from being second order to being first order. For one thing, in the supersymmetric limit L is not a relevant parameter, as the five dimensional dynamics of the system is independent of L (indeed, one can send the 7-branes on which the 5-brane prongs end all the way to infinity without any change in the dynamics [211]). This does not seem to be the case after we break supersymmetry. From the 7-brane theory point of view, this does not come as a surprise, since L is related to a Coulomb branch modulus of the eight-dimensional theory living on the 7-branes. By rotating the brane system this modulus is lifted, but only a detailed study of the 7-brane dynamics could tell whether this would be stabilized to some finite value or, say, sent all the way to infinity. This is hard to figure out since the brane system of section 6.6 is intricate and more complicated than a system of branes at angle in isolation. This is again an important aspect worth investigating further, even though present string techniques do not seem to be enough to tackle it. This said, it is reassuring that whenever the phase transition is second order, the value of h at which the phase transition occurs, $h = \tilde{h}$, does not depend on L. Notice, further, that if the supersymmetry breaking deformation is taken to be small, ℓ_φ can be made parametrically large, and hence one can take L large as well, still having the phase transition being second order. In this regime, the 7-branes are far from the stack compared to the scale $\tilde{h}$ at which the transition happens. Therefore, the 7-brane metric, which would change non-trivially the background and which we have not considered in our analysis, would not have any sensible effect on the dynamics triggering the phase transition.

The property of the $X_{1,N}$ theory may be shared by other systems, some of which could also admit a holographic dual description. While no fully stable non-supersymmetric AdS_6 backgrounds are known (see [310–313] for recent works addressing this point), this is yet an interesting and potentially far reaching direction to be pursued.

Bibliography

[1] N. Seiberg and E. Witten, *Electric - magnetic duality, monopole condensation, and confinement in N=2 supersymmetric Yang-Mills theory* Nucl. Phys. B **426** (1994) 19–52, arXiv:hep-th/9407087. [Erratum: Nucl.Phys.B 430, 485–486 (1994)].

[2] N. Seiberg and E. Witten, *Monopoles, duality and chiral symmetry breaking in N=2 supersymmetric QCD* Nucl. Phys. B **431** (1994) 484–550, arXiv:hep-th/9408099.

[3] O. Aharony, S. S. Razamat, N. Seiberg, and B. Willett, *3d dualities from 4d dualities* JHEP **07** (2013) 149, arXiv:1305.3924 [hep-th].

[4] O. Bergman and G. Zafrir, *Lifting 4d dualities to 5d* JHEP **04** (2015) 141, arXiv:1410.2806 [hep-th].

[5] M. Martone and G. Zafrir, *On the compactification of 5d theories to 4d* JHEP **08** (2021) 017, arXiv:2106.00686 [hep-th].

[6] M. Sacchi, O. Sela, and G. Zafrir, *Compactifying 5d superconformal field theories to 3d* JHEP **09** (2021) 149, arXiv:2105.01497 [hep-th].

[7] C. Turner, *Dualities in 2+1 Dimensions* PoS **Modave2018** (2019) 001, arXiv:1905.12656 [hep-th].

[8] D. Gaiotto, A. Kapustin, N. Seiberg, and B. Willett, *Generalized Global Symmetries* JHEP **02** (2015) 172, arXiv:1412.5148 [hep-th].

[9] G. V. Dunne, *Aspects of Chern-Simons theory* in *Les Houches Summer School in Theoretical Physics, Session 69: Topological Aspects of Low-dimensional Systems*. 1998. arXiv:hep-th/9902115.

[10] C. Closset, T. T. Dumitrescu, G. Festuccia, Z. Komargodski, and N. Seiberg, *Comments on Chern-Simons Contact Terms in Three Dimensions* JHEP **09** (2012) 091, arXiv:1206.5218 [hep-th].

[11] N. Seiberg and E. Witten, *Gapped Boundary Phases of Topological Insulators via Weak Coupling* PTEP **2016** no. 12, (2016) 12C101, arXiv:1602.04251 [cond-mat.str-el].

[12] L. V. Avdeev, G. V. Grigorev, and D. I. Kazakov, *Renormalizations in Abelian Chern-Simons field theories with matter* Nucl. Phys. B **382** (1992) 561–580.

[13] E. Witten, *Quantum Field Theory and the Jones Polynomial* Commun. Math. Phys. **121** (1989) 351–399.

[14] D. Tong, *Lectures on the Quantum Hall Effect* 2016. arXiv:1606.06687 [hep-th].

[15] P.-S. Hsin and N. Seiberg, *Level/rank Duality and Chern-Simons-Matter Theories* JHEP **09** (2016) 095, arXiv:1607.07457 [hep-th].

[16] N. Seiberg, T. Senthil, C. Wang, and E. Witten, *A Duality Web in 2+1 Dimensions and Condensed Matter Physics* Annals Phys. **374** (2016) 395–433, arXiv:1606.01989 [hep-th].

[17] X. Chen, Z.-C. Gu, Z.-X. Liu, and X.-G. Wen, *Symmetry protected topological orders and the group cohomology of their symmetry group* Phys. Rev. B **87** no. 15, (2013) 155114, arXiv:1106.4772 [cond-mat.str-el].

[18] T. Senthil, *Symmetry-protected topological phases of quantum matter* Annual Review of Condensed Matter Physics **6** no. 1, (Mar, 2015) 299–324, arXiv:1405.4015 [cond-mat.str-el].

[19] A. Kapustin, *Bosonic Topological Insulators and Paramagnets: a view from cobordisms* arXiv:1404.6659 [cond-mat.str-el].

[20] A. Kapustin, R. Thorngren, A. Turzillo, and Z. Wang, *Fermionic Symmetry Protected Topological Phases and Cobordisms* JHEP **12** (2015) 052, arXiv:1406.7329 [cond-mat.str-el].

[21] D. S. Freed and M. J. Hopkins, *Reflection positivity and invertible topological phases* Geom. Topol. **25** (2021) 1165–1330, arXiv:1604.06527 [hep-th].

[22] K. Yonekura, *On the cobordism classification of symmetry protected topological phases* Commun. Math. Phys. **368** no. 3, (2019) 1121–1173, arXiv:1803.10796 [hep-th].

[23] D. Gaiotto and T. Johnson-Freyd, *Symmetry Protected Topological phases and Generalized Cohomology* JHEP **05** (2019) 007, arXiv:1712.07950 [hep-th].

[24] M. Barkeshli, Y.-A. Chen, P.-S. Hsin, and N. Manjunath, *Classification of (2+1)D invertible fermionic topological phases with symmetry* Phys. Rev. B **105** no. 23, (2022) 235143, arXiv:2109.11039 [cond-mat.str-el].

[25] A. Armoni, T. T. Dumitrescu, G. Festuccia, and Z. Komargodski, *Metastable vacua in large-N QCD_3* JHEP **01** (2020) 004, arXiv:1905.01797 [hep-th].

[26] A. J. Niemi and G. W. Semenoff, *Axial Anomaly Induced Fermion Fractionization and Effective Gauge Theory Actions in Odd Dimensional Space-Times* Phys. Rev. Lett. **51** (1983) 2077.

[27] S. Rao and R. Yahalom, *Parity Anomalies in Gauge Theories in (2+1)-Dimensions* Phys. Lett. B **172** (1986) 227–230.

[28] S. R. Coleman and B. R. Hill, *No More Corrections to the Topological Mass Term in QED in Three-Dimensions* Phys. Lett. B **159** (1985) 184–188.

[29] E. Witten, *Fermion Path Integrals And Topological Phases* Rev. Mod. Phys. **88** no. 3, (2016) 035001, `arXiv:1508.04715 [cond-mat.mes-hall]`.

[30] M. F. Atiyah and I. M. Singer, *The index of elliptic operators on compact manifolds* Bull. Am. Math. Soc. **69** (1969) 422–433.

[31] Z. Komargodski and N. Seiberg, *A symmetry breaking scenario for QCD_3* JHEP **01** (2018) 109, `arXiv:1706.08755 [hep-th]`.

[32] A. Agarwal and V. P. Nair, *Supersymmetry and Mass Gap in 2+1 Dimensions: A Gauge Invariant Hamiltonian Analysis* Phys. Rev. D **85** (2012) 085011, `arXiv:1201.6609 [hep-th]`.

[33] A. Agarwal and V. P. Nair, *Fermions, mass-gap and Landau levels: gauge invariant Hamiltonian for QCD in D = 2+1* J. Phys. A **48** no. 46, (2015) 465401, `arXiv:1504.07201 [hep-th]`.

[34] N. Seiberg, *Electric - magnetic duality in supersymmetric nonAbelian gauge theories* Nucl. Phys. B **435** (1995) 129–146, `arXiv:hep-th/9411149`.

[35] K. G. Wilson and M. E. Fisher, *Critical exponents in 3.99 dimensions* Phys. Rev. Lett. **28** (1972) 240–243.

[36] Z. Komargodski, *Lectures on Dynamics of quantum fields.*

[37] A. M. Polyakov, *Quark Confinement and Topology of Gauge Groups* Nucl. Phys. B **120** (1977) 429–458.

[38] A. M. Polyakov, *Gauge Fields and Strings*, vol. 3. 1987.

[39] M. E. Peskin, *Mandelstam 't Hooft Duality in Abelian Lattice Models* Annals Phys. **113** (1978) 122.

[40] C. Dasgupta and B. I. Halperin, *Phase Transition in a Lattice Model of Superconductivity* Phys. Rev. Lett. **47** (1981) 1556–1560.

[41] S. R. Coleman, *The Quantum Sine-Gordon Equation as the Massive Thirring Model* Phys. Rev. D **11** (1975) 2088.

[42] A. M. Polyakov, *Fermi-Bose Transmutations Induced by Gauge Fields* Mod. Phys. Lett. A **3** (1988) 325.

[43] M. A. Metlitski and A. Vishwanath, *Particle-vortex duality of two-dimensional Dirac fermion from electric-magnetic duality of three-dimensional topological insulators* Phys. Rev. B **93** no. 24, (2016) 245151, arXiv:1505.05142 [cond-mat.str-el].

[44] F. Wilczek, *Magnetic Flux, Angular Momentum, and Statistics* Phys. Rev. Lett. **48** (1982) 1144–1146.

[45] C. Wang, A. Nahum, M. A. Metlitski, C. Xu, and T. Senthil, *Deconfined quantum critical points: symmetries and dualities* Phys. Rev. X **7** no. 3, (2017) 031051, arXiv:1703.02426 [cond-mat.str-el].

[46] D. T. Son, *Is the Composite Fermion a Dirac Particle?* Phys. Rev. X **5** no. 3, (2015) 031027, arXiv:1502.03446 [cond-mat.mes-hall].

[47] C. Wang and T. Senthil, *Dual Dirac Liquid on the Surface of the Electron Topological Insulator* Phys. Rev. X **5** no. 4, (2015) 041031, arXiv:1505.05141 [cond-mat.str-el].

[48] C. Wang and T. Senthil, *Composite fermi liquids in the lowest Landau level* Phys. Rev. B **94** no. 24, (2016) 245107, arXiv:1604.06807 [cond-mat.str-el].

[49] O. Aharony, *Baryons, monopoles and dualities in Chern-Simons-matter theories* JHEP **02** (2016) 093, arXiv:1512.00161 [hep-th].

[50] P. Di Francesco, P. Mathieu, and D. Senechal, *Conformal Field Theory*. Graduate Texts in Contemporary Physics. Springer-Verlag, New York, 1997.

[51] M. Blau and G. Thompson, *Derivation of the Verlinde formula from Chern-Simons theory and the G/G model* Nucl. Phys. B **408** (1993) 345–390, arXiv:hep-th/9305010.

[52] A. Giveon and D. Kutasov, *Seiberg Duality in Chern-Simons Theory* Nucl. Phys. B **812** (2009) 1–11, arXiv:0808.0360 [hep-th].

[53] F. Benini, C. Closset, and S. Cremonesi, *Comments on 3d Seiberg-like dualities* JHEP **10** (2011) 075, arXiv:1108.5373 [hep-th].

[54] O. Aharony and D. Fleischer, *IR Dualities in General 3d Supersymmetric SU(N) QCD Theories* JHEP **02** (2015) 162, arXiv:1411.5475 [hep-th].

[55] F. Benini, *Three-dimensional dualities with bosons and fermions* JHEP **02** (2018) 068, arXiv:1712.00020 [hep-th].

[56] F. Benini, P.-S. Hsin, and N. Seiberg, *Comments on global symmetries, anomalies, and duality in (2 + 1)d* JHEP **04** (2017) 135, arXiv:1702.07035 [cond-mat.str-el].

[57] D. Radičević, *Disorder Operators in Chern-Simons-Fermion Theories* JHEP **03** (2016) 131, arXiv:1511.01902 [hep-th].

[58] E. Dyer, M. Mezei, and S. S. Pufu, *Monopole Taxonomy in Three-Dimensional Conformal Field Theories* arXiv:1309.1160 [hep-th].

[59] T. T. Wu and C. N. Yang, *Dirac Monopole Without Strings: Monopole Harmonics* Nucl. Phys. B **107** (1976) 365.

[60] V. Gorbenko, S. Rychkov, and B. Zan, *Walking, Weak first-order transitions, and Complex CFTs* JHEP **10** (2018) 108, arXiv:1807.11512 [hep-th].

[61] V. Gorbenko, S. Rychkov, and B. Zan, *Walking, Weak first-order transitions, and Complex CFTs II. Two-dimensional Potts model at $Q > 4$* SciPost Phys. **5** no. 5, (2018) 050, arXiv:1808.04380 [hep-th].

[62] C. Vafa and E. Witten, *Restrictions on Symmetry Breaking in Vector-Like Gauge Theories* Nucl. Phys. B **234** (1984) 173–188.

[63] C. Vafa and E. Witten, *Eigenvalue Inequalities for Fermions in Gauge Theories* Commun. Math. Phys. **95** (1984) 257.

[64] C. Vafa and E. Witten, *Parity Conservation in QCD* Phys. Rev. Lett. **53** (1984) 535.

[65] D. Gaiotto, Z. Komargodski, and N. Seiberg, *Time-reversal breaking in QCD_4, walls, and dualities in 2 + 1 dimensions* JHEP **01** (2018) 110, arXiv:1708.06806 [hep-th].

[66] E. Witten, *Global Aspects of Current Algebra* Nucl. Phys. B **223** (1983) 422–432.

[67] E. Witten, *Current Algebra, Baryons, and Quark Confinement* Nucl. Phys. B **223** (1983) 433–444.

[68] D. S. Freed, Z. Komargodski, and N. Seiberg, *The Sum Over Topological Sectors and θ in the 2+1-Dimensional $\mathbb{CP}^1$ σ-Model* Commun. Math. Phys. **362** no. 1, (2018) 167–183, arXiv:1707.05448 [cond-mat.str-el].

[69] D. K. Hong and H.-U. Yee, *Holographic aspects of three dimensional QCD from string theory* JHEP **05** (2010) 036, arXiv:1003.1306 [hep-th]. [Erratum: JHEP 08, 120 (2010)].

[70] F. Wilczek and A. Zee, *Linking Numbers, Spin, and Statistics of Solitons* Phys. Rev. Lett. **51** (1983) 2250–2252.

[71] S. M. H. Wong, *What exactly is a skyrmion?* arXiv:hep-ph/0202250.

[72] T. Appelquist, D. Nash, and L. C. R. Wijewardhana, *Critical Behavior in (2+1)-Dimensional QED* Phys. Rev. Lett. **60** (1988) 2575.

[73] T. Appelquist and D. Nash, *Critical Behavior in (2+1)-dimensional QCD* Phys. Rev. Lett. **64** (1990) 721.

[74] A. Sharon, *QCD_3 dualities and the F-theorem* JHEP **08** (2018) 078, arXiv:1803.06983 [hep-th].

[75] O. Aharony, G. Gur-Ari, and R. Yacoby, *d=3 Bosonic Vector Models Coupled to Chern-Simons Gauge Theories* JHEP **03** (2012) 037, arXiv:1110.4382 [hep-th].

[76] S. Giombi, S. Minwalla, S. Prakash, S. P. Trivedi, S. R. Wadia, and X. Yin, *Chern-Simons Theory with Vector Fermion Matter* Eur. Phys. J. C **72** (2012) 2112, arXiv:1110.4386 [hep-th].

[77] O. Aharony, G. Gur-Ari, and R. Yacoby, *Correlation Functions of Large N Chern-Simons-Matter Theories and Bosonization in Three Dimensions* JHEP **12** (2012) 028, arXiv:1207.4593 [hep-th].

[78] G. Gur-Ari and R. Yacoby, *Correlators of Large N Fermionic Chern-Simons Vector Models* JHEP **02** (2013) 150, arXiv:1211.1866 [hep-th].

[79] O. Aharony, S. Giombi, G. Gur-Ari, J. Maldacena, and R. Yacoby, *The Thermal Free Energy in Large N Chern-Simons-Matter Theories* JHEP **03** (2013) 121, arXiv:1211.4843 [hep-th].

[80] S. Jain, S. Minwalla, T. Sharma, T. Takimi, S. R. Wadia, and S. Yokoyama, *Phases of large N vector Chern-Simons theories on $S^2 \times S^1$* JHEP **09** (2013) 009, arXiv:1301.6169 [hep-th].

[81] S. Jain, S. Minwalla, and S. Yokoyama, *Chern Simons duality with a fundamental boson and fermion* JHEP **11** (2013) 037, arXiv:1305.7235 [hep-th].

[82] G. 't Hooft, *A Planar Diagram Theory for Strong Interactions* Nucl. Phys. B **72** (1974) 461.

[83] A. Armoni and V. Niarchos, *Phases of QCD_3 from Non-SUSY Seiberg Duality and Brane Dynamics* Phys. Rev. D **97** no. 10, (2018) 106001, arXiv:1711.04832 [hep-th].

[84] O. Aharony, T. T. Dumitrescu, and Z. Komargodski, *Work in progress.*

[85] J. M. Maldacena, *The Large N limit of superconformal field theories and supergravity* Adv. Theor. Math. Phys. **2** (1998) 231–252, arXiv:hep-th/9711200.

[86] E. Witten, *Anti-de Sitter space, thermal phase transition, and confinement in gauge theories* Adv. Theor. Math. Phys. **2** (1998) 505–532, arXiv:hep-th/9803131.

[87] M. Kruczenski, D. Mateos, R. C. Myers, and D. J. Winters, *Towards a holographic dual of large N(c) QCD* JHEP **05** (2004) 041, arXiv:hep-th/0311270.

[88] S. Sugimoto and K. Takahashi, *QED and string theory* JHEP **04** (2004) 051, arXiv:hep-th/0403247.

[89] T. Sakai and S. Sugimoto, *Low energy hadron physics in holographic QCD* Prog. Theor. Phys. **113** (2005) 843–882, arXiv:hep-th/0412141.

[90] M. Fujita, W. Li, S. Ryu, and T. Takayanagi, *Fractional Quantum Hall Effect via Holography: Chern-Simons, Edge States, and Hierarchy* JHEP **06** (2009) 066, arXiv:0901.0924 [hep-th].

[91] S. R. Coleman, R. Jackiw, and H. D. Politzer, *Spontaneous Symmetry Breaking in the O(N) Model for Large N** Phys. Rev. D **10** (1974) 2491.

[92] D. J. Gross and A. Neveu, *Dynamical Symmetry Breaking in Asymptotically Free Field Theories* Phys. Rev. D **10** (1974) 3235.

[93] A. N. Vasiliev, Y. M. Pismak, and Y. R. Khonkonen, *Simple Method of Calculating the Critical Indices in the 1/N Expansion* Theor. Math. Phys. **46** (1981) 104–113.

[94] T. W. Appelquist, M. J. Bowick, D. Karabali, and L. C. R. Wijewardhana, *Spontaneous Chiral Symmetry Breaking in Three-Dimensional QED* Phys. Rev. D **33** (1986) 3704.

[95] J. D. Bekenstein, *Black holes and entropy* Phys. Rev. D **7** (1973) 2333–2346.

[96] G. T. Horowitz and A. Strominger, *Black strings and P-branes* Nucl. Phys. B **360** (1991) 197–209.

[97] C. V. Johnson, *D-branes*. Cambridge Monographs on Mathematical Physics. Cambridge University Press, 2005.

[98] M. Ammon and J. Erdmenger, *Gauge/gravity duality: Foundations and applications*. Cambridge University Press, Cambridge, 2015.

[99] J. Polchinski, *Dirichlet Branes and Ramond-Ramond charges* Phys. Rev. Lett. **75** (1995) 4724–4727, arXiv:hep-th/9510017.

[100] E. D'Hoker and D. Z. Freedman, *Supersymmetric gauge theories and the AdS / CFT correspondence* in *Theoretical Advanced Study Institute in Elementary Particle Physics (TASI 2001): Strings, Branes and EXTRA Dimensions*, pp. 3–158. 2002. arXiv:hep-th/0201253.

[101] O. Aharony, S. S. Gubser, J. M. Maldacena, H. Ooguri, and Y. Oz, *Large N field theories, string theory and gravity* Phys. Rept. **323** (2000) 183–386, arXiv:hep-th/9905111.

[102] K. Skenderis, *Lecture notes on holographic renormalization* Class. Quant. Grav. **19** (2002) 5849–5876, arXiv:hep-th/0209067.

[103] M. Henningson and K. Skenderis, *The Holographic Weyl anomaly* JHEP **07** (1998) 023, arXiv:hep-th/9806087.

[104] K. A. Intriligator and N. Seiberg, *Lectures on supersymmetric gauge theories and electric-magnetic duality* Nucl. Phys. B Proc. Suppl. **45BC** (1996) 1–28, arXiv:hep-th/9509066.

[105] D. J. Gross, I. R. Klebanov, A. V. Matytsin, and A. V. Smilga, *Screening versus confinement in (1+1)-dimensions* Nucl. Phys. B **461** (1996) 109–130, arXiv:hep-th/9511104.

[106] Z. Komargodski and A. Schwimmer, *On Renormalization Group Flows in Four Dimensions* JHEP **12** (2011) 099, arXiv:1107.3987 [hep-th].

[107] D. Z. Freedman, S. S. Gubser, K. Pilch, and N. P. Warner, *Renormalization group flows from holography supersymmetry and a c theorem* Adv. Theor. Math. Phys. **3** (1999) 363–417, arXiv:hep-th/9904017.

[108] J. M. Maldacena and C. Nunez, *Supergravity description of field theories on curved manifolds and a no go theorem* Int. J. Mod. Phys. A **16** (2001) 822–855, arXiv:hep-th/0007018.

[109] I. R. Klebanov and M. J. Strassler, *Supergravity and a confining gauge theory: Duality cascades and chi SB resolution of naked singularities* JHEP **08** (2000) 052, arXiv:hep-th/0007191.

[110] M. Bertolini, *Four lectures on the gauge / gravity correspondence* Int. J. Mod. Phys. A **18** (2003) 5647–5712, arXiv:hep-th/0303160.

[111] L. Girardello, M. Petrini, M. Porrati, and A. Zaffaroni, *Novel local CFT and exact results on perturbations of N=4 superYang Mills from AdS dynamics* JHEP **12** (1998) 022, arXiv:hep-th/9810126.

[112] L. Girardello, M. Petrini, M. Porrati, and A. Zaffaroni, *The Supergravity dual of N=1 superYang-Mills theory* Nucl. Phys. B **569** (2000) 451–469, arXiv:hep-th/9909047.

[113] J. Erlich, E. Katz, D. T. Son, and M. A. Stephanov, *QCD and a holographic model of hadrons* Phys. Rev. Lett. **95** (2005) 261602, arXiv:hep-ph/0501128.

[114] S.-J. Rey, *String theory on thin semiconductors: Holographic realization of Fermi points and surfaces* Prog. Theor. Phys. Suppl. **177** (2009) 128–142, arXiv:0911.5295 [hep-th].

[115] R. Argurio, A. Armoni, M. Bertolini, F. Mignosa, and P. Niro, *Vacuum structure of large N QCD_3 from holography* JHEP **07** (2020) 134, arXiv:2006.01755 [hep-th].

[116] S. W. Hawking and D. N. Page, *Thermodynamics of Black Holes in anti-De Sitter Space* Commun. Math. Phys. **87** (1983) 577.

[117] N. Itzhaki, J. M. Maldacena, J. Sonnenschein, and S. Yankielowicz, *Supergravity and the large N limit of theories with sixteen supercharges* Phys. Rev. D **58** (1998) 046004, arXiv:hep-th/9802042.

[118] A. Karch and E. Katz, *Adding flavor to AdS / CFT* JHEP **06** (2002) 043, arXiv:hep-th/0205236.

[119] E. Witten, *Baryons and branes in anti-de Sitter space* JHEP **07** (1998) 006, arXiv:hep-th/9805112.

[120] E. Witten, *Current Algebra Theorems for the U(1) Goldstone Boson* Nucl. Phys. B **156** (1979) 269–283.

[121] E. Witten, *Large N Chiral Dynamics* Annals Phys. **128** (1980) 363.

[122] O. Aharony, J. Sonnenschein, and S. Yankielowicz, *A Holographic model of deconfinement and chiral symmetry restoration* Annals Phys. **322** (2007) 1420–1443, arXiv:hep-th/0604161.

[123] M. Fujita, C. M. Melby-Thompson, R. Meyer, and S. Sugimoto, *Holographic Chern-Simons Defects* JHEP **06** (2016) 163, arXiv:1601.00525 [hep-th].

[124] R. Argurio, M. Bertolini, F. Mignosa, and P. Niro, *Charting the phase diagram of QCD_3* JHEP **08** (2019) 153, arXiv:1905.01460 [hep-th].

[125] M. A. Metlitski, A. Vishwanath, and C. Xu, *Duality and bosonization of (2+1) -dimensional Majorana fermions* Phys. Rev. B **95** no. 20, (2017) 205137, arXiv:1611.05049 [cond-mat.str-el].

[126] F. F. Hansen, T. Janowski, K. Langæble, R. B. Mann, F. Sannino, T. G. Steele, and Z.-W. Wang, *Phase structure of complete asymptotically free $SU(N_c)$ theories with quarks and scalar quarks* Phys. Rev. D **97** no. 6, (2018) 065014, arXiv:1706.06402 [hep-ph].

[127] C. Choi, *Phases of Two Adjoints QCD_3 And a Duality Chain* JHEP **04** (2020) 006, arXiv:1910.05402 [hep-th].

[128] S. R. Coleman and E. Witten, *Chiral Symmetry Breakdown in Large N Chromodynamics* Phys. Rev. Lett. **45** (1980) 100.

[129] G. Ferretti, S. G. Rajeev, and Z. Yang, *The Effective Lagrangian of three-dimensional quantum chromodynamics* Int. J. Mod. Phys. A **7** (1992) 7989–8000, arXiv:hep-th/9204075.

[130] G. Ferretti, S. G. Rajeev, and Z. Yang, *Baryons as solitons in three-dimensional quantum chromodynamics* Int. J. Mod. Phys. A **7** (1992) 8001–8020, arXiv:hep-th/9204076.

[131] M. Akhond, A. Armoni, and S. Speziali, *Phases of* $\mathbf{U}(\mathbf{N_c})$ *QCD_3 from Type 0 Strings and Seiberg Duality* JHEP **09** (2019) 111, arXiv:1908.04324 [hep-th].

[132] K. Jensen and A. Karch, *Embedding three-dimensional bosonization dualities into string theory* JHEP **12** (2017) 031, arXiv:1709.07872 [hep-th].

[133] D. Kutasov, J. Lin, and A. Parnachev, *Conformal Phase Transitions at Weak and Strong Coupling* Nucl. Phys. B **858** (2012) 155–195, arXiv:1107.2324 [hep-th].

[134] C. Kristjansen and G. W. Semenoff, *The D3-probe-D7 brane holographic fractional topological insulator* JHEP **10** (2016) 079, arXiv:1604.08548 [hep-th].

[135] D. Kutasov, J. Lin, and A. Parnachev, *Holographic Walking from Tachyon DBI* Nucl. Phys. B **863** (2012) 361–397, arXiv:1201.4123 [hep-th].

[136] A. W. Peet and J. Polchinski, *UV / IR relations in AdS dynamics* Phys. Rev. D **59** (1999) 065011, arXiv:hep-th/9809022.

[137] E. Witten, *Theta dependence in the large N limit of four-dimensional gauge theories* Phys. Rev. Lett. **81** (1998) 2862–2865, arXiv:hep-th/9807109.

[138] D. Gaiotto, A. Kapustin, Z. Komargodski, and N. Seiberg, *Theta, Time Reversal, and Temperature* JHEP **05** (2017) 091, arXiv:1703.00501 [hep-th].

[139] N. Kan, R. Kitano, S. Yankielowicz, and R. Yokokura, *From 3d dualities to hadron physics* Phys. Rev. D **102** no. 12, (2020) 125034, arXiv:1909.04082 [hep-th].

[140] Q. Bonnefoy, E. Dudas, and S. Lüst, *On the weak gravity conjecture in string theory with broken supersymmetry* Nucl. Phys. B **947** (2019) 114738, arXiv:1811.11199 [hep-th].

[141] R. Argurio, M. Bertolini, F. Bigazzi, A. L. Cotrone, and P. Niro, *QCD domain walls, Chern-Simons theories and holography* JHEP **09** (2018) 090, arXiv:1806.08292 [hep-th].

[142] D. B. Kaplan, J.-W. Lee, D. T. Son, and M. A. Stephanov, *Conformality Lost* Phys. Rev. D **80** (2009) 125005, arXiv:0905.4752 [hep-th].

[143] K. Jensen, A. Karch, D. T. Son, and E. G. Thompson, *Holographic Berezinskii-Kosterlitz-Thouless Transitions* Phys. Rev. Lett. **105** (2010) 041601, arXiv:1002.3159 [hep-th].

[144] N. Iqbal, H. Liu, M. Mezei, and Q. Si, *Quantum phase transitions in holographic models of magnetism and superconductors* Phys. Rev. D **82** (2010) 045002, arXiv:1003.0010 [hep-th].

[145] N. Seiberg, *Five-dimensional SUSY field theories, nontrivial fixed points and string dynamics* Phys. Lett. B **388** (1996) 753–760, arXiv:hep-th/9608111.

[146] R. Dijkgraaf and E. Witten, *Topological Gauge Theories and Group Cohomology* Commun. Math. Phys. **129** (1990) 393.

[147] N. Lambert, C. Papageorgakis, and M. Schmidt-Sommerfeld, *Instanton Operators in Five-Dimensional Gauge Theories* JHEP **03** (2015) 019, arXiv:1412.2789 [hep-th].

[148] E. Witten, *Phase transitions in M theory and F theory* Nucl. Phys. B **471** (1996) 195–216, arXiv:hep-th/9603150.

[149] K. A. Intriligator, D. R. Morrison, and N. Seiberg, *Five-dimensional supersymmetric gauge theories and degenerations of Calabi-Yau spaces* Nucl. Phys. B **497** (1997) 56–100, arXiv:hep-th/9702198.

[150] M. Banados, L. J. Garay, and M. Henneaux, *The Dynamical structure of higher dimensional Chern-Simons theory* Nucl. Phys. B **476** (1996) 611–635, arXiv:hep-th/9605159.

[151] M. Banados, L. J. Garay, and M. Henneaux, *The Local degrees of freedom of higher dimensional pure Chern-Simons theories* Phys. Rev. D **53** (1996) 593–596, arXiv:hep-th/9506187.

[152] A. Nedelin, *Exact Results in Five-Dimensional Gauge Theories : On Supersymmetry, Localization and Matrix Models*. PhD thesis, Uppsala U., 2015.

[153] C. Closset, M. Del Zotto, and V. Saxena, *Five-dimensional SCFTs and gauge theory phases: an M-theory/type IIA perspective* SciPost Phys. **6** no. 5, (2019) 052, arXiv:1812.10451 [hep-th].

[154] P. Benetti Genolini and L. Tizzano, *Instantons, symmetries and anomalies in five dimensions* JHEP **04** (2021) 188, arXiv:2009.07873 [hep-th].

[155] P. Benetti Genolini, M. Honda, H.-C. Kim, D. Tong, and C. Vafa, *Evidence for a Non-Supersymmetric 5d CFT from Deformations of 5d $SU(2)$ SYM* JHEP **05** (2020) 058, arXiv:2001.00023 [hep-th].

[156] Y. Tanii, *Introduction to supergravities in diverse dimensions* in *YITP Workshop on Supersymmetry*. 1998. arXiv:hep-th/9802138.

[157] D. Z. Freedman and A. Van Proeyen, *Supergravity*. Cambridge Univ. Press, Cambridge, UK, 2012.

[158] A. Hebecker, *5-D superYang-Mills theory in 4-D superspace, superfield brane operators, and applications to orbifold GUTs* Nucl. Phys. B **632** (2002) 101–113, arXiv:hep-ph/0112230.

[159] T. W. Grimm and A. Kapfer, *Self-Dual Tensors and Partial Supersymmetry Breaking in Five Dimensions* JHEP **03** (2015) 008, arXiv:1402.3529 [hep-th].

[160] S. M. Kuzenko and A. E. Pindur, *Massless particles in five and higher dimensions* Phys. Lett. B **812** (2021) 136020, arXiv:2010.07124 [hep-th].

[161] L. Alvarez-Gaume, S. Della Pietra, and G. W. Moore, *Anomalies and Odd Dimensions* Annals Phys. **163** (1985) 288.

[162] T. T. Dumitrescu and N. Seiberg, *Supercurrents and Brane Currents in Diverse Dimensions* JHEP **07** (2011) 095, arXiv:1106.0031 [hep-th].

[163] S. Yokoyama, *Supersymmetry Algebra in Super Yang-Mills Theories* JHEP **09** (2015) 211, arXiv:1506.03522 [hep-th].

[164] I. A. Popescu and A. D. Shapere, *BPS equations, BPS states, and central charge of N=2 supersymmetric gauge theories* JHEP **10** (2002) 033, arXiv:hep-th/0102169.

[165] Y. Tachikawa, *N=2 supersymmetric dynamics for pedestrians.* 2013. arXiv:1312.2684 [hep-th].

[166] K. Hosomichi, R.-K. Seong, and S. Terashima, *Supersymmetric Gauge Theories on the Five-Sphere* Nucl. Phys. B **865** (2012) 376–396, arXiv:1203.0371 [hep-th].

[167] F. Quevedo, S. Krippendorf, and O. Schlotterer, *Cambridge Lectures on Supersymmetry and Extra Dimensions* arXiv:1011.1491 [hep-th].

[168] P. C. Argyres, M. R. Plesser, and N. Seiberg, *The Moduli space of vacua of N=2 SUSY QCD and duality in N=1 SUSY QCD* Nucl. Phys. B **471** (1996) 159–194, arXiv:hep-th/9603042.

[169] S. Minwalla, *Restrictions imposed by superconformal invariance on quantum field theories* Adv. Theor. Math. Phys. **2** (1998) 783–851, arXiv:hep-th/9712074.

[170] J. Kinney, J. M. Maldacena, S. Minwalla, and S. Raju, *An Index for 4 dimensional super conformal theories* Commun. Math. Phys. **275** (2007) 209–254, arXiv:hep-th/0510251.

[171] F. A. Dolan and H. Osborn, *On short and semi-short representations for four-dimensional superconformal symmetry* Annals Phys. **307** (2003) 41–89, arXiv:hep-th/0209056.

[172] J. Bhattacharya, S. Bhattacharyya, S. Minwalla, and S. Raju, *Indices for Superconformal Field Theories in 3,5 and 6 Dimensions* JHEP **02** (2008) 064, arXiv:0801.1435 [hep-th].

[173] V. K. Dobrev and V. B. Petkova, *All Positive Energy Unitary Irreducible Representations of Extended Conformal Supersymmetry* Phys. Lett. B **162** (1985) 127–132.

[174] S. Ferrara and E. Sokatchev, *Representations of (1,0) and (2,0) superconformal algebras in six-dimensions: Massless and short superfields* Lett. Math. Phys. **51** (2000) 55–69, arXiv:hep-th/0001178.

[175] V. K. Dobrev, *Positive energy unitary irreducible representations of D = 6 conformal supersymmetry* J. Phys. A **35** (2002) 7079–7100, arXiv:hep-th/0201076.

[176] C. Cordova, T. T. Dumitrescu, and K. Intriligator, *Deformations of Superconformal Theories* JHEP **11** (2016) 135, arXiv:1602.01217 [hep-th].

[177] C. Cordova, T. T. Dumitrescu, and K. Intriligator, *Multiplets of Superconformal Symmetry in Diverse Dimensions* JHEP **03** (2019) 163, arXiv:1612.00809 [hep-th].

[178] H.-C. Kim, S.-S. Kim, and K. Lee, *5-dim Superconformal Index with Enhanced En Global Symmetry* JHEP **10** (2012) 142, arXiv:1206.6781 [hep-th].

[179] S. Cremonesi, G. Ferlito, A. Hanany, and N. Mekareeya, *Instanton Operators and the Higgs Branch at Infinite Coupling* JHEP **04** (2017) 042, arXiv:1505.06302 [hep-th].

[180] N. Mekareeya, K. Ohmori, Y. Tachikawa, and G. Zafrir, *E_8 instantons on type-A ALE spaces and supersymmetric field theories* JHEP **09** (2017) 144, arXiv:1707.04370 [hep-th].

[181] M. Bullimore, T. Dimofte, and D. Gaiotto, *The Coulomb Branch of 3d $\mathcal{N} = 4$ Theories* Commun. Math. Phys. **354** no. 2, (2017) 671–751, arXiv:1503.04817 [hep-th].

[182] H. Nakajima, *Towards a mathematical definition of Coulomb branches of 3-dimensional $\mathcal{N} = 4$ gauge theories, I* Adv. Theor. Math. Phys. **20** (2016) 595–669, arXiv:1503.03676 [math-ph].

[183] A. Braverman, M. Finkelberg, and H. Nakajima, *Coulomb branches of 3d $\mathcal{N} = 4$ quiver gauge theories and slices in the affine Grassmannian* Adv. Theor. Math. Phys. **23** (2019) 75–166, arXiv:1604.03625 [math.RT].

[184] G. Ferlito and A. Hanany, *A tale of two cones: the Higgs Branch of Sp(n) theories with 2n flavours* arXiv:1609.06724 [hep-th].

[185] G. Ferlito, A. Hanany, N. Mekareeya, and G. Zafrir, *3d Coulomb branch and 5d Higgs branch at infinite coupling* JHEP **07** (2018) 061, arXiv:1712.06604 [hep-th].

[186] S. Cabrera and A. Hanany, *Quiver Subtractions* JHEP **09** (2018) 008, arXiv:1803.11205 [hep-th].

[187] S. Cabrera, A. Hanany, and F. Yagi, *Tropical Geometry and Five Dimensional Higgs Branches at Infinite Coupling* JHEP **01** (2019) 068, arXiv:1810.01379 [hep-th].

[188] S. Cabrera, A. Hanany, and M. Sperling, *Magnetic quivers, Higgs branches, and 6d N=(1,0) theories* JHEP **06** (2019) 071, arXiv:1904.12293 [hep-th]. [Erratum: JHEP 07, 137 (2019)].

[189] A. Bourget, S. Cabrera, J. F. Grimminger, A. Hanany, M. Sperling, A. Zajac, and Z. Zhong, *The Higgs mechanism — Hasse diagrams for symplectic singularities* JHEP **01** (2020) 157, arXiv:1908.04245 [hep-th].

[190] A. Bourget, S. Cabrera, J. F. Grimminger, A. Hanany, and Z. Zhong, *Brane Webs and Magnetic Quivers for SQCD* JHEP **03** (2020) 176, arXiv:1909.00667 [hep-th].

[191] S. Cabrera, A. Hanany, and M. Sperling, *Magnetic quivers, Higgs branches, and 6d $\mathcal{N} = (1, 0)$ theories — orthogonal and symplectic gauge groups* JHEP **02** (2020) 184, arXiv:1912.02773 [hep-th].

[192] J. F. Grimminger and A. Hanany, *Hasse diagrams for 3d $\mathcal{N} = 4$ quiver gauge theories — Inversion and the full moduli space* JHEP **09** (2020) 159, arXiv:2004.01675 [hep-th].

[193] A. Bourget, J. F. Grimminger, A. Hanany, M. Sperling, and Z. Zhong, *Magnetic Quivers from Brane Webs with O5 Planes* JHEP **07** (2020) 204, arXiv:2004.04082 [hep-th].

[194] A. Bourget, J. F. Grimminger, A. Hanany, M. Sperling, G. Zafrir, and Z. Zhong, *Magnetic quivers for rank 1 theories* JHEP **09** (2020) 189, arXiv:2006.16994 [hep-th].

[195] M. Akhond, F. Carta, S. Dwivedi, H. Hayashi, S.-S. Kim, and F. Yagi, *Five-brane webs, Higgs branches and unitary/orthosymplectic magnetic quivers* JHEP **12** (2020) 164, arXiv:2008.01027 [hep-th].

[196] A. Bourget, S. Giacomelli, J. F. Grimminger, A. Hanany, M. Sperling, and Z. Zhong, *S-fold magnetic quivers* JHEP **02** (2021) 054, arXiv:2010.05889 [hep-th].

[197] A. Dancer, A. Hanany, and F. Kirwan, *Symplectic duality and implosions* Adv. Theor. Math. Phys. **25** no. 6, (2021) 1367–1387, arXiv:2004.09620 [math.SG].

[198] A. Bourget, A. Hanany, and D. Miketa, *Quiver origami: discrete gauging and folding* JHEP **01** (2021) 086, arXiv:2005.05273 [hep-th].

[199] A. Bourget, J. F. Grimminger, A. Hanany, R. Kalveks, M. Sperling, and Z. Zhong, *Magnetic Lattices for Orthosymplectic Quivers* JHEP **12** (2020) 092, arXiv:2007.04667 [hep-th].

[200] M. Akhond, F. Carta, S. Dwivedi, H. Hayashi, S.-S. Kim, and F. Yagi, *Factorised 3d $\mathcal{N} = 4$ orthosymplectic quivers* JHEP **05** (2021) 269, arXiv:2101.12235 [hep-th].

[201] A. Bourget, J. F. Grimminger, A. Hanany, M. Sperling, and Z. Zhong, *Branes, Quivers, and the Affine Grassmannian* arXiv:2102.06190 [hep-th].

[202] A. Bourget, A. Dancer, J. F. Grimminger, A. Hanany, F. Kirwan, and Z. Zhong, *Orthosymplectic implosions* JHEP **08** (2021) 012, arXiv:2103.05458 [hep-th].

[203] M. Akhond and F. Carta, *Magnetic quivers from brane webs with $O7^+$-planes* JHEP **10** (2021) 014, arXiv:2107.09077 [hep-th].

[204] J. Bao, A. Hanany, Y.-H. He, and E. Hirst, *Some Open Questions in Quiver Gauge Theory* arXiv:2108.05167 [hep-th].

[205] K. Gledhill and A. Hanany, *Coulomb branch global symmetry and quiver addition* JHEP **12** (2021) 127, arXiv:2109.07237 [hep-th].

[206] O. Bergman and D. Rodriguez-Gomez, *A Note on Instanton Operators, Instanton Particles, and Supersymmetry* JHEP **05** (2016) 068, arXiv:1601.00752 [hep-th].

[207] O. Aharony, A. Hanany, and B. Kol, *Webs of (p,q) five-branes, five-dimensional field theories and grid diagrams* JHEP **01** (1998) 002, arXiv:hep-th/9710116.

[208] Y. Tachikawa, *Instanton operators and symmetry enhancement in 5d supersymmetric gauge theories* PTEP **2015** no. 4, (2015) 043B06, arXiv:1501.01031 [hep-th].

[209] O. J. Ganor, D. R. Morrison, and N. Seiberg, *Branes, Calabi-Yau spaces, and toroidal compactification of the N=1 six-dimensional E(8) theory* Nucl. Phys. B **487** (1997) 93–127, arXiv:hep-th/9610251.

[210] H. Hayashi, S.-S. Kim, K. Lee, and F. Yagi, *6d SCFTs, 5d Dualities and Tao Web Diagrams* JHEP **05** (2019) 203, arXiv:1509.03300 [hep-th].

[211] O. DeWolfe, A. Hanany, A. Iqbal, and E. Katz, *Five-branes, seven-branes and five-dimensional E(n) field theories* JHEP **03** (1999) 006, arXiv:hep-th/9902179.

[212] D. R. Morrison and N. Seiberg, *Extremal transitions and five-dimensional supersymmetric field theories* Nucl. Phys. B **483** (1997) 229–247, arXiv:hep-th/9609070.

[213] D.-E. Diaconescu and R. Entin, *Calabi-Yau spaces and five-dimensional field theories with exceptional gauge symmetry* Nucl. Phys. B **538** (1999) 451–484, arXiv:hep-th/9807170.

[214] H. Hayashi, C. Lawrie, and S. Schafer-Nameki, *Phases, Flops and F-theory: SU(5) Gauge Theories* JHEP **10** (2013) 046, arXiv:1304.1678 [hep-th].

[215] H. Hayashi, C. Lawrie, D. R. Morrison, and S. Schafer-Nameki, *Box Graphs and Singular Fibers* JHEP **05** (2014) 048, arXiv:1402.2653 [hep-th].

[216] M. Del Zotto, J. J. Heckman, and D. R. Morrison, *6D SCFTs and Phases of 5D Theories* JHEP **09** (2017) 147, arXiv:1703.02981 [hep-th].

[217] D. Xie and S.-T. Yau, *Three dimensional canonical singularity and five dimensional $\mathcal{N}$ = 1 SCFT* JHEP **06** (2017) 134, arXiv:1704.00799 [hep-th].

[218] P. Jefferson, H.-C. Kim, C. Vafa, and G. Zafrir, *Towards Classification of 5d SCFTs: Single Gauge Node* arXiv:1705.05836 [hep-th].

[219] P. Jefferson, S. Katz, H.-C. Kim, and C. Vafa, *On Geometric Classification of 5d SCFTs* JHEP **04** (2018) 103, arXiv:1801.04036 [hep-th].

[220] L. Bhardwaj and P. Jefferson, *Classifying* 5*d SCFTs via* 6*d SCFTs: Rank one* JHEP **07** (2019) 178, arXiv:1809.01650 [hep-th]. [Addendum: JHEP 01, 153 (2020)].

[221] L. Bhardwaj and P. Jefferson, *Classifying 5d SCFTs via 6d SCFTs: Arbitrary rank* JHEP **10** (2019) 282, arXiv:1811.10616 [hep-th].

[222] F. Apruzzi, L. Lin, and C. Mayrhofer, *Phases of 5d SCFTs from M-/F-theory on Non-Flat Fibrations* JHEP **05** (2019) 187, arXiv:1811.12400 [hep-th].

[223] F. Apruzzi, C. Lawrie, L. Lin, S. Schäfer-Nameki, and Y.-N. Wang, *5d Superconformal Field Theories and Graphs* Phys. Lett. B **800** (2020) 135077, arXiv:1906.11820 [hep-th].

[224] F. Apruzzi, C. Lawrie, L. Lin, S. Schäfer-Nameki, and Y.-N. Wang, *Fibers add Flavor, Part I: Classification of 5d SCFTs, Flavor Symmetries and BPS States* JHEP **11** (2019) 068, arXiv:1907.05404 [hep-th].

[225] F. Apruzzi, C. Lawrie, L. Lin, S. Schäfer-Nameki, and Y.-N. Wang, *Fibers add Flavor, Part II: 5d SCFTs, Gauge Theories, and Dualities* JHEP **03** (2020) 052, arXiv:1909.09128 [hep-th].

[226] L. Bhardwaj, *On the classification of 5d SCFTs* JHEP **09** (2020) 007, arXiv:1909.09635 [hep-th].

[227] L. Bhardwaj, P. Jefferson, H.-C. Kim, H.-C. Tarazi, and C. Vafa, *Twisted Circle Compactifications of 6d SCFTs* JHEP **12** (2020) 151, arXiv:1909.11666 [hep-th].

[228] L. Bhardwaj, *Dualities of 5d gauge theories from S-duality* JHEP **07** (2020) 012, arXiv:1909.05250 [hep-th].

[229] V. Saxena, *Rank-two 5d SCFTs from M-theory at isolated toric singularities: a systematic study* JHEP **04** (2020) 198, arXiv:1911.09574 [hep-th].

[230] F. Apruzzi, S. Schafer-Nameki, and Y.-N. Wang, *5d SCFTs from Decoupling and Gluing* JHEP **08** (2020) 153, arXiv:1912.04264 [hep-th].

[231] C. Closset and M. Del Zotto, *On 5d SCFTs and their BPS quivers. Part I: B-branes and brane tilings* arXiv:1912.13502 [hep-th].

[232] L. Bhardwaj, *Do all 5d SCFTs descend from 6d SCFTs?* JHEP **04** (2021) 085, arXiv:1912.00025 [hep-th].

[233] L. Bhardwaj and G. Zafrir, *Classification of 5d $\mathcal{N} = 1$ gauge theories* JHEP **12** (2020) 099, arXiv:2003.04333 [hep-th].

[234] J. Eckhard, S. Schäfer-Nameki, and Y.-N. Wang, *Trifectas for T_N in 5d* JHEP **07** no. 07, (2020) 199, arXiv:2004.15007 [hep-th].

[235] L. Bhardwaj, *More 5d KK theories* JHEP **03** (2021) 054, arXiv:2005.01722 [hep-th].

[236] M. Hubner, *5d SCFTs from (E_n, E_m) conformal matter* JHEP **12** (2020) 014, arXiv:2006.01694 [hep-th].

[237] L. Bhardwaj, *Flavor symmetry of 5d SCFTs. Part I. General setup* JHEP **09** (2021) 186, arXiv:2010.13230 [hep-th].

[238] L. Bhardwaj, *Flavor symmetry of 5d SCFTs. Part II. Applications* JHEP **04** (2021) 221, arXiv:2010.13235 [hep-th].

[239] L. Bhardwaj and S. Schäfer-Nameki, *Higher-form symmetries of 6d and 5d theories* JHEP **02** (2021) 159, arXiv:2008.09600 [hep-th].

[240] C. Closset, S. Giacomelli, S. Schafer-Nameki, and Y.-N. Wang, *5d and 4d SCFTs: Canonical Singularities, Trinions and S-Dualities* JHEP **05** (2021) 274, arXiv:2012.12827 [hep-th].

[241] F. Apruzzi, L. Bhardwaj, J. Oh, and S. Schafer-Nameki, *The Global Form of Flavor Symmetries and 2-Group Symmetries in 5d SCFTs* arXiv:2105.08724 [hep-th].

[242] C. Closset and H. Magureanu, *The U-plane of rank-one 4d $\mathcal{N} = 2$ KK theories* SciPost Phys. **12** no. 2, (2022) 065, arXiv:2107.03509 [hep-th].

[243] A. Collinucci, A. Sangiovanni, and R. Valandro, *Genus zero Gopakumar-Vafa invariants from open strings* JHEP **09** (2021) 059, arXiv:2104.14493 [hep-th].

[244] A. Collinucci, M. De Marco, A. Sangiovanni, and R. Valandro, *Higgs branches of 5d rank-zero theories from geometry* JHEP **10** no. 18, (2021) 018, arXiv:2105.12177 [hep-th].

[245] O. Aharony and A. Hanany, *Branes, superpotentials and superconformal fixed points* Nucl. Phys. B **504** (1997) 239–271, arXiv:hep-th/9704170.

[246] H. Hayashi, S.-S. Kim, K. Lee, and F. Yagi, *Complete prepotential for 5d $\mathcal{N} = 1$ superconformal field theories* JHEP **02** (2020) 074, arXiv:1912.10301 [hep-th].

[247] O. Bergman, D. Rodríguez-Gómez, and G. Zafrir, *5-Brane Webs, Symmetry Enhancement, and Duality in 5d Supersymmetric Gauge Theory* JHEP **03** (2014) 112, arXiv:1311.4199 [hep-th].

[248] O. Bergman, D. Rodríguez-Gómez, and G. Zafrir, *5d superconformal indices at large N and holography* JHEP **08** (2013) 081, arXiv:1305.6870 [hep-th].

[249] O. Bergman, D. Rodríguez-Gómez, and G. Zafrir, *Discrete θ and the 5d superconformal index* JHEP **01** (2014) 079, arXiv:1310.2150 [hep-th].

[250] A. Brandhuber and Y. Oz, *The D-4 - D-8 brane system and five-dimensional fixed points* Phys. Lett. B **460** (1999) 307–312, arXiv:hep-th/9905148.

[251] E. D'Hoker, M. Gutperle, A. Karch, and C. F. Uhlemann, *Warped $AdS_6 \times S^2$ in Type IIB supergravity I: Local solutions* JHEP **08** (2016) 046, arXiv:1606.01254 [hep-th].

[252] E. D'Hoker, M. Gutperle, and C. F. Uhlemann, *Warped $AdS_6 \times S^2$ in Type IIB supergravity II: Global solutions and five-brane webs* JHEP **05** (2017) 131, arXiv:1703.08186 [hep-th].

[253] E. D'Hoker, M. Gutperle, and C. F. Uhlemann, *Warped $AdS_6 \times S^2$ in Type IIB supergravity III: Global solutions with seven-branes* JHEP **11** (2017) 200, arXiv:1706.00433 [hep-th].

[254] M. Gutperle, A. Trivella, and C. F. Uhlemann, *Type IIB 7-branes in warped AdS_6: partition functions, brane webs and probe limit* JHEP **04** (2018) 135, arXiv:1802.07274 [hep-th].

[255] A. Legramandi and C. Nunez, *Electrostatic description of five-dimensional SCFTs* Nucl. Phys. B **974** (2022) 115630, arXiv:2104.11240 [hep-th].

[256] O. Bergman, D. Rodríguez-Gómez, and C. F. Uhlemann, *Testing AdS_6/CFT_5 in Type IIB with stringy operators* JHEP **08** (2018) 127, arXiv:1806.07898 [hep-th].

[257] O. Bergman and G. Zafrir, *5d fixed points from brane webs and O7-planes* JHEP **12** (2015) 163, arXiv:1507.03860 [hep-th].

[258] G. Zafrir, *Brane webs and O5-planes* JHEP **03** (2016) 109, arXiv:1512.08114 [hep-th].

[259] H. Hayashi, S.-S. Kim, K. Lee, M. Taki, and F. Yagi, *More on 5d descriptions of 6d SCFTs* JHEP **10** (2016) 126, arXiv:1512.08239 [hep-th].

[260] G. Zafrir, *Brane webs in the presence of an O5$^-$-plane and 4d class S theories of type D* JHEP **07** (2016) 035, arXiv:1602.00130 [hep-th].

[261] H. Hayashi, S.-S. Kim, K. Lee, and F. Yagi, *Discrete theta angle from an O5-plane* JHEP **11** (2017) 041, arXiv:1707.07181 [hep-th].

[262] H. Hayashi, S.-S. Kim, K. Lee, and F. Yagi, *5-brane webs for 5d $\mathcal{N} = 1$ G_2 gauge theories* JHEP **03** (2018) 125, arXiv:1801.03916 [hep-th].

[263] M. R. Douglas, *Branes within branes* NATO Sci. Ser. C **520** (1999) 267–275, arXiv:hep-th/9512077.

[264] O. Bergman and D. Rodriguez-Gomez, *5d quivers and their AdS(6) duals* JHEP **07** (2012) 171, arXiv:1206.3503 [hep-th].

[265] P. B. Genolini and L. Tizzano, *Comments on Global Symmetries and Anomalies of* 5*d SCFTs* arXiv:2201.02190 [hep-th].

[266] O. Bergman, M. R. Gaberdiel, and G. Lifschytz, *String creation and heterotic type I' duality* Nucl. Phys. B **524** (1998) 524–544, arXiv:hep-th/9711098.

[267] J. Polchinski and E. Witten, *Evidence for heterotic - type I string duality* Nucl. Phys. B **460** (1996) 525–540, arXiv:hep-th/9510169.

[268] J. Polchinski, S. Chaudhuri, and C. V. Johnson, *Notes on D-branes* arXiv:hep-th/9602052.

[269] A. Karch, *Field theory dynamics from branes in string theory* other thesis, 1998.

[270] A. Sen, *String network* JHEP **03** (1998) 005, arXiv:hep-th/9711130.

[271] J. Polchinski, *String theory. Vol. 2: Superstring theory and beyond*. Cambridge Monographs on Mathematical Physics. Cambridge University Press, 2007.

[272] M. R. Gaberdiel, T. Hauer, and B. Zwiebach, *Open string-string junction transitions* Nucl. Phys. B **525** (1998) 117–145, arXiv:hep-th/9801205.

[273] M. R. Gaberdiel and B. Zwiebach, *Exceptional groups from open strings* Nucl. Phys. B **518** (1998) 151–172, arXiv:hep-th/9709013.

[274] O. DeWolfe and B. Zwiebach, *String junctions for arbitrary Lie algebra representations* Nucl. Phys. B **541** (1999) 509–565, arXiv:hep-th/9804210.

[275] O. DeWolfe, T. Hauer, A. Iqbal, and B. Zwiebach, *Constraints on the BPS spectrum of N=2, D = 4 theories with A-D-E flavor symmetry* Nucl. Phys. B **534** (1998) 261–274, arXiv:hep-th/9805220.

[276] O. DeWolfe, *Affine Lie algebras, string junctions and seven-branes* Nucl. Phys. B **550** (1999) 622–637, arXiv:hep-th/9809026.

[277] O. DeWolfe, T. Hauer, A. Iqbal, and B. Zwiebach, *Uncovering infinite symmetries on [p, q] 7-branes: Kac-Moody algebras and beyond* Adv. Theor. Math. Phys. **3** (1999) 1835–1891, arXiv:hep-th/9812209.

[278] C. G. Callan and J. M. Maldacena, *Brane death and dynamics from the Born-Infeld action* Nucl. Phys. B **513** (1998) 198–212, arXiv:hep-th/9708147.

[279] E. Witten, *Solutions of four-dimensional field theories via M theory* Nucl. Phys. B **500** (1997) 3–42, arXiv:hep-th/9703166.

[280] A. Hanany and E. Witten, *Type IIB superstrings, BPS monopoles, and three-dimensional gauge dynamics* Nucl. Phys. B **492** (1997) 152–190, arXiv:hep-th/9611230.

[281] O. Bergman, A. Hanany, A. Karch, and B. Kol, *Branes and supersymmetry breaking in three-dimensional gauge theories* JHEP **10** (1999) 036, arXiv:hep-th/9908075.

[282] A. Collinucci and R. Valandro, *The role of U(1)'s in 5d theories, Higgs branches, and geometry* JHEP **10** (2020) 178, arXiv:2006.15464 [hep-th].

[283] O. Bergman and D. Rodríguez-Gómez, *The Cat's Cradle: deforming the higher rank E_1 and $\tilde{E}_1$ theories* JHEP **02** (2021) 122, arXiv:2011.05125 [hep-th].

[284] B. Kol and J. Rahmfeld, *BPS spectrum of five-dimensional field theories, (p,q) webs and curve counting* JHEP **08** (1998) 006, arXiv:hep-th/9801067.

[285] A. Sen, *F theory and orientifolds* Nucl. Phys. B **475** (1996) 562–578, arXiv:hep-th/9605150.

[286] O. DeWolfe, T. Hauer, A. Iqbal, and B. Zwiebach, *Uncovering the symmetries on [p,q] seven-branes: Beyond the Kodaira classification* Adv. Theor. Math. Phys. **3** (1999) 1785–1833, arXiv:hep-th/9812028.

[287] S.-S. Kim, M. Taki, and F. Yagi, *Tao Probing the End of the World* PTEP **2015** no. 8, (2015) 083B02, arXiv:1504.03672 [hep-th].

[288] V. Mitev, E. Pomoni, M. Taki, and F. Yagi, *Fiber-Base Duality and Global Symmetry Enhancement* JHEP **04** (2015) 052, arXiv:1411.2450 [hep-th].

[289] F. Benini, S. Benvenuti, and Y. Tachikawa, *Webs of five-branes and N=2 superconformal field theories* JHEP **09** (2009) 052, arXiv:0906.0359 [hep-th].

[290] C. Bachas and M. B. Green, *A Classical manifestation of the Pauli exclusion principle* JHEP **01** (1998) 015, arXiv:hep-th/9712187.

[291] L. Fei, S. Giombi, and I. R. Klebanov, *Critical $O(N)$ models in $6-\epsilon$ dimensions* Phys. Rev. D **90** no. 2, (2014) 025018, arXiv:1404.1094 [hep-th].

[292] Y. Nakayama and T. Ohtsuki, *Five dimensional $O(N)$-symmetric CFTs from conformal bootstrap* Phys. Lett. B **734** (2014) 193–197, arXiv:1404.5201 [hep-th].

[293] J.-B. Bae and S.-J. Rey, *Conformal Bootstrap Approach to O(N) Fixed Points in Five Dimensions* arXiv:1412.6549 [hep-th].

[294] S. M. Chester, S. S. Pufu, and R. Yacoby, *Bootstrapping $O(N)$ vector models in $4 < d < 6$* Phys. Rev. D **91** no. 8, (2015) 086014, arXiv:1412.7746 [hep-th].

[295] Z. Li and N. Su, *Bootstrapping Mixed Correlators in the Five Dimensional Critical O(N) Models* JHEP **04** (2017) 098, arXiv:1607.07077 [hep-th].

[296] G. Arias-Tamargo, D. Rodriguez-Gomez, and J. G. Russo, *On the UV completion of the $O(N)$ model in $6-\epsilon$ dimensions: a stable large-charge sector* JHEP **09** (2020) 064, arXiv:2003.13772 [hep-th].

[297] Z. Li and D. Poland, *Searching for gauge theories with the conformal bootstrap* JHEP **03** (2021) 172, arXiv:2005.01721 [hep-th].

[298] S. Giombi, R. Huang, I. R. Klebanov, S. S. Pufu, and G. Tarnopolsky, *The $O(N)$ Model in $4<d<6$: Instantons and complex CFTs* Phys. Rev. D **101** no. 4, (2020) 045013, arXiv:1910.02462 [hep-th].

[299] S. Giombi and J. Hyman, *On the large charge sector in the critical O(N) model at large N* JHEP **09** (2021) 184, arXiv:2011.11622 [hep-th].

[300] A. Florio, J. a. M. V. P. Lopes, J. Matos, and J. a. Penedones, *Searching for continuous phase transitions in 5D SU(2) lattice gauge theory* JHEP **12** (2021) 076, arXiv:2103.15242 [hep-lat].

[301] F. De Cesare, L. Di Pietro, and M. Serone, *Five-dimensional CFTs from the ε-expansion* Phys. Rev. D **104** no. 10, (2021) 105015, arXiv:2107.00342 [hep-th].

[302] M. Bertolini and F. Mignosa, *Supersymmetry breaking deformations and phase transitions in five dimensions* JHEP **10** (2021) 244, arXiv:2109.02662 [hep-th].

[303] M. Bertolini, F. Mignosa, and J. van Muiden, *On non-supersymmetric fixed points in five dimensions* arXiv:2207.11162 [hep-th].

[304] S. A. Cherkis, *Moduli Spaces of Instantons on the Taub-NUT Space* Commun. Math. Phys. **290** (2009) 719–736, arXiv:0805.1245 [hep-th].

[305] A. Sen, *NonBPS states and Branes in string theory* in *Advanced School on Supersymmetry in the Theories of Fields, Strings and Branes*, pp. 187–234. 1999. arXiv:hep-th/9904207.

[306] G. Aldazabal, S. Franco, L. E. Ibanez, R. Rabadan, and A. M. Uranga, *D = 4 chiral string compactifications from intersecting branes* J. Math. Phys. **42** (2001) 3103–3126, arXiv:hep-th/0011073.

[307] K. Hashimoto and S. Nagaoka, *Recombination of intersecting D-branes by local tachyon condensation* JHEP **06** (2003) 034, arXiv:hep-th/0303204.

[308] A. Giveon and D. Kutasov, *Gauge Symmetry and Supersymmetry Breaking From Intersecting Branes* Nucl. Phys. B **778** (2007) 129–158, arXiv:hep-th/0703135.

[309] E. A. Bergshoeff, M. de Roo, S. F. Kerstan, T. Ortin, and F. Riccioni, *SL(2,R)-invariant IIB Brane Actions* JHEP **02** (2007) 007, arXiv:hep-th/0611036.

[310] I. Bena, K. Pilch, and N. P. Warner, *Brane-Jet Instabilities* JHEP **10** (2020) 091, arXiv:2003.02851 [hep-th].

[311] M. Suh, *The non-SUSY AdS_6 and AdS_7 fixed points are brane-jet unstable* JHEP **10** (2020) 010, arXiv:2004.06823 [hep-th].

[312] G. Itsios, P. Panopoulos, K. Sfetsos, and D. Zoakos, *On the stability of AdS backgrounds with λ-deformed factors* JHEP **07** (2021) 054, arXiv:2103.12761 [hep-th].

[313] F. Apruzzi, G. Bruno De Luca, G. Lo Monaco, and C. F. Uhlemann, *Non-supersymmetric AdS_6 and the swampland* JHEP **12** (2021) 187, arXiv:2110.03003 [hep-th].